LATE PRECAMBRIAN PALAEOMAGNETISM OF AUSTRALIA AND AFRICA

by

MICHAEL OTIS McWILLIAMS

A thesis submitted for the degree of

DOCTOR OF PHILOSOPHY

in the

AUSTRALIAN NATIONAL UNIVERSITY

Research School of Earth Sciences
Institute of Advanced Studies
Canberra

September, 1977

STATEMENT

The studies described herein were conducted during my tenure of an Australian National University scholarship from March, 1974 to September, 1977. The results and interpretations presented are entirely my own work except where otherwise acknowledged.

All samples from Australia were collected by myself with assistance from Drs. M.W. McElhinny, P.W. Schmidt and R.T. Merrill or Messrs. D.J. Edwards and J.L. Kirschvink. Samples from Africa were collected by Prof. A. Kröner. Mrs. J. Cowley assisted with some of the remanence and susceptibility measurements. Mass spectrometer measurements were done by Mr. I. Williams.

No part of this work has been previously submitted to any other university or institution.

M.O. McWilliams

(M.O. McWilliams)

ACKNOWLEDGEMENTS

It is a great pleasure to acknowledge the advice, encouragement and assistance of some of the many individuals and organizations who contributed to this endeavour.

I wish to thank my supervisor Dr. M.W. McElhinny, who originally suggested the project and provided beneficial and stimulating discussion and comment throughout its course. Thanks are also due my advisors, Drs. W. Compston and B.J.J. Embleton for their continuing support and advice, and to Professor A. Kröner (Johannes Gutenberg Universität, Mainz, FRG) for enthusiastic collaboration in the Nama/Damara study.

Fieldwork assistance by Drs. M.W. McElhinny, P.W. Schmidt and R.T. Merrill and Mr. D.J. Edwards is greatly appreciated, as is laboratory assistance by Mrs. J.A. Cowley and Mr. D.J. Edwards. Thanks are due Mr. I. Williams for considerable assistance in the U-Pb geochronological studies. Mrs. J.A. Cowley proofread the manuscript.

I should like to thank the many persons of the Bureau of Mineral Resources and South Australian Department of Mines who provided valuable support and advice. I gratefully acknowledge financial support from the Australian National University during my course of study.

My special thanks are due to my wife Barbara for her continuing support throughout.

LATE PRECAMBRIAN PALAEOMAGNETISM OF AUSTRALIA AND AFRICA

Table of Contents

ABSTRACT

Palaeomagnetic studies of late Precambrian sedimentary and volcanic rocks from Australia and Southern Africa are described. The data are obtained mainly from stratigraphic sequences where absolute isotopic age information is sparse or absent; however stratigraphic control enables the construction of a relative polar chronology from the major cratonic units.

Australian palaeomagnetic data are derived from the Adelaide 'Geosyncline', from the Amadeus, Kimberley and Officer Basins, from King Island and from the Burke River outlier. Apparent polar wander path (APWP) segments for the various structural units suggest that the present distribution of older Precambrian domains may have resulted from a late Precambrian - early Palaeozoic rifting episode which caused fission of a contiguous proto-Australian plate into a number of subplates. Such a rifting episode is consistent with some proposed models of the structural evolution of Australia and of the Australian-Antarctic platform.

African palaeomagnetic data are derived from the Nama and Damara Systems of Namibia, stratigraphic equivalents deposited on the Kalahari and Congo cratons respectively. In conjunction with previously published data, the new data support the view that the two cratons have maintained approximately their present relative positions since at least -1000 my, that no large scale relative motion has occurred between the two units, and that the intervening Damara mobile belt did not result from a plate collision mechanism.

When compared on a Smith-Hallam reconstruction of Gondwanaland, the proposed late Precambrian APWPs for Africa and

Australia are distinctly different before about -550 my, but form a common path after this time. Palaeomagnetic and geological evidence suggest that Australia, India and Antarctica may have comprised an east Gondwanaland assemblage, colliding at about -550 my with a west Gondwanaland assemblage consisting of Africa and possibly South America. Such a collision could account for some, but not all of the late Precambrian to early Palaeozoic Pan-African mobile belts.

Many of the sedimentary sequences studied contain excellent examples of late Precambrian glaciogenic rocks. Palaeolatitude information obtained from these units strongly suggests that the nonsynchronous circumpolar model for the late Precambrian glaciations is not applicable. A synchronous global event may be indicated.

LIST OF ABBREVIATIONS

α_{95} (A_{95})	semi-angle of the cone whose apex lies at the origin and whose axis coincides with the estimated mean direction (pole) calculated from a population of directions (poles) and within which the true mean direction (pole) lies with 95% probability. The intersection of this cone with a surrounding sphere describes the 'circle of confidence' at the 95% probability level. (Fisher, 1953).
B/C	bedding-corrected : structurally corrected magnetization directions, *ie* restored to palaeohorizontal orientation.
by	billion (10^9) years.
CRM	chemical remanent magnetization.
γ	gamma; magnetic field unit (18 equivalent to 10^{-9}T).
D(D')	declination with respect to present (palaeo-) horizontal.
dp,dm	semi-minor and semi-major axes of the polar error ellipse (degrees): the ellipse describes a region surrounding an estimated palaeomagnetic pole position within which the true pole lies at the 95% probability level. The α_{95} circle about the mean direction of magnetization transforms to an ellipse about the palaeomagnetic pole.
F/C	field-corrected : structurally uncorrected magnetization directions, *ie* with respect to present horizontal orientation.
I(I')	inclination with respect to present (palaeohorizontal).
$\hat{I}_o$	estimated mean inclination from borehole samples (Briden and Ward, 1960).

J	magnetitude of the magnetization vector $\vec{J}$.
$k(k')$	estimate of the precision parameter for a population of directions of magnetization referred to present (palaeo-) horizontal.
$\hat{k}$	estimate of precision parameter k for a population of inclination values from borehole samples (Briden and Ward, 1960).
mAm^{-1}	unit of magnetization : milliamperes per metre.
mT	unit of magnetic field : milli Tesla.
my	million (10^6) years.
$N(n)$	number of sites (samples) in population used to calculate mean direction.
NRM	natural remanent magnetization, prior to application of any magnetic cleaning method.
palaeomagnetic pole	a time averaged representation of the palaeomagnetic field calculated over a sufficient time span such that the effects of palaeosecular variation are minimised. On an axial geocentric dipole model, the palaeomagnetic and palaeogeographic poles are coincident.
PEF	present earth's field : the present geomagnetic field direction at a particular point on the earth's surface.
PTRM	partial thermoremanent magnetization.
R	the magnitude of the resultant vector of a population of unit vectors.
TRM	thermoremanent magnetization.
VGP	virtual geomagnetic pole : an instantaneous estimate of the palaeomagnetic field represented by an equivalent geomagnetic pole.
VRM	viscons remanent magnetization.

1. With the exception of the substitution of γ for nT, all units are SI throughout.

2. Latitudes reckoned positive north; longitudes reckoned positive east.

Chapter 1

Introduction

§1.1 Approach to project

Palaeomagnetic studies conducted in the late 1950s and early 1960s were a major factor in helping to convince earth scientists that relative continental motion had occurred. These studies, coupled with the detailed study of magnetic lineations in the ocean basins, led to the formulation of an elegant and widely applied global tectonic theory which has met with unqualified success in explaining much of the earth's present behaviour and recent history. Endowed with uniformitarian dogma, many earth scientists have naturally suggested that the tectonic mechanisms envisaged as operative in recent times are also responsible for the geological events we see recorded in the older Palaeozoic and Precambrian domains where marine geophysical and geological studies are not applicable.

In recent years, considerable evidence has accumulated primarily in the study of Proterozoic orogenic zones which strongly suggests that such an application of uniformitarian principles may be incorrect; indeed, as recently as 500 million years ago, global tectonics may have taken a different form compared to modern plate tectonics. A considerable amount of debate has been centred around the problem, uniformitarianists to the one side, while other workers support an evolutionary scheme of global tectonics, with plate tectonics being only the most recent form to have been developed. A solution to the problem, *i.e.* discovery of different tectonic mechanisms or confirmation of the existence

of present plate-type tectonics in pre-Mesozoic times is intimately related to the history of crustral motions and therefore can probably only be accomplished by the detailed application of palaeomagnetic methods.

The study of palaeomagnetism has too undergone an evolutionary process. First generation palaeomagnetism sought to convince the earth science community that the study of remanent magnetizations in rocks could yield useful information concerning the history of lateral crustal displacements. This phase of palaeomagnetism was characterized by the discrete study of favourable younger rock units from many localities, culminating in the construction and reconstruction of apparent polar wander paths for the continents. The end result was the confirmation of relative continental motions in post-Palaeozoic times. With second generation palaeomagnetism came magnetic reversal stratigraphy and the study and correlation of continental and oceanic polarity sequences for this recent 200 million year interval. Neither of these subsets of palaeomagnetism have yet been completed; nevertheless present knowledge in both these areas is complete enough to enable earth scientists to attempt more localized, second-order problems.

Third generation palaeomagnetism, the detailed study of crustal displacements and behaviour of the earth's magnetic field in the earlier 90% of earth history is in its infancy. Examination of the palaeomagnetic data compilations produced by the Earth Physics Branch (Ottawa) shows that as of 1975, roughly 850 palaeomagnetic results which meet minimum reliability requirements are available for the Carboniferous to Recent interval, an average density of about 2.4 poles/my.

For the preceding Proterozoic to Devonian interval, only 350 poles are available which meet the same criteria for reliability, a pole density of 0.16 poles/my, depleted by a factor of 15 with respect to the younger interval. Even in the Cambrian to Devonian interval, data are depleted by the factor of 3 compared to the more recent 250 my period. The present state of third generation palaeomagnetism is therefore not unlike the state of first generation palaeomagnetism 15 to 20 years ago, when the first systematic continental displacements were discovered.

Understandably, one of the obvious thrusts of current palaeomagnetic research is to extend and clarify the palaeomagnetic record back to Proterozoic and Archaean times. Probably the most logical procedure for this extension is to work backwards from a relatively well known Phanerozoic point. The accumulation in recent years of Phanerozoic palaeomagnetic data of good quality from Australia and Africa provides such a starting point. At the initiation of this project, only two palaeomagnetic results were available for Australia in the 1200-600 my interval. Although the state of the African data was better, significant time gaps were also present. In both continents, little attention had been given to the isolation and interpretation of superimposed secondary magnetizations which could be of potential significance in their tectonic history.

The palaeomagnetic studies described in this thesis form the framework of a detailed history of apparent polar motions of Australia and Africa in the 900-500 my interval. The guiding philosophy was to sample well represented and little deformed late Precambrian stratigraphic sequences in

both continents. The obvious advantage of this scheme is that a relative polar chronology can be constructed based upon stratigraphic relationships. An APWP segment based upon such a relative chronology can be calibrated if rocks suitable for isotopic dating are present; in the absence of radiometric ages within the stratigraphic column, the APWP segment can be compared with isolated palaeomagnetic poles of known age from the same structural block.

By sampling folded strata and by conducting detailed demagnetization experiments, it was hoped that reliable information could be obtained regarding not only the original (primary) magnetizations, but also the nature and mode of occurrence of any secondary magnetizations which might be present. Sequences of poles of similar age in a known relative chronology from different regions may then be compared, making judgements possible about the existence of motions between the continental blocks or cratons from which the data are derived, and ultimately about the mechanisms which may have caused orogenic zones to form between the blocks.

Sampling of late Precambrian (Adelaidean) rocks was conducted in six structurally distinct regions in Australia (Figure 1.1a) : the Adelaide 'Geosyncline', Amadeus Basin, Kimberley Basin, Officer Basin, Burke River Inlier and on King Island. Samples of late Precambrian rocks of similar age were obtained from the Congo and Kalahari cratons of Africa, and from the intervening Damara mobile belt (Figure 1.1b). Palaeomagnetic data from the well documented Adelaide 'Geosyncline' were intended to be used as a reference pole path (Chapter 2), with which late Precambrian Poles from elsewhere

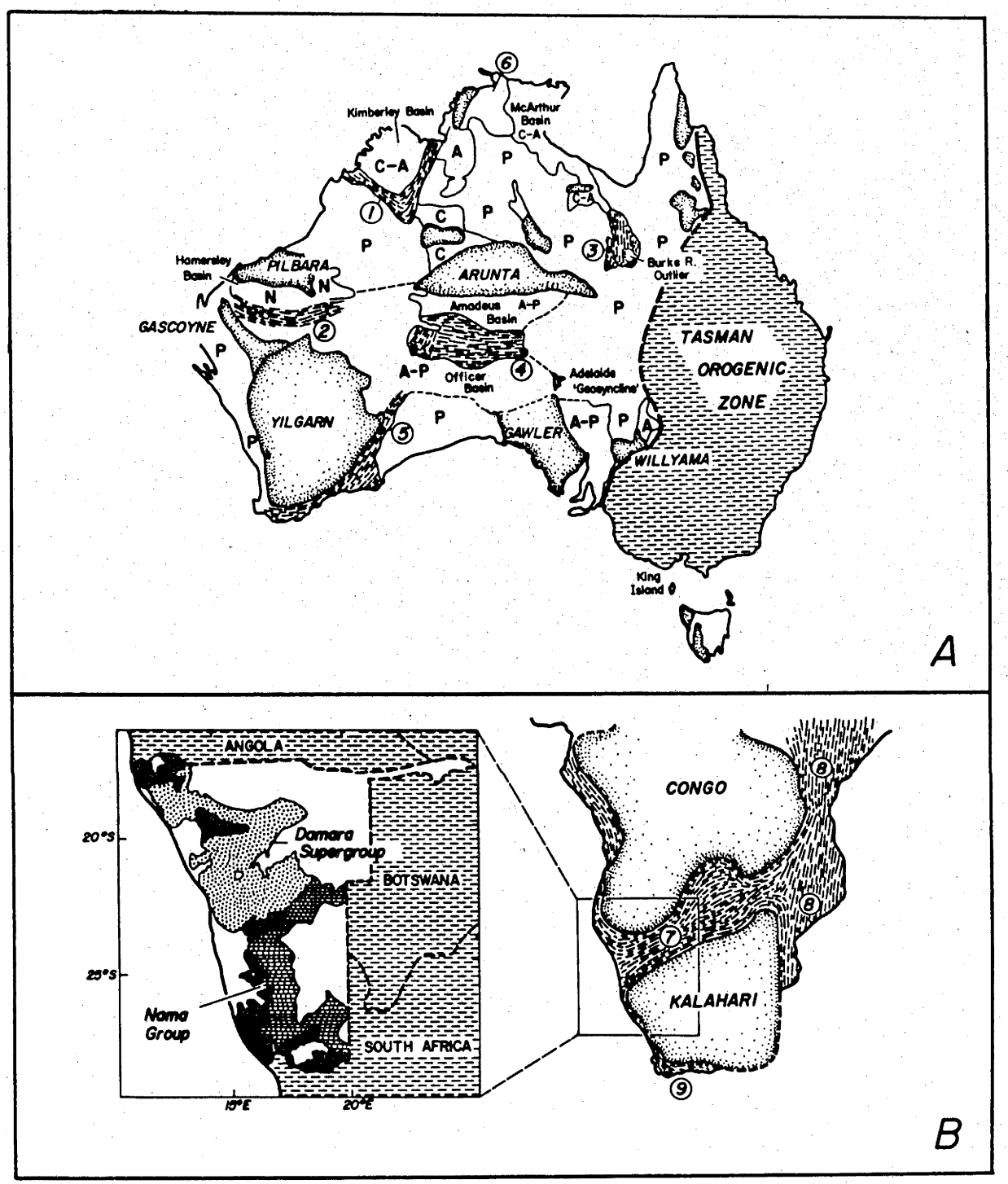

Figure 1.1 : Generalized structural map of (A) Australia and (B) Africa, after McElhinny and McWilliams (1977). Stable cratonic areas stippled; younger intervening mobile belts labelled 1-8: 1) Halls Creek-King Leopold mobile belt (ca. 1.8 by), 2) Ophthalmian mobile belt (ca. 1.7 by), 3) Mt. Isa Geosyncline (1.4-1.8 by), 4) Musgrave mobile belt (1.2-1.4 by), 5) Albany-Fraser mobile belt (1.0-1.3 by), 6) Pine Creek Geosyncline 7) Damara mobile belt (0.6-0.45 by), 8) Mozambique mobile belt (0.6-0.46 by), 9) Cape mobile belt (Permo-Triassic). Age of Australian sedimentary basins indicated as N (Nullaginian, 2.2-1.8 by), C (Carpentarian, 1.8-1.4 by), A (Adelaidean, (?) 1.4-0.6 by) and P (Phanerozoic, 0.6 by). Inset: relationship of Nama and Damara sediments to Damara mobile belt and Congo and Kalahari cratons.

in Australia could be compared (Chapter 3). Data from southern Africa are first compared internally (Chapter 4), then with the Australian and other data on a reconstruction of the supercontinent Gondwanaland (Chapter 5).

An important aspect of this study of late Precambrian sedimentary sequences in Australia and Africa has been determination of the palaeolatitudes of the glacial deposits contained in many of the sequences (Plates 1-7, Figure 1.2). Ever since the original suggestion of a synchronous global glaciation was made (Harland, 1964), stratigraphers and palaeomagnetists have debated the usefulness of such deposits as intra- and intercontinental chronostratigraphic marker horizons. As little direct palaeomagnetic data from the glacial deposits was available at the start of the project, considerable effort was devoted to the study of some of the well exposed and well documented late Precambrian glacial deposits of Australia and Africa. Although palaeolatitudes of the tillites and related sediments become obvious as the data of Chapters 2,3 and 4 accumulate, a discussion of the implications of the data to the various models for the late Precambrian glaciations which have been proposed is deferred until Chapter 5.

§1.2 Palaeomagnetic methods

An overall summary of palaeomagnetism and rock magnetism is not presented here. A comprehensive discussion of palaeomagnetism and palaeomagnetic methods can be found in texts by Irving (1964) and McElhinny (1973), and of rock magnetism in texts by Nagata (1961) and Stacey and Bannerjee (1974). A number of specific points relevant to the studies

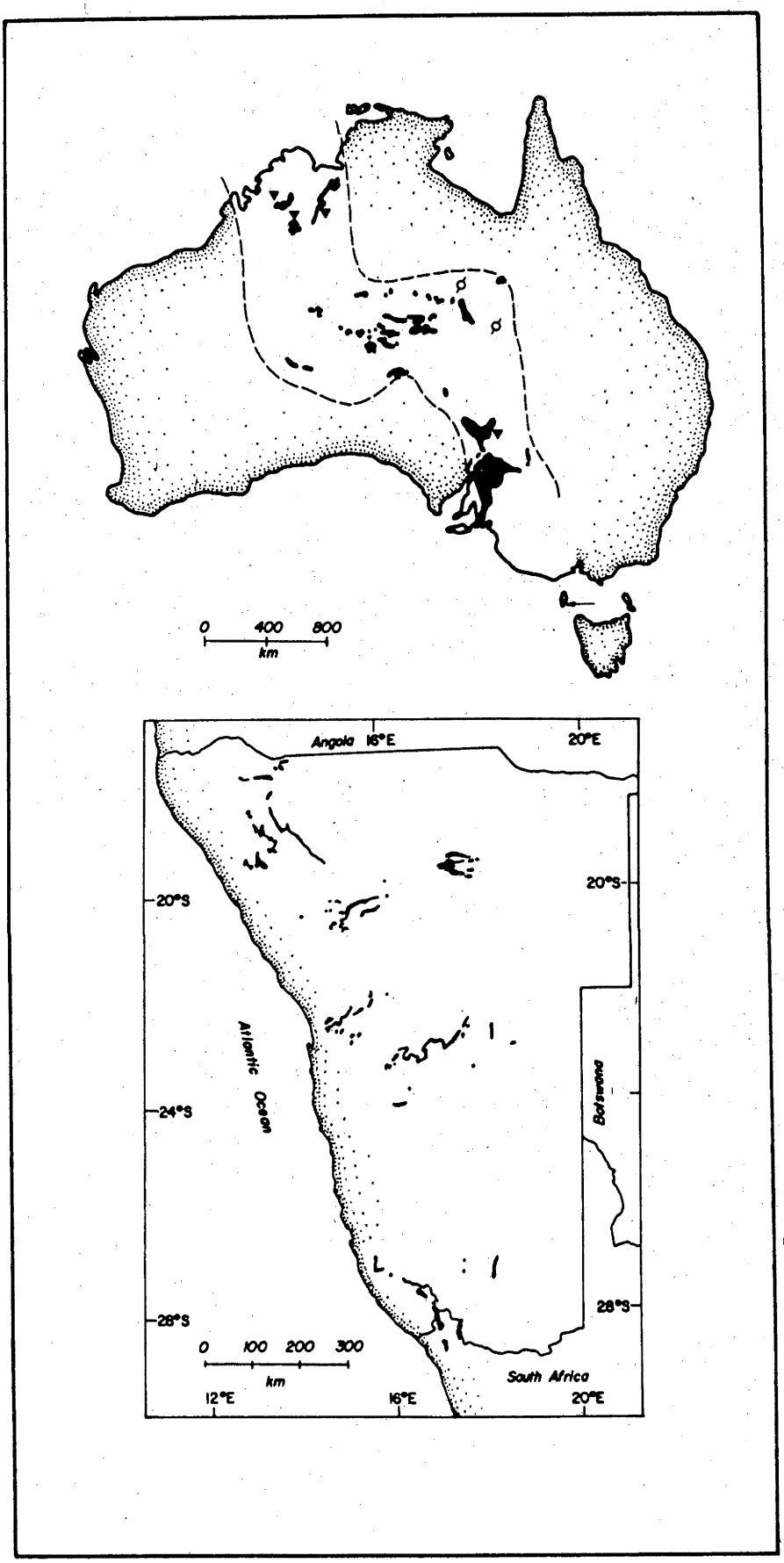

Figure 1.2 : Distribution of proven and possible late Precambrian glaciogenic rocks in Australia (above : after Dunn *et al.*, 1971) and Namibia (below : after Kröner and Rankema, 1973). Solid areas indicate surface exposures, triangles denote observed glacial pavements, circles with slash denote borehole intersections of (?) glaciogenic rocks. Dotted lines on Australian map mark probable limits of preserved late Precambrian glacial sediments.

described in Chapters 2,3 and 4 are discussed below:

§1.2.1 Sampling hierarchy

In this work, the following nomenclature for collection of samples is applicable:

locality - a geographical point where one or more sites in a rock unit were sampled.

site - the basic sampling unit; a thickness or areal extent of rock from which a number (usually 3-5) of samples are collected. The averaged direction of magnetization of these samples defines the *site mean direction*, an instantaneous or 'spot' recording of the ancient geomagnetic field. In the case of sedimentary rocks, a narrow (∿1-2 m) stratigraphic interval is considered to be a site, while with volcanic and intrusive rocks, flows and dykes are equated with sites. Site mean directions collectively representing a much longer time span than the individual sites are averaged to form the overall *formation mean direction*, in which the effects of palaeosecular variation have (hopefully) been cancelled.

sample - an individually oriented piece of rock, usually a drill core or block from which a number (3-5) of specimens are obtained. Orientation of samples was done by both solar and magnetic compass to eliminate spurious effects due to intensely magnetized outcrops; random errors in azimuth and dip are estimated to be $\pm 1°$ or less.

specimen - the basic measurement unit; a 2.53 cm diameter x 2.30 cm height (2.20 cm diameter x 1.91 cm height for Nama Group specimens) cylindrical core slice.

§1.2.2 Magnetic measurements and demagnetization apparatus

Measurements of remanent magnetizations were conducted using one of three commerically available magnetometers : a DIGICO slow speed (∿7Hz) fluxgate spinner magnetometer interfaced with a minicomputer, or one of two 3.8 cm access 2 axis SQUID (Superconducting QUantum Interference Device) magnetometers with either a 6ℓ or 30ℓ liquid helium storage dewar (Superconducting Technology, Inc.) interfaced to the DIGICO minicomputer. A practical lower intensity limit for remanence measurements was found to be $\sim 5 \times 10^{-2} mAm^{-1}$ for the fluxgate instrument and $1\text{-}2 \times 10^{-2} mAm^{-1}$ for the cryogenic magnetometer.

Thermal demagnetization experiments were done in air in an apparatus described by McElhinny *et al.* (1971), a non-magnetic furnace capable of attaining temperatures in excess of 700° surrounded by a 10 coil feedback controlled field cancellation system. DC magnetic field levels during cooling periods were kept below $\pm 2\gamma$. Alternating field (AF) demagnetization was done in an instrument modified after Evans (1969), a 3-axis specimen tumbler within a large coil capable of attaining peak fields of 210 mT. DC field cancellation within the AF demagnetization apparatus was kept within $\pm 10\gamma$. Chemical leaching was performed in the same field-controlled space used for thermal demagnetization. Specimens were serrated twice to facilitate more rapid acid

penetration; in the initial 24 hour leaching period, HCℓ concentration was kept at 6N. Subsequent leaching was done in 12N HCℓ. Specimens were repeatedly rinsed in fresh water during a period of about 1 hour prior to measuring.

Transferral of partially demagnetized specimens from the particular demagnetizing apparatus to the magnetometer was done using mu-metal shields inside which DC magnetic field cancellation was generally better than $\pm 50\gamma$. Specimens were loaded in the magnetometer inside special Helmholtz coil sets which cancelled the ambient magnetic field in the specimen handling region to within $\pm 100\text{-}250\gamma$.

§1.2.3 Statistical analysis of magnetization directions

Errors in mean magnetization directions have been estimated by the methods developed by Fisher (1953). An explanation of the symbols relevant to the analysis is to be found in the List of Abbreviations.

The "randomness test" (Watson, 1956a; Vincenz and Bruckshaw, 1960) was used as an objective criterion for rejecting widely scattered directions at the sample or site mean level.

In Chapters 2,3 and 4, considerable use is made of two statistical methods, the fold test (Graham, 1949) and the comparison of mean directions (Watson, 1956b). The object of the fold test is to determine whether or not a particular component magnetization was acquired before or after folding of a rock unit occurred by comparing the precision of the structurally corrected formation mean direction (k') with the precision of the *in situ* formation mean direction (k). The variance ratio k'/k (or k/k') for N directions may be

compared with F-ratio tables with equal 2(N-1) degrees of freedom to determine whether a change in precision is statistically significant at a given probability level (McElhinny, 1964). The test can be used to infer when a formation mean magnetization direction was acquired relative to the age of folding, and is applicable to both positive ($k'/k \geq 1.0$) and negative ($k'/k \leq 1.0$) changes in precision.

Populations of magnetization directions whose mean direction and associated circles of confidence at a chosen probability level do not overlap are statistically significantly different at that level. Population means with overlapping circles of confidence may still be different, and thus a special method must be employed to determine whether or not the populations are indeed different. The statistic

$$\frac{2\ (\Sigma N_i - s)}{2\ (s-1)} \quad \frac{\Sigma R_i - R}{\Sigma (N_i - R_i)}$$

where:

s = number of populations to be tested

N_i = number of individual directions in the ith population

R_i = vector resultant of the ith population

R = vector resultant of all the individual directions

may be compared with F-ratio tables with $2(s-1)$ and $2(\Sigma N_i - S)$ degrees of freedom to test whether the populations are identical, assuming the precisions of the s populations are statistically the same. Large values of this statistic indicate that the assumption of an identical mean direction for the s populations may be false.

§1.2.4 Multicomponent analysis

The total natural remanent magnetization (NRM) of a rock is commonly a vector sum of several component parts, each possibly dating from a different time in the rock's history. Consider as an example a hypothetical sedimentary rock which originally contained only a diagenetically acquired primary CRM. A subsequent low grade metamorphic event may superimpose a secondary PTRM component upon the original magnetization; more recent lightning strikes may have resulted in a secondary IRM component being added (Figure 1.3). These three magnetizations might be completely different in age, direction, intensity, rock magnetic properties and importance to a palaeomagnetic investigation. Such a collection of magnetizations is called a *multicomponent system.*

In all but the most recent palaeomagnetic studies the analysis of multicomponent magnetization systems has been commonly treated rather superficially. Samples are often treated in progressively higher peak AF's or temperatures in an attempt to fully remove any low H_c or T_b components and isolate a single, stable magnetization as indicated by a stable directional endpoint. Little emphasis has been placed upon study of the nature of the removed magnetizations. In recent years however, the detailed palaeomagnetic study of mainly Precambrian igneous, sedimentary and metamorphic rocks with complex thermal and tectonic histories has led to considerable discussion about the mode of occurrence, isolation, and interpretation of multicomponent systems (*e.g.* Hargraves and Burt, 1967; Buchan and Dunlop, 1976; Irving and McGlynn, 1976; Roy and Lapointe, 1976; Ueno and Irving, 1976). Attention was given to the occurrence and interpretation of

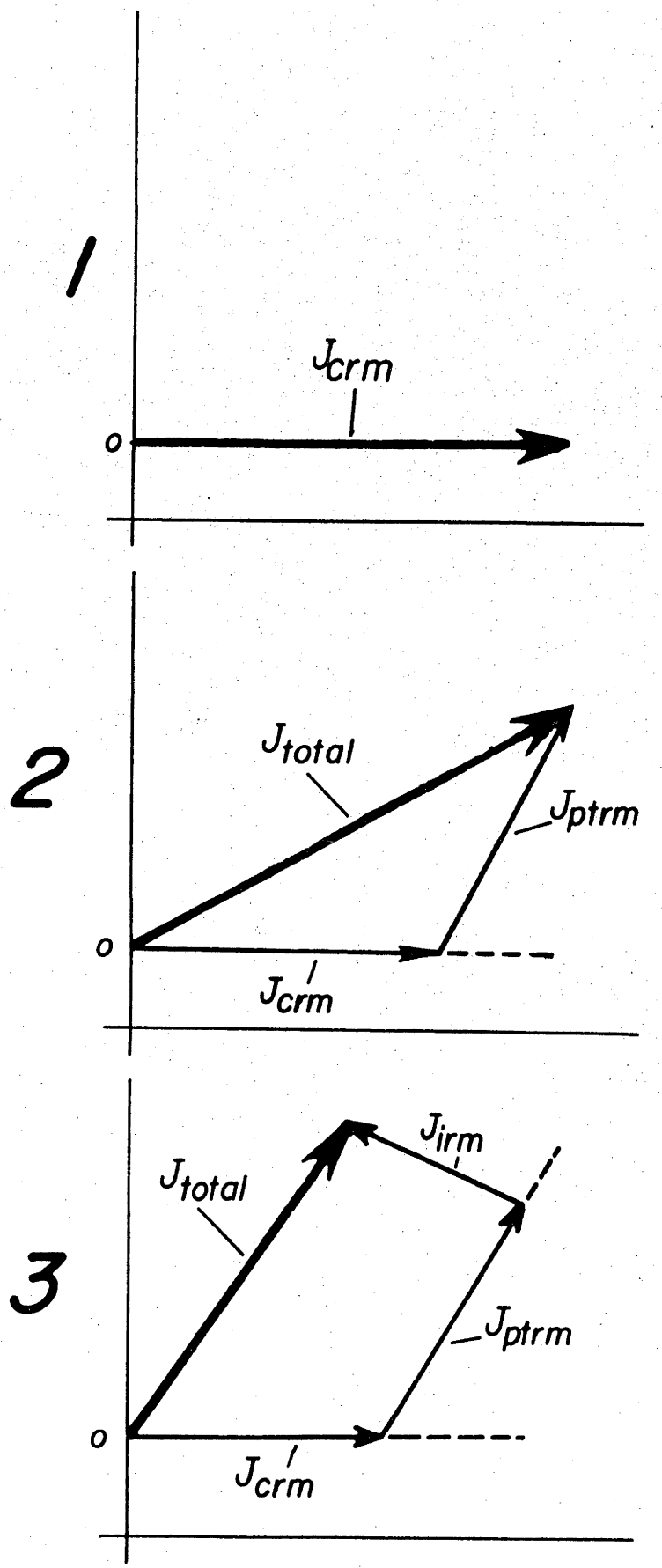

Figure 1.3 : To illustrate a multicomponent magnetization system : magnetization vectors J_{crm}, J_{ptrm} and J_{irm} combine to form the total observed NRM J_{total}.

multicomponent magnetizations in the palaeomagnetic investigations described herein, largely as a result of an advance knowledge of the complex geological history of many of the rocks studied.

The observed remanence vector J can be written

$$\vec{J} = X_i \cdot \vec{\mu}_i \quad (i = 1,2,3)^* \tag{1}$$

where the X_i are scalar magnitudes of the projection of the vector upon a cartesian coordinate system (the magnitudes of the commonly used X,Y and Z components), and the $\vec{\mu}_i$ are unit vectors in each of the directions of a coordinate system which is fixed with respect to a present geographical frame.

Two additional complexities in notation are introduced. The magnetization vector $\vec{J}$ following the kth demagnetization step is denoted by

$$\vec{J}(k) = X_i(k) \cdot \vec{\mu}_i \quad (k = 0,1,2...n) \tag{2}$$

for any of n successive demagnetization steps. The untreated NRM vector is thus $\vec{J}(0)$. The *subtracted vector* is the vector difference between magnetization vectors after any two demagnetization steps which may somehow change the state of the magnetization vector and is simply

$$\begin{aligned} \Delta\vec{J}(m-n) &= \vec{J}(m) - \vec{J}(n) \quad (n>m) \\ &= (X_i(m) - X_i(n)) \cdot \vec{\mu}_i \end{aligned} \tag{3}$$

For a single component 'system', demagnetization may produce only a change in intensity of the remanence vector (Figure 1.4a) thus

$$\Delta\vec{J}(m-n) = F_{m-n} \cdot \vec{J}(0) \tag{4}$$

---

* Summation implied upon repeated indicies.

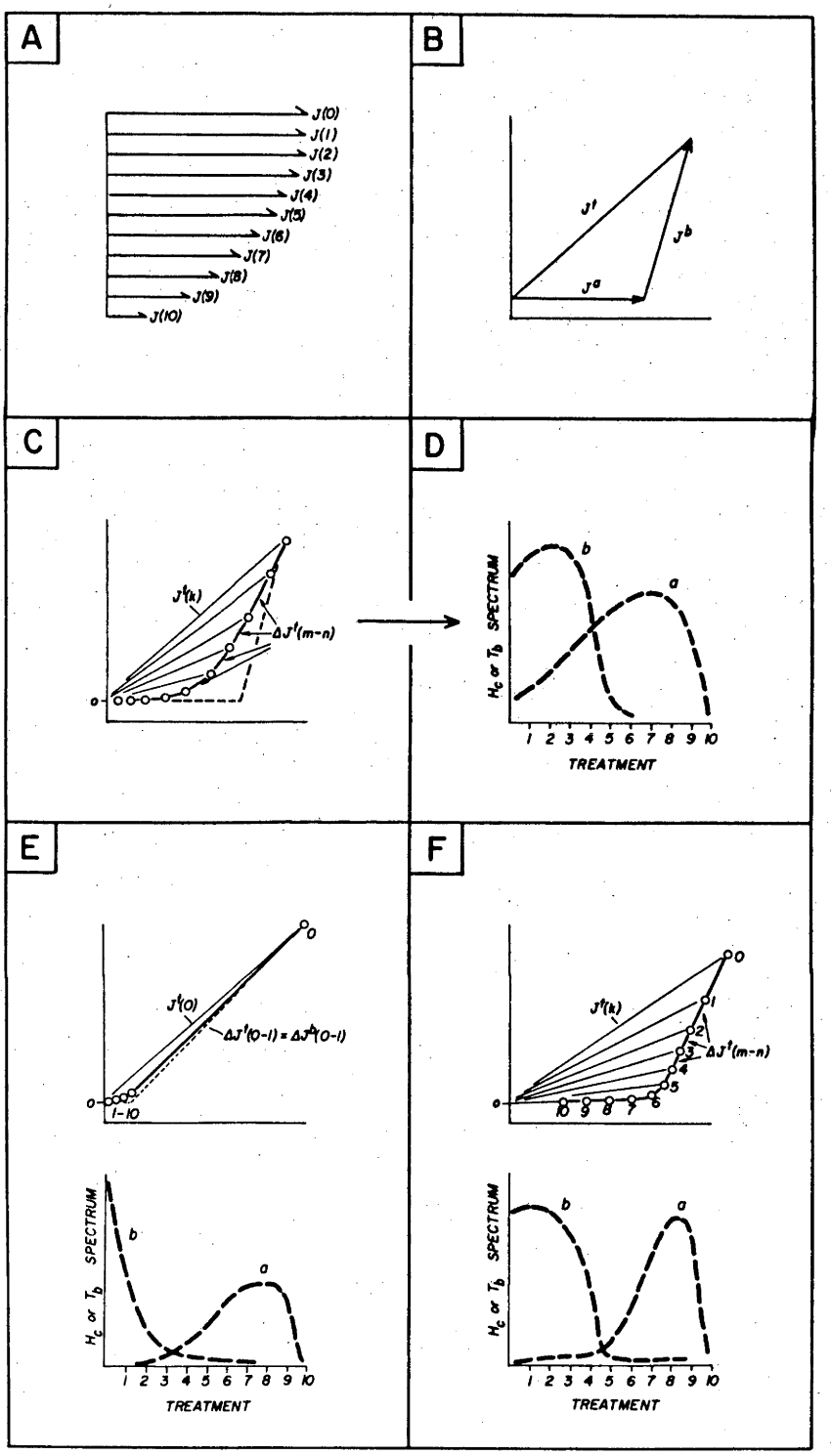

Figure 1.4 : Demagnetization systematics in multicomponent assemblages. See text for detailed explanation.

where F_{m-n} is a scalar related to the coercivity spectrum, blocking temperature spectrum or acid leaching resistance spectrum in the case of alternating field, thermal or chemical demagnetization, respectively.

Consider now a two-component magnetization system. The total and component vectors are denoted by superscripts such that after the kth demagnetization step

$$\vec{J}^t(k) = \vec{J}^a(k) + \vec{J}^b(k) \tag{5}$$

as illustrated in 2 dimensions in Figure 1.4b. After demagnetization, each component may have a different intensity from its previous value such that

$$\begin{aligned} \vec{J}^a(n) &= F^a_{m-n} \cdot \vec{J}^a(m) \quad \text{and} \\ \vec{J}^b(n) &= F^b_{m-n} \cdot \vec{J}^a(m) \end{aligned} \tag{6}$$

The individual components change in intensity but not direction and the F^a_{m-n} and F^b_{m-n} values are analogous to F_{m-n} in (5). The subtracted vector in the two-component system is then

$$\begin{aligned} \Delta\vec{J}^t(m-n) &= \Delta\vec{J}^a(m-n) + \Delta\vec{J}^b(m-n) \\ &= (X^a_i(m) - X^a_i(n))\ \vec{\mu}_i + \\ &\quad (X^b_i(m) - X^b_i(n))\ \vec{\mu}_i \end{aligned} \tag{7}$$

The subtracted vector $\Delta\vec{J}^t(m-n)$ can be calculated from the observed changes in the remanence vector, but obviously no unique solution of (7) exists unless one of $\Delta\vec{J}^a(m-n)$ or $\Delta\vec{J}^b(m-n)$ is zero and the other nonzero. This is the familiar problem of non-uniqueness in resolution of individual components of a multicomponent system : if during demagnetization more than one component suffers a change in intensity, a unique and direct resolution of the components cannot be made. Such a

condition can arise in one of several ways. The most commonly encountered situation is when the coercivity or blocking temperature spectra of the various components overlap; in the peak AF intensity or temperature range of the overlap, both $\Delta\vec{J}^a(m\text{-}n)$ and $\Delta\vec{J}^b(m\text{-}n)$ are nonzero for the two-component system (Figure 1.4c). A more trivial case would be when both $\Delta\vec{J}^a(m\text{-}n)$ and $\Delta\vec{J}^b(m\text{-}n)$ were zero, reflecting extreme magnetic "hardness", or resistance to change of both components when subjected to a particular demagnetization method. The two component system can be extended to the general case of many components

$$\vec{J}^t(k) = \vec{J}^a(k) + \vec{J}^b(k) + \ldots + \vec{J}^z(k) \qquad (8)$$

and

$$\Delta\vec{J}^t(m\text{-}n) = \Delta\vec{J}^a(m\text{-}n) + \vec{J}^b(m\text{-}n) + \ldots + \Delta\vec{J}^z(m\text{-}n) \qquad (9)$$

with a corresponding increase in complexity of interpretation. Only the two component system is considered here for simplicity.

Given a known $\Delta\vec{J}^t(m\text{-}n)$, we seek solutions to (9) which yield the directions (not necessarily intensities) of $\vec{J}^a$ and $\vec{J}^b$. An indirect method exists for obtaining both directions, called the "remagnetization circles" technique.

The total magnetization vector $\vec{J}^t(k)$ at any time during demagnetization is a linear combination of two component vectors $\vec{J}^a(k)$ and $\vec{J}^b(k)$. If the H_c or T_b spectra overlap but are not coincident as shown in Figure 1.4d, the observed vectors $\vec{J}t(k)$ and removed vectors $\Delta\vec{J}^t(m\text{-}n)$, since they are also linear combinations of $\vec{J}^a$ and $\vec{J}^b$, will sweep through a plane which contains both $\vec{J}^a$ and $\vec{J}^b$. If a second set of vectors $\vec{J}^t(k)$ is available from demagnetization of a second

sample with coexistent $\vec{J}^a$ and $\vec{J}^b$ magnetizations these vectors will also describe a plane containing $\vec{J}^a$ and $\vec{J}^b$. The planes will be coincident if both components have exactly identical directions in each of the samples. Small variations of the components due to secular variation or to tectonic disturbance will give rise however to noncoincident planes. The intersection(s) of these planes (or their representation on a sphere as great circles) may yield an estimate of one or both components in favourable circumstances. Commonly the planes described by the *in situ* $\vec{J}^t$ and structurally corrected $\vec{J}^t$ vectors rather than the uncorrected $\vec{J}^t$ are tested for intersection to determine whether or not the magnetizations were acquired before or after folding in sedimentatary rocks. Halls (1976) has described a least squares method for estimating the mean directions of two components with overlapping H_c or T_b spectra based upon the remagnetization circles technique. The method has practical application only in situations where tectonic control is good (to ensure significant convergence) and becomes complicated where more than 2 components are present. It has the advantage of being the only method of estimating a mean direction for the two components where H_c and T_b spectra completely overlap and stable endpoints are not attained by the $\vec{J}^t(k)$.

Fortunately, multicomponent systems in many rocks have H_c and T_b spectra which do not completely overlap. By careful and detailed demagnetization experiments, it is often possible to discover a range of AF or thermal treatment in which only one component is removed while the remaining components are unaffected. It is important to note that the complete absence of an overlap is not required for if

$$\Delta\vec{J}^{t}(m\text{-}n) = \Delta\vec{J}^{a}(m\text{-}n) + \Delta\vec{J}^{b}(m\text{-}n)$$

where

$$\Delta\vec{J}^{a}(m\text{-}n) >> \Delta\vec{J}^{b}(m\text{-}n) \qquad (10)$$

then

$$\Delta\vec{J}^{t}(m\text{-}n) \cong \Delta\vec{J}^{a}(m\text{-}n)$$

and thus it is possible to obtain approximately the $\Delta\vec{J}^{a}$ subtracted vector direction. Situations like this are frequently encountered; for example when a very large component with a relatively low H_c or T_b coexists with a much smaller component with an overlapping but higher H_c or T_b spectrum, as illustrated in Figure 1.4e. While both components undoubtedly change in intensity during the initial demagnetization steps, the change in the smaller component is insignificant compared to the change in the larger, and (10) is indeed reasonable. The approximation is especially valid when the two components are of pre- and post-folding age, as any systematic bias in the estimated subtracted vector direction $\Delta\vec{J}^{a}(m\text{-}n)$ is reduced.

Probably the best indicator of uniqueness in multicomponent analysis is consistency of directions of the subtracted vectors throughout a particular treatment range. During demagnetization, if both components of a two-component system with differing H_c or T_b spectra are simultaneously reduced, the subtracted vectors will define a great-circle path identical to that generated by the observed vectors. However if only one component is being removed, subtracted vectors will be constant in direction (Figure 1.4f). Care must be exercised, as it is possible to construct a special system in which the subtracted vectors remain constant in direction but both components are being reduced (Figure 1.4f).

The situation arises of course because the subtracted vectors are linear combinations of the component vectors, but requires a very special arrangement of H_c or T_b spectra such that

$$\Delta\vec{J}^a(m-n) = \Delta\vec{J}^b(m-n) \qquad (11)$$

for each and every step. However, considering the wide variation in H_c and T_b spectra generally encountered in a large sample collection, the probabilities of consistency obtaining such a false "unique" solution are small, especially when folded rocks are involved.

The approach to analysis of demagnetization data described herein was conducted with these conditions in mind. Individual subtracted vector directions from a specimen which were consistent and well grouped throughout a particular demagnetization range were averaged to form specimen mean directions; demagnetization intervals were chosen to be small enough to facilitate delineation of components. Specimen means were then averaged to form sample mean directions in the case where more than one specimen was subjected to progressive demagnetization. Sample mean subtracted directions were subsequently averaged to create site mean subtracted directions, and the hierarchical system was completed by calculating an overall mean removed direction from the site means. By carefully combining results from sites with differing lithologies and differing structural orientations, it was hoped that systematic effects produced by the overlap of H_c of T_b spectra could be eliminated. The internal consistency of many of these results combined with the good agreement of many of the mean observed and subtracted components testifies to the applicability of the method.

§1.2.5 Presentation of demagnetization data

The discussion of multicomponent analysis of the previous section demonstrated the need for careful and detailed analysis of demangetization data. A family of data handling programmes was developed during the course of this investigation, some of which tested for systematics in subtracted and observed components and others for directional stability of the remanence vector.

The demagnetization plots presented are produced by parts of two such data analysis routines. In Chapters 2,3 and 4 conventional stereographic plots with normalized intensity curves for typical specimens are shown together with orthogonal vector projections. Each method of presentation has particular advantages. The conventional plots allow a rapid assessment of directional behaviour and stability, but are not nearly as diagnostic as the orthogonal plots in evaluating the nature of component vectors which may be present as illustrated in Figure 1.5. Used in conjunction the two methods of presentation are probably the most useful tools in multicomponent analysis. An explanation of the intricacies of methods of presentation is given in Appendix B.

§1.3 Representation of Precambrian Pole paths

When considering Phanerozoic palaeomagnetic data, it is common to be able to assign results to a particular subdivision of a geological period either from stratigraphic evidence and fossil control or from radiometric dating. The accumulation of results from a single continental block for each of these periods enables overall means to be calculated

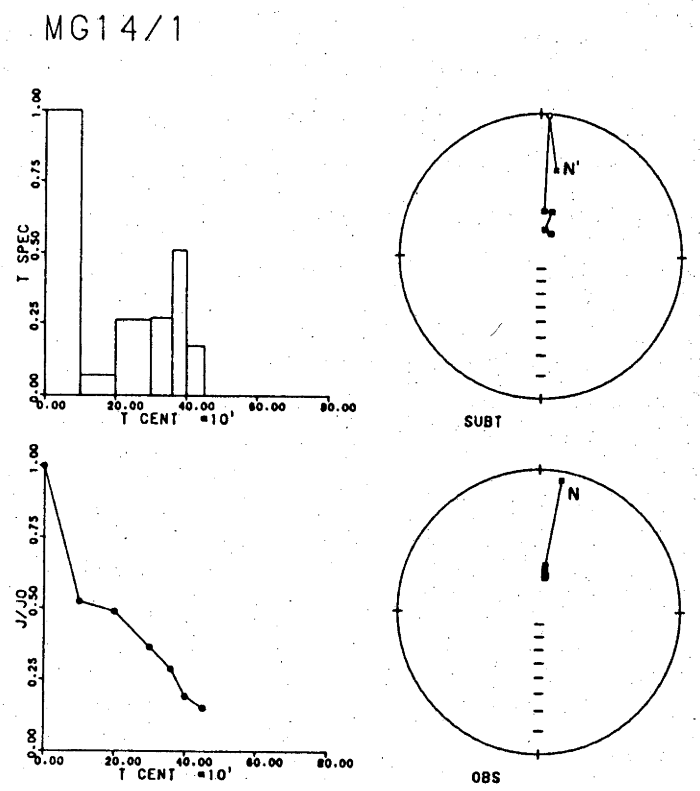

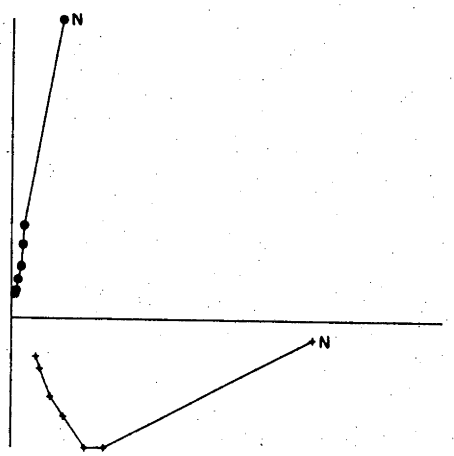

Figure 1.5 : A comparison of a conventional stereographic demagnetization plot with an orthogonal vector plot. The conventional plot clearly shows stable directional behaviour in the higher demagnetization steps, however the orthogonal plot illustrates better the nature of the multicomponent system.

by period or subdivision. Whereas there may be some internal scatter of the order 10°-15° between results from the same period for a particular block, the period means themselves can be determined with high precision and relatively small errors. The resulting pole paths can in many cases be defined fairly precisely (McElhinny, 1973). This is not the case in Precambrian studies, because one is forced to rely exclusively on radiometric ages; in the 10^9 year region, age uncertainties are often greater than the length of the Phanerozoic geological periods. Thus, it is not possible to average results period by period and it is necessary to plot all the data and determine the general trend as representing the best estimate of the apparent polar wander path. The inability to determine sequentially averaged results amplifies the inherent inaccuracies present in individual palaeomagnetic results. These inaccuracies arise in a number of ways: they may be associated with sampling errors due to minor local tectonics or they may be due to laboratory problems associated with isolating and measuring a primary remanence. Also, periods of rapid apparent polar motion combined with frequent reversals of the earth's magnetic field can lead to difficulty in the interpretation of already sparse data. The result is that Precambrian apparent polar wander paths are not represented by period means as in the Phanerozoic, but must be represented by swathes of width 10°-15° arising from the inherent inaccuracies in individual results. The concept of a swathe was first suggested by Beck (1970) and introduced by Piper *et al.* (1973).

There are other complications assoicated with Precambrian palaeomagnetism which are more serious than in

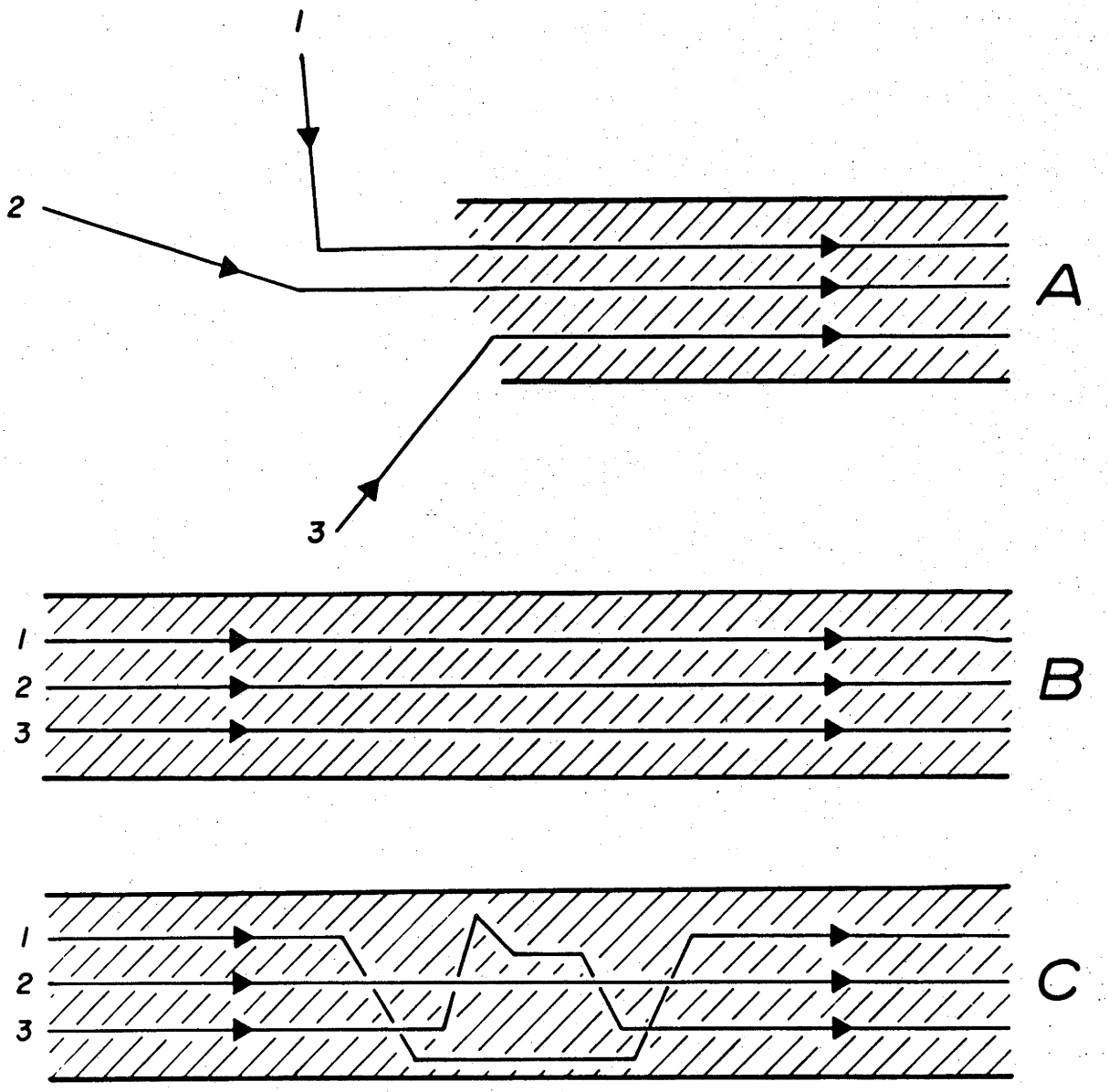

Figure 1.6 : Expected APWPs for differing tectonic mechanisms (after Piper *et al.*, 1973). A: plate tectonic model, B: fixed plate model, C: combination of A and B representing opening and closing of small intercratonic oceans.

Phanerozoic studies. The older the rock formation, the more likely it is to have been subjected to thermal or chemical overprinting of the original (primary) magnetization, with possible concomitant tectonic re-orientation. Laboratory studies using a variety of techniques such as alternating field demagnetization, high- and low-temperature thermal demagnetization, and chemical demagnetization coupled with detailed vector analysis of the various magnetic components can reveal the presence of magnetizations acquired at different times under different conditions (Roy and Park, 1974; Buchan and Dunlop, 1976). However, only field tests (baked contact or fold tests) can establish the relative timing of such multicomponent magnetizations. Alternatively, it can be assumed that the magnetizations with the higher blocking temperatures are the oldest in any slowly cooled rock (Irving *et al.*, 1974a); this is strictly true only if all the magnetic components are of thermal origin (TRM). This situation arises commonly in Precambrian terrains and is due either to slow initial cooling or to subsequent heating during burial and regional metamorphism and slow cooling during post-orogenic uplift. The magnetizations may be related to radiometric ages determined by different methods, whole-rock Rb-Sr ages to the higher blocking temperatures and mineral K-Ar ages to the lower blocking temperature magnetizations (Irving *et al.*, 1974) However, without a clear understanding of the evidence related to the timing of the various magnetizations which may be present in a particular rock unit, an interpretation could be completely incorrect.

On the assumption that the time-averaged field is that of an axial geocentric dipole, palaeomagnetic poles of

the same general age from regions that have not suffered relative displacement should agree with one another. Extended to a time-sequence of poles represented by an apparent polar wander path various situations arise according to the applicable tectonic model for intercratonic orogenesis as illustrated in Figure 1.6. In the diagram we imagine three cratonic blocks each defined by its separate apparent polar wander path, 1, 2 or 3. If the plate-tectonic model of convergence of widely separated blocks is valid to explain the orogenic belts then Figure 1.6a should describe the apparent polar wander paths of each of the blocks. The three paths will diverge prior to the time of collision and after convergence of all three blocks, a unified common path results represented by the swathe. Generally speaking, the separate paths would be represented by a widening of the swathe beyond its normal limits coupled with an inability to contain all the data within a single swathe. If on the other hand the orogenic belts were formed by internal deformation without relative movement, the data from all three blocks can be constrained to a single common swathe, as illustrated in Figure 1.6b. The width of the swathe is large enough to allow limited relative movement and/or the opening and closing of relatively small (500-1000 km) oceans, as illustrated in Figure 1.6c. The "small-movement" model illustrated in Figure 1.6c, therefore cannot be distinguished from the static model, Figure 1.6b.

Chapter 2

Late Precambrian Palaeomagnetism of the Adelaide 'Geosyncline', South Australia

§2.1 Introduction

The Adelaide 'Geosyncline' comprises a major belt of Late Precambrian and Cambrian sediments with minor volcanics and extends across South Australia from the Mount Lofty Ranges to the Musgrave Block (Figure 2.1). The term *Adelaidean*, originally introduced by David (1922) and formally defined by Glaessner (1948) and Raggatt (1950), refers to the time interval recorded by the Precambrian part of the 'Geosyncline'. The stratigraphic sections, especially those in the North Flinders Ranges, are so well exposed and completely represented that outcrops in the area have achieved worldwide recognition as standard records of Adelaidean time. Some of the best known examples of Late Precambrian glacial sedimentation are found in the Adelaide 'Geosyncline'. For these reasons, a detailed palaeomagnetic study of these rocks forms the central part of Late Precambrian palaeomagnetism in Australia, and serves as a basis for testing both intercontinental and intracontinental correlations of Adelaidean strata.

The Adelaide 'geosyncline' sediments were deposited in a downwarping or trough of appreciable size; the Precambrian part of the stratigraphic sequence reaches a thickness of 15,000 m in places. There is some question as to whether the geosynclinal concept originally introduced by Sprigg (1952) has relevance. Rutland (1973) suggested that the Adelaide 'Geosyncline' was in fact a fault-bounded intracratonic basin

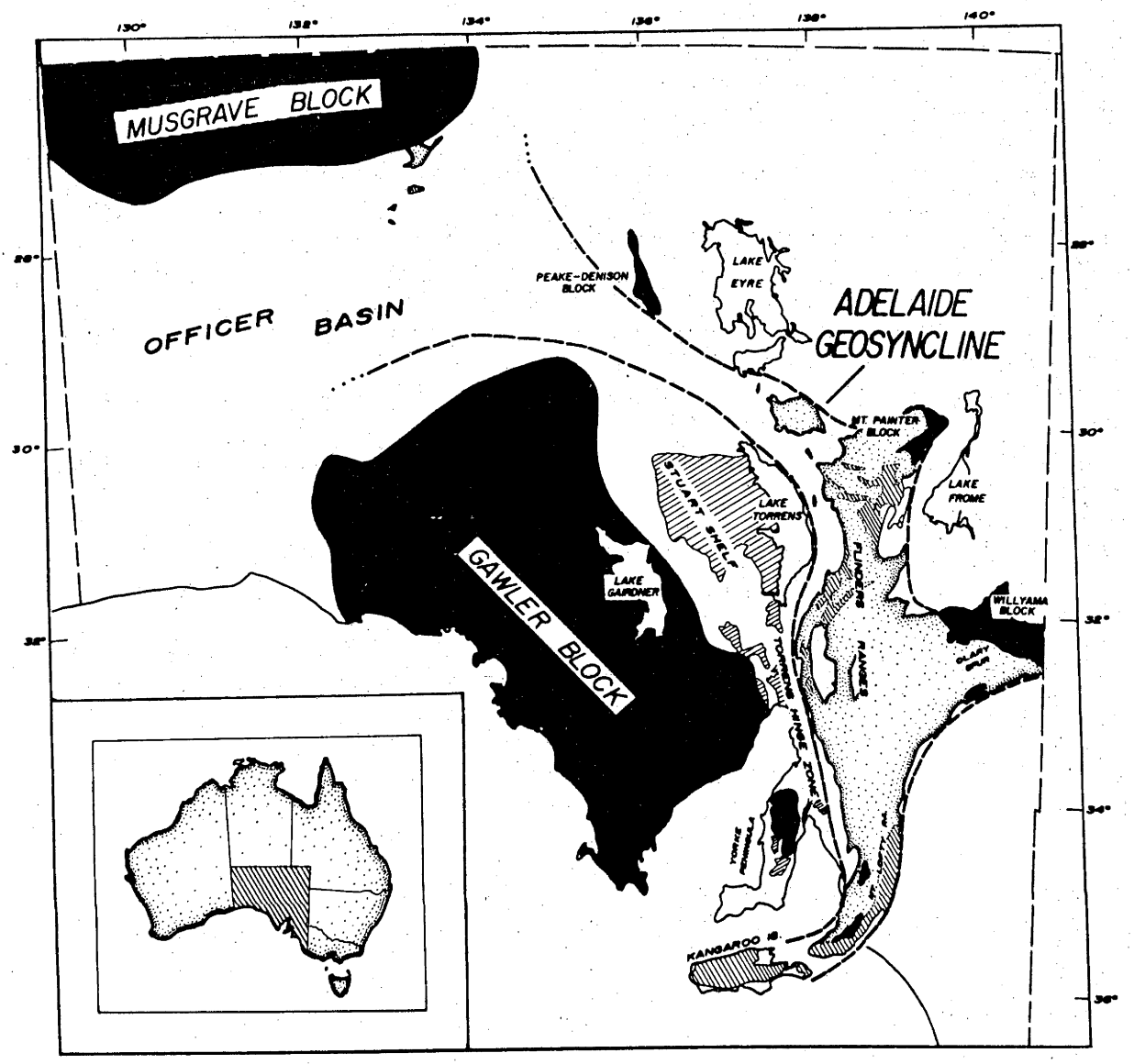

Figure 2.1 : Simplified geological sketch of South Australia showning Adelaide 'Geosyncline' and geographical names used in this thesis. Older Proterozoic structures are shown in black; Adelaidean strata are stippled; Cambrian strata are cross-hatched; younger rocks uncoloured.

or *aulacogene*, but has more recently stated that the aulacogene concept is not applicable (Rutland and Murrell, 1976) and adopted the term *Adelaide Fold Belt*. Controversy concerning the mechanics of basin formation still exists. For this reason, the common term Adelaide 'Geosyncline' is used here, the quotes signifying uncertainty in its usage.

§2.2 Stratigraphy

Mawson and Sprigg (1950) and Sprigg (1952) originally defined the chronostratigraphic terminology for Adelaidean rocks. In order of increasing age they are the Marinoan, Sturtian, Torrensian and Willouran Series. Thomson (1969) grouped the Adelaide 'geosyncline' rocks into four major lithostratigraphic units, the Wilpena Group, Umberatana Group, Burra Group and Callana Beds, in order of increasing age. The relationship between lithostratigraphic and chronostratigraphic names is shown in Figure 2.2. The following outlines of stratigraphy and structure of the Adelaide 'Geosyncline' draw from the comprehensive reviews of Thomson (1969) and Coats and Blissett (1971).

The Callana Beds, the oldest lithostratigraphic unit in Adelaide System, lie unconformably upon crystalline basement rocks of Carpentarian (Middle Proterozoic) age. Coats and Blissett (1971) have divided the sequence into two parts separated by an unconformity, the Upper and Lower Callana Beds. The stratotype for the Lower Callana Beds near Mount Painter consists mainly of quartzite and dolomite with basaltic and trachytic lavas. Attempts to obtain a satisfactory isotopic age for these lavas and thereby date the base of the Adelaide System are discussed in §2.4 and §2.5. The Upper Callana

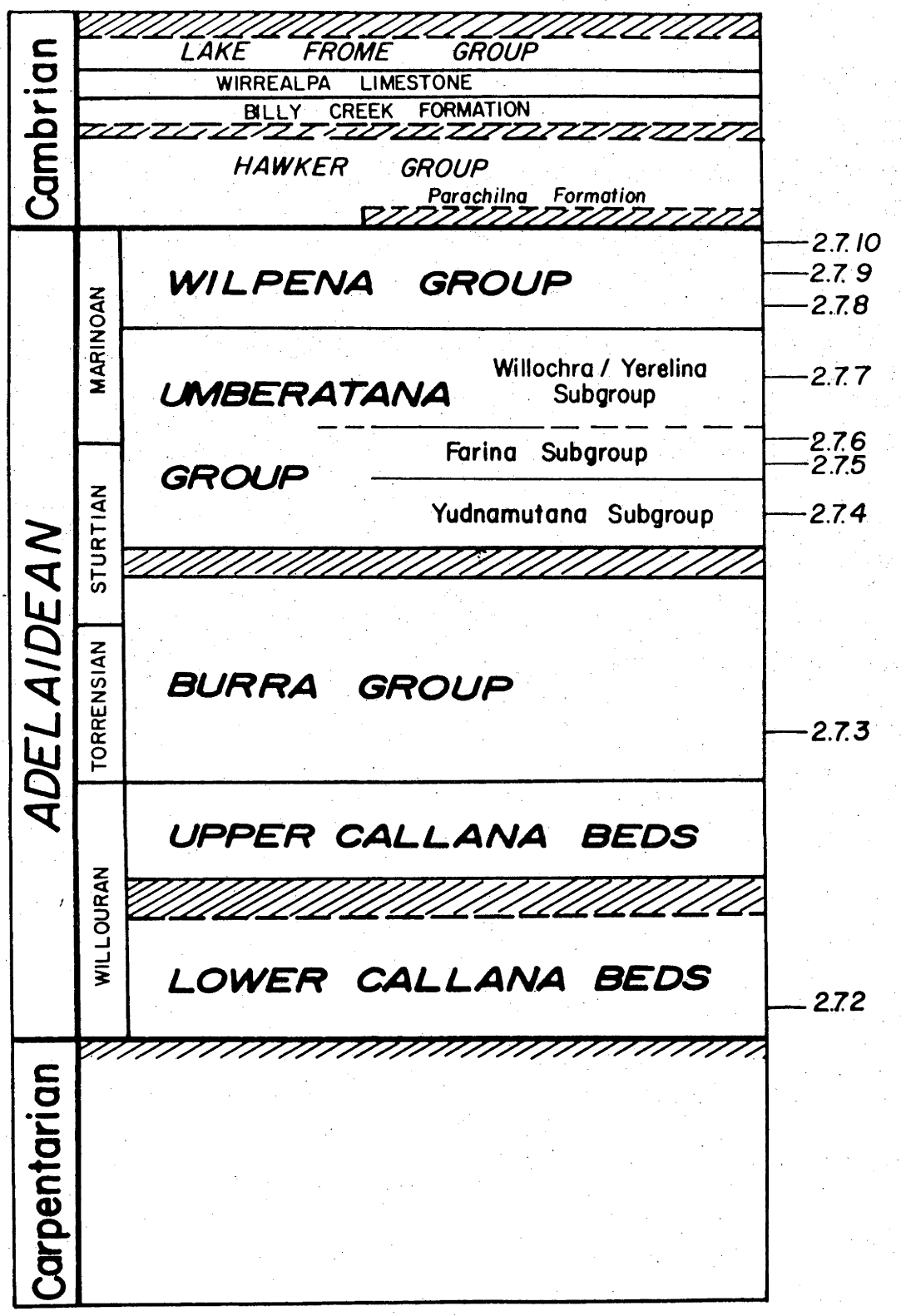

Figure 2.2 : Stratigraphic relationships in the Adelaide System, after Thomson (1969). Figures at right refer to palaeomagnetic studies discussed in this chapter.

Beds lie with apparent unconformity and consist of alternating sandstones and siltstones at the reference locality in the Willouran Ranges.

Burra Group sediments lie with local unconformity upon the Upper Callana Beds. This unit is characterized by a basal sandstone-conglomerate member overlain by an argillite-carbonate succession containing columnar stromatolites of the groups *Tungussia* and *Baicalia* (Preiss 1971 in Walter 1972). The Burra Group is in turn overlain, unconformably in places, by sediments of the Umberatana Group. Three subdivisions of the Umberatana Group have been made. The lower Yudnamutana Sub-Group commences with a glacial sequence including massive tillites with a great variety of erratic boulders and cobbles. Arkose and quartzite horizons are common, while in some places massive tillites interchange with siltstone shale and sandstone. The glacial sequence passes upwards and laterally into a thick glacial marine sequence of argillites with occasional tillites. In some areas a sedimentary iron formation or "ironstone" of near economic quality is found immediately above the tillite horizons.

The overlying interglacial Farina Sub-Group comprises a thick (up to 3000 m) pile of laminated siltstones and shales. No tillites have been found in the sequence; however some workers have suggested that the regular laminations resemble varves. The upper part of the section includes calcareous sediments with stromatolites in places. Walter (1972) lists six stromatolite groups found in the Umberatana Group : *Acaciella, Boxonia, Inerzia, Jurusania, Kulparia* and *Linella*. In the eastern part of the 'Geosyncline', the Farina Sub-Group is overlain by the Yerelina Sub-Group, a sequence of glacial marine

sediments including tillite, tillitic sandstone, sandstone and siltstone. In the west, the uppermost part of the Farina Sub-Group and the Yerelina Sub-Group are represented by the Willochra Sub-Group, a shallower water nonglacial facies of red sandstones and siltstones.

The Umberatana Group is in turn overlain by the Wilpena Group, a sequence of shales, siltstones, limestones and quartzites with pronounced red-bed affinities. The upper member of the Wilpena Group contains an abundance of Late Precambrian trace and body fossils, including the well known *Ediacara* fauna (Glaessner and Daily, 1959; Glaessner, 1971). The Wilpena Group passes conformably into the overlying Cambrian succession in most places.

§2.3 Structure and tectonics

The present rugged physiography of most of the Adelaide 'Geosyncline' is to a large degree due to Tertiary faulting and uplift, but the dominant tectonic trends are largely a result of several dramatic events which occurred in early Paleozoic times. Three events are significant in an understanding of the tectonics of the Adelaide 'Geosyncline', a late Precambrian - early Cambrian folding episode, a later period of trough subsidence and rapid sedimentation, culminating in a major Cambro-Ordovician orogenic episode.

A period of epeirogenic uplift and gentle folding occurred in late Marinoan or early Cambrian times, affecting mainly the Mount Lofty Ranges and Yorke Peninsula. This event, named the Duttonian folding (Thomson, 1969), resulted in erosion of Wilpena and Umberatana Group sediments as recorded by an unconformity which separates lower Adelaidean sediments

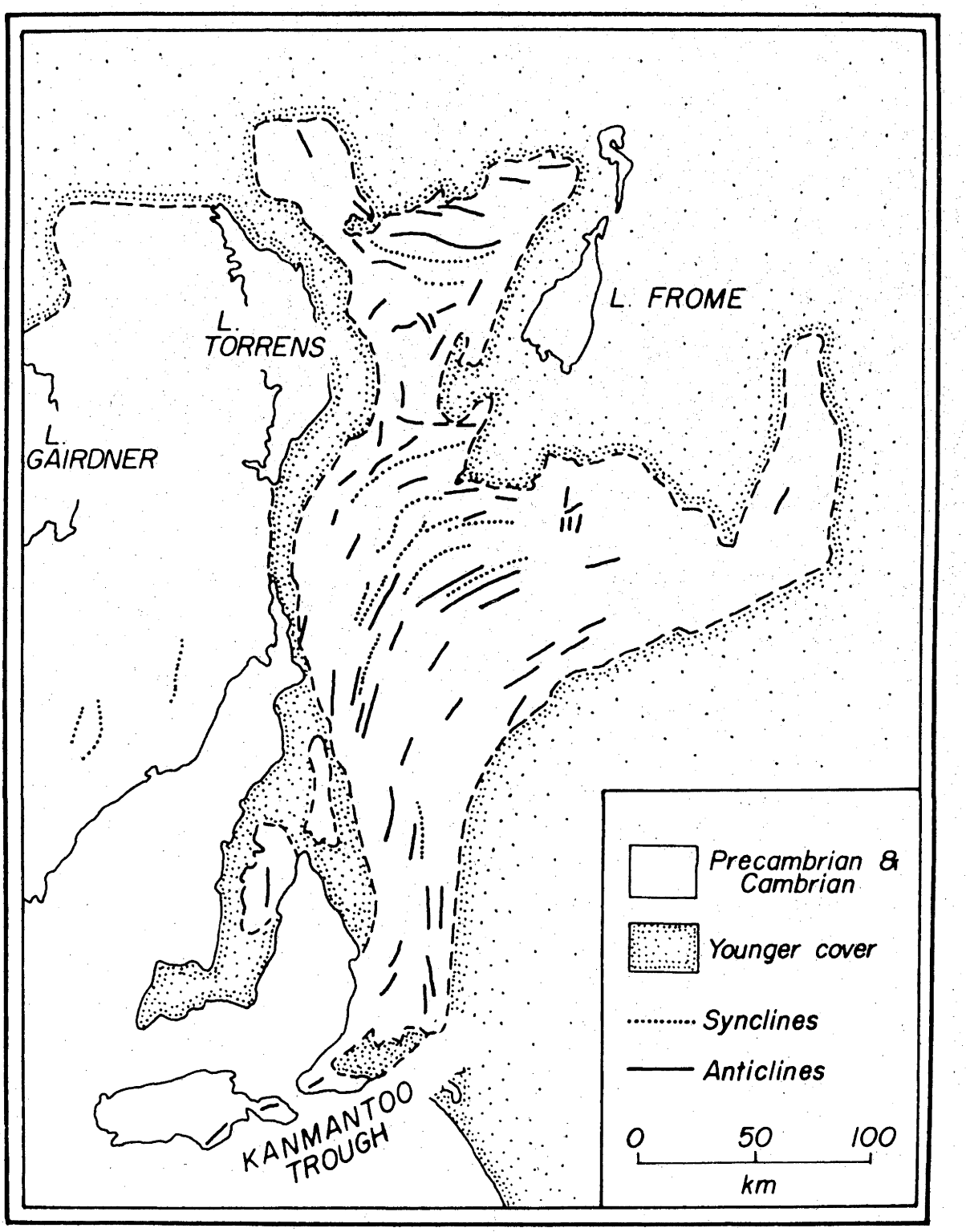

Figure 2.3 : Simplified structural map of the Adelaide 'Geosyncline' showing the sigmoidal trend of folds in the central and southern regions.

from Cambrian rocks in the region. Following the Duttonian folding, activity of major submarine faults in the eastern Mount Lofty Ranges and Kangaroo Island areas caused a rapid subsidence of the sea floor and formed the Kanmantoo Trough (Figure 2.3). Complementary uplift to the north and west provided source areas for up to 18,000 m of greywacke and related sediment which rapidly filled the trough.

The present structures of the Adelaide 'geosyncline' and Kanmantoo Trough result from a major orogenic episode, the Delamerian Orogeny, commencing in late Cambrian times. Several orogenic phases are evident in this event, which involved metamorphism, shearing and deformation of the Adelaidean and Cambrian cover rocks, reactivation of basement complexes such as the Willyama and Mount Painter blocks, and culminated in the emplacement of granitic plutons. These intrusions form part of a great metamorphic arc with a characteristic sigmoidal shape extending from Kangaroo Island to the Willyama block (Figure 2.3). The close of the orogeny has been established as early Ordovician by isotopic ages from these granites and from overprinted (metamorphic) ages from Adelaidean and older rocks (Compston *et al.*, 1966; White *et al.*, 1967).

Great variations in structural style in the Adelaide 'Geosyncline' are apparent. In the east and south, elevated temperatures and regional shearing resulted in flow-folding and medium to high grade metamorphism. Adelaidean sediments in the North Flinders Ranges were less stressed and deformed at low temperatures into broad, open folds with some reactivation of preexisting basement faults. Diapiric breccias containing rafts of underlying sediments intrude the gentle folds. Owing to the near absence of metamorphic effects in the north,

palaeomagnetic sampling was confined to this region.

§2.4 Age of the Adelaide System

The term *Adelaidean* refers to the time interval recorded by deposition of the Precambrian part of the Adelaide 'Geosyncline' sediments. By definition, the younger limit of Adelaidean time is the Precambrian-Cambrian boundary, currently represented in the Adelaide 'Geosyncline' by the surface separating the uppermost member of the Wilpena Group from the lower-most member of the overlying Hawker Group. While there has been controversy about the exact placement of the Precambrian-Cambrian boundary within the upper part of the Wilpena Group, the Hawker Group is undoubtedly Cambrian as it contains abundant *archaeocyathid* limestones, trilobites and brachiopods. The younger limit to Adelaidean time is thus well established.

An older limit to Adelaidean time is much more difficult to assess. By definition, the Lower Callana Beds are the oldest unit in the Adelaide System. A reliable age for the Wooltana Volcanics, one of the members of the Lower Callana Beds and one of the few igneous units in the whole of the Adelaide 'Geosyncline', would provide a good estimate for the commencement of Adelaidean sedimentation. Efforts to data the volcanics have met with only minimal success due to their altered nature. At Roopena and elsewhere on Eyre Peninsula (Figure 2.1), petrologically similar lavas are found and have been correlated with the Wooltana Volcanics. The Roopena lavas have been well dated at 1345±30 my by the Rb/Sr isochron method (Compston *et al.*, 1966). Adopting the tentative Wooltana-Roopena correlation, many workers have assigned an age of 1350-1400 my to be the beginning of Adelaidean time. From

detailed Rb/Sr studies on the Wooltana Volcanics, Compston *et al.*, (1966) suggested that the Wooltana-Roopena correlation might not be valid and quote a preferred age of "... approximately 850±50 my" as a reliable minimum age of extrusion. Cooper and Compston (1971) and Cooper (1975) lend further support to a younger age for Adelaidean sedimentation with Rb/Sr measurements of the Wooltana lavas. Cooper (1975) concludes that the Callana beds in the Mount Painter area are "... less than 900 (possibly 800) my old ...".

At present, geochronologic evidence would seem to favour an age of approximately 850 my as the older limit of Adelaidean time. However, recent isotopic studies have suggested that the use of the Rb/Sr isochron technique with basaltic rocks may lead to serious error in age determination. Brooks *et al.*, (1976) and Duncan and Compston (1977) have shown that Rb/Sr isochron ages of volcanic rocks may not be directly relevant to ages of extrusion and emplacement, but rather reflect Sr isotopic conditions in the source region at the time of partial melting. These ages would then reflect the age at which the mantle source region was last homogenized, if the isotopic composition of the basaltic liquid was the same as that of the source region. With this in mind, the data from the Haughton Inlier metamorphic rocks (867±32 my) could be the best indication of an older limit to Adelaidean time. All that can be said with certainty however is that the Burra Group sediments are younger than the metamorphism of the Haughton Inlier rocks.

§2.5 U-Pb Zircon studies of the Wooltana Volcanics

Due to the problems associated with Rb/Sr and K/Ar age determinations of the Wooltana Volcanics, age determination by

TABLE 2.1

Wooltana Volcanics : zircon U-Pb age determinations

	$^{208}Pb/^{206}Pb$	$^{207}Pb/^{206}Pb$	$^{206}Pb/^{204}Pb$
Blank Pb isotopic composition:	2.1452	0.9046	17.028

	$^{208}Pb/^{204}Pb$	$^{207}Pb/^{204}Pb$	$^{206}Pb/^{204}Pb$
Common Pb isotopic composition:	37.6	15.6	17.7

Final isotopic data:

Fraction	U ppm	Pb ppm	206/204	atom % radiogenic Pb 206	207	208	atomic ratios 206/238	207/235	207/206
Z66 euhedral	15.4	238.8	583.4	83.6	5.1	11.2	0.061024	0.508013	0.060377
Z102 rounded	21.1	108.5	803.2	81.1	8.8	10.1	0.180742	2.70495	0.108542

the U-Pb zircon method has been attempted. The results to date are summarized here. Pilot mineral separation studies showed that the concentration of zircon in the volcanics was extremely low as expected. Following the pilot study, approximately 60 kg of rock was crushed with very careful attention paid to possible contamination by previously processed material. Using standard mineral separation techniques (Wilfley Table, heavy liquid centrifuge, magnetic separator, static heavy liquids) a total zircon yield of approximately 0.2 mg was realized. Two types of zircon in roughly equal proportion were present in the final concentrate : transparent, euhedral, often broken grains with a characteristic pink cast, and rounded translucent grains with a yellow-orange stain. The two fractions were separated and purified by hand picking and analysed separately.

Dissolution of the two fractions was done by a method modified after Krogh (1973), followed by separation of U and Pb in anion exchange columns. Isotopic analyses were carried out on a 23 cm 60° sector solid source mass spectrometer. Samples were loaded on the spectrometer source filament using the silica gel technique.

Correction for blank Pb concentration was estimated from current laboratory blank levels and was assumed to be 0.4 pmol total. Isotopic ratios of blank Pb as measured from dust trapped in laboratory filters were used for correction; these ratios are listed in Table 2.1. After correction for blank contamination, all remaining ^{204}Pb was assumed to be common lead. Isotopic composition of the common Pb component was estimated from Cumming and Richards (1975). The final results are relatively insensitive to common Pb compositional changes

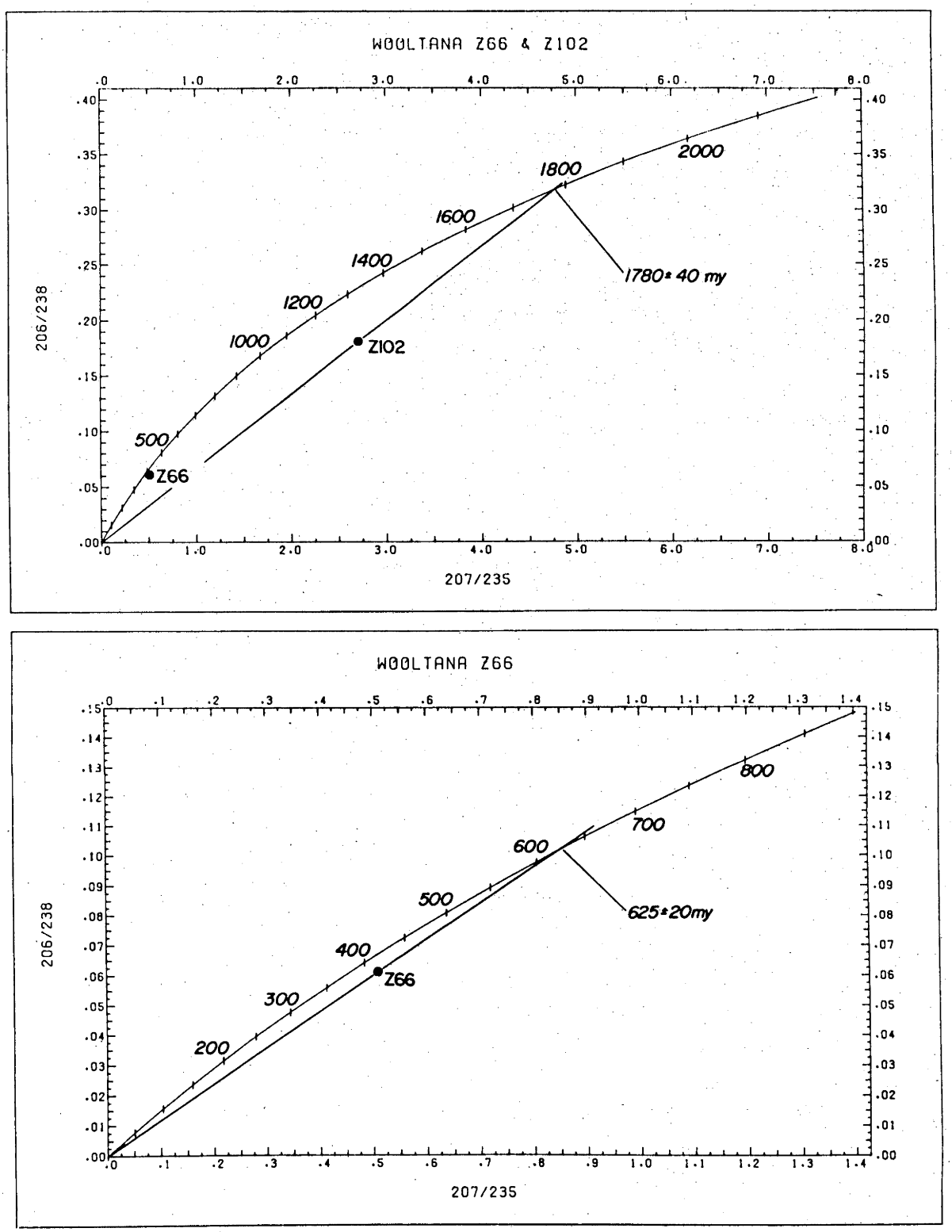

Figure 2.4 : U-Pb concordia plots, Wooltana Volcanics. Results from zircon fractions Z66 and Z102 are shown above, while Z66 alone is shown below on an expanded scale. Axis labels refer to isotopic ratios.

in the 1000-500 my range. Chosen isotopic ratios (corresponding to ∿ 600 my abundances) are listed in Table 2.1 with the final results.

Both results (Figure 2.4) are clearly discordant. There being only 2 analyses, any conclusions are necessarily tenuous. Assuming a continuous diffusion model (inspection of the concordia plots of Figure 2.4 shows that an episodic loss at ∿ 500 my is not realistic) the intercept age for the rounded fraction is approximately 1780 my, while the transparent euhedral grains have an intercept age of about 625 my. Conservative estimates of uncertainty in the final isotopic ratios for the two fractions lead to uncertainties in intercept ages of ±20 and ±40 my respectively.

An inherited history for the rounded zircons seems the best interpretation of the older age. These grains could be part of a refractory residue left during remobilization and melting of crustal materials at a low level which became incorporated as part of a source region for the volcanics. Alternatively they might have been picked up from underlying basement complexes during upwelling of basalt magma. Basement ages in the Mt. Painter area are sparse; two age determinations for the Pepegoona Porphyry (Compston *et al.*, 1966) yielded a Rb/Sr total-rock age of 1650 my while microcline feldspars were dated at 1900 my. More recently however, Cooper (1975) reports two Rb/Sr ages from a suite of indistinguishable samples of the Pepegoona Porphyry, one 1309±129 my and the other 1035±62 my. Cooper regards the older age as the age of emplacement, while the younger may be an updating due to local igneous activity.

The intercept age from the euhedral grains is regarded as having more relevance to actual emplacement of the lavas,

although an age of 615-645 my is difficult to accept for the beginning of Adelaidean time. However, there is no evidence for any major thermo-tectonic event in the region at about this time, thus any hypothesis other than primary crystallization and cooling is difficult to invoke to explain such a young age. More work (in progress) needs to be done; it would be incorrect to place more emphasis on this single result than is justified. For the present, perhaps the best estimate of the start of Adelaidean time is somewhere between 870 and 625 my. It is interesting to note that the palaeomagnetic evidence reported in the following sections of this chapter and in following chapters does suggest a much younger age for the Adelaide System than is currently accepted.

§2.6 Previous palaeomagnetic work

Briden (1967) reported palaeomagnetic studies of Adelaidean rocks from the southern part of the Adelaide 'Geosyncline'. In what was largely a disappointing study, Briden found that many of the samples had remanence directions which were either too weak to measure accurately using instruments then available, or too widely scattered to be meaningful. Other samples exhibited stable directions consistent with a Mesozoic or Tertiary age; negative fold tests reinforced this conclusion. Many of the results were based upon uncleaned remanence directions from surface samples and borecore material.

Embleton and Giddings (1974) studied latest Adelaidean and Cambrian rocks from the North Flinders Ranges. They obtained significant results after thermal demagnetization of three units, the Pound Quartzite (Wilpena Group), Aroona Dam sediments (Hawker Group) and Lake Frome Group. Karner (1975) reported a

study of red beds of the Brachina Formation (Wilpena Group) sampled at Hallett Cove, south of Adelaide. His results, based upon thermally cleaned remanence directions, showed that the magnetization in these rocks was most likely acquired before late Cambrian (Delamerian) folding.

A discussion of these results in the context of the present work is deferred until §2.8.

§2.7 Palaeomagnetic results

§2.7.1 Sampling and locality details

Site localities for the units sampled are shown in Figure 2.5. Sampling details are listed in Appendix A. Samples were collected either as oriented blocks or field-drilled cores using both magnetic and solar compass for orientation. In most cases, sampling localities were selected in order to facilitate application of a fold test (Graham, 1949) in determining the age of magnetization with respect to Cambrian folding. Three or four cylindrical specimens 25 mm diameter and 22 mm in height were obtained from nearly all the samples. Orientation information in the form of azimuth and dip of cores and block samples is estimated to be correct to within $\pm 1°$.

§2.7.2 Wooltana Volcanics (Lower Callana Beds)

Following Crawford (1963), the Wooltana Volcanics outcrop in an area about 8 km by 25 km in the Mount Painter district and comprise up to 2500 m of lavas and pyroclastics, mainly sodic trachytes with minor andesite and rhyolite (Figure 2.5). Minor occurrences of interbedded sediments suggest that at least some of the flows were submarine, although

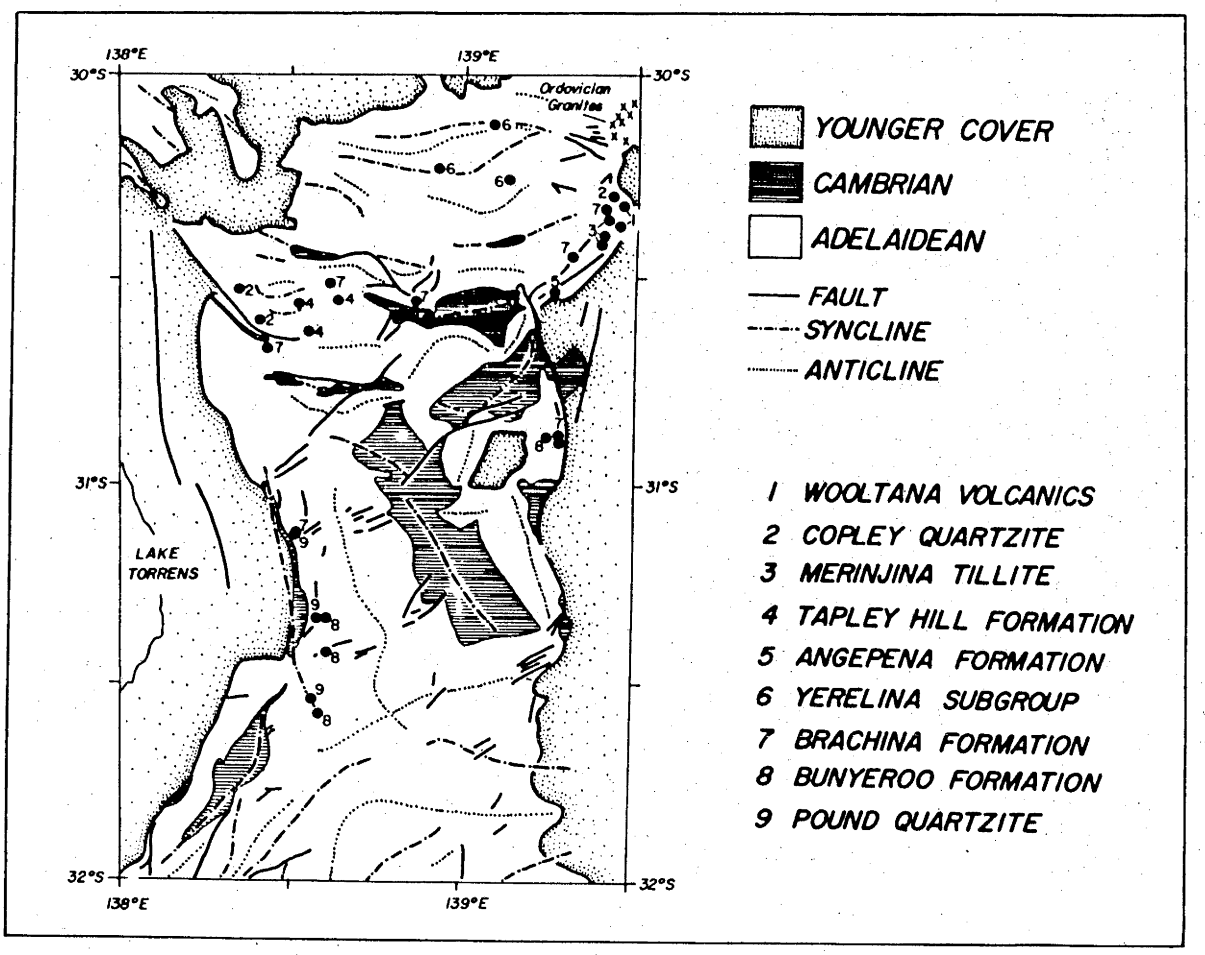

Figure 2.5 : Sampling localities in the Northern Flinders Ranges, with detailed structural trends. Crosses denote occurrences of Ordovician granites.

no pillow lavas have been found. The volcanics overlie rocks of probable lower Proterozoic age and are disconformably overlain by Torrensian rocks of the Burra Group.

The structural geology of the Wooltana district is complex and not yet well understood. No detailed structural studies have been made to date. The dominant structure in the region is the Paralana fault system, a network of related thrust, wrench and splinter faults trending approximately northeast - southwest (Figure 2.5). Folding of the volcanics possibly associated with compression on the east side of the Paralana system further complicates understanding of the structure.

Sampling was confined to two areas which appeared to have reasonably simple structure, at Woodnamoka Well and at Arkaroola Creek near Groan Creek (Figure 2.5). A total of 72 samples were taken at 24 sites through several rock types including vesicular, amygdaloidal and epidotized lavas as well as the characteristic massive purple-grey trachyte. In places an accurate determination of flow orientation was hampered by paucity of vesicular flow tops.

Palaeomagnetic results are summarized in Table 2.2. Examples of alternating field (AF) and thermal, demagnetization studies are shown in Figures 2.6 and 2.7 respectively. Stable directional behaviour was suggested by pilot stepwise AF demagnetization to 200 mT. The high coercive forces exhibited by some of the specimens indicated that at least part of the total NRM was carried by a mineral in the hematite-ilmenite solid solution series, confirming the presence of 'hematite' noted by Crawford (1963) and by Fander (1963) in petrographic description. Subsequent examination of polished sections in

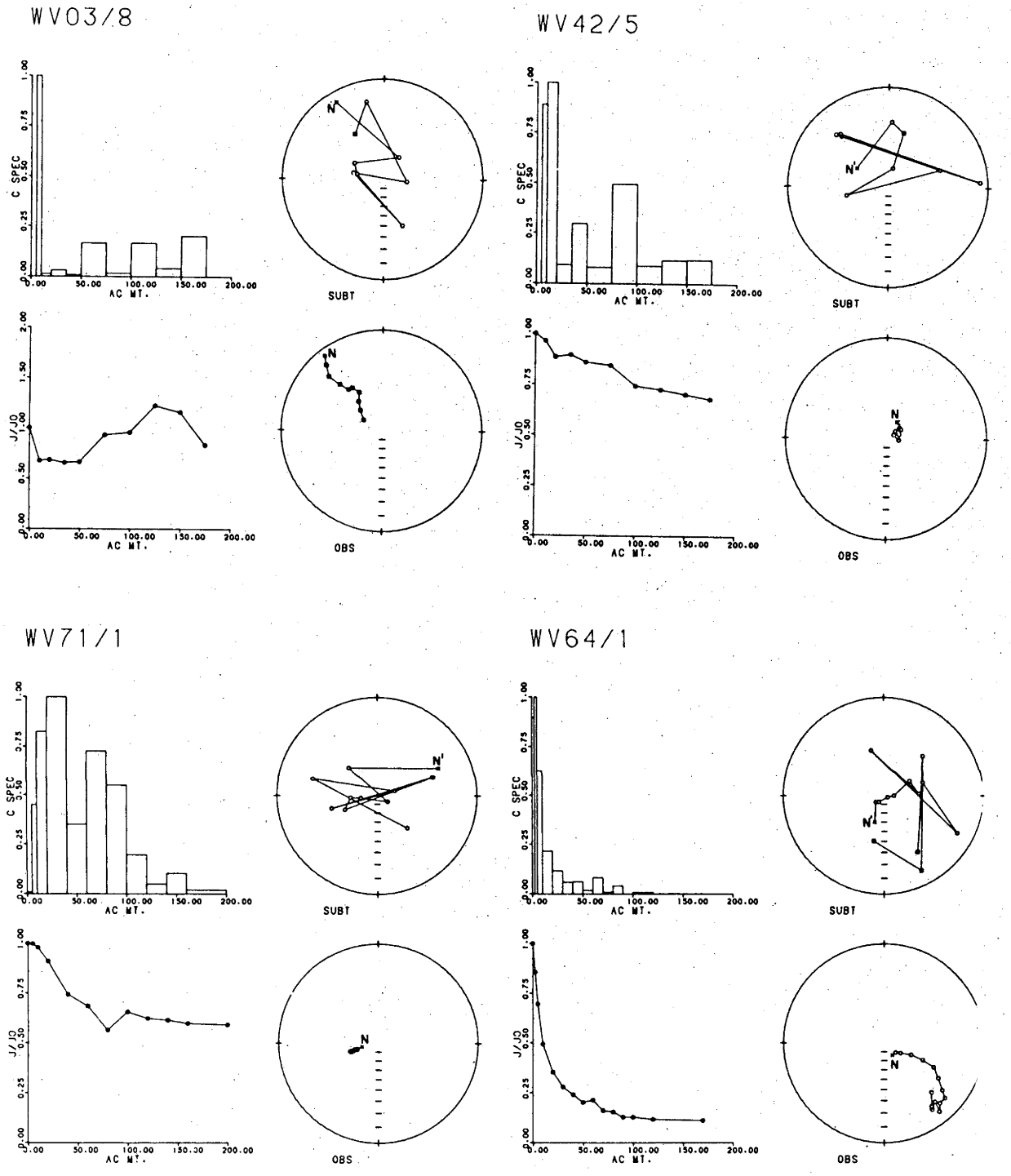

Figure 2.6(A) : AF demagnetization, Wooltana Volcanics.

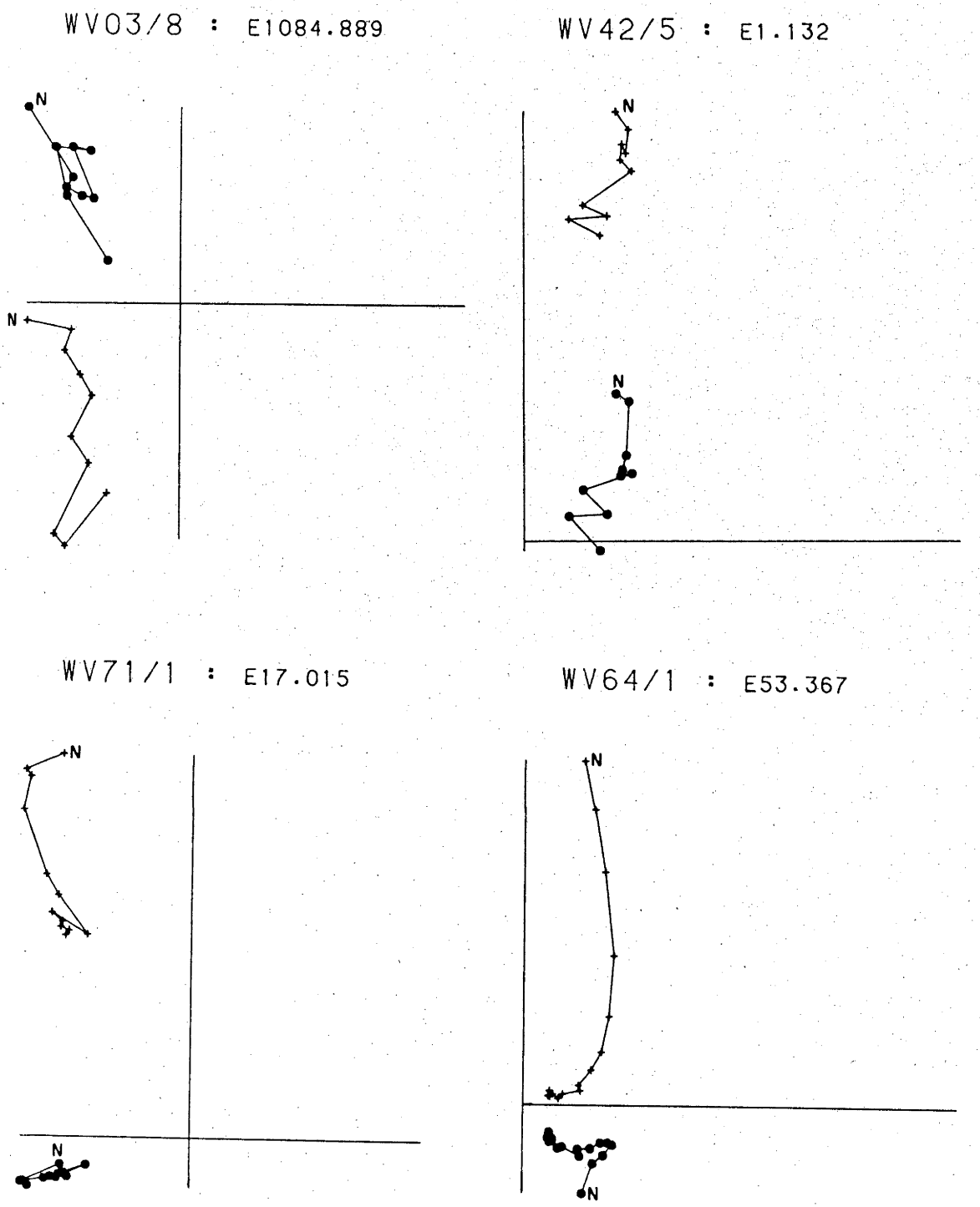

Figure 2.6(B) : AF demagnetization Wooltana Volcanics (continued).

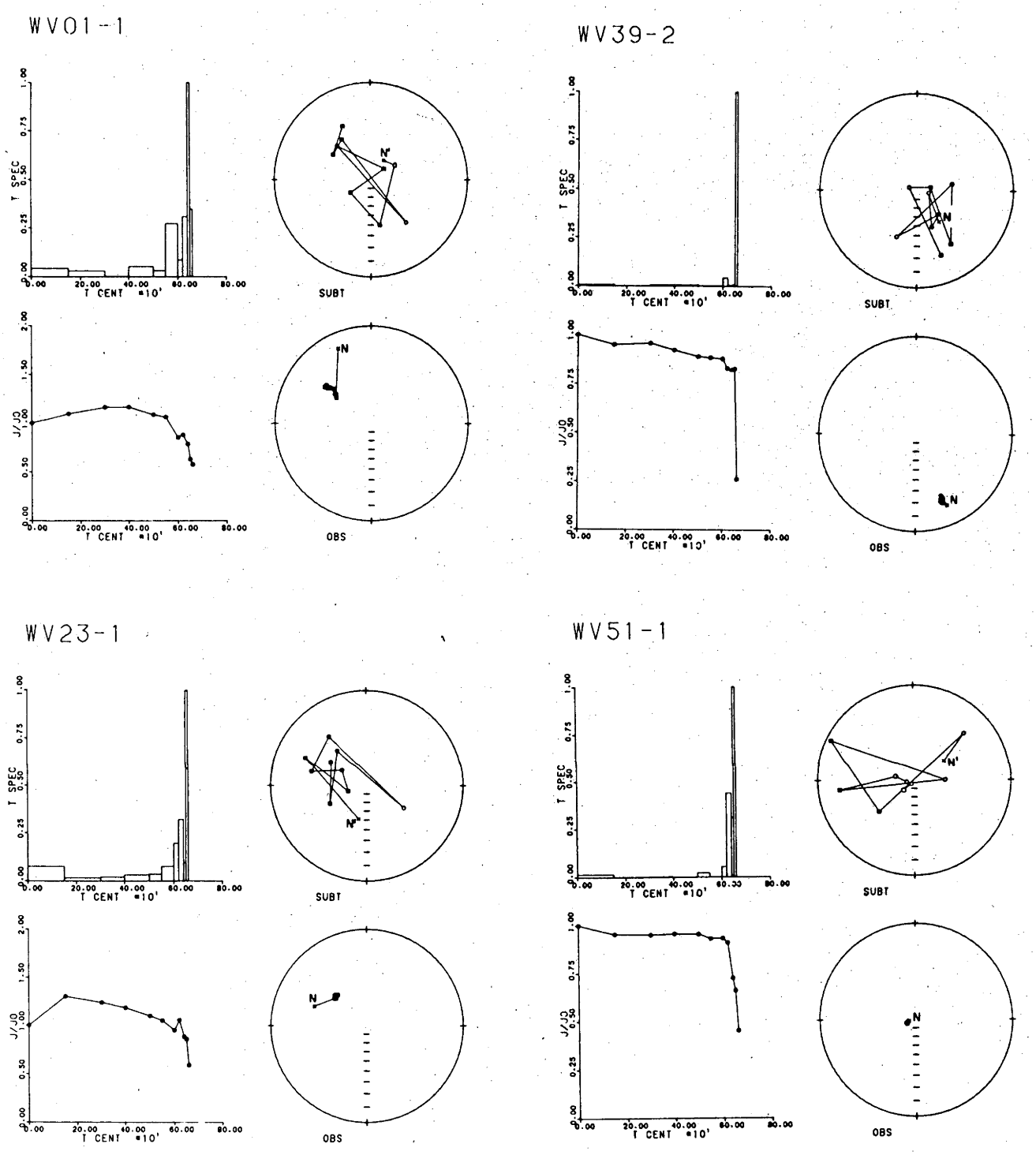

Figure 2.7(A) : Thermal demagnetization, Wooltana Volcanics.

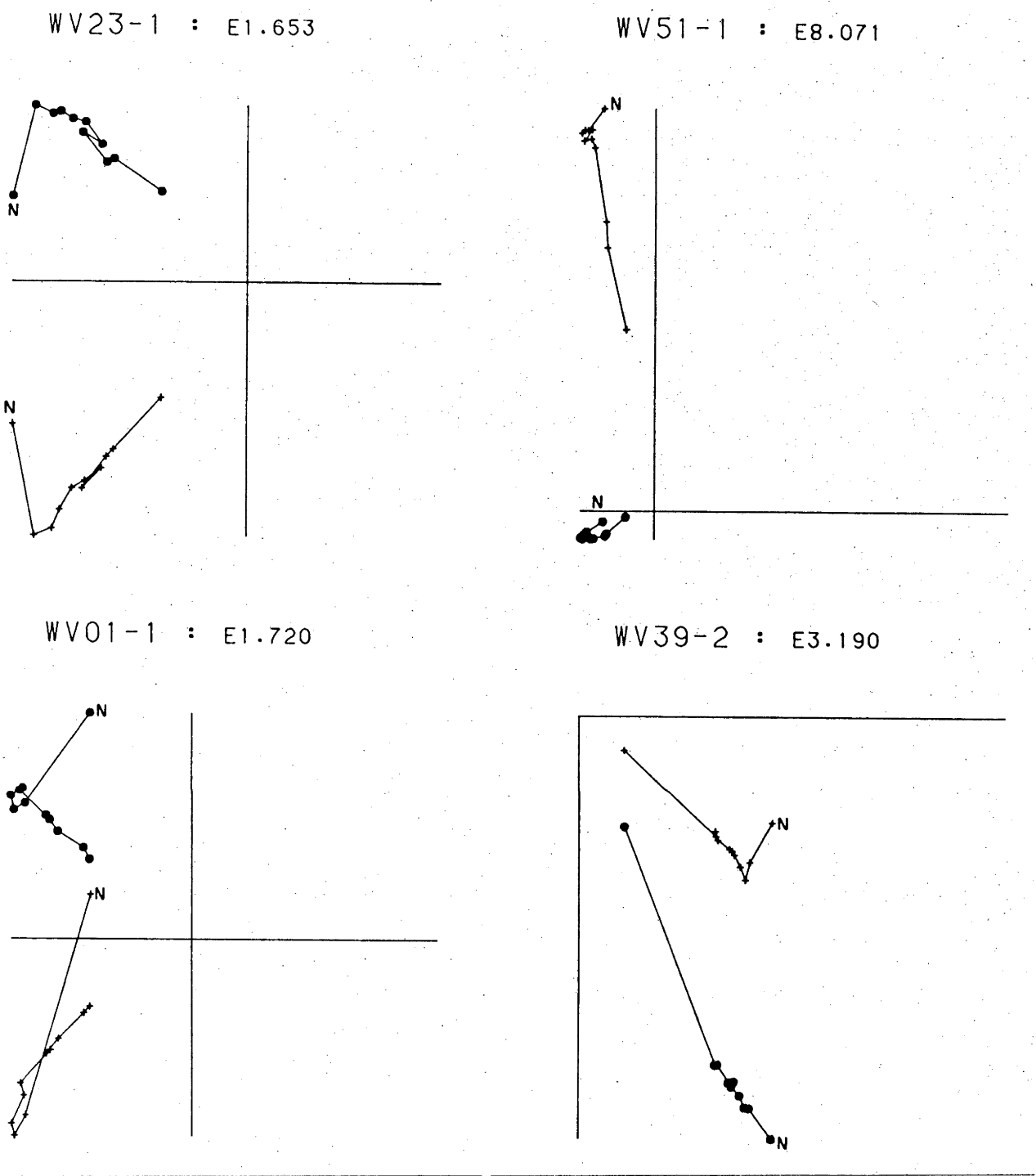

Figure 2.7(B) : Thermal demagnetization, Wooltana Volcanics (continued).

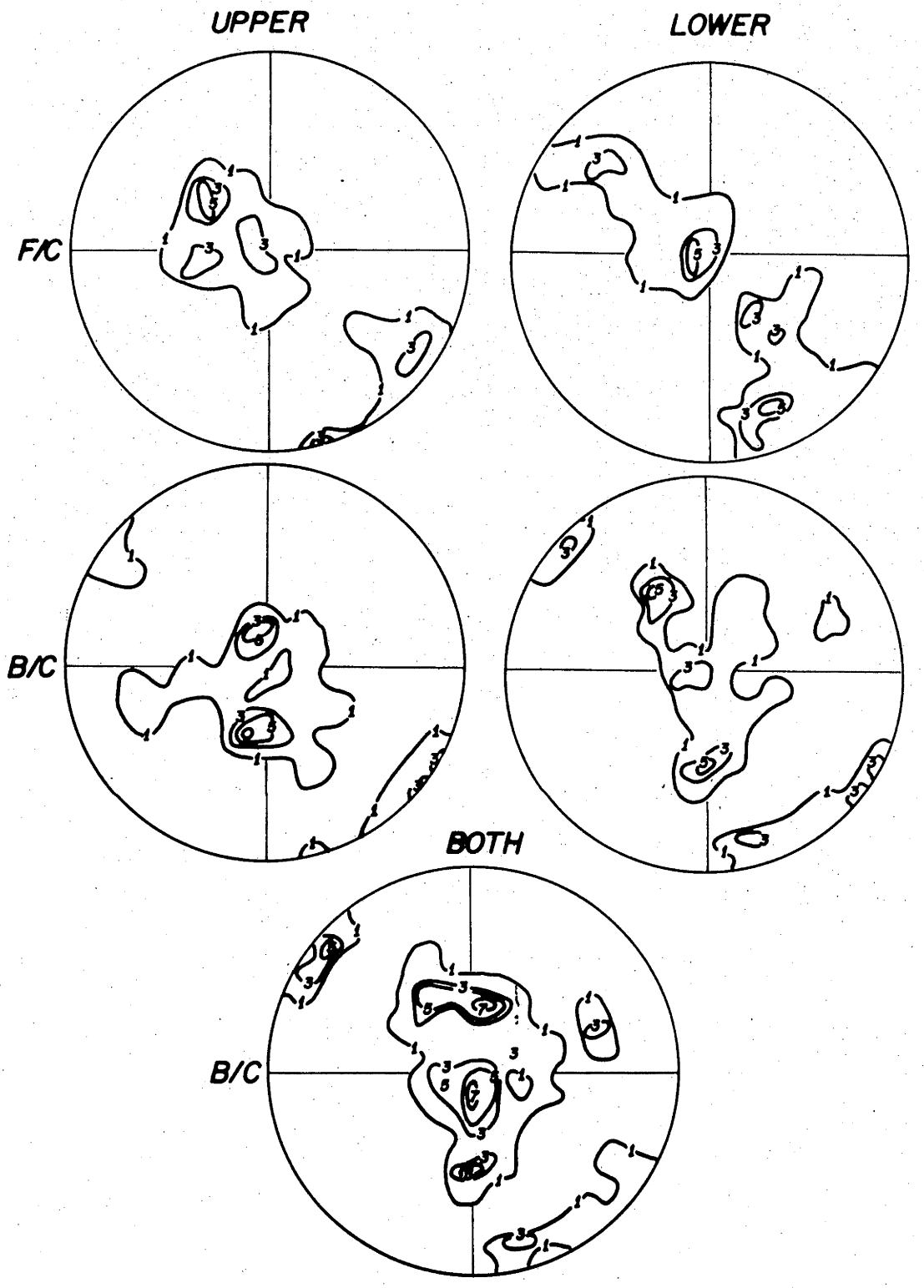

Figure 2.8 : Frequency analysis of cleaned site mean directions from Wooltana samples. Upper and lower hemispheres of the equal-area projection shown. 'Both' refers to combined upper and (reversed) lower hemispheres for structurally corrected directions. See text for details.

TABLE 2.2 (A)

WOOLTANA VOLCANICS : Site mean directions before and after thermal demagnetization

	NRM				400°C						
SITE	n	R	D	I	n	R	D	I	D'	I'	MAGNETIZATION
1	3	2.932	339	-01	3	2.983	315	28	342	-14	WV3
2	3	2.845	326	-12	3	2.940	307	21	333	-28	WV3
3	3	2.958	328	-67	3	2.960	324	-66	40	-76	WV1
4	3	2.701	330	-48	3	2.992	304	-57	339	-80	WV1
5	4	3.963	315	-55	3	2.973	312	-56	350	-76	WV2
6	4	3.807	165	-68	4	3.783	165	-66	244	-41	WV2
7	4	3.726	296	49	4	3.858	302	55	59	64	WV2
8	3	2.579	145	32	2	1.985	121	49	92	85	WV1
9	3	2.871	187	50	2	1.988	146	51	213	77	WV1
10	3	2.434	141	29	3	2.909	138	43	170	77	WV1
11	3	2.974	167	26	3	2.844	152	32	179	61	WV1
12	3	2.983	158	16	2	1.987	158	20	175	48	WV1
13	2	1.981	165	29	2	1.999	165	21	184	46	WV1
14	2	1.995	54	-71	2	1.980	56	-84	143	-60	WV2
15	3	2.995	327	83	3	2.999	287	85	328	56	WV2
16	3	2.984	326	78	3	2.979	273	81	321	55	WV2
17	2	1.999	258	-84	2	1.996	243	-80	174	-58	WV2
18	2	1.276	26	-38	1	-	315	-80	165	-69	WV2
19	2	1.999	16	-63	2	1.947	195	-81	165	-53	WV2
20	5	4.807	309	-69	5	4.920	271	-62	186	-65	WV2
21	1	-	127	-03	1	-	306	-68	319	-71	WV1
22	5	4.540	121	-34	5	4.792	133	-15	132	-08	WV3
23	3	2.993	164	05	3	2.994	163	07	167	13	WV3
24	3	2.979	249	-65	3	2.996	241	-60	86	-87	WV1

TABLE 2.2 (B)

WOOLTANA VOLCANICS : Mean directions after thermal demagnetization

	Before structural correction									After structural correction						
							pole							pole		
MAGNETIZATION	N	n	R	k	D_m	I_m	lat	long	dp,dm	R'	k'	D_m'	I_m'	lat	long	dp,dm
WV1	10	24	9.169	10.8	140	50	56S	218E	14,21	9.615	23.4	178	73	62S	142E	16,18
WV2	10	29	9.393	14.8	36	87	26S	143E	26,26	9.222	11.6	358	68	09N	138E	21,25
WV3	4	14	3.787	14.1	320	15	36N	87E	13,26	3.796	14.7	333	-12	55N	88E	13,25

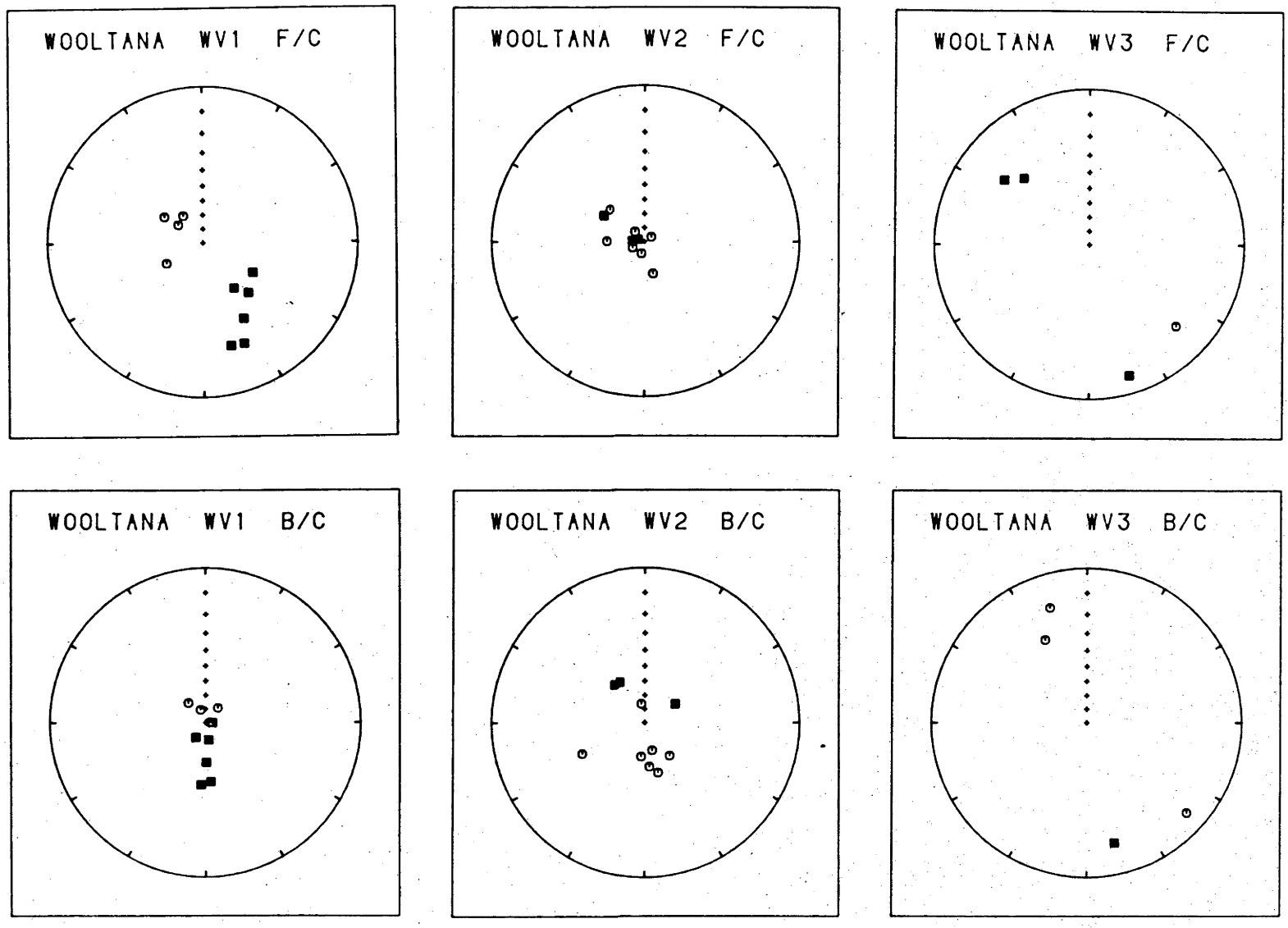

Figure 2.9 : Cleaned site mean magnetization directions for the WV1, WV2 and WV3 components; equal-angle projection. Open (closed) symbols refer to negative (positive) inclination.

reflected light indicates that the magnetic minerals are highly oxidized. Original magnetite lamellae have been altered to hematite, while the ilmenite lamellae have been almost completely replaced by pseudobrookite. Tiny rutile rods are visible. The volcanics are probably best described as class 5 or higher in oxidation state (Wilson and Watkins, 1967). Thermal demagnetization experiments were conducted on one specimen from each sample in an attempt completely to demagnetize the high coercive force hematite minerals and to detect whether or not multicomponent magnetizations were present.

Examples of thermal demagnetization studies are illustrated in Figure 2.7. A component of magnetization with a steep negative inclination is removed in the 20°-200° heating step, after which the magnetization vector remains directionally stable and decreases in intensity. This low blocking temperature (T_b) component has a mean direction 352,-68 (α_{95} = 13°, n = 19 sites) and is not significantly different from the PEF direction at the sampling locality. The most plausible explanation for the low T_b component is that it is a VRM acquired in Recent times.

Excluding the very low T_b component, only a single magnetization direction was isolated in any one specimen. As magnetizations generally became directionally stable in or below the 300°-400° range, 400° was chosen as a final temperature for bulk treatment of the remaining specimens from each sample. Cleaned site mean directions are listed in Table 2.2 and illustrated in Figures 2.8 and 2.9. Although only a single stable magnetization was isolated at each site, the frequency analyses of directions shown in Figure 2.8 suggest that the distribution of magnetization directions is not Fisherian, both

before and after structural correction.

The elongated distribution of uncorrected directions (Figure 2.8a) is due to structural causes. The major axis of the distribution pattern is perpendicular to the dominant strike direction and is what would be the expected distribution if a Fisherian population were structurally modified by folding with variable dip but nearly constant strike. After tectonic correction, a different non-Fisherian distribution is seen (Figure 2.8b) and three groups of site mean directions are apparent. These three groups have been labeled the WV1, WV2 and WV3 magnetizations in the figures and in Table 2.2. Each of the magnetizations is statistically distinct at the 95% confidence level, whether structurally corrected or not, e.g. the WV1 mean direction is significantly different from the WV2 mean direction in both its corrected and uncorrected position. Precision of the WV1 magnetization increases significantly upon structural correction (k'/k=2.17, 95% significance point $\cong$ 2.16). Both the WV2 and WV3 magnetization have nonsignificant changes in precision upon correction (WV2 : k'/k=0.78, 95% significance point $\cong$ 0.46); WV3 : k'/k = 1.04, 95% significance point $\cong$ 3.79).

There are two possible explanations for such a trimodal distribution. One possibility is that the geological structure is much more complicated than was apparent during superficial structural mapping whilst sampling, making an accurate reconstruction of a single primary magnetization difficult. The occurrence of both the WV1 and WV2 magnetizations at sites separated by only a few metres and with almost certainly a common structural orientation (*cf.* sites 7 and 8) could be cited as evidence contrary to the possibility of such a

"structurally induced" multicomponent system. An alternative possibility is that the various magnetizations make up a true multicomponent system and that the WV1-WV3 magnetizations were acquired at different times. Here, the facts that only one stable magnetization is found at a particular site during demagnetization experiments and that there are no consistent physical differences (such as gross texture or petrology, colour, bulk susceptibility etc.) between samples which carry the various components argue against this possibility.

It is difficult to determine conclusively whether the WV2 and WV3 magnetizations are parts of a true multicomponent system or simply result from inadequate structural reorientation. As discussed in §2.7.4, similar components of magnetization have been found in the Merinjina Tillite, an immediately overlying unit in the Wooltana district. The similarities between magnetizations from the two units in conjunction with their interpretation in terms of geological events in the area would tend to support real rather than artificial multicomponents. Further discussion of the problem is deferred until the results of §2.7.4 have been presented. It can be stated with some confidence however that the WV1 magnetization was acquired before folding of the volcanics occurred. Initially, this would suggest that the WV1 magnetization predates only the Cambrian folding episode, however Crawford (1963) has noted that a marked angular unconformity exists between the folded volcanics and the overlying pre-Sturtian (Burra Group) sediments. This would imply that the WV1 magnetization was probably acquired in Willouran times and is most likely a true primary age acquired during cooling after extrusion. Combined with the evidence for a pre-folding age, the presence

of pseudobrookite as a presumed original high temperature oxidation product would suggest that the WV1 magnetization is a primary TRM (Haggerty and Lindsley, 1969).

§2.7.3 Copley/Wortupa Quartzite (Burra Group)

The Burra Group overlies the Upper Callana Beds and records a sedimentary cycle which commences with a basal clastic unit followed by a carbonate-siltstone succession and terminated by an association of shallow water clastic sediments. The carbonate members (Skillogallee Dolomite and equivalents) contain columnar stromatolites of the group *Tungussia* and *Baicalia* (Preiss, 1971 in Walter, 1972). The basal unit at the stratotype, called the Rhynie Sandstone, has equivalents in other areas of the Adelaide 'Geosyncline'. Two of these equivalents in the North Flinders Ranges were sampled, the Copley Quartzite and Wortupa Quartzite.

The Copley Quartzite was sampled at two localities west and northwest of Copley (Figure 2.5) where the structure is relatively simple and beds dip steeply to the northeast. Samples of the Wortupa Quartzite were taken in the Mount Painter area near Lady Buxton Creek (Figure 2.5) where the beds have a shallow easterly dip. At both localities, the lithology which was sampled was predominantly a crossbedded white feldspathic quartzite with heavy mineral banding.

Palaeomagnetic results are summarized in Table 2.3. Directions of NRM were highly scattered both before and after structural correction. During pilot thermal demagnetization of one speciment from each of the 30 samples (examples shown in Figure 2.10), a magnetization with a steep negative inclination (028,-57, α_{95}=17°, n=7 sites) was consistently removed in the

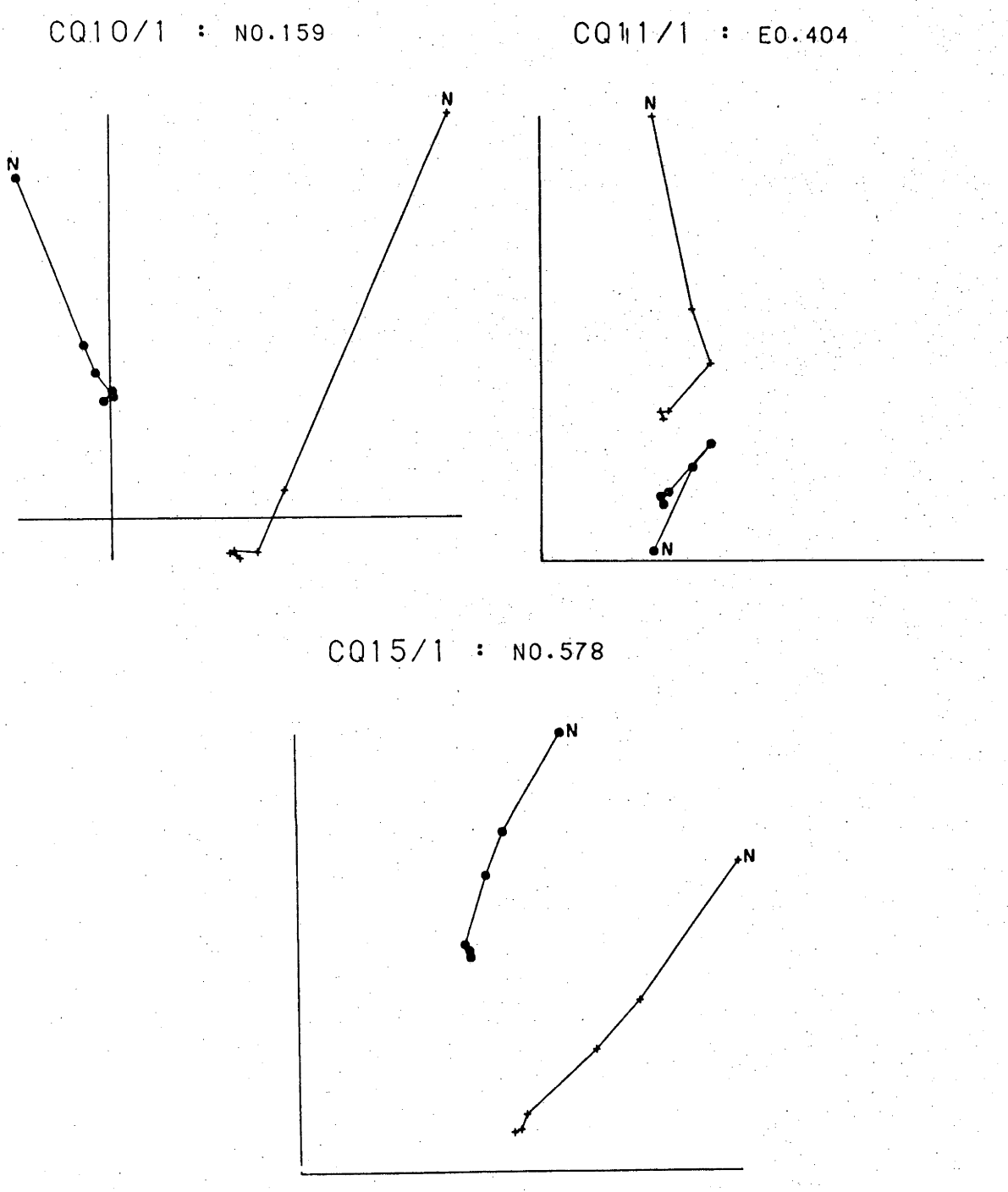

Figure 2.10(A) : Thermal demagnetization, Copley Quartzite.

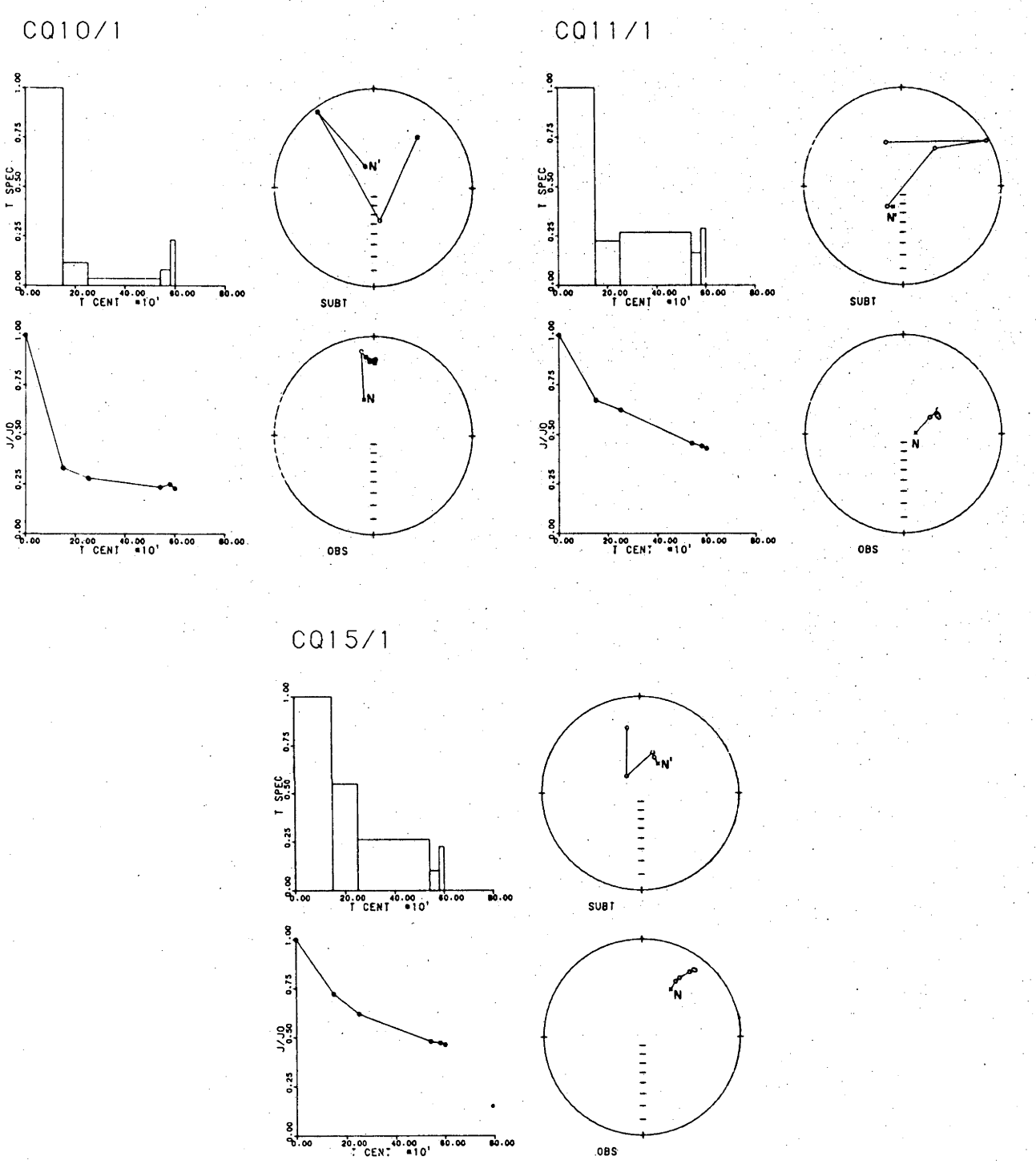

Figure 2.10(B) : Thermal demagnetization, Copley Quartzite.

TABLE 2.3(A)

COPLEY QUARTZITE : Site mean directions before and after thermal demagnetization

	NRM				300°C				
SITE	n	R	D	I	n	R	D	I	D'	I'
1	5	4.023	288	51	4	3.948	287	78	038	41
2	6	5.572	023	-53	3	2.967	037	-05	038	00
3	3	2.571	031	17	3	2.987	004	76	035	-04
4	3	2.178	075	-59	3	2.884	212	74	044	25
5	4	2.773	024	-09	3	2.812	330	88	040	11
6	4	2.991	258	-28	2	1.743	242	78	043	17
7	5	4.314	159	66	(random)					

TABLE 2.3(B)

COPLEY QUARTZITE : Mean direction after thermal demagnetization

		Before structural correction							After structural correction						
N	(n)	R	k	D_m	I_m	lat	long	dp,dm	R'	k'	D_m'	I_m'	lat	long	dp,dm
6	18	4.866	4.4	005	81	85N	261E	67,69	5.784	23.1	40	15	50S	345E	7,15

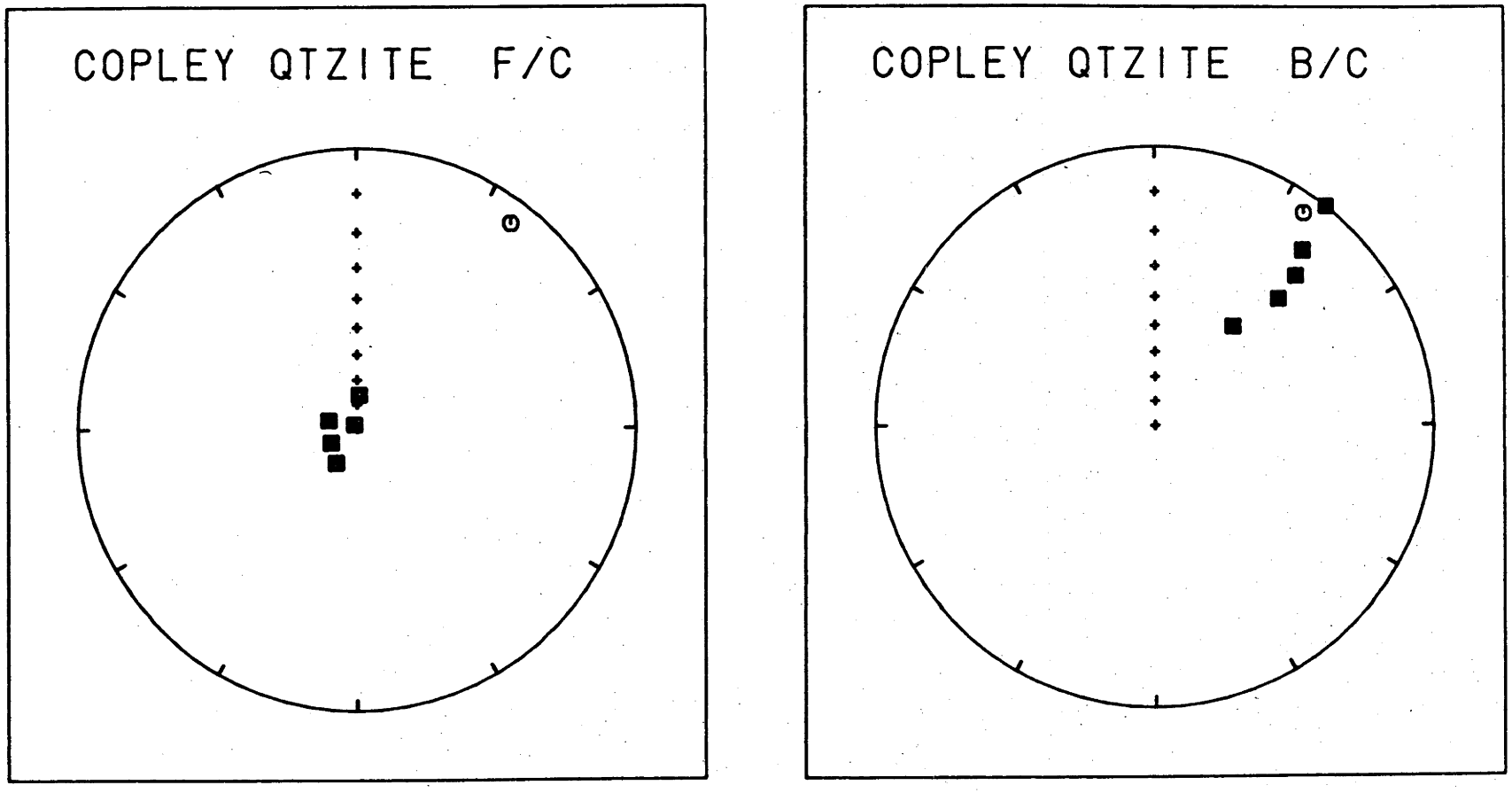

Figure 2.11 : Cleaned magnetization directions, Copley Quartzite; equal-angle projection. Open (closed) symbols refer to negative (positive) inclination.

20°-150° heating step. This mean direction is not significantly different from the PEF direction at the sampling localities and is probably a recently acquired VRM. Stable directions were generally realized between 250° and 500°, although many specimens exhibited stable directions only up to 400°. Two remaining specimens from each sample were treated in bulk at 350° for final cleaning.

Final cleaned site mean directions uncorrected for bedding tilt are still quite scattered. Upon making structural corrections, a significant improvement in precision is realized with k increasing from 4.4 to 23.1 (k'/k=5.25, 95% significance point ≅2.82). The positive fold text thus indicates that the stable magnetization of the Copley Quartzite was probably acquired before the rocks were folded in Cambrian times.

There is a marked angular difference of about 68° between the pole positions for the Copley Quartzite and the pole from the WV1 component of the Wooltana Volcanics (Figure 2.27). A possible explanation of this difference is that there was a significant time interval separating magnetization ages of the two units. Coats and Blissett (1971) have demonstrated that a major unconformity exists between the Lower and Upper Callana Beds in the North Flinders area. The exact stratigraphic position of this unconformity is still under study (W. Preiss, *pers.comm.*); in any case it lies between the Wooltana Volcanics and the Copley Quartzite. Depending upon early Adelaidean rates of apparent polar motion, the discordance of these poles suggests that the unconformity could represent quite a significant time break in Adelaidean sedimentation. Rotational motion about a local vertical axis between times of magnetization could account for part of the difference without invoking a large time

difference, however the two results differ by over 50° in palaeolatitude, indicative of true displacement on the sphere.

§2.7.4 Merinjina Tillite (Yudnamutana Sub-Group)

Sediments of the Umberatana Group overlie the Burra Group with a marked glacially produced unconformity. The group contains two distinct tillitic successions and has received worldwide recognition as one of the best preserved examples of late Precambrian glaciation. The Umberatana Group has been divided into three Sub-Groups, the lower Yudnamutana Sub-Group containing the Sturtian glacials, overlain by the interglacial Farina Sub-Group, in turn overlain by Marinoan glacial beds of the Yerelina Sub-Group. At the type area in the Mount Painter region, the Yudnamutana Sub-Group has four members which attain a thickness of over 5000 m in places. The lowest member, the Fitton Formation, is a massive tillite made up of granitic debris with some dolomitic siltstone, arkose and quartzite. Overlying and interfingering with the Fitton Formation, massive tillites of the Bolla Bollana Formation contain a wide variety of striated and polished erratics. The overlying Lyndhurst Formation is a sequence of shallow marine sediments with recurrent tillite horizons. In the Wooltana area, a massive tillite horizon occurs unconformably above the Wooltana Volcanics just east of the Paralana fault. This tillite is called the Merinjina Tillite (Coats and Preiss, in preparation) and contains a wide variety of polished and fragmented erratics in a quartzitic matrix, iron rich in places. Photographs of the tillite are shown in Plates 1 and 2. Samples of the Merinjina Tillite were taken at several localities through nearly its entire thickness (Figure 2.5).

Plate 1 - Merinjina Tillite

Plate 2 - (?) Striated Pavement underlying Merinjina Tillite

The interpretation of palaeomagnetic data from the Merinjina Tillite is problematic. Detailed thermal demagnetization studies of 1 pilot specimen from each of 64 samples showed that a complex system of magnetizations may be present. Wide variation in blocking temperature spectra of the various components present has made isolation of individual directions difficult, as discussed below.

Examples of typical thermal demagnetization experiments are shown in Figure 2.12. Two components of magnetization are evident at most sites. One magnetization is characterized by very steep, relatively stable directions similar to observed and subtracted directions found in other Adelaide 'Geosyncline' sediments (see §2.7.2, 2.7.3, 2.7.6, 2.7.7). A second frequently observed magnetization has a stable shallow inclination and southwesterly or northeasterly declination. A third less frequently observed component exhibits a shallow to moderate negative (positive) inclination and northwest (southeast) declination.

A major problem in interpretation is caused by the apparent close interrelationship of these three magnetizations. Upon determining a range for stable directional behaviour in each sample, remaining specimens were heated in bulk to the appropriate temperature. In some cases, all specimens from a particular sample gave consistent directions after treatment. In many other samples, after heating to an optimum temperature, sample mean directions were widely scattered and essentially random at the 15% confidence level. Closer inspection revealed that although the sample means were random, in many cases individual specimen directions could be grouped in one of the three types of magnetization observed during pilot studies

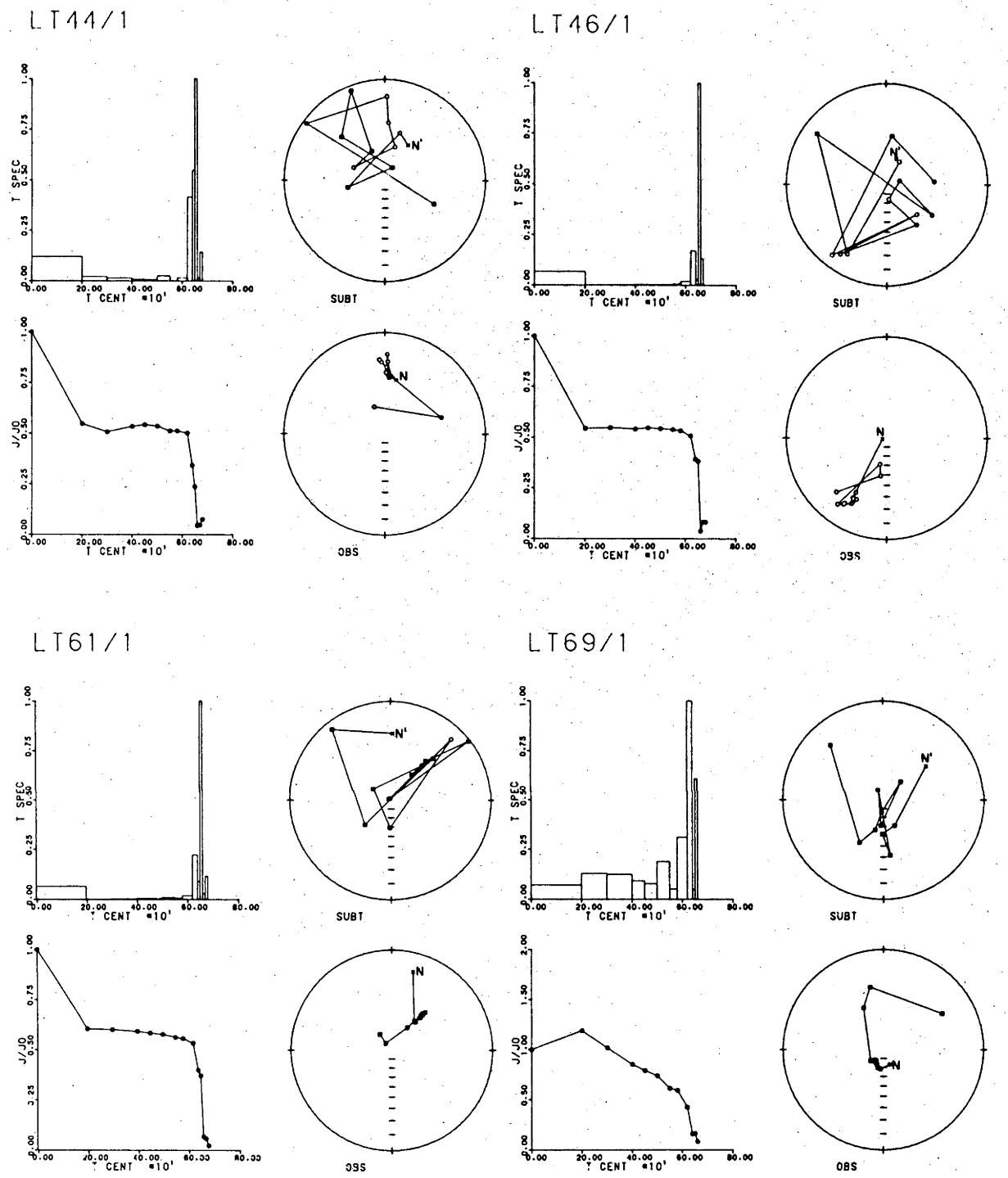

Figure 2.12(A) : Thermal demagnetization, Merinjina Tillite.

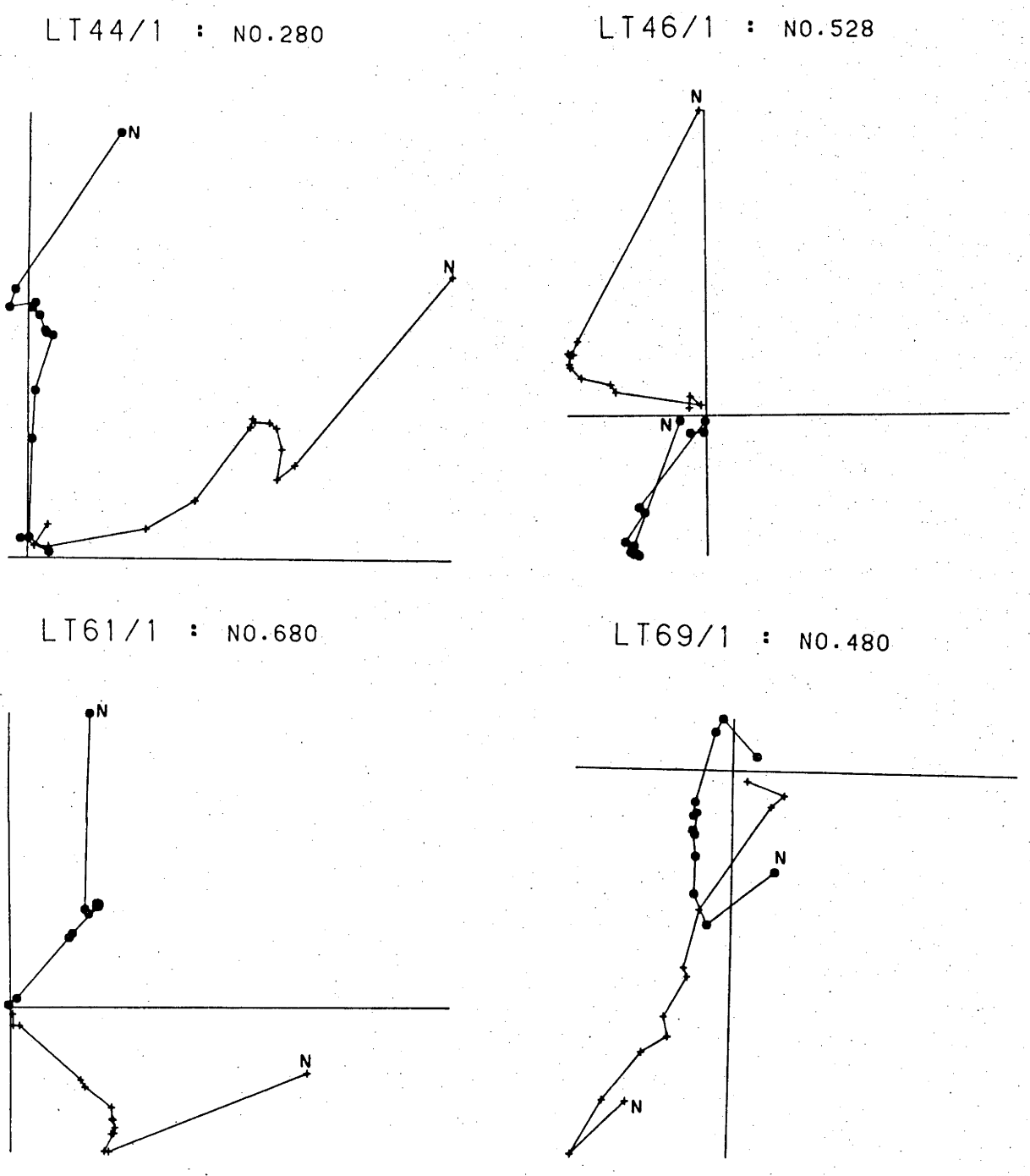

Figure 2.12(B) : Thermal demagnetization, Merinjina Tillite (continued).

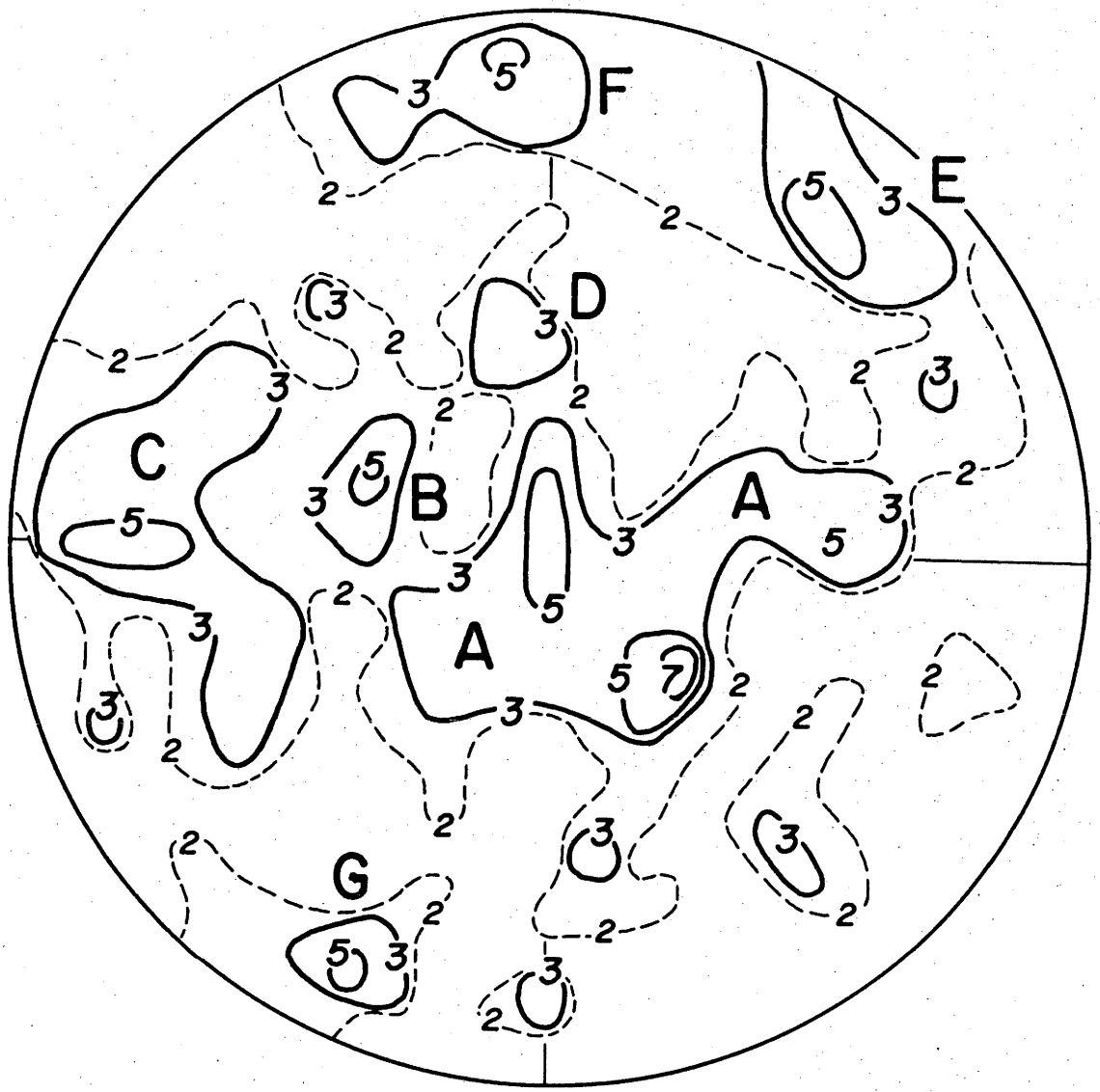

Figure 2.13 : Frequency analysis of cleaned specimen magnetization directions from Merinjina Tillite samples : upper hemisphere of equal-area projection shown. Directions from lower hemisphere have been reversed and plotted on upper hemisphere. See text for details.

TABLE 2.4 (A)

MERINJINA TILLITE : Site mean directions after thermal demagnetization

MAGNETIZATION	SITE	n	R	D	I	D'	I'
	1	2	1.845	021	23	039	36
	5	1	-	220	-16	214	-27
	6	2	1.908	033	15	016	47
	7	3	2.703	194	-20	189	-23
	9	1	-	193	-26	187	-29
	10	2	1.944	018	-06	018	-01
	11	1	-	191	-18	186	-20
MT1	12	3	2.944	229	-11	225	-21
	13	3	2.794	036	-05	037	05
	14	2	1.901	206	08	202	-01
	15	1	-	207	-25	199	-29
	17	3	2.791	199	03	194	-11
	18	1	-	170	13	172	-02
	19	2	1.939	042	07	041	28
	20	3	2.735	345	-13	347	00
	21	2	1.864	202	-17	198	-37
	1	4	3.869	126	85	195	59
	5	1	-	009	-81	066	-68
	6	1	-	344	60	319	51
	7	2	1.912	298	-82	297	-82
	8	3	2.719	199	-87	102	-79
	10	3	2.841	299	69	288	55
	11	2	1.963	136	73	193	77
MT2	12	1	-	325	-65	006	-74
	13	1	-	331	-61	357	-62
	15	1	-	127	61	151	72
	16	2	1.989	260	-64	241	-78
	17	1	-	281	-67	078	-69
	18	1	-	353	-67	014	-48
	19	1	-	047	-61	048	-40
	20	1	-	265	80	234	61
	21	2	1.946	161	68	187	52
	1	4	3.854	288	51	267	39
	5	2	1.924	099	-47	097	-28
	6	3	2.953	266	13	266	-06
	7	1	-	160	-45	149	-41
	8	1	-	091	-21	090	-09
	9	1	-	081	-31	081	-19
MT3	12	2	1.834	110	-15	109	01
	13	1	-	088	-14	088	01
	14	3	2.724	267	18	267	04
	15	3	2.720	283	20	282	05
	16	2	1.940	262	-05	261	-19
	17	1	-	253	-03	246	-43
	18	2	1.911	096	-43	083	-28
	20	2	1.944	301	39	286	34

TABLE 2.4 (B)

MERINJINA TILLITE : Mean directions after thermal demagnetization

			Before structural correction							After structural correction						
MAGNETIZATION	N	n	R	k	D_m	I_m	pole lat	pole long	dp,dm	R'	k'	D_m'	I_m'	pole lat	pole long	dp,dm
MT1	16	32	14.914	13.8	202	-09	49S	354E	05,10	14.915	13.8	199	-21	45S	346E	06,11
MT2	16	27	15.087	16.4	147	81	45S	153E	17,18	14.642	11.0	205	74	56S	117E	19,21

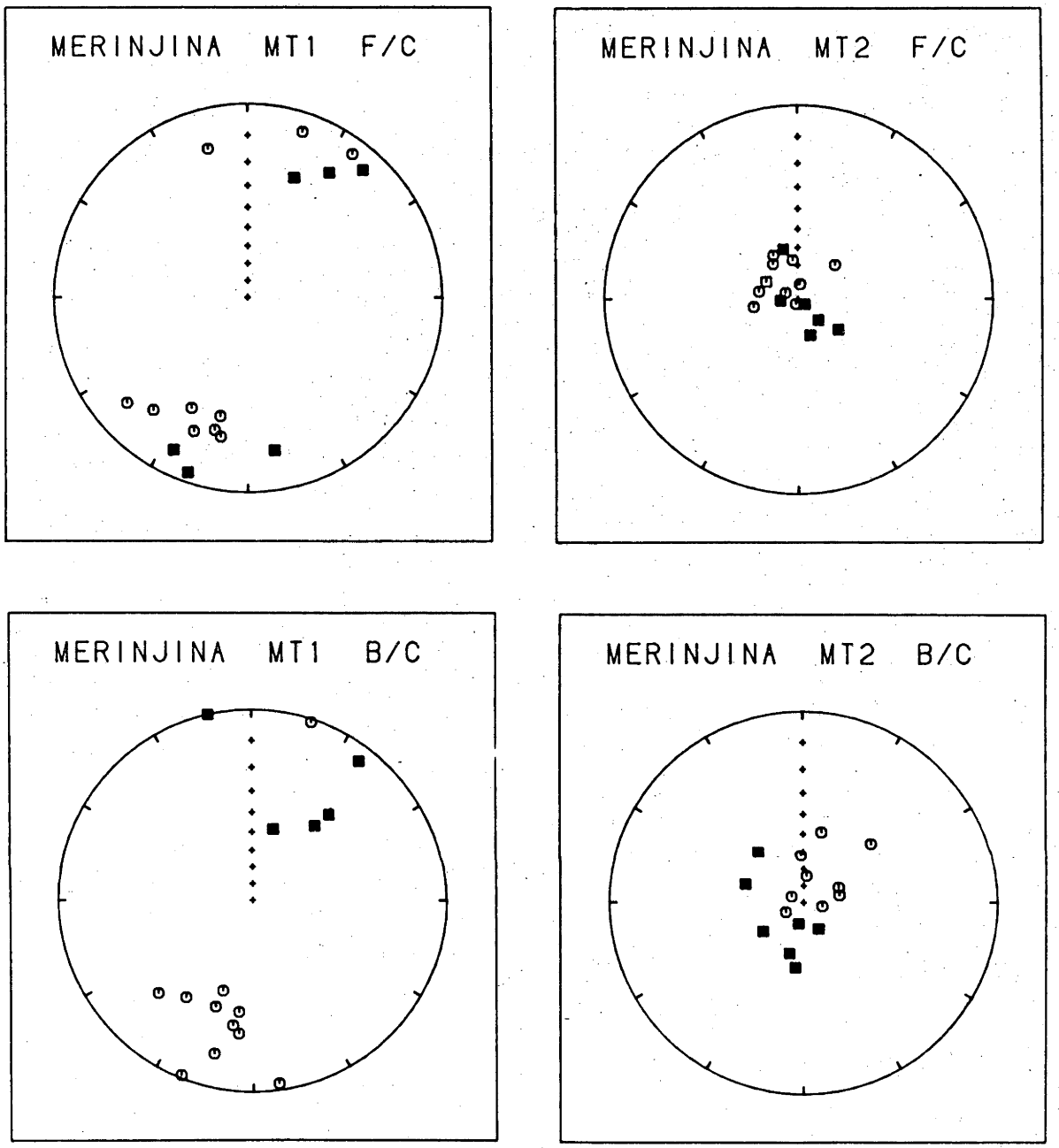

Figure 2.14(A) : Cleaned site mean directions, MT1 and MT2 components; equal angle projection. Open (closed) symbols refer to negative (positive) inclination.

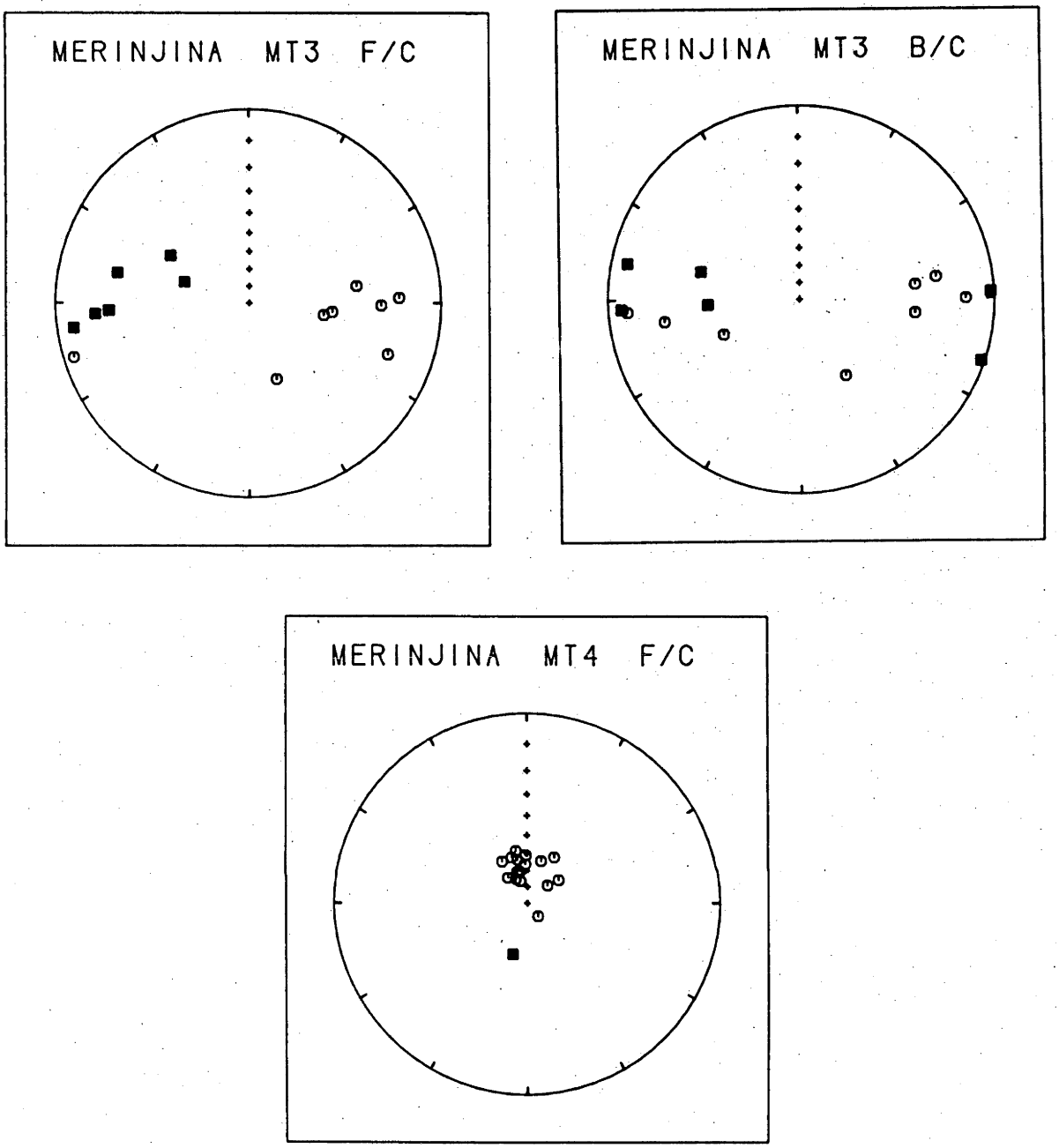

Figure 2.14(B) : Cleaned site mean directions, MT3 and MT4 components; equal angle projection. Open (closed) symbols refer to negative (positive) inclination.

described above. This implies that more than one component of magnetization is present in an individual sample. The difficulty stems from the fact that in multicomponent systems, individual components often have T_b or H_c spectra which facilitate separation of the components. In such systems, specimens from one sample have generally similar responses to demagnetization and will generally exhibit the same component at a particular temperature or peak AF intensity. The various components can be extracted using a variety of vector techniques. In the Merinjina samples however, specimens from the same sample treated at a particular optimum temperature have differing magnetizations, possibly implying that the nature of the remanence carriers and/or the thermochemical histories of adjacent specimens differ. This latter possibility seems almost impossible to successfully argue, in light of the proximity of any two specimens cored from the same block sample. Considering the petrographic nature of these tillitic sediments which contain an extremely heterogeneous mixture of rock types and grain sizes (from a few metres to fine rock flour, although large pebbles were avoided during coring) it seems plausible that the possibility of wide variations in grain size and composition of remanence carriers cannot be excluded. If this is indeed the case, individual specimens obtained from the same sample might be expected to respond differently to thermal and chemical events in the rock's later history.

With this in mind, individual specimen directions have been subjected to frequency analysis as illustrated in Figure 2.13 (only 1 hemishpere is shown, directions on the obscured hemisphere have been reversed). It is obvious that

the distribution of directions is non-Fisherian and that more than one magnetic component is present, to judge by the contoured 'peaks' which occur. However it is somewhat difficult to decide at what level grouping of directions become significant, as directions in the various groups tend to spread into one another. The occurrence of three or more directions in a given areal subdivision (in Figure 2.13 the hemisphere is divided into 387 equal area units) is used here as a basis for describing the regions described below.

As seen in pilot demagnetization studies, three dominant components are present. One is characterized by southerly trending declinations and steep positive inclinations. Another component exhibits moderate to shallow inclination and westerly declination. Although it is not obvious from Figure 2.13, both polarities of these components are observed. The third component has shallow inclination and NNE-SSW declination; again both polarities are present. The directions have been contoured and divided into regions labelled A-G. Although the distributions are clearly not Fisherian, and tend to merge together, the directions contained in regions A and C are certainly quite distinct. Departure from a Fisherian distribution might be expected if the heterogeneity of remanence carriers suggested above is indeed true. Similarly, regions E, F and G collectively do not form a Fisherian distribution but are quite separate from regions A-D and are probably a separate population of directions.

The problem of obtaining mean directions for each of the components is somewhat difficult as the methods outwardly appear to be purely subjective. As is later shown however, the mean directions obtained do have a meaningful interpretation in

terms of the tectonic and thermal history of the area and thus tend to justify the means employed. There being no obvious alternative basis for subdivision such as locality, stratigraphic position or gross physical appearance, directions have been grouped on their proximity to the three most frequently observed components. These three components have been labelled MT1, MT2 and MT3 in Table 2.4 and Figure 2.14. All specimens from a sample which exhibit the same component have been grouped to form a sample mean direction; the sample means are then used to calculate a site mean direction. Since some samples show more than one component, their corresponding sites have more than one entry in the table. A fourth magnetization MT4 has a very low blocking temperature and was calculated from the vector directions subtracted in the 20°-200° and 200°-300° pilot heating steps.

The mean directions for each of the MT1-MT3 components are reasonably well grouped and significantly different from each other. The MT3 mean direction is similar to the WV3 mean direction (Figure 2.14). A fold test on the MT1 magnetization is inconclusive as the values for the precision parameter k remain constant. This is most likely due to the similar structural style in the sampling area, with consistent westerly dips ranging from 12° to 43°. The precision of both the MT2 and MT3 mean directions decreases upon making the structural corrections, suggesting that these components are of a post-folding age. Unfortunately, the fold test is not significant at the 95% level (MT2: k'/k=0.67, 95% significance point ≅0.57; MT3: k'/k=0.78, 95% significance point ≅0.53). The MT4 magnetization is not significantly different from the PEF direction at the sampling site.

Although the fold test on the MT1 magnetization cannot supply information about the age of magnetization relative to folding, the pole position calculated from this direction falls between pole positions for the older Copley Quartzite and the overlying Angepena Formation, a position which suggests that the magnetization is original. The pole position for the immediately overlying Tapley Hill Formation is problematical as it is displaced some 10°-15° to the east (Figure 2.27).

The MT3 magnetization probably dates from past folding times, and its pole position (Figure 2.27) is near poles of Ordovician age from elsewhere in Australia. Massive granite plutons were emplaced in the Mount Painter area during Ordovician times. Support for an Ordovician thermal event in the sampling area comes from the isotopic work of Compston *et al.* (1966), who reported Rb/Sr results from samples of the Wooltana Volcanics which immediately underly the Merinjina Tillite in the sampling area, and from the Arkaroola Creek Pegmatite, an intrusive offshoot probably related to the Mudnawatana Granite (Figure 2.5). Their results suggested a major isotopic reorganization at about 465 my in the volcanics, while the hydrothermal activity recorded by emplacement of the pegmatite was dated at 460 my. A similar age is inferred for the MT3 magnetization, which could be a CRM or TRM. It is interesting to note that the MT3 component has a counterpart in the underlying volcanics in the form of the WV3 magnetization, the pole from which falls in a similar area. Both magnetizations are probably due to thermochemical effects during igneous activity in the area.

The MT2 magnetization is quite similar to

magnetizations observed in other rocks from the North Flinders (see §2.72, 2.73, 2.76, 2.77). If the magnetization is indeed of post-folding age as suggested by the negative fold test, it could be related to uplift and stabilization of the region during early Tertiary tectonic movements (Rutland, 1973). Considering the high blocking temperatures of the MT2 component, it is probably a CRM and not a low temperature PTRM as in the Angepena Formation, for example. Again, an analogue to the MT2 component is found in the underlying Wooltana lavas; the WV2 component could be of Tertiary or late Cretaceous age (Figure 2.27). The MT4 magnetization is almost certainly a VRM acquired in Recent times.

§2.7.5 Tapley Hill Formation (Farina Sub-Group)

A persistant finely laminated shale unit occurs immediately above the Sturtian glacial horizons. Overlying this unit, a thick sequence of shales, siltstones and occasional limestones called the Tapley Hill Formation forms the lower part of the Farina Sub-Group. These sediments are of shallow marine origin and together with some of the immediately overlying sediments are referred to as the "interglacial sequence", occurring between the Sturtian and Marinoan glacial horizons.

Briden (1967) reported uncleaned results from samples of the Tapley Hill 'slates' collected near Adelaide. His results, weak and widely scattered NRM directions from 10 samples, were largely inconclusive. One complication in Briden's study was that the rocks studied had most likely suffered low to moderate grade metamorphism, and it is probable that the directions measured, even if cleaned, would have

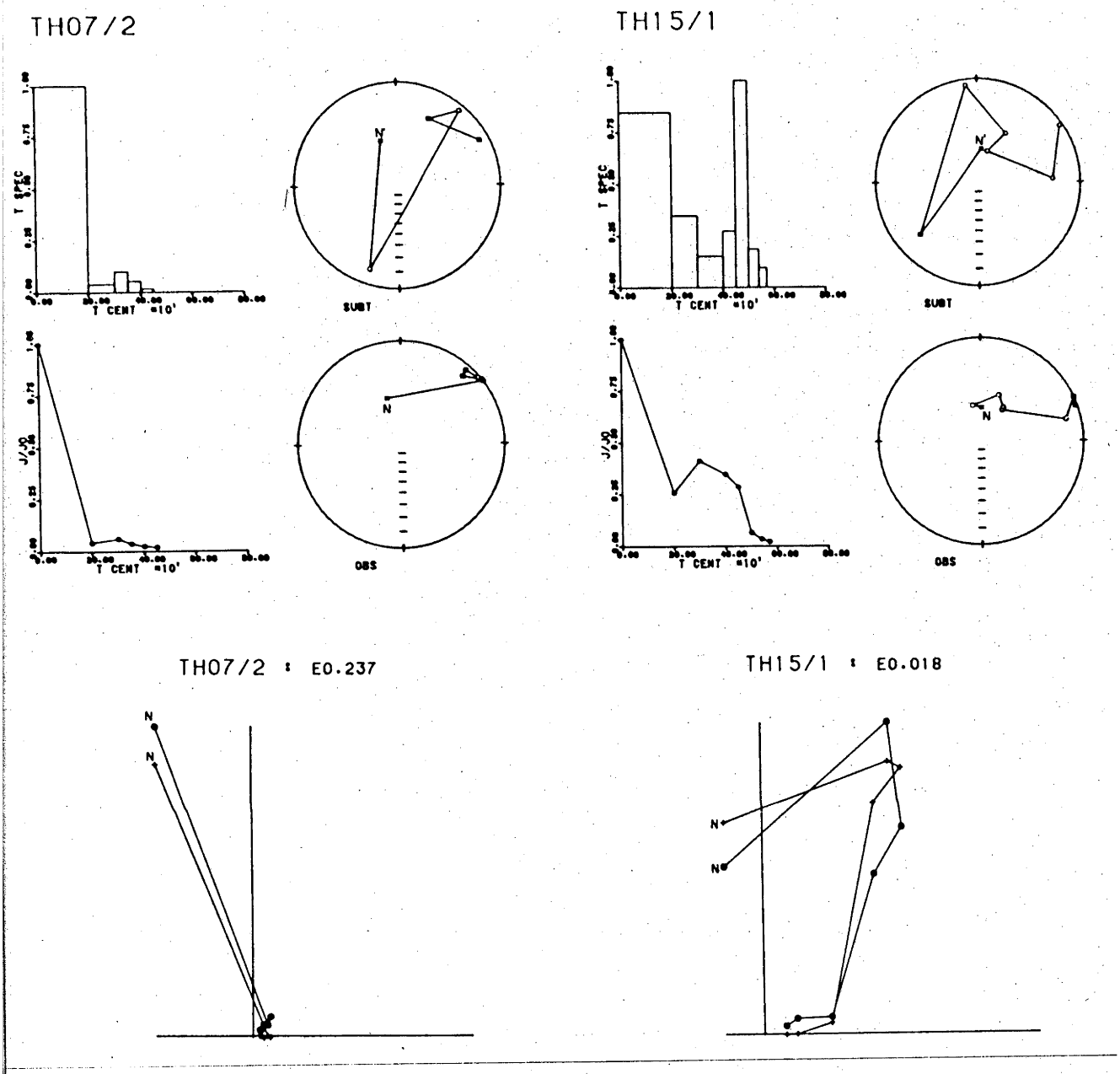

Figure 2.15 : Thermal demagnetization, Tapley Hill Formation.

TABLE 2.5

TAPLEY HILL FORMATION : Sample mean directions after thermal demagnetization, selected samples

Sample	N,R	D,I	D',I'
4	1, -	058,-32	062,-17
6	2,1.939	055,-30	058,-17
7B	2,1.939	055,-30	058,-17
8	2,1.975	027,-42	040,-48
9	1, -	053,-01	052,+13
10	2,1.957	055,-35	062,-09
11	3,2.690	004,-27	018,-23
12	2,1.979	351,-39	017,-39
27	2,1.995	126,+66	047,+13
28	3,2.706	055,-36	069,-10
31	3,2.703	029,+05	025,+07
32	2,1.950	061,-11	061,+13
MEAN:		043,-19 (k=4.6,R=9.621)	047,-09 (k'=9.2,R'-10.810)

CORRECTED POLE POSITION : 39S,028E dp,dm=08,15

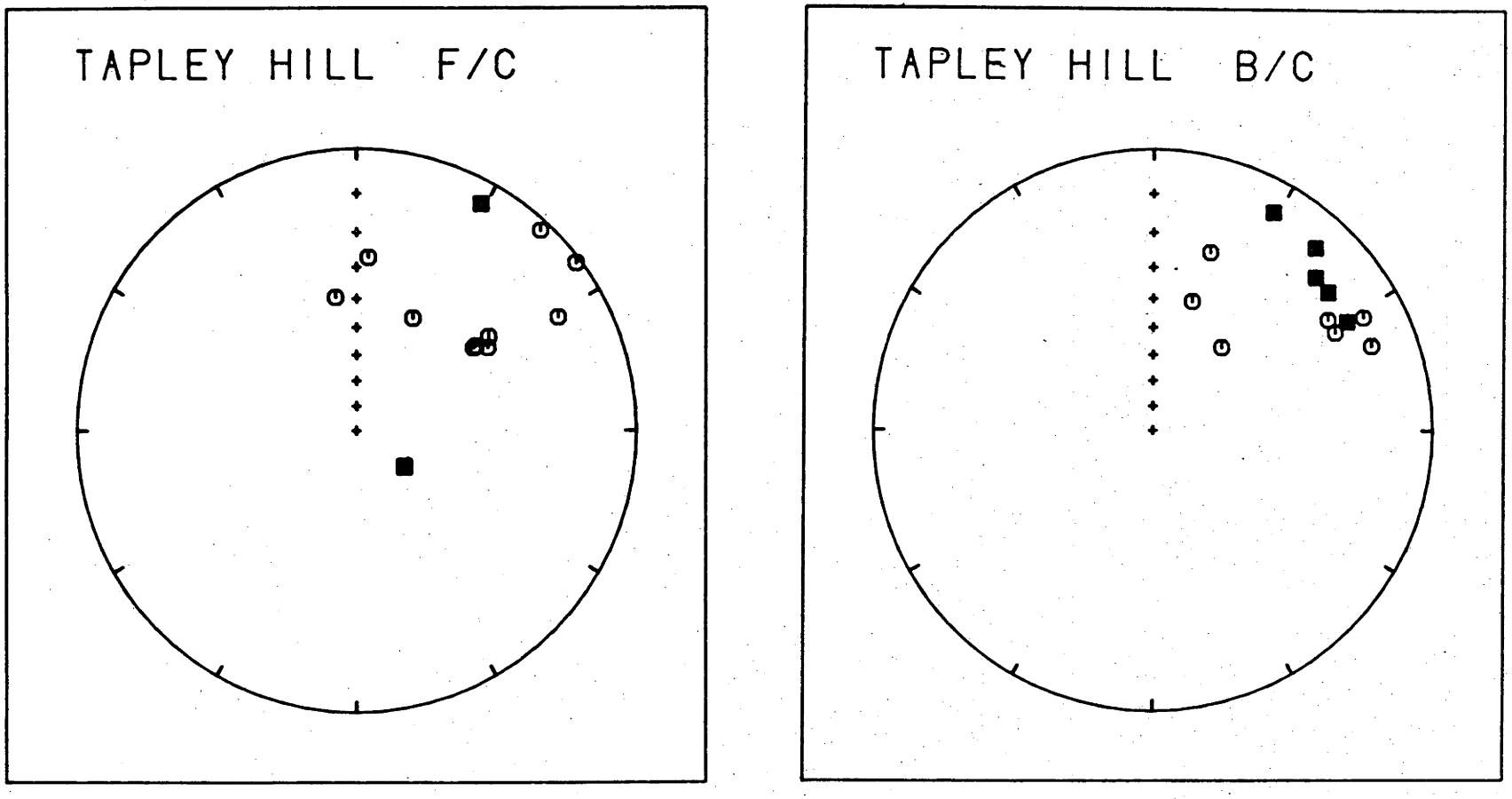

Figure 2.16 : Cleaned sample mean directions, Tapley Hill Formation; equal-angle projection. Open (closed) symbols refer to negative (positive) inclination.

reflected not a depositional or diagenetic magnetization, but a magnetization acquired during or just after the Cambro-Ordovician Delamerian metamorphism.

Samples of the Tapley Hill Formation were collected at a number of sites in the North Flinders Ranges (Figure 2.5). The dominant lithologies sampled were dark grey laminated shales and siltstones. NRM directions were not significantly different from the PEF direction, to judge by the site mean directions and associated error circles. Pilot thermal demagnetization studies of 1 specimen from each of the samples revealed three types of magnetization. Some pilot specimens exhibited weak but stable magnetizations directed along the PEF direction with no indication of another magnetic component. Others showed no signs of directional stability; magnetizations in these specimens became extremely weak at low temperatures, with large fluctuations in direction between heating steps. The remanence vector of the third class of pilot specimens (12 total) tended to swing away from the PEF direction and reach a moderately stable endpoint in the 300°-450° range, with a shallow northeasterly trend (Figure 2.15). Remaining specimens from these 12 samples were treated in bulk at 350°. Cleaned results are listed in Table 2.5.

Upon structural correction, the mean direction (unit weight to samples) changes by about 10°, however the increase in precision is nearly significant at the 95% level (k'/k=2.00, 95% significance point ≅2.02). The pole position calculated from the corrected mean direction is near the pole from the Ordovician Tumblagooda Sandstone (Embleton and Giddings, 1974). While the improvement in precision is marginally short of being significant at the 95% level, the fold test strongly

suggests that the magnetization dates from pre-folding times. A Precambrian rather than Paleozoic age of magnetization is favoured.

§2.7.6 Angepena Formation (Farina Sub-Group)

In the Copley area the Tapley Hill Formation intertongues with, and is overlain by the Balcanoona Formation, a series of oolitic algal limestones passing gradually upwards into dolomitic layers with minor red shales at the top. The Angepena Formation, a group of red and purple micaceons siltstones and shales, intertongues with the upper part of the Balcanoona Formation and also contains oolites and stromatolites. The Angepena Formation therefore occupies a slightly higher stratigraphic position in the Farina Sub-Group than the Tapley Hill Formation. Samples of the Angepena Formation were taken at one locality, a steep cliff face east of the main Paralana fault system just north of Balcanoona Station (Figure 2.5).

Palaeomagnetic results are summarized in Table 2.6. The NRM directions are widely scattered with a general shallow northeasterly trend. Upon progressive thermal demagnetization (Figure 2.17), magnetizations become very weak but stabilize in direction in the 500°-580° range. Cleaned directions form a reasonably tight grouping, here designated the AF1 magnetization. During thermal demagnetization, a component with a southerly trending declination and steep positive inclination is consistently removed in the 350°-400° and 400°-450° heating steps. This component is called the AF2 magnetization and is significantly different from the stable direction reached at higher temperatures.

As samples were taken from only one locality with a

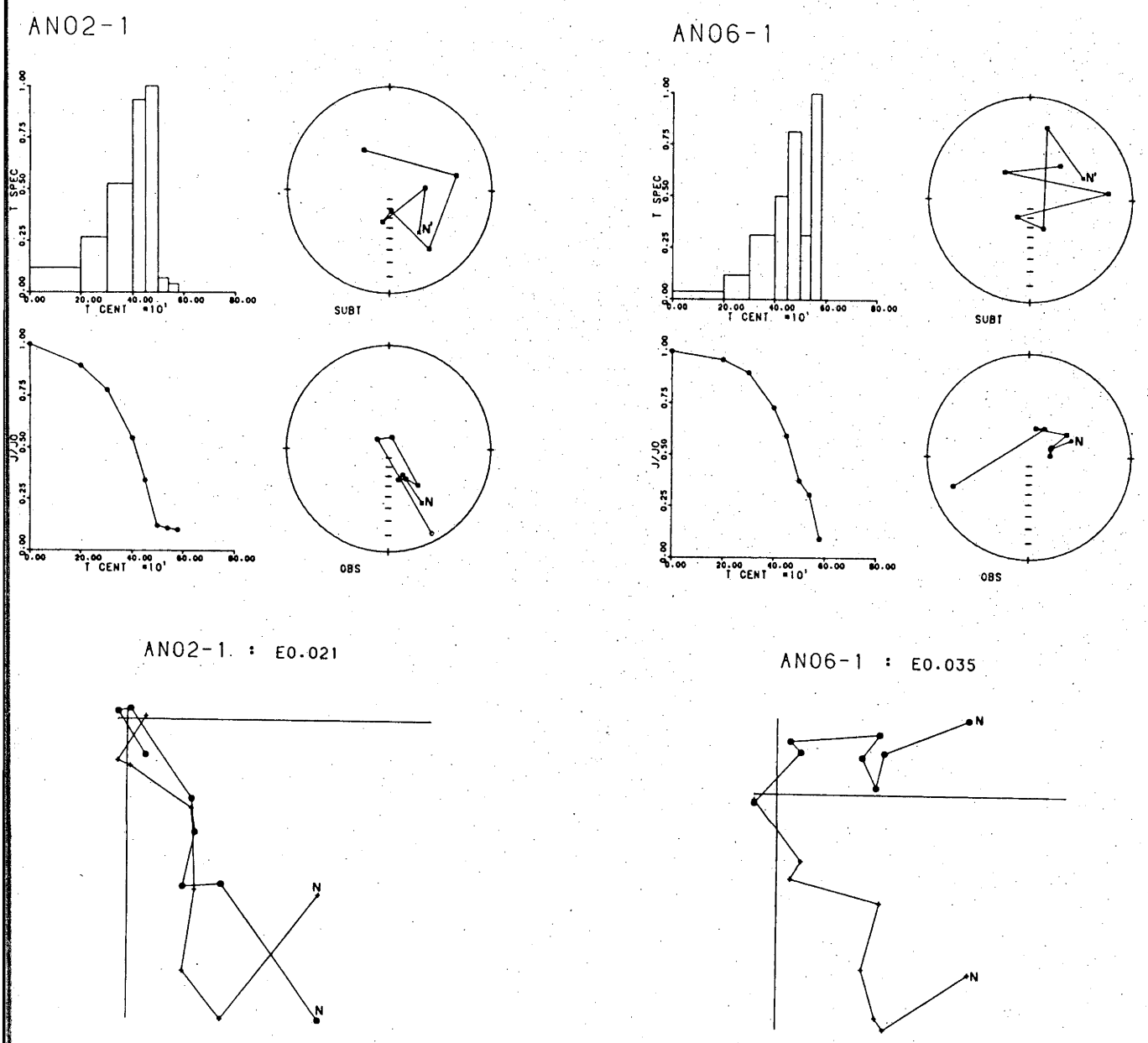

Figure 2.17 : Thermal demagnetization, Angepena Formation.

TABLE 2.6 (A)

ANGEPENA FORMATION : Site mean directions before and after thermal demagnetization

		NRM				540°C					
MAGNETIZATION	SITE	n	R	D	I	n	R	D	I	D'	I'
	1	3	1.388	087	65	3	2.849	003	48	001	48
	2	3	2.580	026	16	3	2.954	030	39	026	36
AF1	3	3	2.397	010	-01	3	2.669	024	44	021	42
	4	3	2.389	058	19	3	2.870	043	28	038	25
	5	3	2.057	012	-11	3	2.661	019	45	017	43
						3	2.939	180	72		
						3	2.972	180	72		
AF2						3	2.975	148	78		
						2	1.981	189	82		
						3	2.951	181	75		

TABLE 2.6 (B)

ANGEPENA FORMATION : Mean directions after thermal demagnetization, observed and subtracted vectors

	Before structural correction									After structural correction						
							pole							pole		
MAGNETIZATION	N	(W)	R	k	D_m	I_m	lat	long	dp,dm	R'	k'	D_m'	I_m'	lat	long	dp,dm
AF1	5	15	4.887	35.3	025	41	31S	346E	10,16	4.887	35.3	022	39	33S	344E	9,16
AF2	5	14	4.982	217	183	76	57S	137E	09,10	4.982	217	157	75	55S	158E	9,10

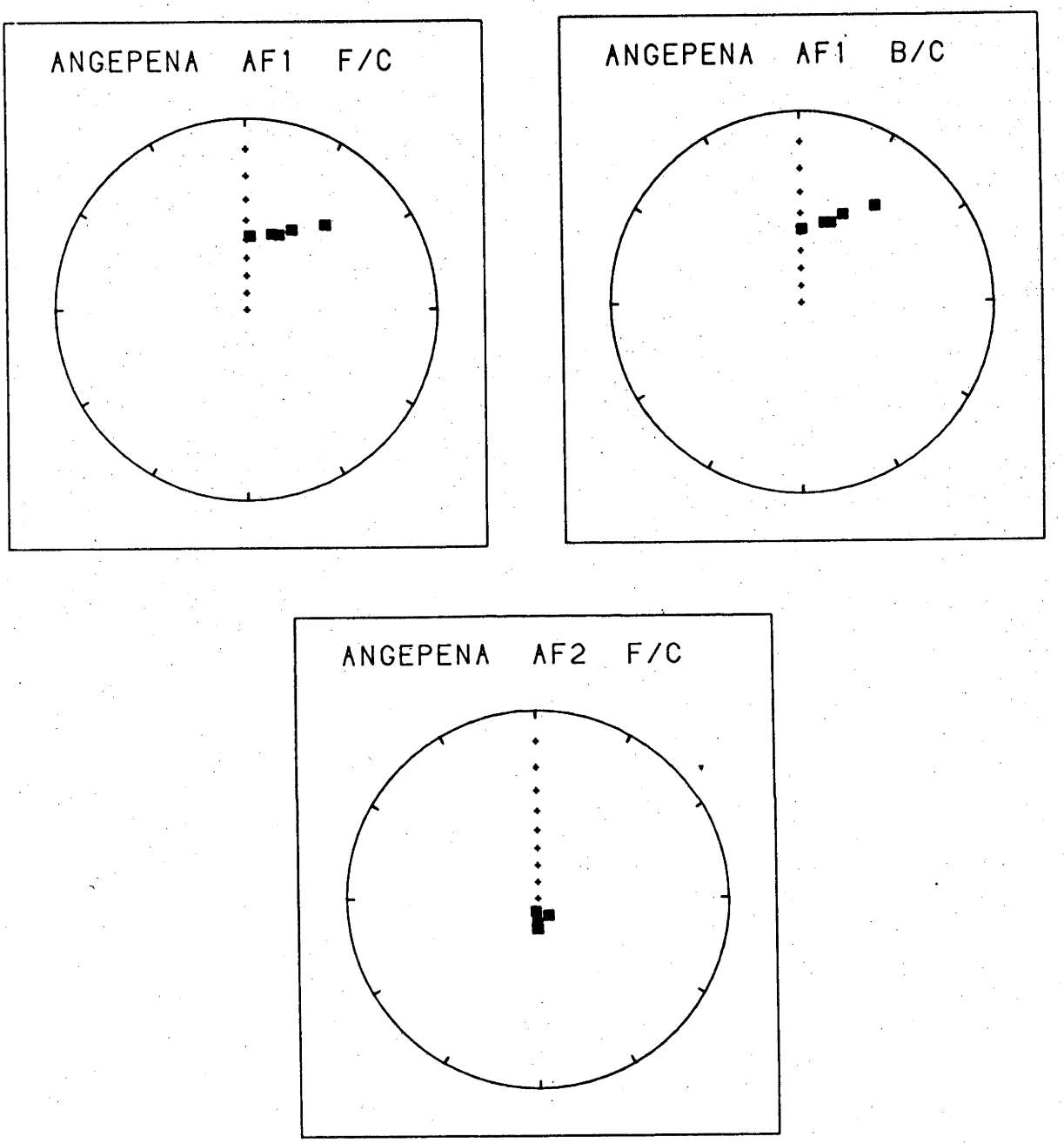

Figure 2.18 : Cleaned site mean magnetization directions, AF1 and AF2 components; equal-angle projection. Open (closed) symbols refer to negative (positive) inclination.

uniform dip, a fold test cannot be employed to test the relative ages of the AF1 and AF2 magnetizations. A simple and straightforward approach would suggest that the AF2 component, with a lower blocking temperature, is younger than the AF1 component. This possibility is supported by the fact that palaeomagnetic pole calculated from the AF1 direction is quite similar to poles from other Adelaidean sediments with positive or near-positive fold tests (Figure 2.27) and dissimilar to any part of the Phanerozoic apparent polar wander path. Further, the AF2 pole is not significantly different from the mean Cretaceous and early Tertiary poles for Australia (Schmidt, 1976). As the main period of epeirogenic uplift, stabilization and dissection of the North Flinders area occurred in early Tertiary times (Thomson, 1969, Coats and Blissett, 1971), it seems feasible that the AF2 magnetization is a low temperature PTRM acquired during or just after uplift, and that the AF1 component is probably a diagenetic CRM. Alternatively, if both magnetizations are CRM's, their relative ages might not be expected to follow the blocking temperature-age relationship suggested. At present an age sequence AF1→AF2 is regarded as most likely to be correct.

§2.7.7 Balparana Sandstone, Mount Curtis Tillite, Fortress Hill Formation (Yerelina Sub-Group)

The Yerelina Sub-Group is the youngest subdivision of the Umberatana Group. It consists of four members, the Elatina Formation, Balparana Sandstone, Mount Curtis Tillite and Fortress Hill Formation. With the exception of the Elatina Formation, all of these units were sampled in detail in order to obtain a reliable palaeomagnetic pole position from the

Plate 3 - Mount Curtis Tillite

Plate 4 - tillite in Areyonga Formation

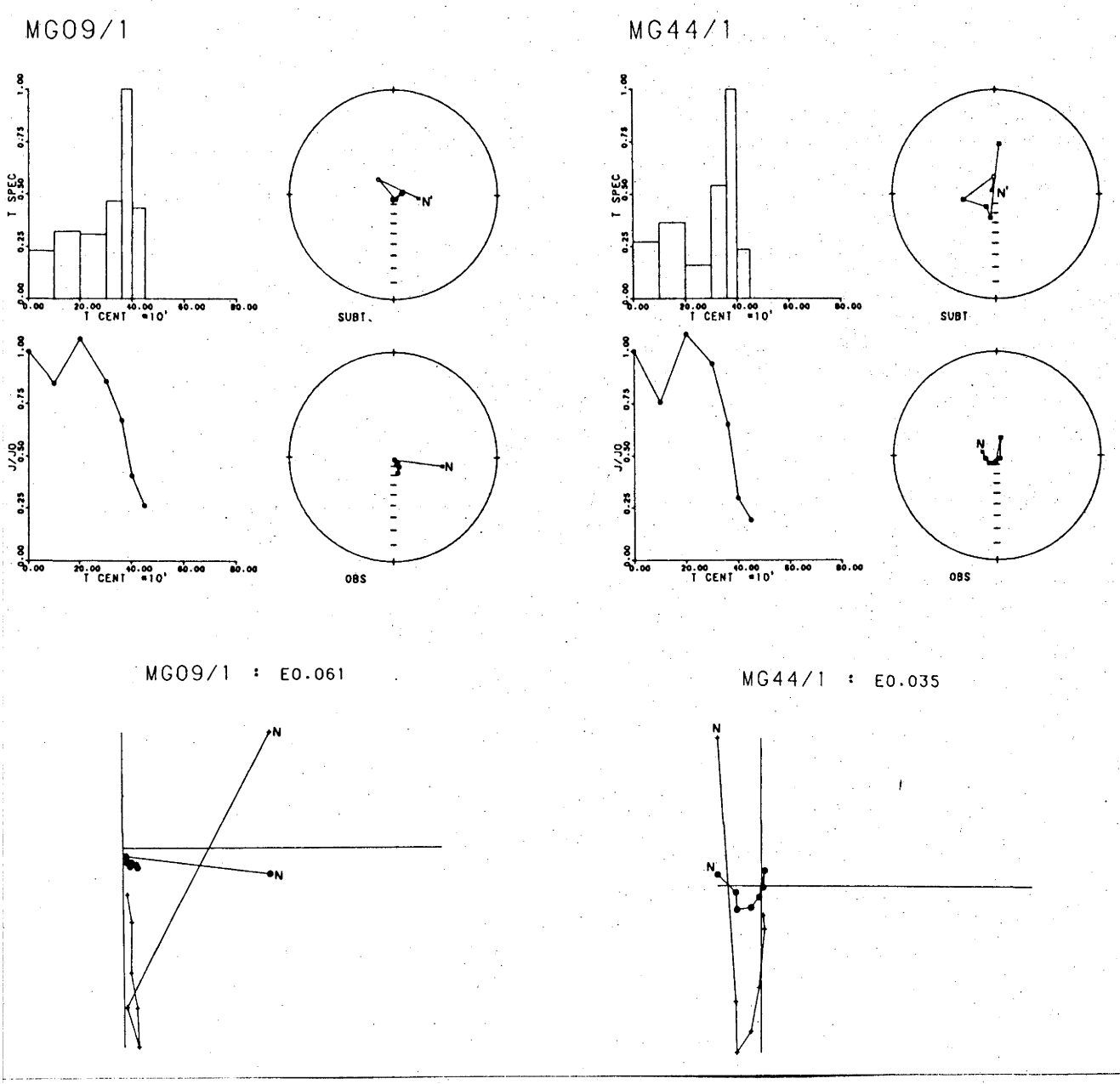

Figure 2.19 : Thermal demagnetization, Yerelina Sub-group.

TABLE 2.7 (A)

YERELINA SUB-GROUP : Site mean directions before and after thermal demagnetization

	NRM				350°					
SITE	N	R	D	I	N	R	D	I	D'	I'
1	3	1.540	167	37	3	2.708	155	52	167	-04
2	2	1.992	102	38	2	1.987	107	56	142	19
3	3	1.699	159	-42	3	2.763	135	72	163	21
4	3	2.379	085	-65	3	2.929	054	82	166	31
5	3	2.621	024	-12	3	2.944	039	70	154	43
6	3	2.390	215	-02	3	2.974	155	68	169	08
7	3	2.343	185	-43	3	2.968	157	64	168	05
8	3	2.761	053	-47	2	1.891	039	-58	087	-38
9	3	1.421	323	-28	2	1.918	241	60	305	28
10	3	2.746	237	57	3	2.856	239	58	279	26
11	2	1.762	280	-46	(random)					
12	2	1.711	284	-56	(random)					
13	2	1.739	182	-83	(random)					
14	2	1.296	086	-11	(random)					
15	2	1.955	075	-70	(random)					
16	4	3.413	015	-57	4	3.710	059	58	082	45
17	4	3.956	309	-71	4	3.887	270	81	023	75

TABLE 2.7 (B)

YERELINA SUB-GROUP : Mean directions after thermal demagnetization

	Before structural correction									After structural correction						
							pole							pole		
MAGNETIZATION	N	n	R	k	D_m	I_m	lat	long	dp,dm	R'	k'	D_m'	I_m'	lat	long	dp,dm
Y1	12	35	9.181	11.0	169	75	58S	149E	26,28	6.513	2.6	184	33	77S	337E	25,43
Y2	12	42	11.660	32.3	028	-81	45S	127E	14,15	8.908	3.6	010	-63	74S	293E	34,43

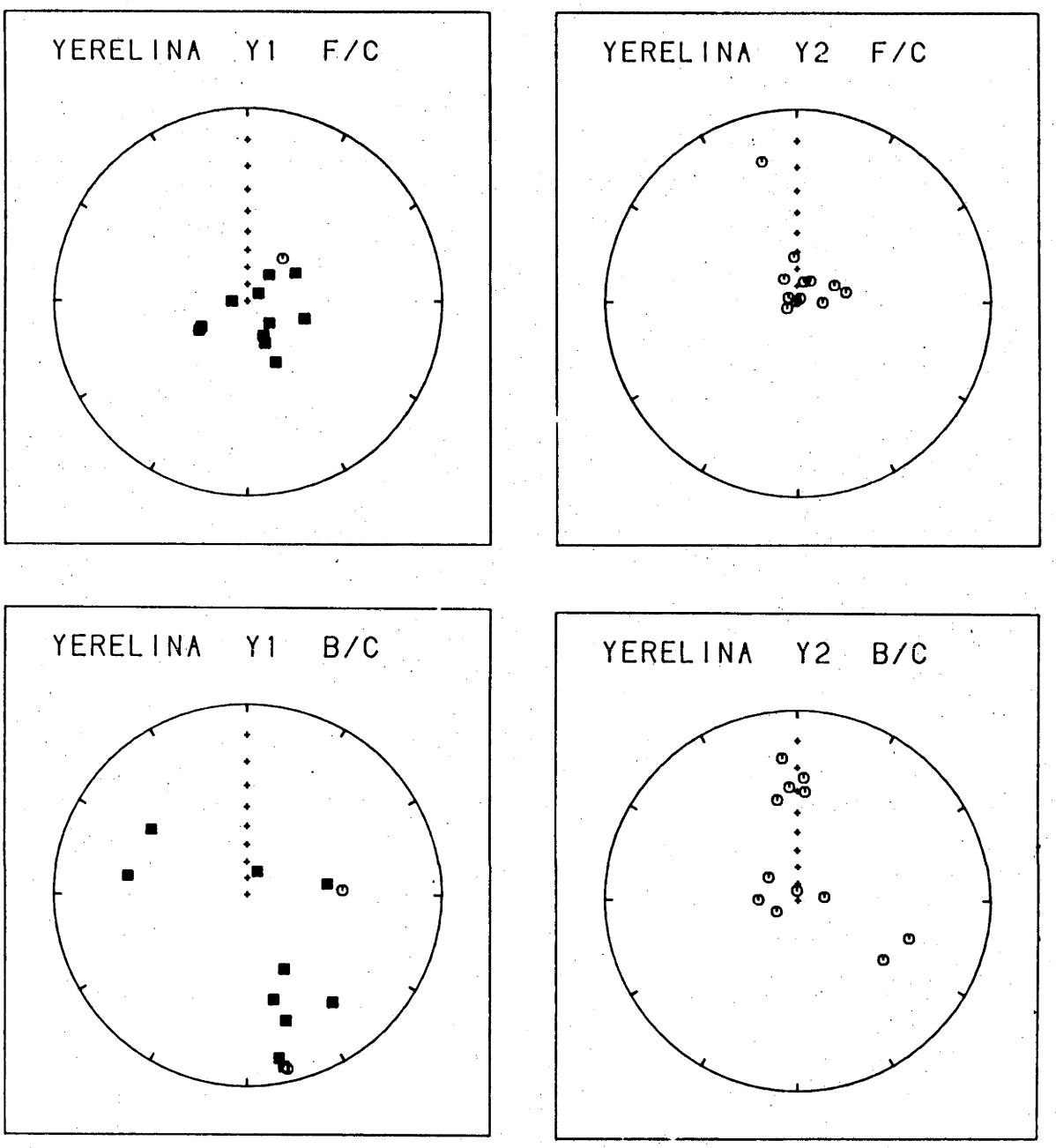

Figure 2.20 : Cleaned site mean magnetization directions, Y1 and Y2 components; equal-angle projection. Open (closed) symbols refer to negative (positive) inclination.

plotted before and after structural correction in Figure 2.20. Clearly the fold test is negative for both the Y1 and Y2 magnetizations. The precision parameter k decreases from 11.0(32.3) to 2.6(3.6) for the Y1(Y2) magnetization (Y1:k'/k=0.24, 95% significance point ≅0.50; Y2:k'/k=0.11, 95% significance point ≅0.50). It must therefore be assumed that both the Y1 and Y2 magnetizations were acquired after folding of the Yerelina Sub-Group occurred. The palaeomagnetic pole calculated from the uncorrected Y1 mean direction is similar to the AF2 pole and also to other Tertiary poles from Australia (Figure 2.27). An explanation for Tertiary remagnetization during or after uplift of the Yerelina Sub-Group similar to that of the AF2 magnetization in the Angepena Formation could be invoked, especially in view of the low blocking temperatures.

The pole from the Y2 direction is not similar to early Tertiary or late Cretaceous poles, but is more consistent with a Permo-Triassic age of magnetization (Figure 2.27). As it has a lower T_b than the Y1 magnetization, the similarity with poles older than Y1 is puzzling, though not inexplicable if both Y1 and Y2 are CRM's as discussed in the previous section.

§2.7.8 Brachina Formation/Ulupa Siltstone (Wilpena Group)

Glacial sedimentation ceased after deposition of the Yerelina Sub-Group. Shallow water continental sediments of the Wilpena Group conformably overlie the Marinoan glacial strata. The uppermost unit in the Wilpena Group, the Pound Quartzite, is immediately overlain by Cambrian sediments of the Hawker Group. The Wilpena Group therefore constitutes the youngest Precambrian stratigraphic unit in the Adelaide 'Geosyncline'. Upper Adelaidean sections from elsewhere in Australia, notably

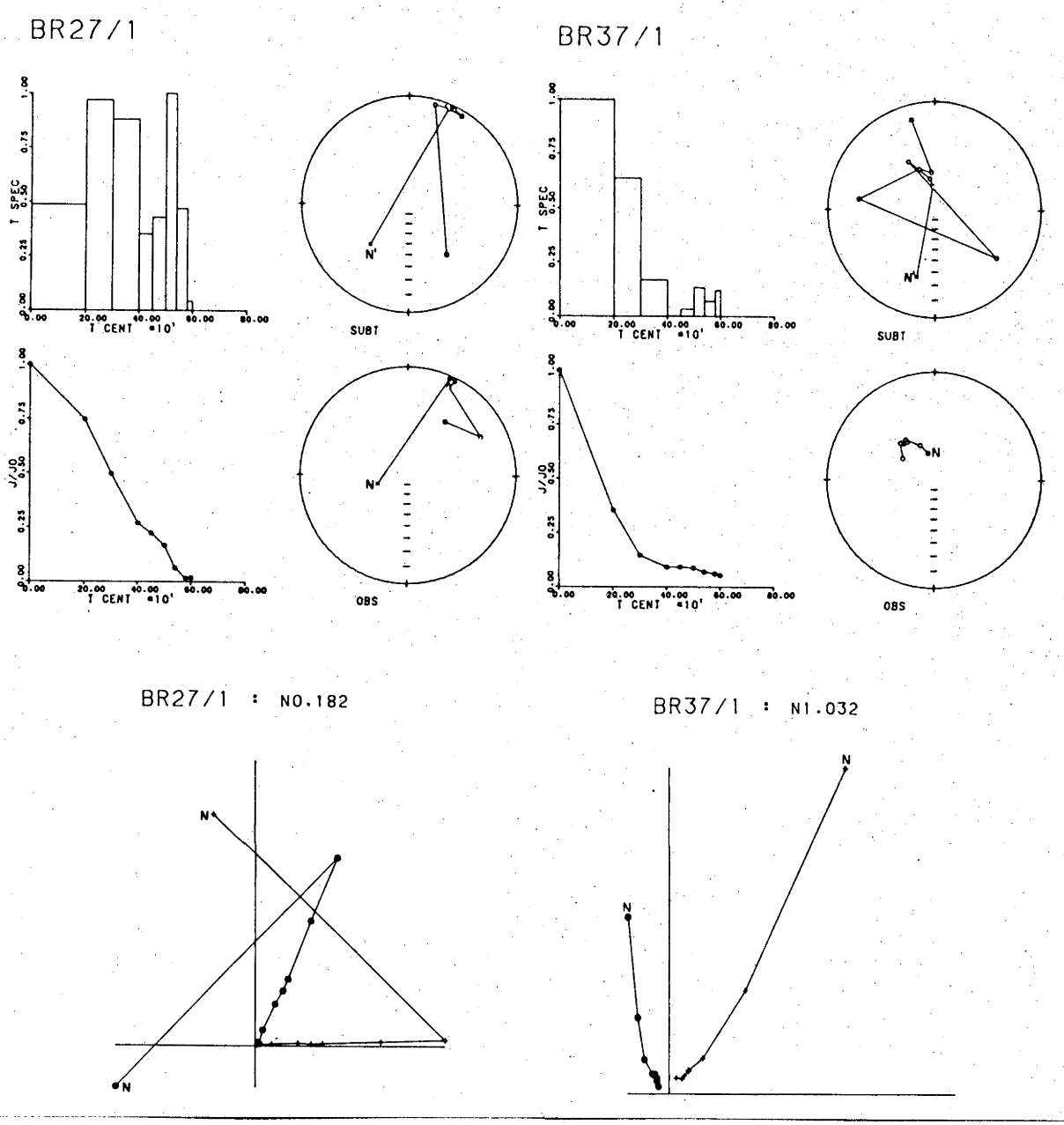

Figure 2.21 : Thermal demagnetization, Brachina Formation.

TABLE 2.8 (A)

BRACHINA FORMATION : Site mean directions before and after thermal demagnetization

	NRM				350°					
SITE	n	R	D	I	n	R	D	I	D'	I'
1	3	2.450	159	-52	3	2.827	186	-29	163	-23
2	3	2.338	302	-80	2	1.901	229	-18	196	-47
3	3	2.313	112	-69	3	2.691	205	-39	158	-36
4	3	2.203	118	-58	3	2.746	203	-19	178	-27
5	4	2.702	256	-78	4	3.259	183	36	004	57
6	4	2.283	124	-84		(random)				
7	4	3.393	332	-73		(random)				
8	4	3.592	045	-38		(random)				
9	4	2.385	115	-81		(random)				
10	3	2.772	239	-29		(random)				
11	3	2.627	313	-49		(random)				
12	3	2.268	013	-17	3	2.812	229	-31	229	-41
13	3	2.555	328	-48	3	2.659	226	-60	203	-56
14	3	2.581	270	-61	3	2.685	231	-50	214	-47

TABLE 2.8 (B)

BRACHINA FORMATION : Mean direction after thermal demagnetization

Before structural correction									After structural correction						
						pole							pole		
N	n	R	k'	D_m	I_m	lat	long	dp,dm	R'	k'	D_m'	I_m'	lat	long	dp,dm
8	24	6.458	4.5	220	-44	22S	357E	23,37	7.477	13.4	189	-44	33S	328E	12,20

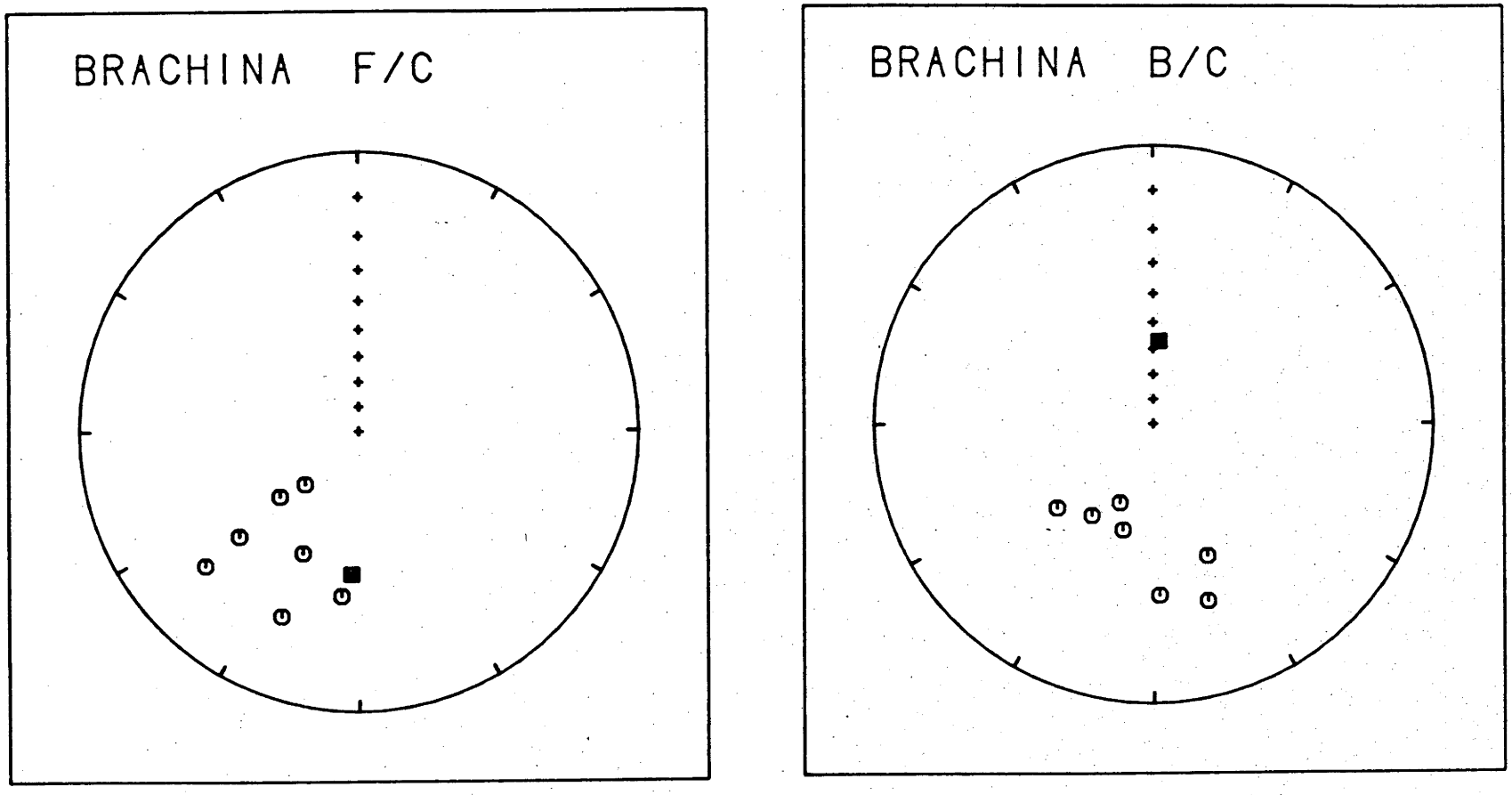

Figure 2.22 : Cleaned site mean magnetization directions, Brachina Formation; equal-angle projection. Open (closed) symbols refer to negative (positive) inclination.

the Amadeus Basin, have lithologies and trace fossils remarkably similar to those of the Wilpena Group.

The base of the Wilpena Group is defined in the North Flinders Ranges by the Nuccalena Formation, a persistent pink dolomitic layer useful as a marker horizon. The Brachina Formation and Ulupa Siltstone immediately overlie the Nuccalena Formation and are the most widespaced units in the Wilpena Group. The Brachina Formation is defined in the western part of the North Flinders and comprises a thick sequence of red and green ripple marked siltstones. To the east the Ulupa Siltstone is a lateral equivalent of the Brachina Formation consisting of a thick monotonous sequence of green siltstones. Samples of the Brachina Formation and Ulupa Siltstone (hereafter referred to as Brachina Formation only) were obtained at 7 localities (Figure 2.5). Palaeomagnetic results are listed in Table 2.9.

NRM directions were scattered but generally directed towards the PEF direction. Pilot thermal demagnetization of one specimen from each sample showed that only one stable magnetization was present (Figure 2.21) at 8 sites; the remaining 6 sites exhibited moderately stable but widely scattered inconsistent directions. Bulk treatment of remaining specimens at 540° yielded significant site mean directions at the former 8 sites. At the latter 6 sites which showed only moderate stability, site mean directions were random at the 95% level.

The 8 significant sites give a mean uncorrected direction of 220,-74, still with marked scatter. Upon structural correction the precision parameter k increases from 4.5 to 13.4, significant at the 95% confidence level (k'/k=2.98, 95%

significance point ≅2.42), suggesting that the magnetization was acquired before Cambrian folding occurred. The palaeomagnetic pole calculated from the formation mean direction is near other poles from the Adelaide 'geosyncline' and is distinctly removed from any part of the Phanerozoic apparent polar wander path, supporting the hypothesis of primary magnetization.

§2.7.9 Bunyeroo Formation (Wilpena Group)

The ABC Range Quartzite overlies the Brachina Formation in the western part of the North Flinders Ranges. The Bunyeroo formation occurs immediately above the ABC Quartzite in the west and just above the Ulupa Siltstone in the east, and is made up of a thin sequence of dark red and purple shales. These are 'typical'red beds, and contain sun cracks and other sedimentary structures indicative of a shallow water to subaerial environment. Samples were taken at four localities distributed about the southern part of the North Flinders (Figure 2.5). Samples were taken at a fifth locality (sites 1-3 omitted from Table 2.9); subsequent mapping revealed that these samples were in a complex structural position and were actually contorted red shales which were part of the overlying Pound Quartzite.

Samples from the former 4 localities exhibited quite stable magnetizations during thermal demagnetization (Figure 2.23). Within-site scatter was minimized generally in the 540°-580° range, and a temperature of 560° was chosen for final bulk treatment. Cleaned site mean directions are listed in Table 2.9 and plotted in Figure 2.24. Overall precision increases markedly upon making structural correction, however the increase is not significant at the 95% confidence level (k'/k=1.64, 95% significance point ≅2.29). The pole position calculated from

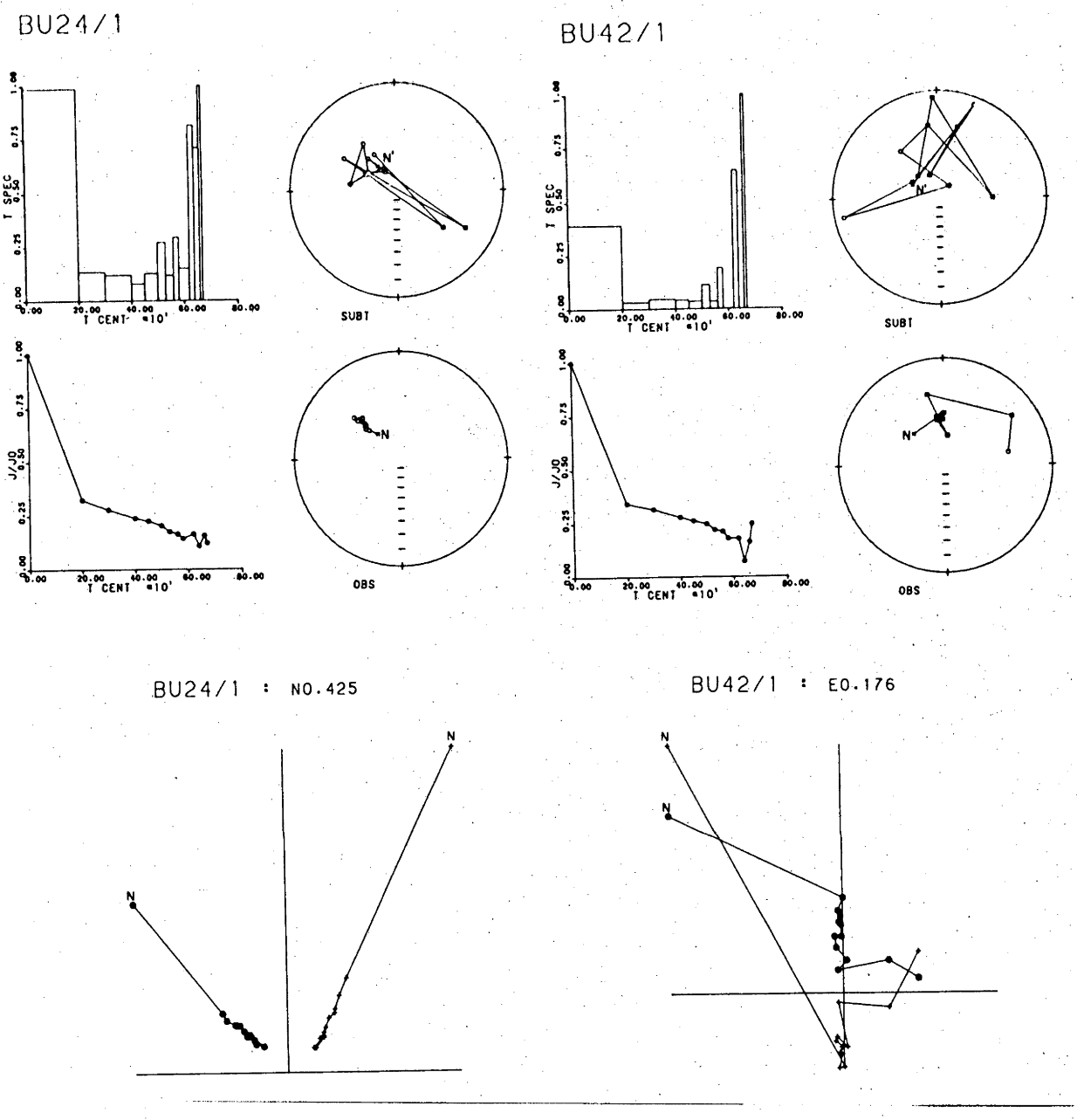

Figure 2.23 : Thermal demagnetization : Bunyeroo Formation.

TABLE 2.9 (A)

BUNYEROO FORMATION : Site mean directions before and after thermal demagnetization

	NRM				350°					
SITE	n	R	D	I	n	R	D	I	D'	I'
4	4	3.707	302	-55	2	1.938	251	-52	241	-59
5	4	3.570	307	-60	4	3.912	240	-32	234	-38
6	4	3.944	025	-48	4	3.968	052	07	051	13
7	4	3.785	297	-51	4	3.543	283	-01	281	-45
8	4	3.765	284	-34	4	3.986	267	-07	262	-31
9	4	3.517	284	-54	4	3.864	254	-07	245	-36
10	3	2.779	285	-02	3	2.921	263	-06	247	-49
11	3	1.960	340	-14	3	2.926	064	-02	052	31
12	3	2.296	006	-48	3	2.931	067	-00	070	49

TABLE 2.9 (B)

BUNYEROO FORMATION : Mean direction after thermal demagnetization

Before structural correction									After structural correction						
N	n.	R	$\hat{k}$	D_m	I_m	pole lat	pole long	dp,dm	R'	$\hat{k}'$	D_m'	I_m'	pole lat	pole long	dp,dm
9	31	8.341	12.1	254	-12	10S	035E	8,16	8.596	19.8	246	-40	07S	017E	9,14

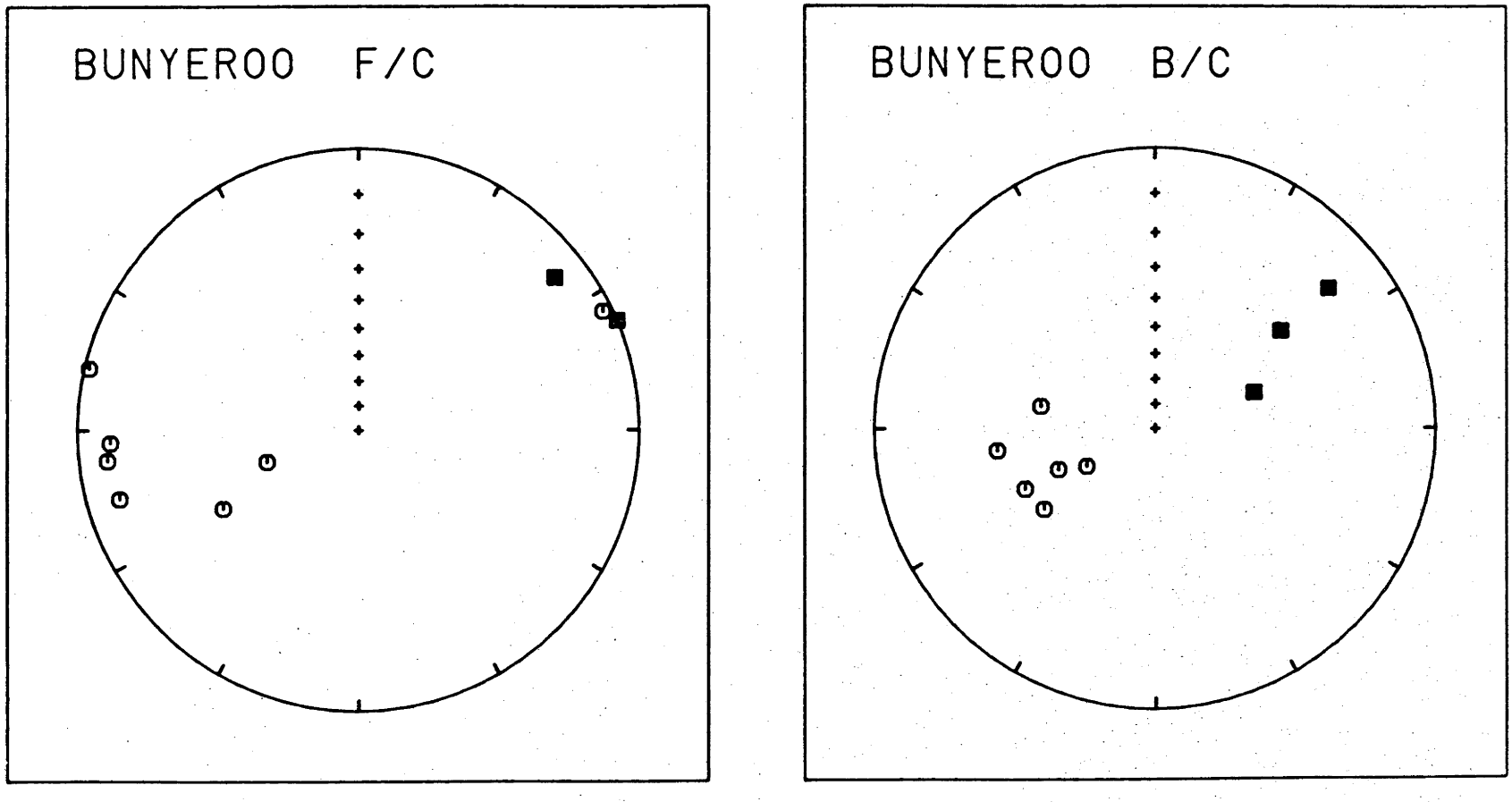

Figure 2.24 : Cleaned site mean magnetization directions, Bunyeroo Formation; equal-angle projection. Open (closed) symbols refer to negative (positive) inclination.

the structurally corrected mean direction is distinct from the underlying units (Figure 2.27), but close to some of the lower Cambrian poles. The pole does not lie near any part of the younger Phanerozoic apparent polar wander path. Although the positive fold test is not statistically significant and therefore does not definitively prove that the stable remanence of the Bunyeroo Formation was acquired before folding, the strong increase in precision combined with the incompatibility of the pole position with the younger Phanerozoic APWP are consistent with an original rather than secondary magnetization.

§2.7.10 Pound Quartzite (Wilpena Group)

The Bunyeroo Formation is overlain by up to 7000 m of sediments which form the upper part of the Wilpena Group. These overlying sediments are grouped into three units, the Wonoka Formation, Billy Springs Beds and Pound Quartzite. The Pound Quartzite is recognized as the youngest Precambrian rock unit in the Adelaide 'Geosyncline', and is overlain in the North Flinders Ranges by the Hawker Group, containing abundant Lower Cambrian fossils, such as *archaeocyathids*, brachiopods and trilobites. The Pound Quartzite contains the well-known *Ediacara* fauna, a rich assemblage of body and trace fossils of which at least 34 different varieties have been identified. Body and trace fossils thought to be elements of the same fauna have been found on other continents and elsewhere in Australia at roughly similar stratigraphic levels (Glaessner, 1971).

The Pound Quartzite includes two members, a white massive quartzite (Rawnsley Quartzite), underlain by a red feldspathic sandstone with heavy mineral bands (Bonney Sandstone; Forbes, 1971). Both members have a wide distribution; the upper

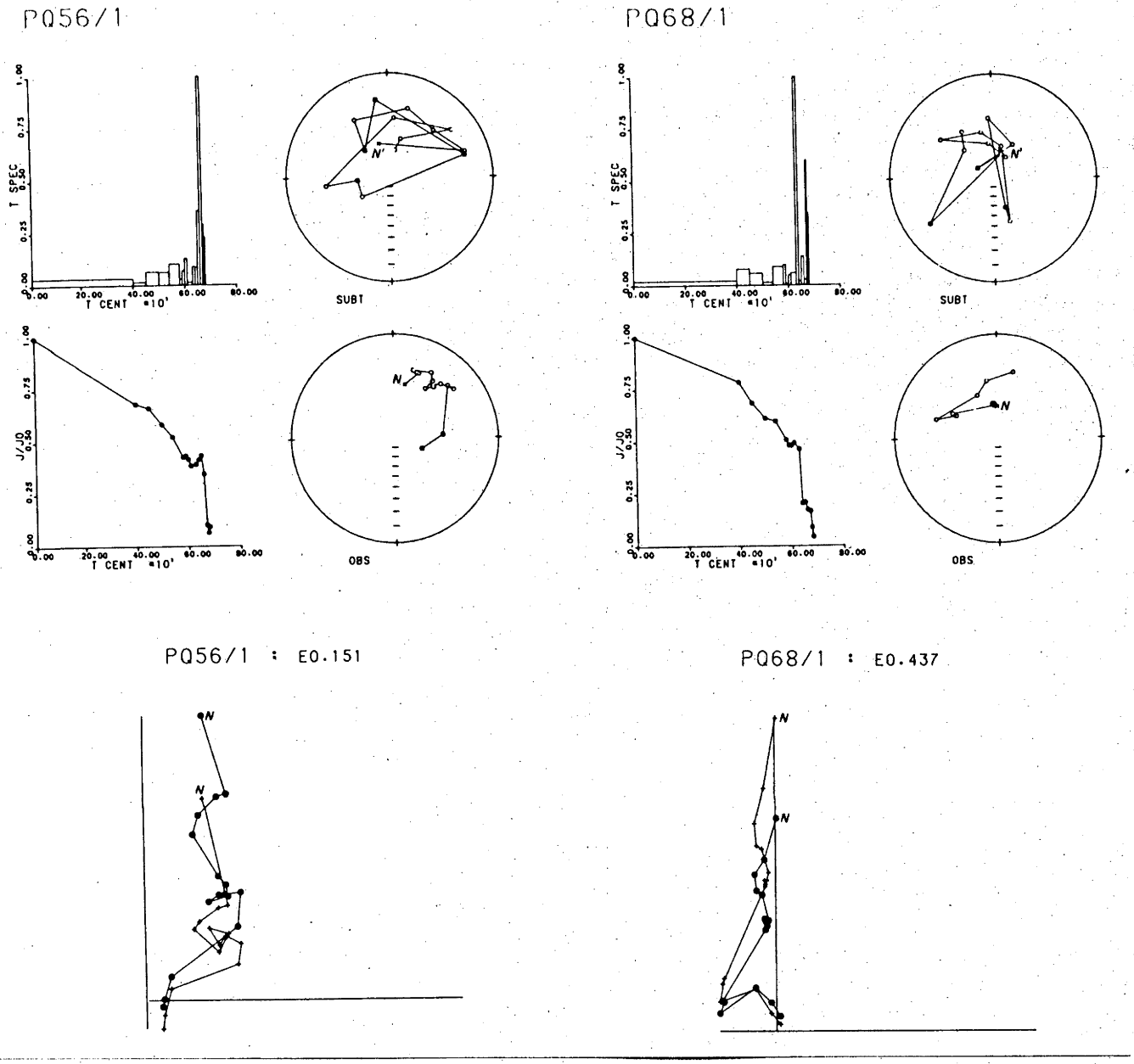

Figure 2.25(A) : Thermal demagnetization, Pound Quartzite.

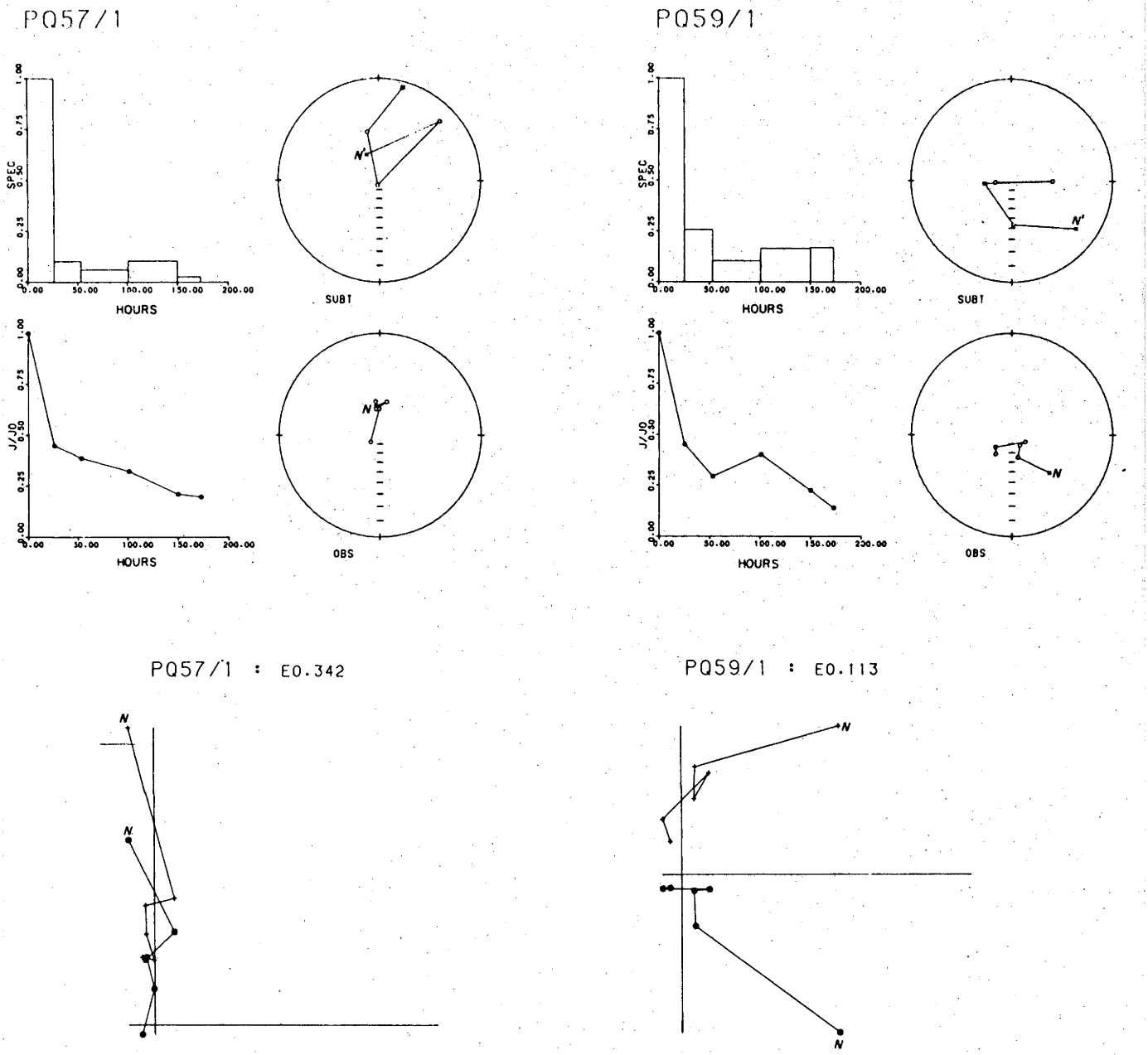

Figure 2.25(B) : Chemical demagnetization, Pound Quartzite.

TABLE 2.10

POUND QUARTZITE : Site mean directions (non-random sites only) after chemical demagnetization; in geographic coordinates

SITE	N,R	D	I
3[1]	3,2.840	309	-77
4[1]	3,2.735	028	-79
5[1]	3,2.786	011	-75
6[1]	3,2.653	330	-58
7[1]	3,2.902	325	-54
1[2]	5,4.245	318	-63
6[2]	5,4.283	005	-73
7[2]	6,5.402	334	-78
Mean :	8,7.825	337	-71

Pole position : 61S,166E (dp,dm = 13,15)

[1] supplementary collection

[2] original collection

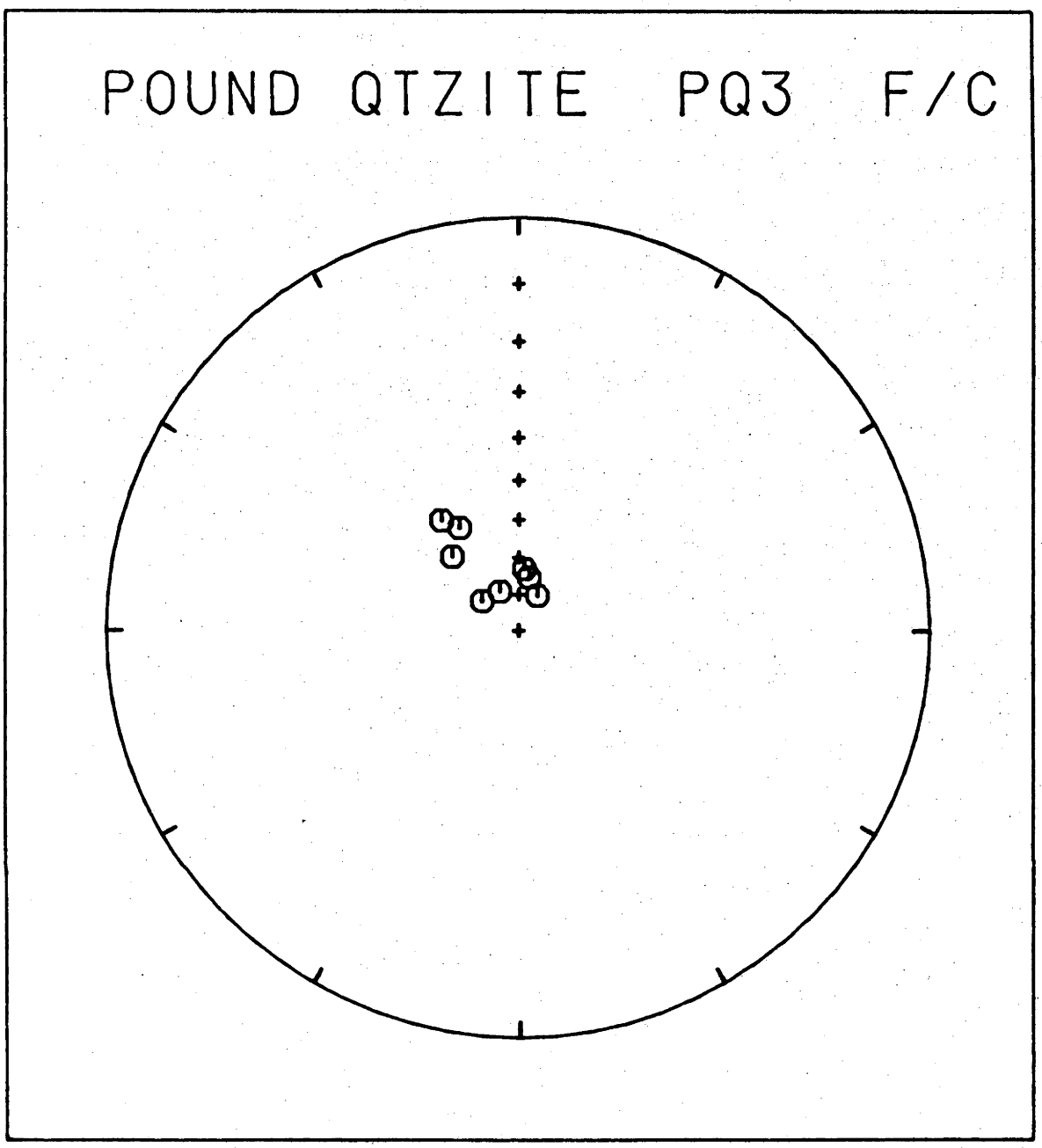

Figure 2.26 : Cleaned site mean magnetization directions, Pound Quartzite PQ3 component; equal-angle projection. Open (closed) symbols refer to negative (positive) inclination.

white quartzite unit is largely responsible for the rugged topography of the North Flinders Ranges and has been a major contributor in the preservation of underlying Adelaidean strata.

Embleton and Giddings (1974) reported palaeomagnetic results from 10 samples of the lower Bonney Sandstone member. They collected 39 samples at 3 localities in the North Flinders Ranges (Figure 2.5). After progressive thermal demagnetization of 9 specimens, three types of magnetization were observed: a) directions initially close to the PEF direction which remained essentially unchanged during demagnetization, b) directions initially removed from the PEF direction which were stable and remained unchanged during demagnetization, and c) directions initially close to the PEF direction which underwent substantial angular changes at low temperatures, stabilizing in the 440°-630° range. After bulk thermal treatment, all but 10 samples had random mean directions at the 95% confidence level. A recalculation of the mean directions listed in Giddings (1974) shows that the structurally uncorrected mean direction has a precision of 5.0 and not 4.7 as listed. The decrease in precision upon making the structural correction is not significant at the 95% level (k'/k=0.94, 95% significance point $\cong$0.46), however the presence of a post-folding magnetization is suggested.

One of the difficulties encountered in the original study was that of measuring the very weak magnetizations using equipment available at the time. Since then, more modern and sensitive magnetometers had been installed in the laboratory, hence a supplementary collection of the Pound Quartzite was made. Samples were taken from three localities in the North Flinders Ranges (Figure 2.5); two of these were where some of the previous samples collected by Embleton and Giddings (1974) were obtained.

Pilot studies of 2 specimens from each of 24 samples showed variable behaviour upon thermal demagnetization (Figure 2.25). Directions from the Wilpena samples remained aligned with the PEF direction up to 675°, whereupon intensities decayed rapidly and random directional behaviour ensued. Samples from the Parachilna and Brachina localities exhibited stable directional behaviour in many cases, however within site and even within sample grouping was often random at the 95% confidence level and no systematic grouping of specimen directions was observed. Embleton and Giddings (1974) noted similar problems with their collection.

Chemical demagnetization studies were conducted on a third specimen cut from each of the above 24 samples and from 24 additional specimens obtained from the original collection which had not been thermally treated. Typical results are shown in Figure 2.25. Directions remain reasonably stable during leaching, while intensities of magnetization decay to 10-15 percent of the NRM value. Internal inspection of test specimens after 150 hours in the acid bath showed that most of the red pigment originally present had been dissolved by this time. Again, although many specimens had attained stable directional characteristics, site mean directions were often random. Eight sites had non-random mean directions and yielded a mean direction just significantly different from the PEF direction (Table 2.10 and Figure 2.26). Precision decreases markedly upon making the structural correction; the negative fold test combined with the proximity of the pole position to the Cenozoic APWP for Australia (Figure 2.27) suggest aTertiary age of magnetization.

It was therefore not possible to duplicate or augment

the result for the Pound Quartzite reported by Embleton and Giddings (1974). Their pole position is problematic, as it lies in a position which does not appear to be consistent with the results from the underlying sediments.

§2.8 Summary of palaeomagnetic results from the Adelaide 'Geosyncline', the Adelaidean Polar Track, and the definition of Adelaidean time

Palaeomagnetic poles from Adelaidean and Cambrian rocks of the Adelaide 'Geosyncline' are listed in Table 2.11. The 12 poles of possible primary age and 10 poles of possible secondary age have been plotted in Figure 2.27. The lower Adelaidean poles form an APWP segment or "polar track" (Irving and Park, 1972) which follows in a logical sequence from the Wooltana Volcanics through to the Brachina Formation. Apart from the angular discordance between the Wooltana Volcanics and the Copley Quartzite, no significant polar gaps appear to be present in the lower and middle parts of the sequence. The polar gap separating poles WV1 and CQ is most likely due to a major unconformity within the Callana Beds, as discussed in §2.7.3. The absence of significant polar gaps in the CQ→BR sequence would imply that no major time gaps are present in the period of sedimentation recorded by the poles, assuming a reasonably constant rate of apparent polar motion.

The marked angular difference between the pole positions for the Wooltana Volcanics and the Copley Quartzite merits discussion in terms of the formal definition of Adelaidean time. Mapping conducted to date has not been able to establish whether or not the unconformity between the Upper and Lower Callana Beds represents a major time break. The palaeomagnetic results demonstrate that the two magnetizations

TABLE 2.11 (A)

Summary of palaeomagnetic poles from the Adelaide 'Geosyncline'

Symbol	Rock Unit	Probable Magnetization Age	Pole Position		dp,dm	Reference
Possible Primary Poles						
WV1	Wooltana Volcanics	PЄ(650-850?)	62S	142E	16,18	this study
CQ	Copley Quartzite	PЄ(<WV1)	50S	345E	07,15	this study
MT1	Merinjina Tillite	PЄ(<CQ)	45S	346E	06,11	this study
TH	Tapley Hill Formation	PЄ(<MT1)	39S	028E	08,15	this study
AF1	Angepena Formation	PЄ(<TH)	33S	344E	09,16	this study
BRK	Brachina Formation	PЄ(=BR?)	46S	356E	10,15	Karner (1975)
BRM	Brachina Formation	PЄ(<AF1)	33S	328E	12,20	this study
BU	Bunyeroo Formation	PЄ(<BR)	07S	017E	09,14	this study
PQ1[1]	Pound Quartzite	?PЄ(<BU)	60S	006E	13,26	Embleton & Giddings (1974)
AD	Aroona Dam sediments	Є&	36S	033E	10,19	Embleton & Giddings (1974)
LFL	Lake Frome Group (lower)	Єm	05S	023E	11,19	Embleton & Giddings (1974)
LFU	Lake Frome Group (upper)	Єu(<LFL)	40S	025E	09,19	Embleton & Giddings (1974)
Possible Secondary Poles						
WV3	Wooltana Volcanics	?O	36N	087E	13,26	this study
MT3	Merinjina Tillite	?O	01S	065E	08,14	this study
PQ3[2]	Pound Quartzite	?S-D	69S	335E	13,25	recalculated from Giddings (1974)
Y2	Yerelina Sub-Group	?P-T_R	45S	127E	14,15	this study
WV2	Wooltana Volcanics	?K-T	26S	143E	26,26	this study
MT2	Merinjina Tillite	?K-T	45S	153E	17,18	this study
AF2	Angepena Formation	?K-T	57S	137E	09,10	this study
Y1	Yerelina Sub-Group	?K-T	58S	149E	26,28	this study
MT4	Merinjina Tillite	?T	68S	139E	09,10	this study
PQ2	Pound Quartzite	?T	61S	166E	13,15	this study

[1]Structurally corrected
[2]Structurally uncorrected

Table 2.11 (B)

Summary of new palaeomagnetic results from the Adelaide 'Geosyncline'

Symbol	Rock Unit	Interpretation[1]
WV1	Wooltana Volcanics	primary
WV2	Wooltana Volcanics	secondary
WV3	Wooltana Volcanics	secondary, €-O(?)
CQ	Copley Quartzite	primary
MT1	Merinjina Tillite	primary
MT2	Merinjina Tillite	secondary, uPz-Mz
MT3	Merinjina Tillite	secondary, €-O(?)
MT4	Merinjina Tillite	secondary, T
TH	Tapley Hill Formation	primary (?)
AF1	Angepena Formation	primary
AF2	Angepena Formation	secondary, T
Y1	Yerelina Sub-Group	secondary, T
Y2	Yerelina Sub-Group	secondary, uPz(?),T(?)
BRM	Brachina Formation	primary
BU	Bunyeroo Formation	primary
PQ3	Pound Quartzite	secondary, T

[1] abbreviations: Pz(Palaeozoic), Mz(Mesozoic)

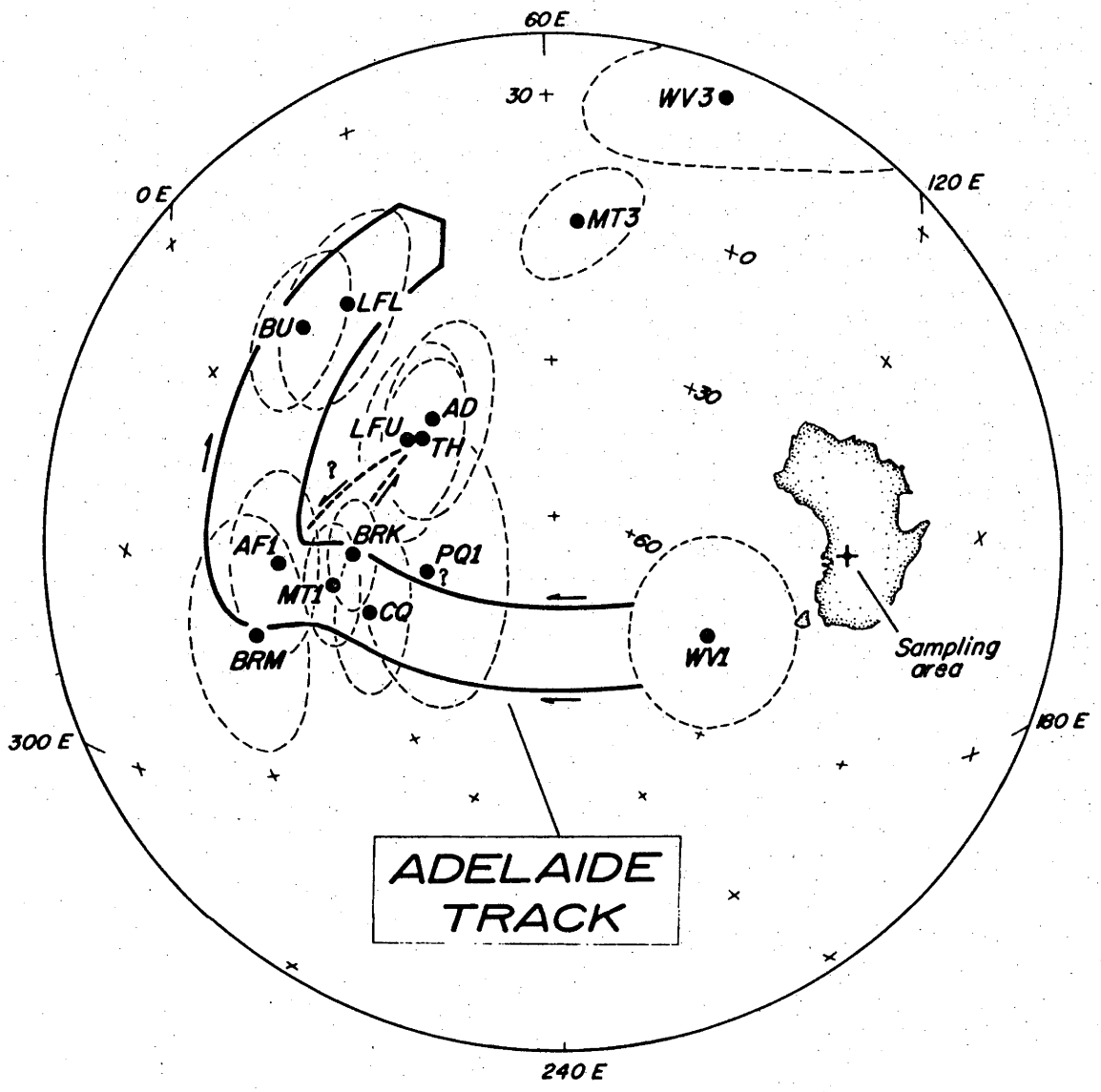

Figure 2.27(A) : The Adelaide Track, the late Precambrian APWP segment derived from Adelaide 'Geosyncline' rocks. Dashed ovals : 95% polar error ellipses dp, dm. Equal-area projection, radius 115°. Swathe width 15° at equator. Symbols as in Table 2.11.

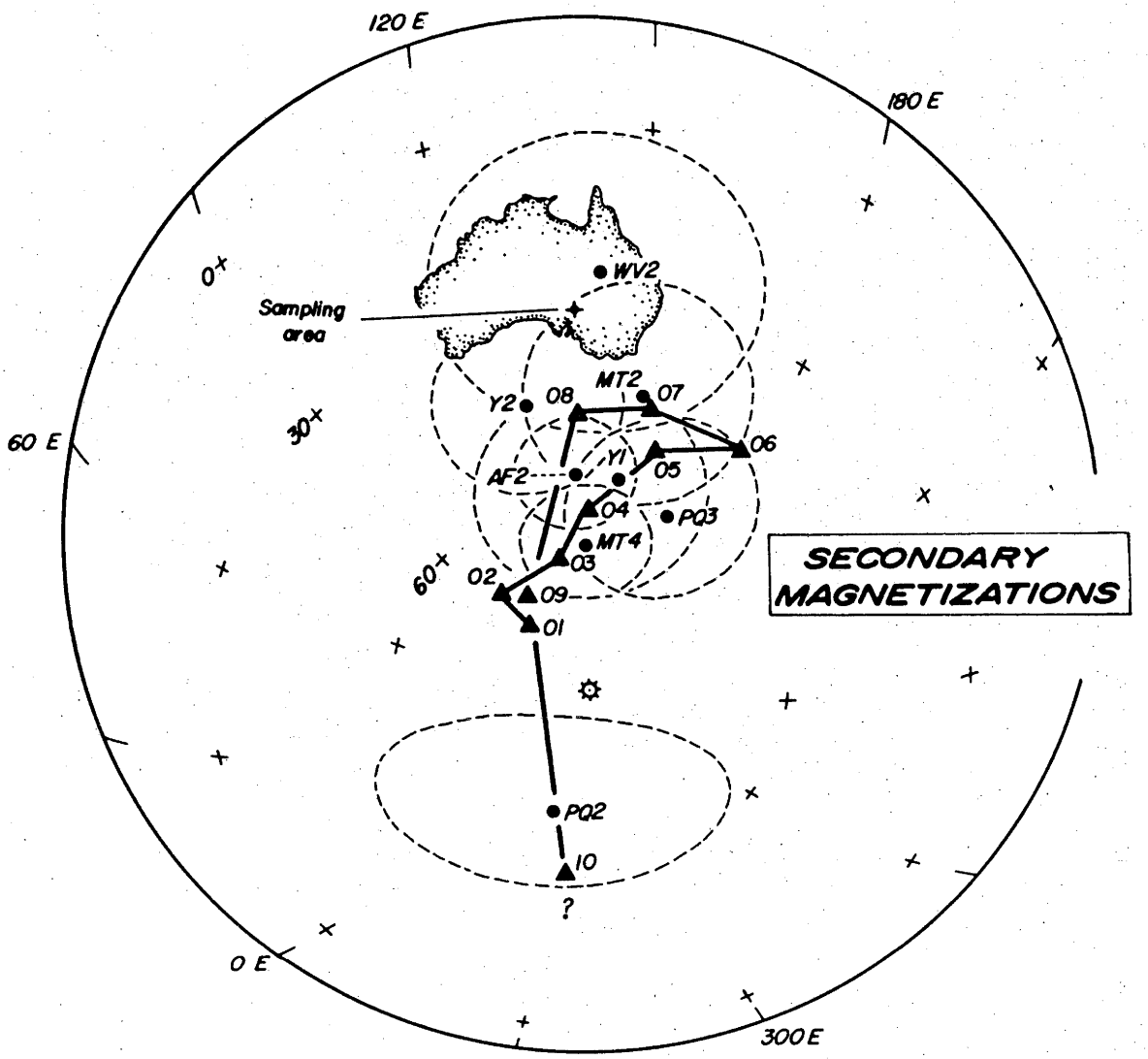

Figure 2.27(B) : Secondary poles from Adelaide 'Geosyncline' rocks, plotted with Phanerozoic period mean poles : 01, Miocene, 02: Oligocene, 03: Eocene, 04: Palaeocene, 05: Cretaceous, 06: Upper Jurassic, 07: Triassic-Lower Jurassic, 08: Upper Carboniferous-Permian, 09: Upper Devonian-Lower Carboniferous, 10: Silurian-Lower Devonian (all shown as triangles). Dashed ovals: 95% error ellipse dp,dm. Equal-area projection, radius 115°. Symbols as in Table 2.11.

(WV1 and CQ) are original and were probably acquired in palaeolatitudes which differ by over 50°. Even with rapid rates of apparent polar motion, this latitudinal difference could represent a highly significant time break. At rates of (15,10,5) cm yr^{-1} of motion relative to the pole, the unrecorded interval would be of the order of (37,55,110) my. Depending upon the age of the Wooltana Volcanics, redefinition of the stratotype Adelaide 'System' or of Adelaidean time might be warranted. If their true age is in the 870-625 my range, the lower Callana Beds might be as much as 200 my older than the unconformably overlying sequence. If an age older than 1000 my is accepted the palaeomagnetic data would suggest (taking the antipole of WV1 rather than in its near Australia position) that the majority of Adelaidean time as defined has not been recorded by deposition. This possibility, discussed by Compston *et al.* (1966), would indicate that a more reasonable definition of the Adelaide 'System' might begin with the Upper Callana Beds or Burra Group. In view of the palaeomagnetic and isotopic data, it seems more plausible that Adelaidean time, at least from deposition of the Upper Callana Beds to the Precambrian-Cambrian boundary, was actually shorter than is commonly thought. The problem is disussed in more detail in Chapter 5 in conjunction with new data from Africa and elsewhere in Australia.

The two pole positions from the Brachina Formation (Karner, 1975 and this study) are clearly different. Again, fold test evidence suggests that the magnetization in both cases is probably original. There are two possible explanations. Either the ages of magnetization are distinctly different for the two localities, or if the ages of magnetization are similar,

relative motion may have taken place between the northern and southern parts of the Adelaide 'Geosyncline'. Many workers (see e.g. Crawford and Campbell, 1973; Harrington *et al*, 1973; Scheibner, 1974) have postulated that the characteristic sigmoidal shape of the Adelaide 'Geosyncline' resulted from tectonic deformation of an initially linear or simple accurate structure. In this type of hypothesis, the deformation is thought to take the form of bending of the sedimentary belt in response to dextral shear and concomitant drag along a major transform to the south (Crawford and Campbell, 1973), or to sinistral shear (Harrington *et al*, 1973), or to compressional forces arising from a southeasterly rotation of the Gawler Block to the northwest (Scheibner, 1974). Embleton and Giddings (1974) demonstrated using paleomagnetic data that the bend in Yorke Peninsula did not arise from such tectonic bending, however no tests have been made of possible bending in the Mount Lofty-Kangaroo Island arc. The discordant results from the Brachina Formation sampled in the North Flinders Ranges and south of Adelaide provide the basis for a simple test.

It is obvious that any hypothesis which postulates a straightening out of the east-west Kangaroo Island trends to coincide with the north-south Mount Lofty trends would require rotation about a local Euler pole which would move the two poles further apart, a negative result. However, Scheibner (1974) has postulated that the Adelaide 'Geosyncline' was originally a northeast-southwest linear structure parallel to the present Darling River lineament. Subsequent deformation occurred when the Gawler Block, originally further to the north, suffered an anticlockwise rotation about a nearby Euler pole to the northeast. Unfolding of the present sigmoidal trends to form a linear

structural pattern requires two rotations about local Euler poles. The first rotation moves the two poles far apart, the second, about a different Euler pole moves them together again. Tests using a variety of possible Euler poles and angular displacements were made, with the conclusion that a straightening of structural trends according to Scheibner's hypothesis does not decrease the angular distance between the two poles for the Brachina Formation. In all cases, the angular difference was either the same or marginally greater as a result of rotation. This fact is a product of the palaeolatitude difference between the two poles ($\sim$18°, when corrected for distance between the sampling localities) which cannot be resolved by rotation about local vertical axes.

While an unfolding and straightening of the central and southern part of the Adelaide 'Geosyncline' cannot be refuted or accepted on the basis of the palaeomagnetic test, it is interesting to note that such unfolding brings the BRK pole near the TH pole from the Tapley Hill Formation. Although the BRK pole is probably younger than the TH pole, the poles can be accommodated in a small anticlockwise bend in the polar track, as shown in Figure 2.27. Such a bend brings all the poles in a reasonable order, especially when it is remembered that the two formations studied are lithostratigraphic equivalents, but may not be chronostratigraphic equivalents. Units in the Adelaide 'Geosyncline' appear in some cases to be time transgressive when considered over large distances. Bearing in mind the 450 km distance between the sampling localities, such transgressive nature may cause differences between poles from the northern and southern parts of the Adelaide 'Geosyncline' without invoking relative motion.

A major polar shift of about 50° is present between the Brachina and Bunyeroo pole positions. This discordance could result from a significant difference in magnetization age during a period of relatively slow apparent polar motion, or from a small age difference during a period of rapid polar motion. The latter possibility is favoured for two reasons. Firstly, the sedimentary sequence appears to be conformable in the Brachina-Bunyeroo depositional interval, and a maximum of only 750 m of sediment separates the two units. Secondly, the magnetizations of both units appear to be original, although it can really only be said that the magnetizations are older than Upper Cambrian. It is important to note that although rapid apparent polar motion is implied, in this case marked displacement of the continent may not have caused the polar shift. As the two results differ by only 4° in inclination (not statistically different) a 50° anticlockwise rotation of at least the North Flinders Ranges about a local Euler pole could account for the shift. Minimal translational motion of the continental lithosphere relative to the mantle is required.

The pole from the Pound Quartzite and the three Cambrian results from the North Flinders Ranges are difficult to incorporate into the polar track without overly contorted paths. The polar shift between the BU and BF poles may record the onset of a period of rapid polar motion which may result in widely separated pole positions in the latest Precambrian and early Palaeozoic. Further discussion regarding possible large polar shifts during these times is reserved until Chapters 3 and 5, when data from elsewhere in Australia and other Gondwana continents are synthesized with the Australian data.

Chapter 3

Adelaidean Palaeomagnetism Exclusive of the Adelaide 'Geosyncline'

§3.1 Introduction

Adelaidean sediments occur in areas throughout Australia exclusive of the Adelaide 'Geosyncline' (Figure 3.1). Correlation of these strata with the stratotype Adelaidean sections has been the subject of much study and debate (*cf.* Dunn *et al.*, 1971). Palaeomagnetic study of some of the Adelaidean and Cambrian rocks from some of these areas was attempted, primarily to complement the study of Adelaide 'Geosyncline' strata described in the previous chapter. The results have potential relevance to

1) testing proposed correlations of Adelaidean strata,
2) testing possible lateral displacements between the various Precambrian crustal nucleii, and
3) obtaining additional palaeolatitude information from Australian late Precambrian glacial deposits outside the Adelaide 'Geosyncline'.

In this chapter, palaeomagnetic results from Adelaidean and Cambrian rocks of the Amadeus, Kimberley and Officer Basins, from northwest Queensland and from King Island, Tasmania are described. Sampling details are as outlined in §2.7.1; locality details are given in Appendix A.

§3.2 Amadeus Basin

§3.2.1 Stratigraphy, structure and tectonic history

The Amadeus Basin is an elongate intracratonic

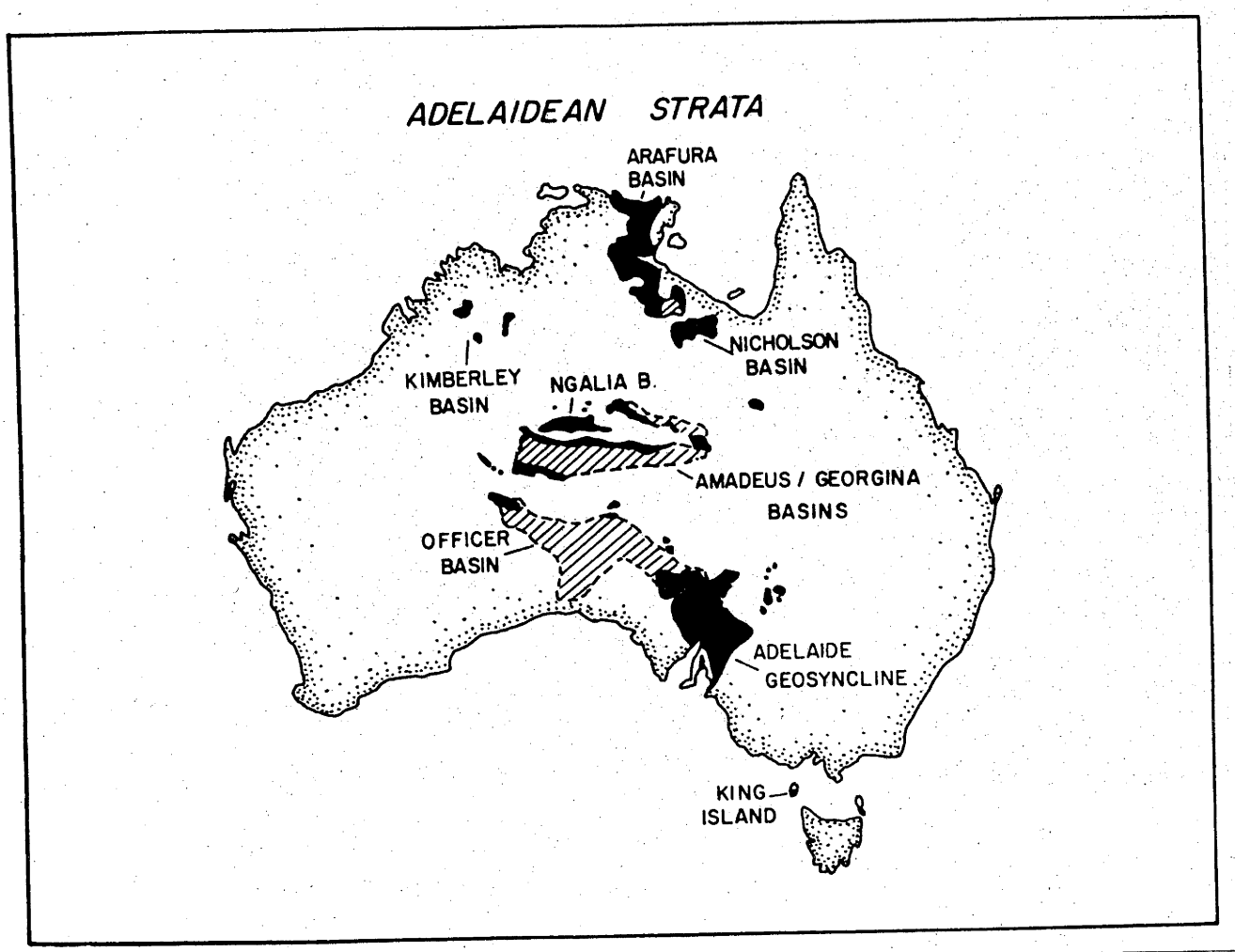

Figure 3.1 : Distribution of Adelaidean strata; solid areas denote surface outcrop, shaded areas denote subsurface occurrence.

depression (or aulacogene) containing over 9000 m of Precambrian and Palaeozoic sediments (see Wells *et al.*, 1970 for detailed descriptions). The Adelaidean part of the Amadeus Basin sediments were unconformably deposited upon older metamorphic and igneous rocks and are conformably overlain by fossiliferous Cambrian strata. The age range of Adelaidean sedimentation in the Amadeus Basin is therefore bracketed by the Precambrian-Cambrian boundary as a younger limit, and by the age of last metamorphism and intrusion of the underlying Arunta and Musgrave Complexes as an older limit. Current estimates of these ages generally restricts the cover rocks of the Amadeus Basin to being younger than about 1100-1200 my.

The Adelaidean sedimentary sequence commences with the Heavitree Quartzite, a massive resistant quartzitic unit which unconformably lies upon the metamorphosed basement complex. The Bitter Springs Formation conformably overlies the Heavitree Quartzite and comprises a thick sequence of calcareous and arenaceous rocks. The calcareous parts of the Bitter Springs Formation contain a wide variety of columnar stromatolites as described in detail by Walter (1972); interbedded chert lenses preserve some of the earliest known algal microbiotas (Schopf, 1968). The Heavitree Quartzite and Bitter Springs Formation have been correlated with the Copley Quartzite and Skillogallee Dolomite of the Adelaide 'Geosyncline' by Wells *et al.* (1970) on a lithological basis. Glaessner *et al.* (1969) and Walter (1972) utilize stromatolite occurrences to reinforce the lithological correlation. Although extensive sampling has been conducted, no palaeomagnetic data are available to date for either the Bitter Springs Formation or the Heavitree Quartzite.

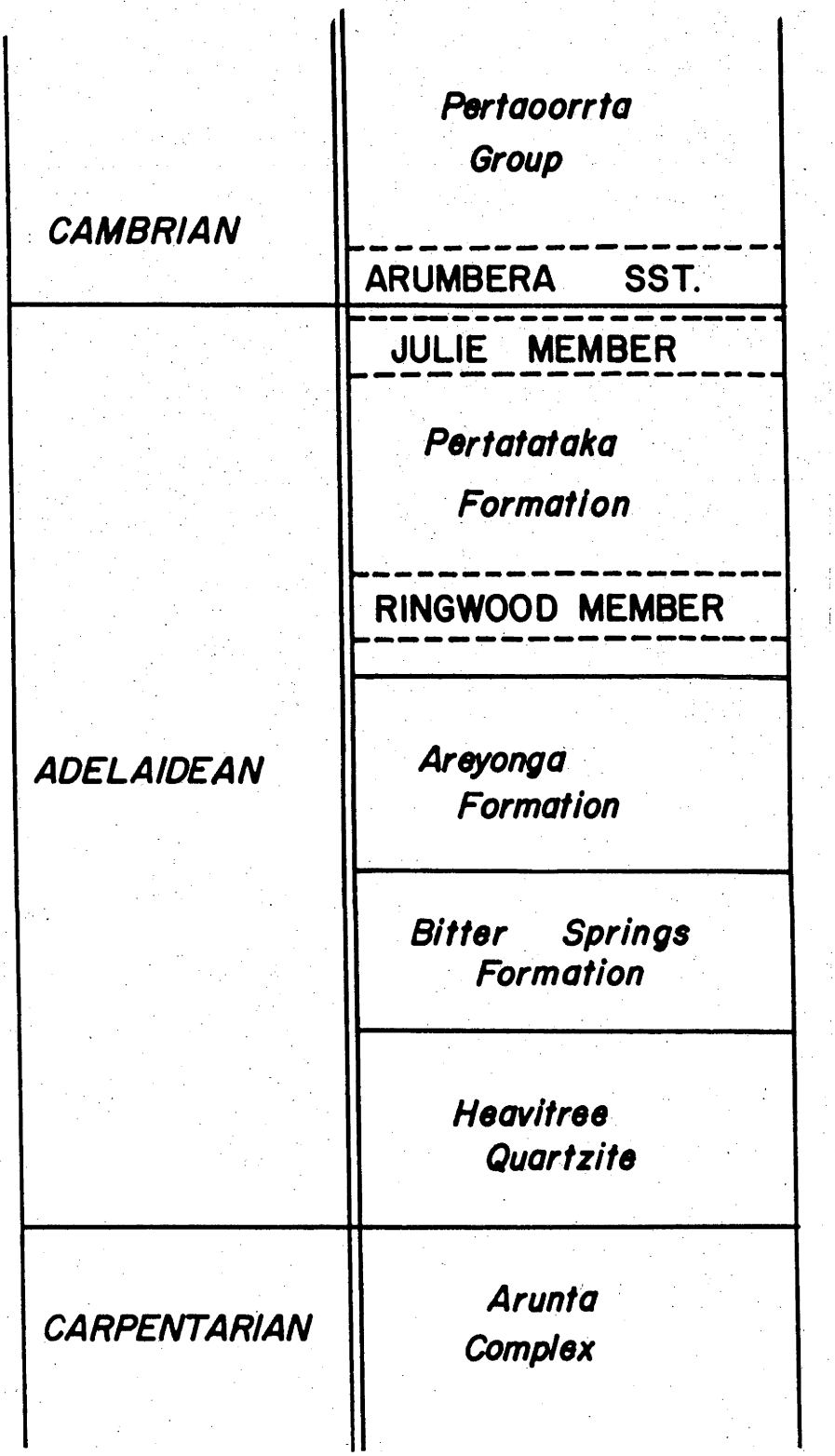

Figure 3.2 : Stratigraphic relationship of Adelaidean rocks of the Amadeus Basin, N.T. The contact between the Arunta Complex and Heavitree Quartzite is unconformable.

The Areyonga Formation disconformably overlies the Bitter Springs Formation. It has a varied lithology, but consists predominantly of a boulder-conglomerate association which has been interpreted as being of glacial origin, overlain by greywackes and sandstones with some algal dolomites. Prichard and Quinlan (1962) have suggested that the Areyonga Formation is the product of a marine glacial environment, which has led to correlation with the Sturtian tillites of the Adelaide 'Geosyncline'.

Stratigraphically above the Areyonga Formation is a thick (over 2100 m) sequence of sandstones, siltstones, shales and carbonates called the Pertatataka Formation. Five members of the Pertatataka Formation are recognized in the eastern Amadeus Basin (Wells *et al.*, 1967): the Julie, Waldo Pedlar, Olympic, Limbla and Ringwood Members, in order of increasing age. Siltstone is the dominant lithology in all the members, which are conformable with the possible exception of the Olympic and Limbla Members, which are probably separated by a disconformity. The occurrence of a possible second horizon of glacial sediments in the Olympic Member has led to the suggestion that this unit be correlated with the Marinoan tillites of the Adelaide 'Geosyncline'. Both the Julie and Ringwood Member contain algal stromatolites.

The Pertatataka Formation is overlain, unconformably in places, by Precambrian and Cambrian sediments of the Pertaoorta Group. The Precambrian-Cambrian boundary is thought to lie within the Arumbera Sandstone (and equivalents), one of the lowest members of the Group.

The first-order structure of the basin is a reasonably simple synclinal downwarping with an east-west axial trend. On

a smaller scale, much more complex structures such as nappes and décollement structures have been produced, largely as a result of late Palaeozoic orogenesis. Local unconformities between various units probably result from diastrophic movements during sedimentation in the basin. Six events are recognized; the most recent of these has the most importance to the present study. Two regional tectonic events are significant in the late Precambrian history of the Basin. These are the so-called Areyonga and Souths Range Movements, which produced unconformities between the Bitter Springs and Areyonga Formations and between the Areyonga and Pertatataka Formations respectively. The Precambrian to Cambrian Petermanns Ranges Orogeny affected mainly the southwestern part of the Basin and produced deformation and low to moderate grade metamorphism in the area. Two Palaeozoic diastrophic movements caused interruptions in sedimentation, the Rodingan Movement and the Pertnjara Movement.

The Alice Springs Orogeny resulted in the formation of the complex nappe and décollement structures found on the northern margin of the Basin and was accompanied by mylonitization, shearing and overthrusting. In some places at least moderate re-heating occurred. Reset K/Ar mineral ages from the Arunta Block to the north range in age from 367 to 420 my. As is later discussed, the Alice Springs Orogeny may have resulted in partial and/or total remagnetization of some of the units studied.

§3.2.2 Previous palaeomagnetic work

Embleton (1972a, b and personal communication) has reported palaeomagnetic results from the Arumbera Sandstone, Hugh River Shale, Pacoota Sandstone, Stairway Sandstone and

Mereenie Sandstone. Although the Precambrian-Cambrian boundary may lie within the Arumbera Sandstone, the other results are from Palaeozoic sediments. Kirschvink (in preparation) has studied in detail the Arumbera Sandstone, overlying Todd River Dolomite and immediately underlying Julie Member of the Pertatataka Formation.

Discussion and interpretation of these results and of new results from the Amadeus Basin is deferred until §3.2.5.

§3.2.3 Areyonga Formation

At the type section at Ellery Creek (Figure 3.3), the Areyonga Formation has two members. The lower member is a tillitic unit with pebble and boulder tillite with tillitic sandstone, which unconformably overlies the Bitter Springs Formation. Most of the erratics are rounded (Plate 4), but some are facetted and striated. The upper member consists of a resistant current bedded quartz greywacke. Due to the fact that much of the matrix material of the lower member was highly weathered, only the upper greywacke member was sampled through about 170 m of section. Samples of a similar greywacke within the Areyonga Formation were taken near Limbla, east of Alice Springs.

NRM directions from most of the sites were scattered but roughly streaked from the PEF direction towards a southeasterly direction. Upon thermal demagnetization, samples from the lower part of the Ellery Creek Section exhibited directional stability after heating to temperatures of 300° and above. During the early heating steps, a magnetization with a moderately steep negative inclination and northerly declination was removed (Figure 3.4). The mean direction of

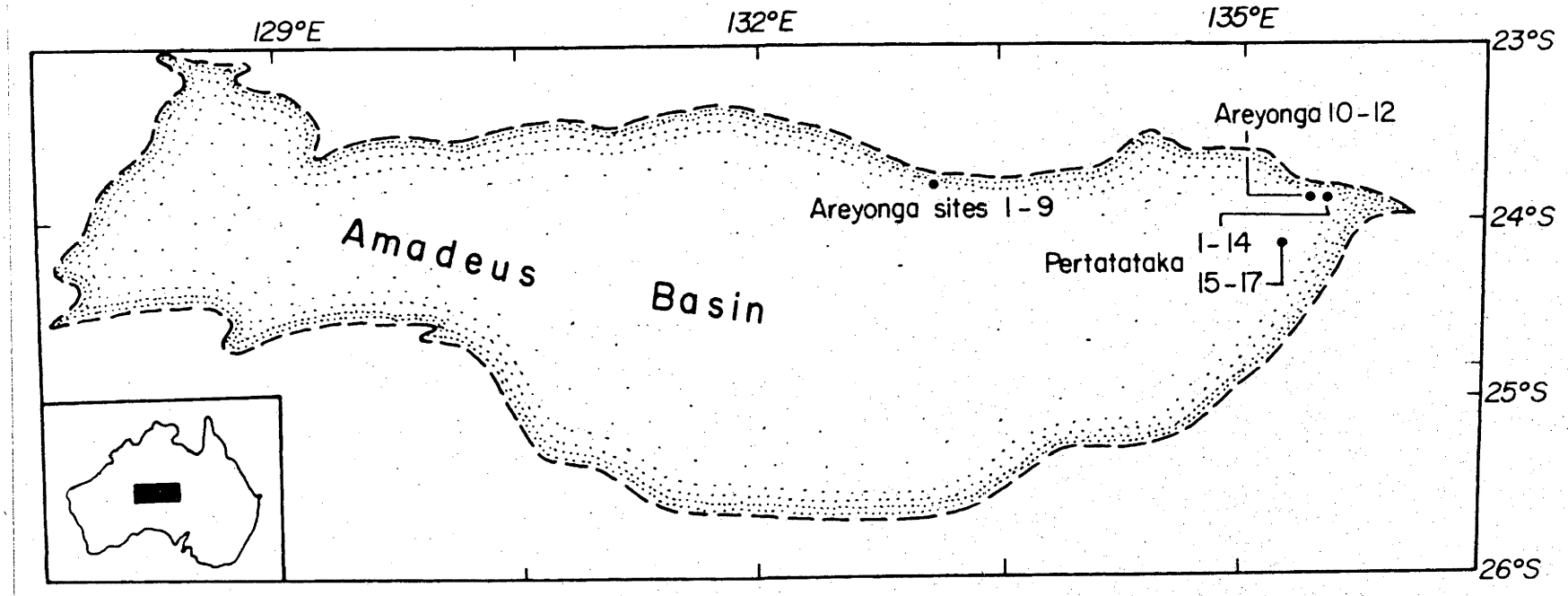

Figure 3.3 : Sampling localities : Areyonga Formation and Ringwood Member, Pertatataka Formation.

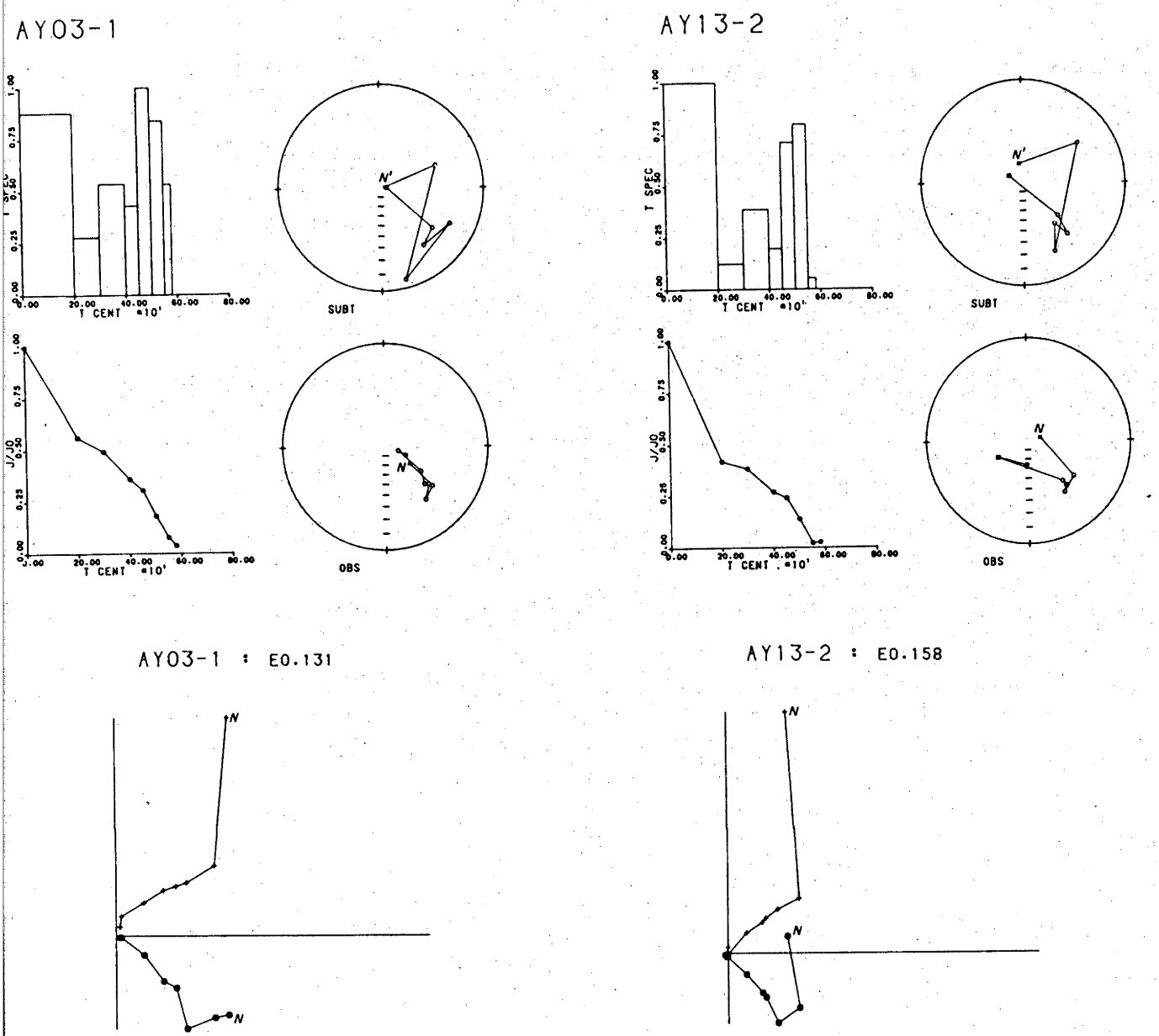

Figure 3.4 : Thermal demagnetization : Areyonga Formation.

this low T_b magnetization is not significantly different from the PEF direction at the sampling site and is probably a VRM acquired in Recent times. The samples collected from the eastern part of the Amadeus Basin responded similarly to thermal treatment, attaining directional stability in the 300°-450° range. After bulk thermal treatment, these samples define the AY1 magnetization (Figure 3.5 and Table 3.1). Dispersion of the AY1 magnetization decreases significantly upon structural correction, indicating that the stable remanence was acquired before folding occurred (k'/k=4.31, 95% significance point ≅2.59). However, as the main episode of folding occurred in late Silurian or Devonian times, all that can be stated with confidence is that the AY1 magnetization is probably pre-Devonian in age.

Samples from the upper part of the sampled section at Ellery Creek had generally a more varied and complicated thermal demagnetization behaviour than did those from the lower part of the section described above. No systematic directional behaviour was observed between these samples during thermal demagnetization. Chemical demagnetization experiments were conducted on these samples in attempt to obtain a meaningful magnetization direction from the upper part of the section. During acid leaching, 13 samples from 4 sites had magnetization vectors which appeared to converge after 560h upon a northerly and shallow negative direction (AY2) before structural correction (Figure 3.5, 3.6). As the AY2 samples were from one locality only, there is a very slight increase in precision upon structural correction.

To judge by its pole position (Table 3.1 and Figure 3.34) the structurally corrected AY1 magnetization could be

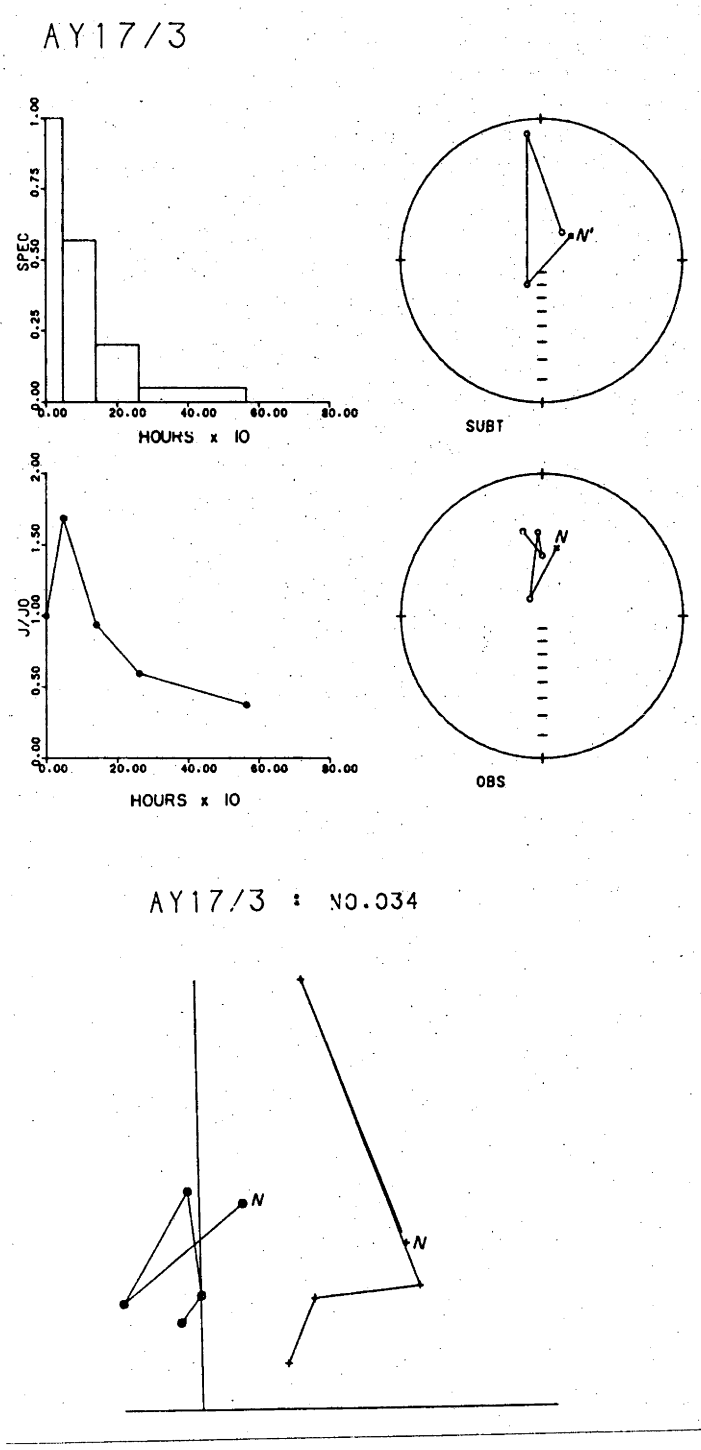

Figure 3.5 : Chemical demagnetization : Areyonga Formation.

TABLE 3.1 (A)

AREYONGA FORMATION : Site mean directions before and after thermal and chemical demagnetization

	NRM				After demagnetization							
SITE	N	R	D	I	N	R	D	I	D'	I'	TREATMENT	MAGNETIZATION
1	3	2.987	114	-56	3	2.995	129	-29	054	-25	450°C	AY1
2	3	2.991	104	-54	3	2.993	129	-30	053	-24	450°C	AY1
3	3	2.945	111	-57	3	2.986	130	-29	054	-26	450°C	AY1
4	3	2.960	111	-74	3	2.996	134	-29	052	-29	450°C	AY1
5	4	3.747	071	-58	3	2.988	133	-32	049	-26	450°C	AY1
6	4	3.163	023	-45	3	2.875	000	-16	337	83	560 h	AY2
7	4	3.069	084	-74	3	2.712	351	-35	341	63	560 h	AY2
8	5	2.701	305	-32	4	3.227	359	-06	228	84	560 h	AY2
9	5	4.438	005	38	3	2.932	003	16	183	64	560 h	AY2
10	6	3.748	014	-40								
11	5	4.037	305	-53	4	3.383	010	-31	359	-34	400°C	AY1
12	5	1.807	356	33	4	3.695	017	-39	008	-35	400°C	AY1

TABLE 3.1 (B)

AREYONGA FORMATION : Mean directions after thermal demagnetization

	Before structural correction									After structural correction						
MAGNETIZATION	N	n	R	k	D_m	I_m	pole lat	pole long	dp,dm	R	k	D_m'	I_m'	pole lat	pole long	dp,dm
AY1	7	23	5.297	3.5	109	-43	05S	255E	29,47	6.603	15.1	040	-30	52S	041E	10,18
AY2	4	13	3.787	14.1	359	-10	71S	310E	13,26	3.789	14.2	277	85	22S	122E	50,50 α=25°

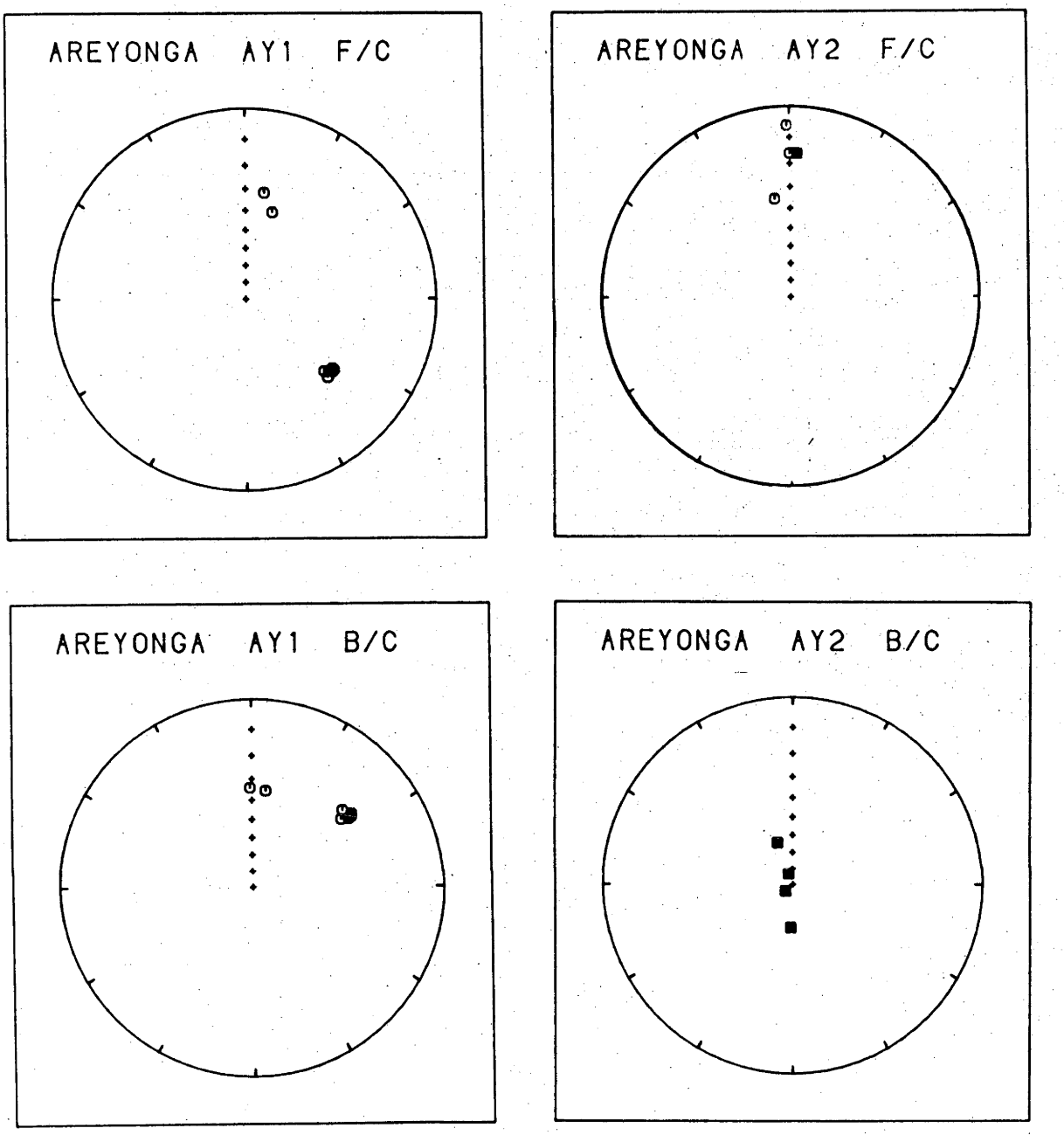

Figure 3.6 : Cleaned site mean magnetization directions, Areyonga AY1 and AY2 components; equal-angle projection. Open (closed) symbols refer to negative (positive) inclination.

secondary and about Silurian in age. Alternatively, it could be a primary magnetization of Precambrian age, as discussed in §3.2.5. The AY2 component has a large polar error and associated uncertainty in its pole position. By comparison with the late Palaeozoic-Mesozoic APWP for Australia, the structurally uncorrected AY2 pole could be of Devonian age. If this is indeed true, the AY2 magnetization might be best interpreted as a thermal or chemical overprint acquired during or just after the Alice Springs Orogeny. The overlying Pertatataka Formation and Arumbera Sandstone exhibit probable overprinted magnetizations of possibly a similar origin, although some of these overprint directions are somewhat scattered. Alternatively, the AY2 magnetization could be of very recent age. In its structurally corrected position, the pole position calculated from the AY2 magnetization does not lie near any part of the post-Silurian APWP, nor does it lie near any other late Precambrian of early Palaeozoic poles.

§3.2.4 Ringwood Member, Pertatataka Formation

In the eastern part of the Amadeus Basin the lowermost member of the Pertatataka Formation is called the Ringwood Member, dominated by algāl dolomite, limestone and siltstone. Samples of the Ringwood Member were taken in the Limbla Syncline near Limbla H.S. and equivalent strata were sampled southeast of Ringwood H.S. (Figure 3.3). At the Limbla locality, massive (∿1 m diameter) columnar stromatolites were present in the section and samples were taken above, below, and occasionally within the algal structures. Grey siltstones and laminated fragmental dolomites or limestones were also samples through about 40 m of stratigraphic section.

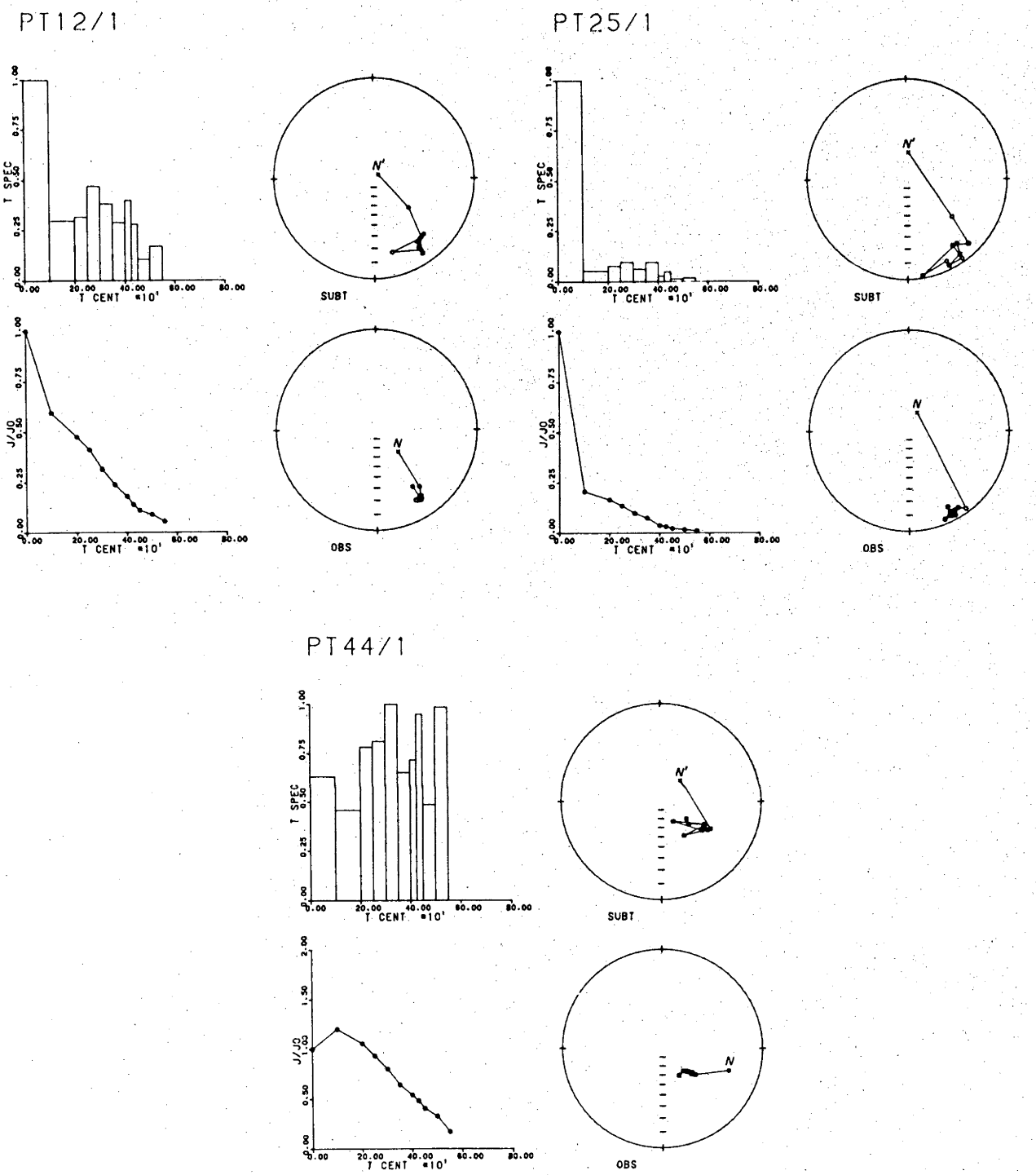

Figure 3.7(A) : Thermal demagnetization, Pertatataka Formation.

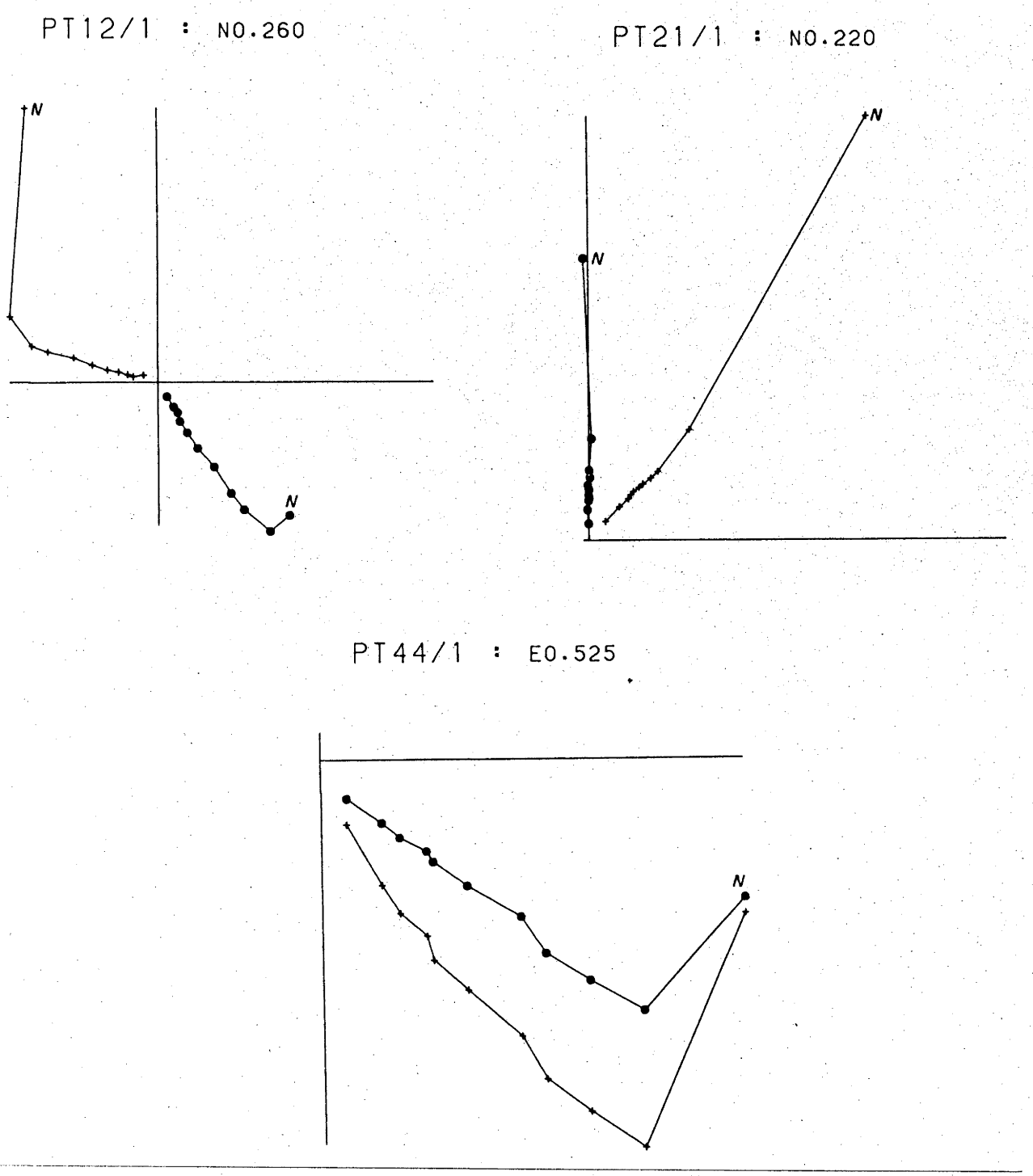

Figure 3.7(B) : Thermal demagnetization, Pertatataka Formation (continued).

TABLE 3.2 (A)

PERTATATAKA FORMATION (RINGWOOD MEMBER) : Site mean directions before and after thermal demagnetization

MAGNETIZATION	SITE	N	R	D	I	D'	I'	T°C
NRM:	1	2	1.979	230	-38			
	2	3	2.981	033	-67			
	3	3	2.977	034	-72			
	4	2	1.996	028	-68			
	5	3	2.610	077	-59			
	6	3	2.770	008	-49			
	7	3	2.973	333	-66			
	8	3	2.142	324	-47			
	9	3	2.969	359	-66			
	10	3	2.967	358	-64			
	11	3	2.976	341	-70			
	12	3	2.949	347	-50			
	13	3	2.779	314	-67			
	14	3	2.977	353	-49			
	15	3	2.882	317	-59			
	16	3	1.689	090	-05			
	17	3	1.576	032	-29			
AFTER THERMAL CLEANING								
PR1:	2	3	2.908	168	07	166	10	450
	3	3	2.843	173	-08	173	-04	450
	4	2	1.912	173	01	172	05	450
	5	2	1.929	158	-04	158	14	450
	9	2	1.963	135	07	134	20	500
	11	4	3.627	159	-02	159	16	450
	16	3	2.806	152	23	154	-13	450
	17	3	2.934	020	-45	020	05	450
PR2:	6	3	2.928	253	80	298	75	400
	7	3	2.977	183	69	204	79	400
	8	2	1.975	170	47	165	58	400
	9	2	1.990	176	49	181	59	400
	10	2	1.999	208	29	218	38	400
	11	2	1.953	191	71	238	78	400
	12	2	1.993	206	62	243	68	400
	13	2	1.995	202	74	276	76	400
	14	3	2.863	279	49	292	37	400
	15	2	1.962	200	50	156	42	400
PR3:	1	2	1.989	272	55	283	62	250-425
(subtracted from	2	3	2.951	214	66	200	75	300-450
PR1 vectors)	3	3	2.969	238	68	238	77	250-450
	4	2	1.983	231	62	228	72	250-425

TABLE 3.2 (B)

PERTATATAKA FORMATION : Mean directions after thermal demagnetization

	Before structural correction									After structural correction						
							pole							pole		
MAGNETIZATION	N	n	R	k	D_m	I_m	lat	long	dp,dm	R	k	D_m'	I_m'	lat	long	dp,dm
PR1	8	22	7.392	11.5	163	10	65S	272E	09,17	7.495	13.9	165	06	65S	278E	08,15
PR2	10	23	9.277	12.5	203	62	63S	097E	17,22	8.927	8.4	218	71	48S	104E	27,31
PR3	4	10	3.925	40.3	241	65	37S	087E	19,23	3.923	39.2	244	74	33S	103E	24,27
PR2+PR3	14	33	12.796	10.8	204	67	58S	105E	17,21	12.820	11.0	225	72	44S	103E	19,22

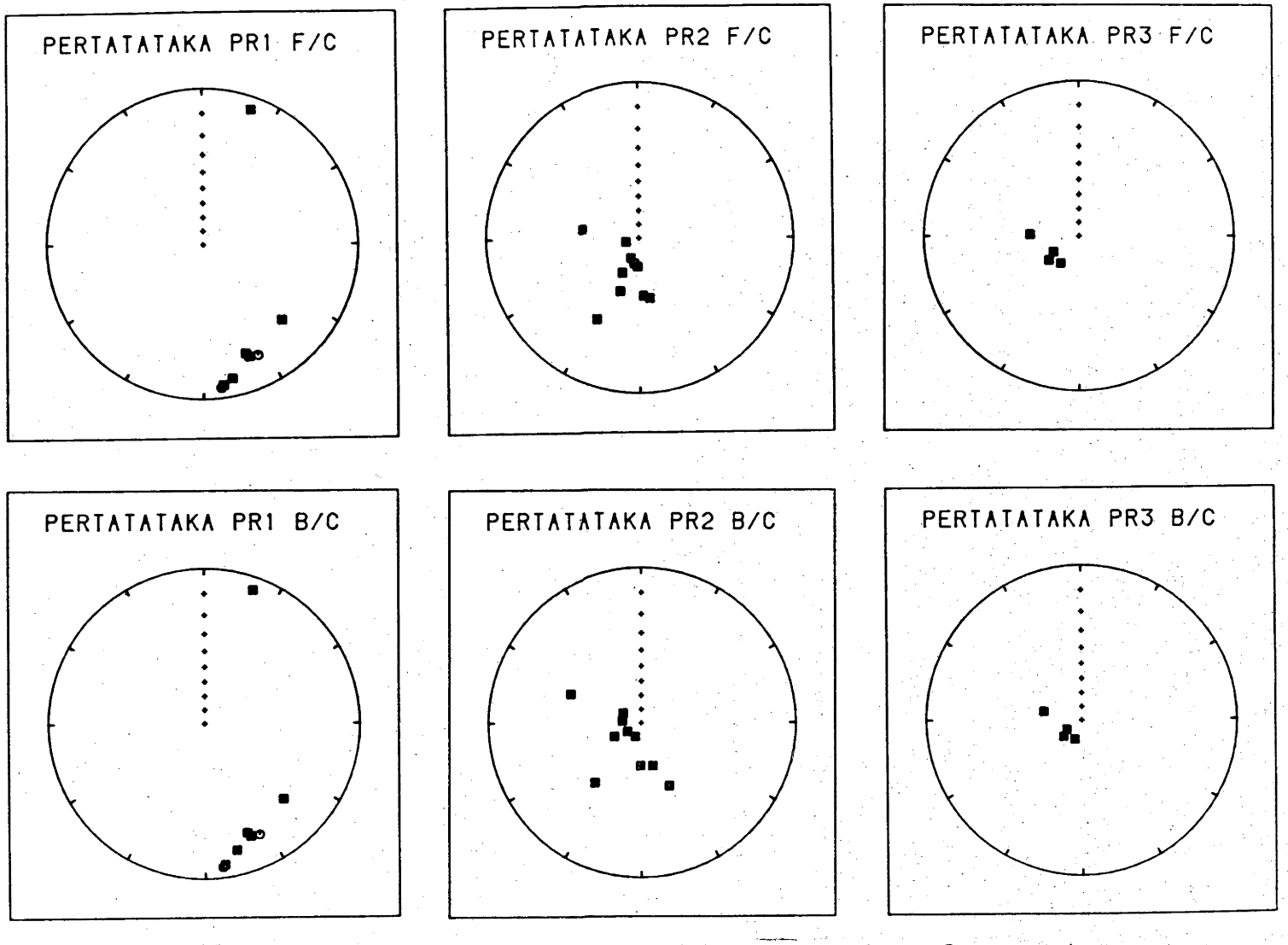

Figure 3.8 : Cleaned site mean magnetization directions, Pertatataka PR1, PR2 and PR3 components; equal-angle projection. Open (closed) symbols refer to negative (positive) inclination.

NRM vectors were generally directed towards the PEF direction with moderate (1.0 mAm^{-1}) intensities. Upon thermal demagnetization of 1 specimen from each sample, a component with a steep negative inclination which made up an average 70% of total NRM intensity was removed from most specimens in the 20°-200° step (Figure 3.7). This removed component is probably a recently acquired VRM and its mean direction is not significantly different from the PEF direction at the 95% confidence level. Directional stability was attained in most specimens in the 400°-500° range, although extremely weak magnetization intensities were encountered at these temperatures ($\sim 10^{-2}$ mAm^{-1})

Bulk treatment of the remaining specimens from each sample was done at temperatures of 400°-500°, according to the stability exhibited by the pilot specimen in this range. A non-Fisherian distribution of cleaned site mean directions was apparent, suggesting the presence of more than one component of magnetization. One component, denoted PR1, was observed at 8 sites and is characterized by shallow negative directions with a southeasterly declination. The second component, called PR2, was seen at 10 sites and has a much more steeply inclined positive direction, with a southwesterly declination. Inspection of vectors removed during thermal demagnetization of specimens from 4 PR1 sites showed that a similar component with a steep positive inclination was consistently removed in the 250°-450° heating range; this removed component is called the PR3 magnetization. The mean PR3 and PR2 magnetizations are not significantly different at the 95% confidence level. The vectors substracted from the PR2 sites are essentially identical to the observed PR2 vectors and no signs of a second

magnetization are seen (Figure 3.7). Assuming a simple high T_b - older magnetization age relationship for the various components present, this would suggest that the pre-existing PR1 magnetizations in many of the sites have been partially (in the case of the PR1 sites) or totally (in the case of the PR2 sites) overprinted by the PR2 direction. Corroborative evidence for this conclusion comes from a positive fold test on the PR1 component and a negative fold test on the PR2 and PR3 components, although unfortunately none are significant at the 95% confidence level as tabulated below:

Magnetization	k'/k	95% significance point
PR1	1.21	2.43
PR2	0.67	0.46
PR3	0.97	0.26

There is therefore the suggestion that the PR1 magnetization may predate the Palaeozoic folding while the PR2 and PR3 magnetizations may postdate the folding. As discussed in the next section, the pole position calculated from the PR1 direction is consistent with a primary Precambrian age. The PR2 and PR3 components are probably overprints acquired during or just after the Alice Springs Orogeny.

§3.2.5 Summary of late Precambrian and Palaeozoic Palaeomagnetism from the Amadeus Basin: the Amadeus Polar Track

All available Precambrian and Palaeozoic palaeomagnetic data from the Amadeus Basin are compiled in Table 3.3 and plotted in Figure 3.9.

Poles PR1 through to MS (excluding AR1) form a

TABLE 1.3 (A)

Summary of palaeomagnetic poles from the Amadeus Basin

Symbol	Rock Unit	Probable Magnetization Age	Pole Position	dp,dm	Reference
Possible Primary Poles					
AY1	Areyonga Formation	PG(?)	52S 041E	10,18	this study
PR1	Pertatataka Formation, Ringwood Member	>PRJ(PG)	65S 278E	08,15	this study
PRJ	Pertatataka Formation, Julie Member; t. Arumbera Sandstone	>AR2(PG)	44S 342E	08,14	Kirschvink (in prep.)
AR1	Arumbera Sandstone	<PRJ(Gt)	09N 325E	28,30	Embleton (1972a)
AR2	Arumbera Sandstone, Upper	>TAE(Gt)	47S 337E	03,05	Kirschvink (in prep.)
TAE	Todd River dolomite, Allua & Eninta Sandstone	>HS(Gt)	44S 342E	05,08	Kirschvink (in prep.)
HS	Hugh River Shale	>PS(Gt-Gm)	11N 037E	05,09	Embleton (1972a)
PS	Pacoota Sandstone	>SS(Gu)	06S 033E	07,13	Embleton (pers. comm.)
SS	Stairway Sandstone	>MS (Om)	02S 051E	05,10	Embleton (1972b)
MS	Mereenie Sandstone	S-D	41S 041E	06,11	Embleton (1972b)
Possible Secondary Poles					
AY1	Areyonga Formation		52S 041E	10,18	this study
AY2	Areyonga Formation		71S 310E	13,26	this study
PP2	Pertatataka Formation, Ringwood Member (observed)		63S 097E	17,22	this study
PR3	Pertatataka Formation, Ringwood Member (subt.)		37S 087E	19,23	this study
PRS	Pertataka Formation Julie Member & Todd River dolomite (subt.)		60S 068E	05,07	Kirschvink (in prep.)
AR3	Arumbera Sandstone		80S 278E	10,17	recalculated from Embleton (1972a)

Table 3.3 (B)

Summary of new palaeomagnetic results from the Amadeus Basin

Symbol	Rock Unit	Interpretation[1]
AY1	Areyonga Formation	secondary (?), ℓPz
AY2	Areyonga Formation	secondary, ℓPz
PR1	Pertatataka Formation Ringwood Member	primary
PR2	Pertatataka Formation, Ringwood Member	secondary, ℓPz
PR3	Pertatataka Formation, Ringwood Member	secondary, ℓPz

[1] age abbreviations as in Table 2.11 (b)

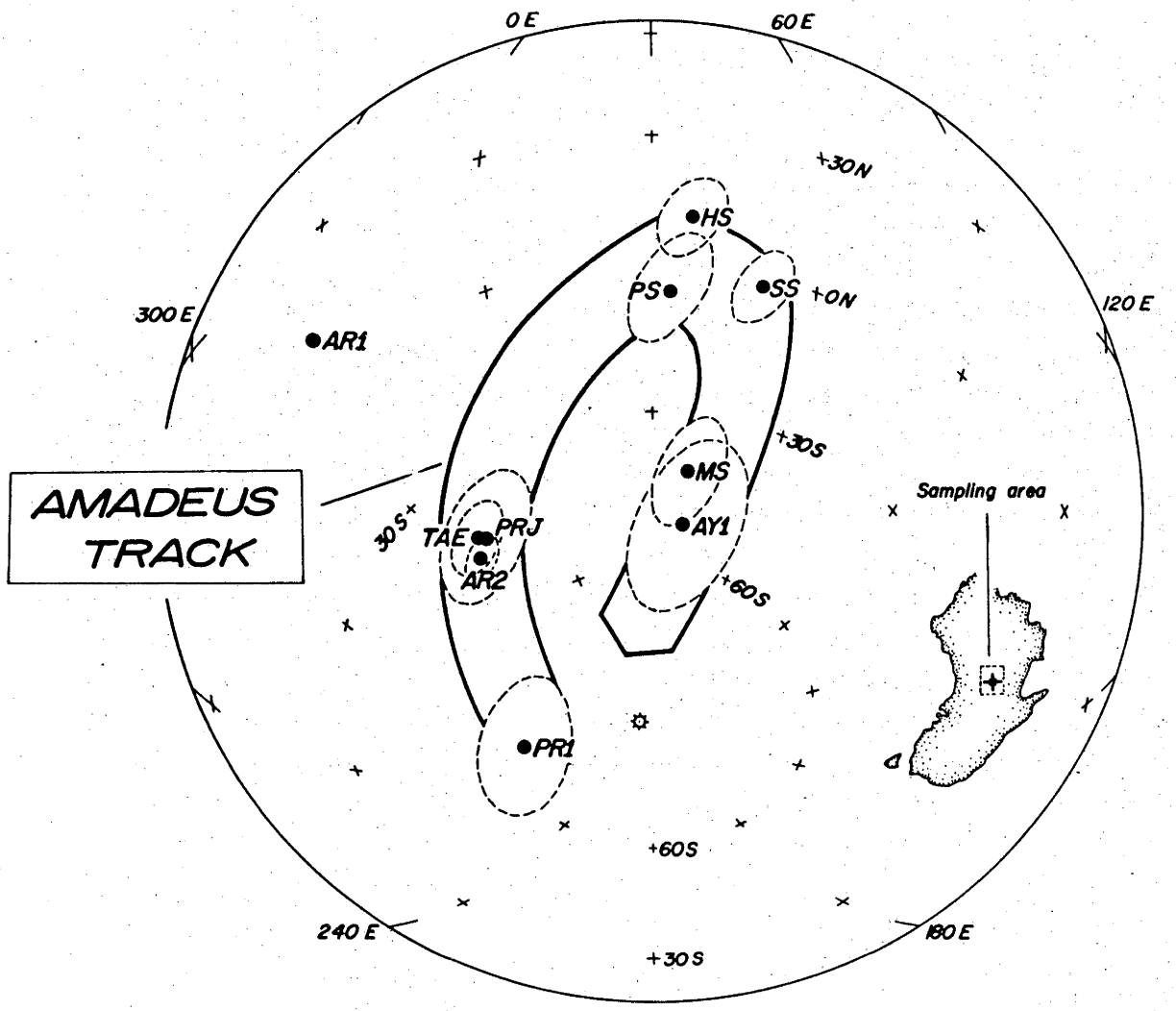

Figure 3.9(A) : The Amadeus Track, the late Precambrian APWP segment derived from Amadeus Basin rocks. Symbols as in Table 3.3; details of projection and APWP as in Figure 2.27(A).

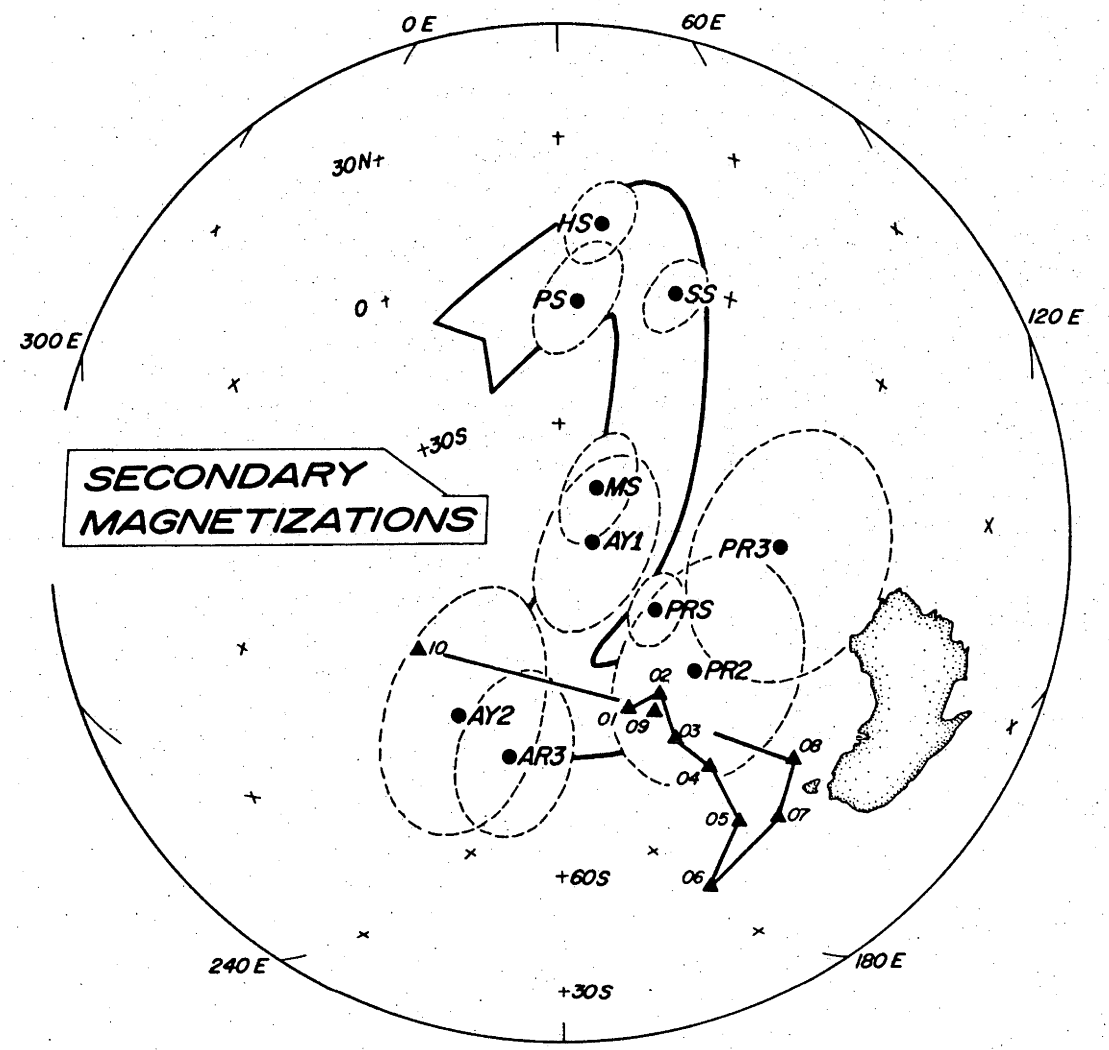

Figure 3.9(B) : Secondary poles from Amadeus Basin rocks, plotted with Phanerozoic period mean poles. Symbols as in Table 3.3; details of projection, APWP and period mean poles as in Figure 2.27(B).

reasonably consistent APWP or polar track, extending from late Precambrian (middle Adelaidean) to Siluro-Devonian times. The exact nature of the connection between the early and late Palaeozoic APW paths is not yet clear, but may follow along the lines suggested in Figure 3.9. A correct interpretation is complicated by (1) the possible presence of middle Palaeozoic overprinting during the Alice Springs Orogeny, (2) the possibility that the late Palaeozoic APWP may double back upon itself, intersecting at early Adelaidean and Siluro-Devonian times, and (3) uncertainty in magnetization ages for some of the rock units for which palaeomagnetic information is available. These problems are disucssed below in relation to the poles which form the Amadeus Polar Track, in order of decreasing age.

To judge by the significant positive fold test, pole AY1 from the Areyonga Formation is probably of pre-folding age, but as discussed above, the folding probably occurred only in pre-Devonian times. If the Siluro-Devonian segment of the Palaeozoic APWP passes through this general area, as indeed it might considering the overprint directions obtained from overlying strata and the paucity of Silurian data from elsewhere in Australia, an early or middle Palaeozoic age of magnetization cannot be discounted. Alternatively, it is possible that the AY1 pole is of early Adelaidean age and defines the older endpoint of the Amadeus Polar Track. A palaeomagnetic result from the underlying Bitter Springs Formation of Heavitree Quartzite might be able to confirm a primary or secondary magnetization age for the AY1 pole.

Poles PR1, PRJ, AR2, TAE, HS, PS, SS and MS form a sequence of poles which can be connected in a logical stratigraphically based sequence to form the Amadeus Polar Track.

The discrepancy between the AR1 and AR2 poles from the Arumbera Sandstone merits discussion as the angular distance between the two presumably contemporaneous poles exceeds 50°. In the earlier of the two studies, Embleton (1972a) sampled at one locality (Ellery Creek, where underlying samples of the Areyonga Formation were taken in the present study) and thus could not employ a fold test to the cleaned directions of remanence. A total of 16 samples defined the final mean direction, which had a large associated uncertainty. Part of the high dispersion may be attributable to difficulty in measuring weak magnetizations using magnetometers then available. Kirschvink (in preparation) collected many more samples at several localities with differing structural orientations, and although weak magnetizations were encountered, newly available more sensitive magnetometers made reliable low level measurements possible. It is therefore probable that the more recent result is the more reliable, but a proper explanation of the directions measured by Embleton (1972a) must be sought.

Two possibilities are apparent; both require that the magnetization from which the AR1 pole is derived is of secondary origin. Considering the relatively simple structural style in the area, major relative tectonic movements can be ruled out. The first possibility is that the AR1 pole represents a magnetization acquired in very late Precambrian or early Cambrian times, but later than the (?) primary AR2 pole. The AR1 pole would in this case be incorporated in the late Precambrian-Cambrian part of the Amadeus Polar Track. Although it is significantly displaced from other results from the Amadeus Basin, the proximity of the AR1 pole and the APV pole from the Antrim Plateau Volcanics could be cited as evidence in

favour of this possibility. Alternatively, a recalculation of the structurally uncorrected mean direction from the data of Embleton (1972a) yields a pole position (AR3) at 60°S, 330°E (dp,dm=10°,16°), which is not significantly different from the AY2 pole and similar to other (?) secondary poles from the Amadeus Basin. The uncorrected AR3 pole could therefore be incorporated in the Palaeozoic part of the Amadeus Polar Track and would imply that the samples collected by Embleton had been completely remagnetized, probably during the Alice Springs Orogeny. Kirschvink noted similar overprinting systematics in his collection, with some samples being completely overprinted, while others had only partial overprints which were removed after high temperature thermal treatment. It is possible that after treatment in higher temperatures, Embleton might have discovered a second component of magnetization, but weak magnetization intensities probably prevented this. Although it is impossible at present to definitively choose between the two possibilities, the latter is favoured as it requires a minimum of APWP extension to incorporate the AR3 pole, and because the uncorrected magnetization is essentially identical to the AY2 magnetization observed in sediments stratigraphically several hundred metres below.

Like the original result for the Arumbera Sandstone, a fold test cannot be applied to the directions from which poles HS, PS, SS and MS are derived. Unlike the original Arumbera result however, no supplementary data are available for these units and therefore these poles describe the best currently available estimate for the early Palaeozoic part of the Amadeus Track. However, these poles are quite distinct from younger Phanerozoic poles in both structurally corrected

and uncorrected positions, suggesting a primary magnetization. As is later demonstrated, poles from elsewhere in Australia of similar age are in reasonable agreement with this segment of the Amadeus Polar Track.

The younger endpoint of the polar track is loosely defined by a number of poles which are most probably of secondary origin. The only (?) primary result is the Siluro-Devonian Mereenie Sandstone (Embleton, 1972b) which also has a somewhat uncertain magnetization age, due to the absence of a fold test. Other possible secondary poles are AY1 and AY2 from the Areyonga Formation, PR2 and PR3 from the Ringwood Member of the Pertatataka Formation, PJS from the Julie Member of the Pertatataka Formation and AR3, the structurally uncorrected result recalculated from the Arumbera Sandstone. The middle and late Phanerozoic APWP for Australia (Schmidt, 1976) is plotted in Figure 3.9 for comparison, beginning with the available Devonian poles and continuing through the Mesozoic and Cenozoic. It can be seen that a continuous APWP segment can be constructed which joins the Amadeus Polar Track with the younger Phanerozoic APWP.

§3.3 Kimberley Basin

§3.3.1 Stratigraphy and tectonic history

Well exposed and essentially undeformed Adelaidean strata outcrop in three regions in the Kimberley Basin (Figure 3.10). Two episodes of glaciation are recorded in the stratigraphic columns, referred to as the Moonlight Valley and Egan glaciations (Dow and Gemuts, 1969). Various efforts to correlate these glacial horizons with the Sturtian and Marinoan

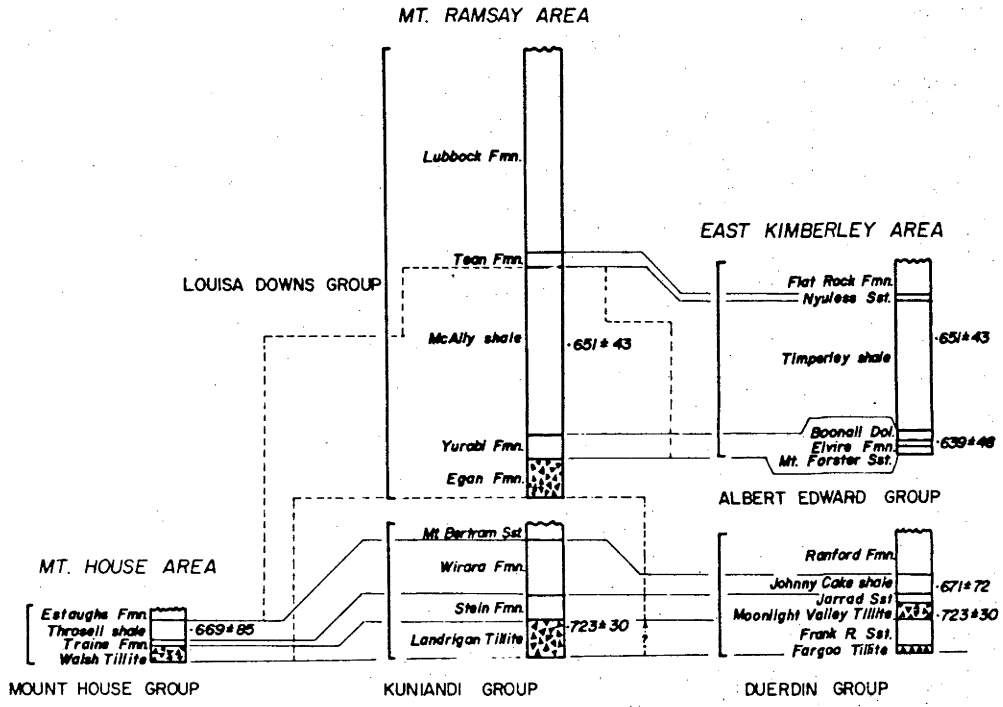

Figure 3.11 : Detailed Adelaidean stratigraphy, Kimberley Basin. Solid and dashed lines represent alternate correlations (Walter, pers. comm. 1977).

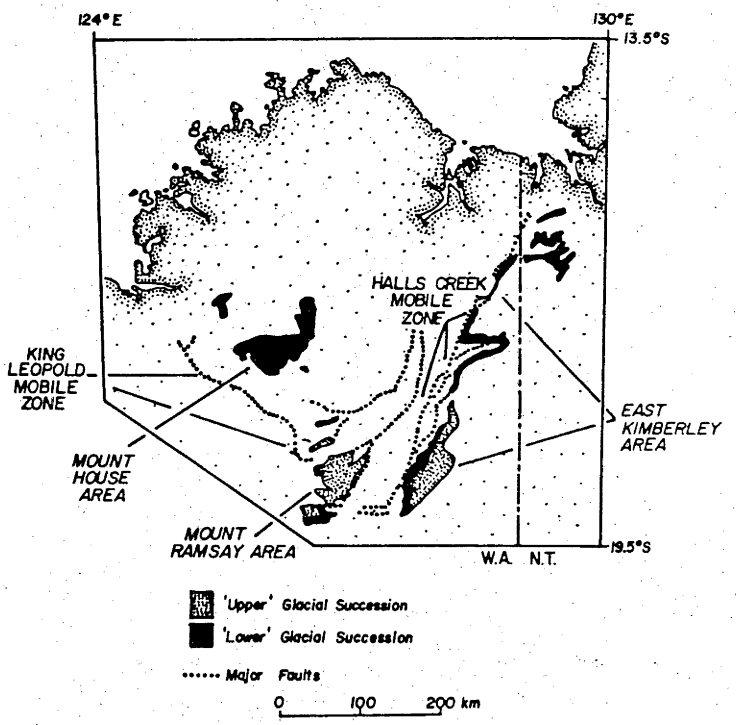

Figure 3.10 : Distribution of Adelaidean strata in the Kimberley region, W.A. Adelaidean rocks are subdivided into the upper and lower glacial successions.

glacials and with other glacial horizons elsewhere have been made. The virtual absence of metamorphism in some of these rocks has allowed geochronological studies to be made on some sediments, yielding the best direct isotopic age information on Adelaidean rocks presently available (Bofinger, 1967).

Only the lower glacial sequence is present in the Mount House area (Figures 3.10, 3.11) and is designated the Mount House Group. At its base is the Walsh Tillite, a tillitic unit with a laminated dolomitic cap which unconformably overlies Carpentarian (Middle Proterozoic) sediments of the Kimberley Group. Conformably above the Walsh Tillite (in order) are the Traine Formation, Throssell Shale and Estaughs Formation. At least 13 glaciated pavements have been reported at or near the base of the Mount House Group. Bofinger (1967) reported a Rb/Sr isochron age of 669±85*my for samples of the Throssell Shale.

The most complete Adelaidean section in the Kimberley Basin is found in the Mount Ramsay area where (?) Adelaidean sediments of the Glidden Group unconformably overlie the Kimberley Group but underlie the lower glacial succession (Figures 3.10, 3.11). The overlying Kuniandi Group begins with the Landrigan Tillite, overlain in turn by the Stein Formation, Wirara Formation and Mount Bertram Sandstone. The upper glacial succession unconformably overlies the Kuniandi Group and is called the Louisa Downs Group. It consists of a basal Egan Tillite (type definition for the Egan glaciation) followed by the Yurabi Formation, McAlly Shale, Tean Formation and Lubbock Formation.

---

* recalculated using $\lambda=1.42\times10^{-11}$ yr^{-1} for ^{87}Rb decay.

In the East Kimberley area, the Duerdin Group is a correlative of the Kuniandi Group (Figure 3.11) and contains the type area for the Moonlight Valley glaciation. The Duerdin Group is overlain by the Albert Edward Group, a correlative of the Louisa Downs Group.

Bofinger (1967) reported model composite ages for two correlative units separated by the Halls Creek Mobile one, the McAlly-Timperley Shales at 651±43*my and the Landrigan/Fargoo Tillites at 723±30*my. Both the Louisa Downs Group and Albert Edward Group are unconformably overlain by thick basalt flows of the Antrim Plateau Volcanics. The volcanics are thought to be latest Precambrian or early Cambrian in age, and are disconformably overlain by fossiliferous middle Cambrian sediments. Depending upon the reliability of the Rb/Sr shale isochrons, the glacial successions would appear to be bracketed in age by the 700 my ages at the base and by the Precambrian-Cambrian boundary at the top.

No direct correlations are possible between the three outlying exposures of Adelaidean strata, and all correlations between them have neccessarily been somewhat tentative. The dashed lines in Figure 3.11 represent alternative correlations.

The Adelaidean deposits of the Kimberley Basin have remained essentially undeformed and unmetamorphosed since deposition. Localized deformation did form tight to open upright and overturned folds in the west. The southernmost outcrops of the Walsh Tillite have suffered intense deformation which probably occurred at about 600 my (Bennett and Gellatly, 1970) when major diastrophic movements occurred in the King Leopold Mobile Zone.

§3.3.2 Previous palaeomagnetic work

Three palaeomagnetic studies have been reported from rocks in the general area. McElhinny and Luck (1970) studied the Precambrian-Cambrian Antrim Plateau Volcanics. Luck (1970) reported palaeomagnetic results from the Cambrian Hudson Formation to the east. McElhinny and Evans (1975) described a palaeomagnetic study of the 1800±25 my Hart Dolerite, which underlies many of the younger Precambrian strata in the Kimberley region.

§3.3.3 Mount House Group (lower glacial succession)

Three members of the Mount House Group were sampled in the West Kimberley region (Figure 3.10). Samples were taken from the Walsh Tillite at 4 localities; tillite as well as dolomite and dolomitic siltstone was collected. The matrix of the tillite had a weathered appearance suggestive of recent ground water activity through the unit. Grey shales and siltstones of the Throssell Shale were taken at 3 localities in the area. Massive purple ferruginous sandstones of the Estaughs Formation were sampled at Mount House, where they form a resistant cap to the lower glacial sequence and tend to dominate the local physiography. All the Adelaidean strata in the area are essentially flat-lying.

Walsh Tillite

NRM vectors from the Walsh Tillite samples were scattered but directed toward the PEF direction with moderate intensities (1-10 mAm^{-1}). Upon pilot thermal demagnetization, intensity of the dolomitic samples had decayed generally to less

than 95% of their NRM value by the 200°-300° heating step, whereupon directionally unstable behaviour ensued. No stable endpoints were observed. The tillite specimens remained very stable in intensity and direction up to about 650°, after which a characteristic 'square-shouldered' decay in intensity was observed. Directions before and during this decay were essentially unchanged and their mean direction not significantly different from the PEF direction, confirming the suspicion that these sediments might have been completely remagnetized in Recent times.

Chemical demagnetization was subsequently attempted on the tillite specimens. The intensity of the remanence vector decayed quite significantly with only minimal leaching, probably due to the porous nature of the samples. The change in intensity was accompanied by directional changes in most samples, however directions tended to move erratically and never converged upon a stable, systematic endpoint. No magnetizations thought to be primary in origin were observed in any of the samples.

Throssell Shale

NRM directions were scattered but again like the underlying Walsh Tillite not significantly different from the PEF direction at the sampling site. During pilot thermal demagnetization of one specimen from each sample, unstable directional behaviour was observed from most of the collection. A low T_b component similar in direction to the PEF direction was removed in the 20°-200° and 200°-300° heating steps, after which directional instability of the remaining weak vector ensued. No systematic stable endpoints were observed during demagnetization.

Estaughs Formation

Of the entire Mount House Group collection, only the samples from the Estaughs Formation had NRM directions which were significantly different from the PEF direction at the sampling locality (Table 3.4). Upon thermal demagnetization, remanence vectors converge upon a direction with a southeasterly declination and moderately steep negative inclination (Figure 3.12, 3.13), and stabilize in the 580°-610° range. After bulk thermal cleaning of the remaining part of the collection at 590°, a marked decrease in dispersion over the NRM mean direction was realized (one site with a random mean direction has been eliminated).

As the beds are flat lying, no fold test was possible. The pole position calculated from the thermally cleaned mean direction lies in the general region of other late Precambrian poles from elsewhere in Australia (figure 3.34). Its antipole does not lie near any part of the younger Phanerozoic APWP. Apart from this indirect evidence, the age of magnetization remains uncertain.

§3.3.4 Louisa Downs Group (upper glacial sequence)

Four members of the Louisa Downs Group were samples in the Mount Ramsay area (Figure 3.10, 3.11). The Egan Tillite was collected at the stratotype and is characterized by a very soft ferruginous matrix containing predominantly angular dolomite clasts of highly variable size. The tillite is overlain by a dolomitic cap. Immediately overlying ripple marked quartzitic and feldspathic sandstones of the Yurabi Formation were sampled at three localities. Siltstones, shales and

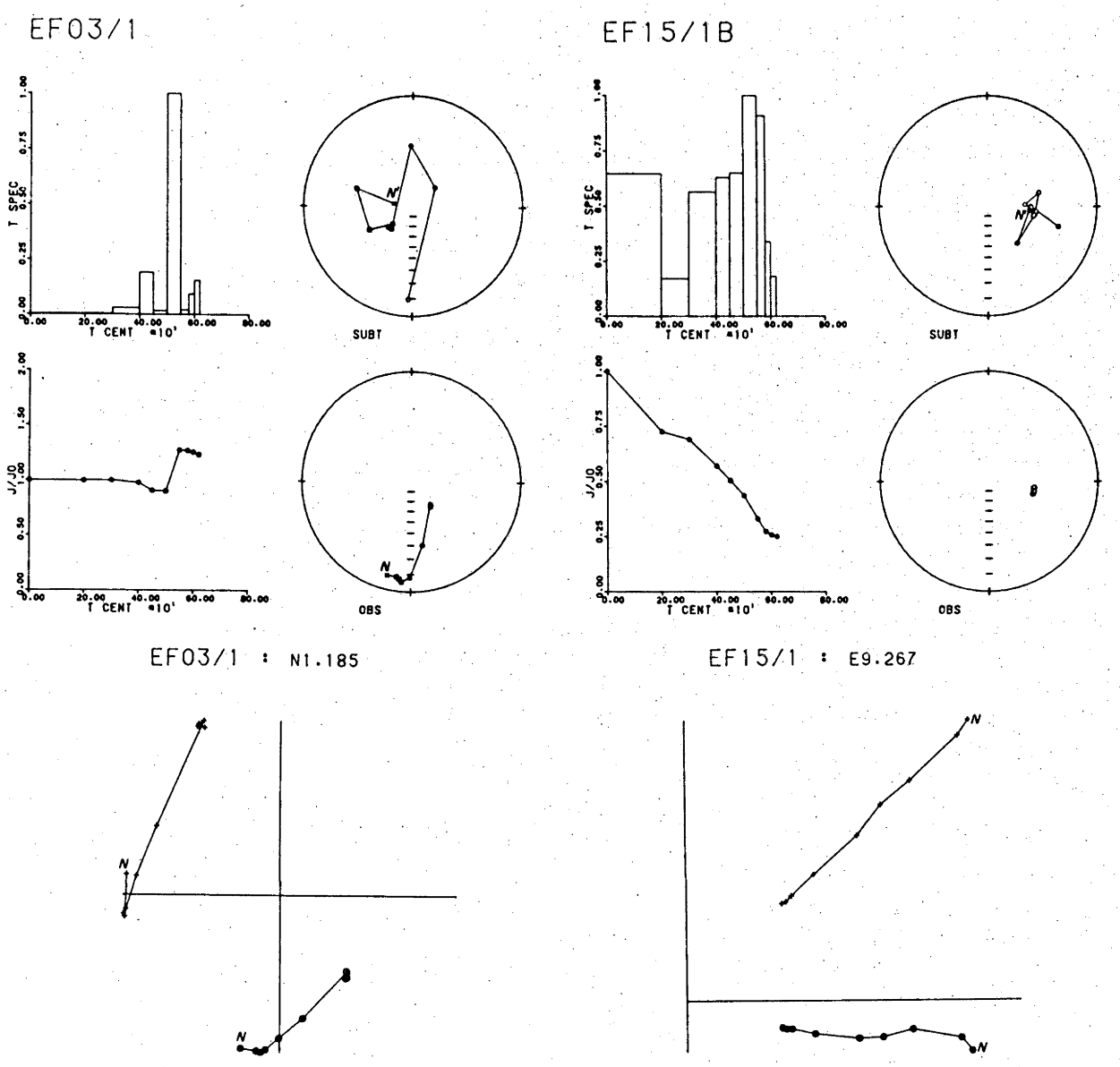

Figure 3.12 : Thermal demagnetization, Estaughs Formation.

TABLE 3.4 (A)

ESTAUGHS FORMATION : Site mean directions before and after thermal demagnetization

	NRM				590°C					
SITE	N	R	D	I	N	R	D	I	D'	I'
1	3	2.628	177	-46	3	2.970	152	-56	152	-56
2	3	2.310	259	-69	3	2.937	167	-52	167	-52
3	3	2.618	318	-59	(random)					
4	2	1.968	129	-83	2	1.945	150	-73	150	-73
5	3	2.447	080	-47	2	1.934	121	-52	121	-52
6	2	1.693	189	-75	2	1.906	144	-74	144	-74

TABLE 3.4 (B)

ESTAUGHS FORMATION : Mean direction and pole position after thermal demagnetization

Before structural correction									After structural correction						
N	n	R	k	D_m	I_m	pole lat	pole long	dp,dm	R	k	D_m'	I_m'	pole lat	pole long	dp,dm
5	12	4.876	32.3	147	-62	23S	280E	17,21	4.876	32.3	147	-62	23S	280E	17,21

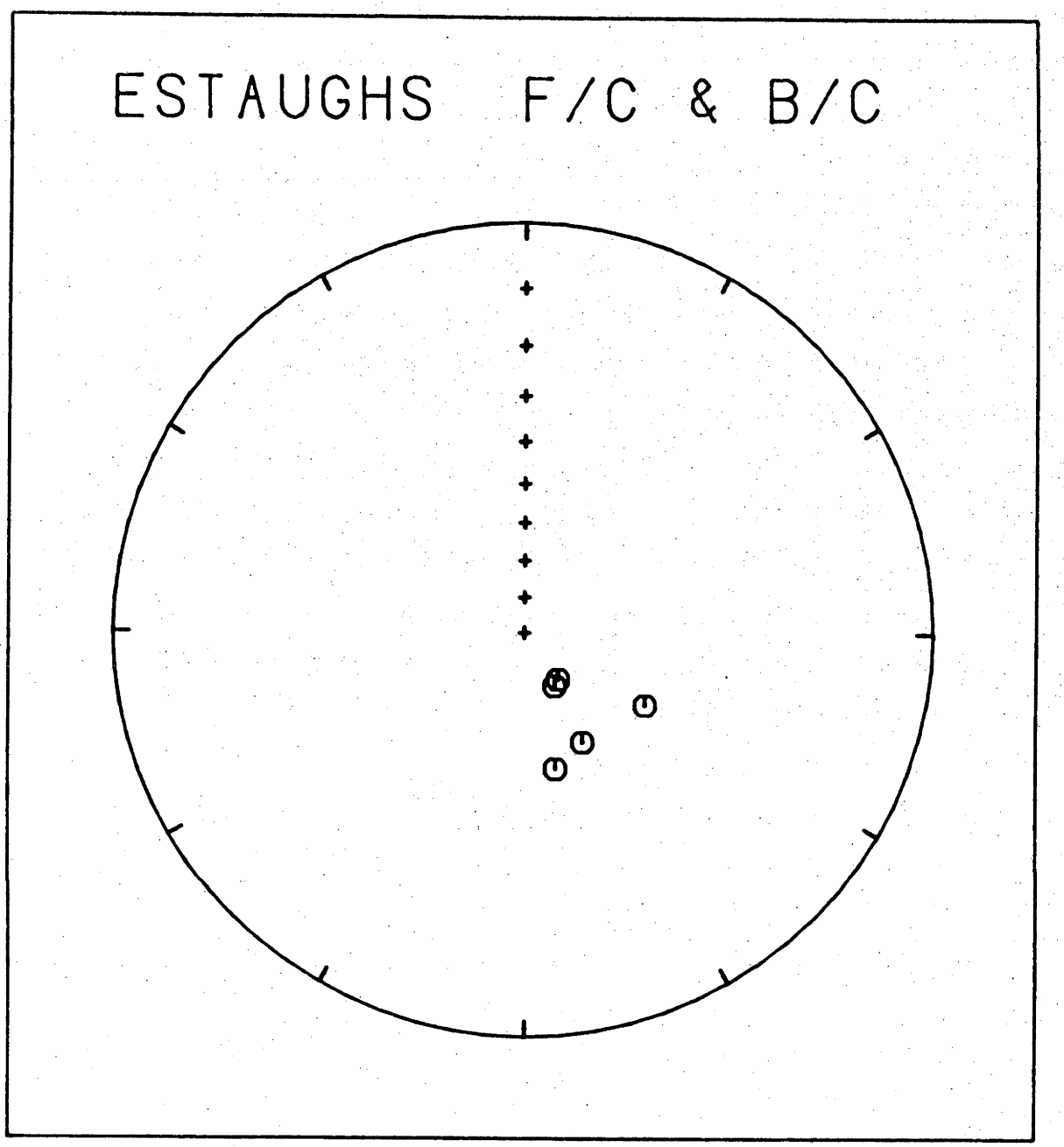

Figure 3.13 : Cleaned site mean magnetization directions, Estaughs Formation; equal-angle projection. Open symbols denote negative inclination.

sandstones of the Lubbock and Tean Formations were sampled at stratigraphically higher levels in the section (Figure 3.11).

Egan Formation

Samples of the Egan Tillite had scattered NRM directions with generally east trending declinations and shallow to moderate negative inclinations. Upon thermal demagnetization, a component averaging 75% of the total NRM intensity was removed from most specimens in the 20°-200° heating step, accompanied by a large directional change (Figure 3.14). The directions of the removed component were widely scattered with a mean direction 117,-14(n=13,R=9.318). After removal of this low T_b component, magnetization directions were weak, but reached a stable endpoint with a steeply inclined northerly trend in the 300°-580° range (Figure 3.15). The mean direction of the samples with stable endpoints is 002,-61(n=11, R=10.293), which is not significantly different from the local PEF direction. As the samples were taken from two localities with a similar structural orientation, overall precision of both these mean directions remains essentially constant upon structural correction and a fold test cannot be employed. Without a fold test, it is probably more correct to assume that the stable high T_b component is of recent origin, probably a CRM aquired during groundwater percolation through the matrix of the tillite. One puzzling aspect is that the pole position calculated from the low T_b subtracted vector direction lies at 23N,051E which could be a Cambrian or Ordovician magnetization (Figure 3.34). This would require that the simple T_b age relationship invoked in earlier sections be reversed, *i.e.* that the low T_b component is older. An alternative to this

Plate 5 - Egan Tillite

Plate 6 - Cottons Breccia

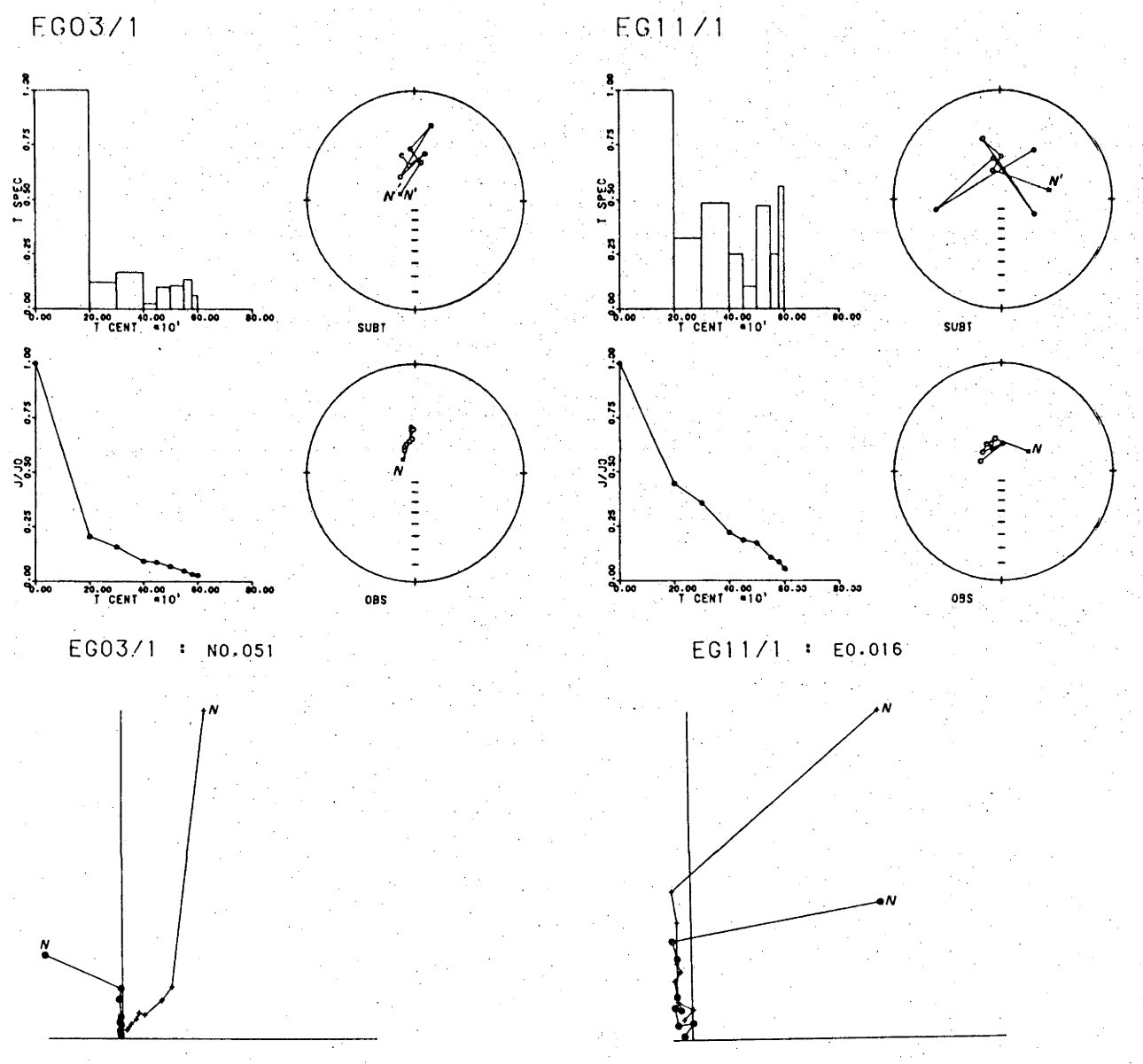

Figure 3.14 : Thermal demagnetization, Egan Formation.

TABLE 3.5

EGAN TILLITE : Low T_b subtracted vectors

SAMPLE	D_m	I_m
01	122	+26
02	128	-57
05	122	-15
06	071	-45
08	134	-02
09	093	+38
10	101	-65
11	080	-41
12	146	+15
13	134	-05
14	103	-31
15	139	+25
Mean :	117	-14
	(n=12,R=9.318,k=4.1)	
Pole :	23N,051E (dp,dm=13,25)	

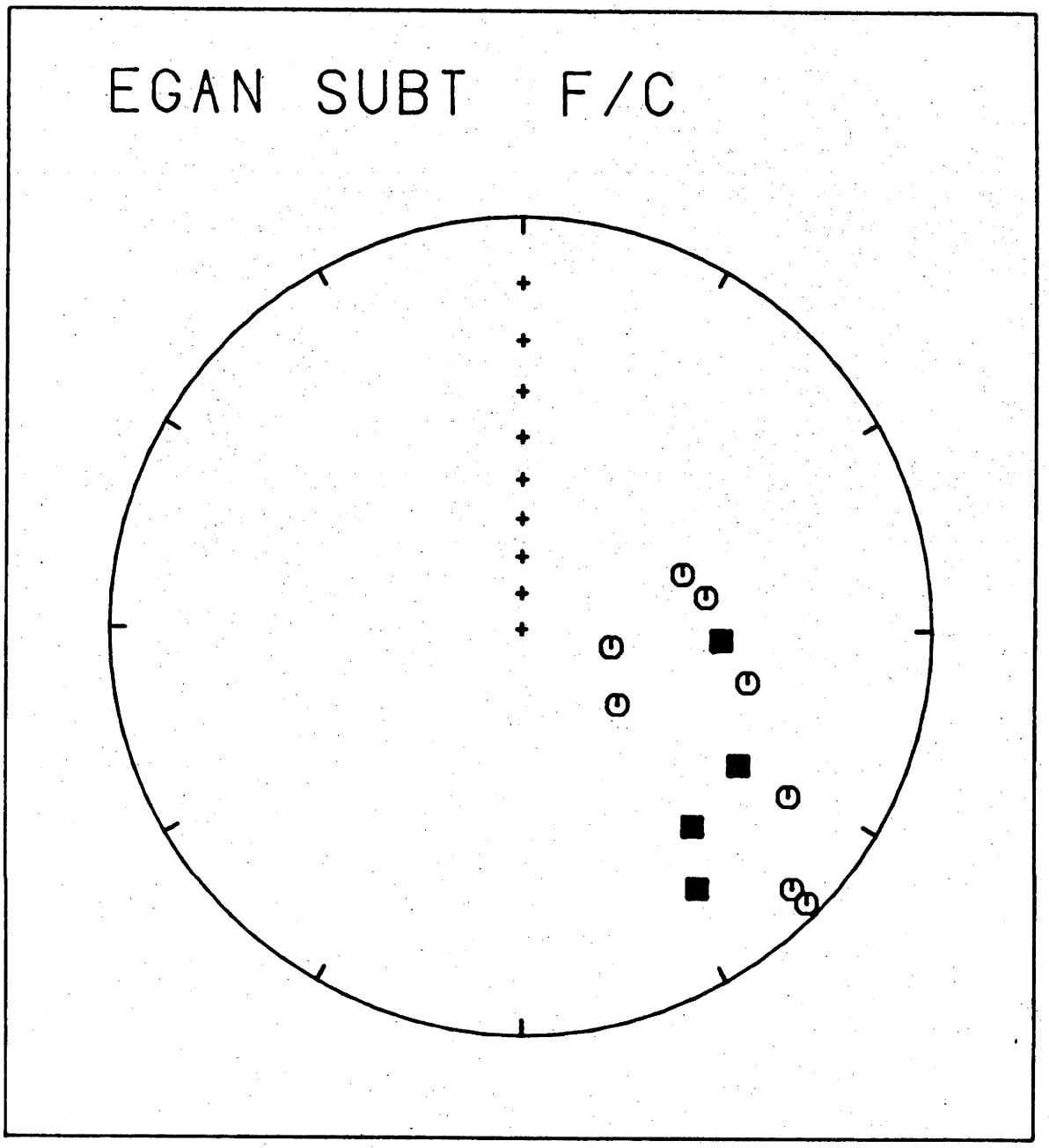

Figure 3.15 : Sample means, low T_b removed component, Egan Formation; equal-angle projection. Open (closed) symbols refer to negative (positive) inclination.

puzzling but not impossible conclusion might be that the low T_b magnetization is a spurious shock induced component acquired during blasting of the road cuttings where the samples were taken.

Yurabi Formation

Most of the mean NRM directions of samples from the Yurabi Formation were aligned very nearly with the PEF direction, although some samples did have positive inclinations. Detailed pilot thermal demagnetization in 13 steps to 580° showed that very high T_b magnetizations were present in about half of the pilot specimens. These specimens exhibited very stable directional behaviour, reaching stable endpoints in the 650°-670° range in most cases. The remaining specimens had relatively low T_b magnetizations which never attained directional stability. While directionally stable, the high T_b magnetizations were dispersed and no systematic grouping of cleaned directions, or subtracted vectors was seen, apart from PEF directions.

Lubbock Formation

Like the Yurabi Formation, sample mean NRM directions of the Lubbock Formation were scattered but not significantly different from the PEF direction. Upon thermal demagnetization, a large PEF component was removed from most pilot specimens and in final analysis 9 samples from 3 sites reached stable endpoints in the 400°-600° range (Figure 3.16). Cleaned mean directions for these three sites are listed in Table 3.6. Dispersion is reduced upon making structural corrections, although the improvement is not significant at the 95% level

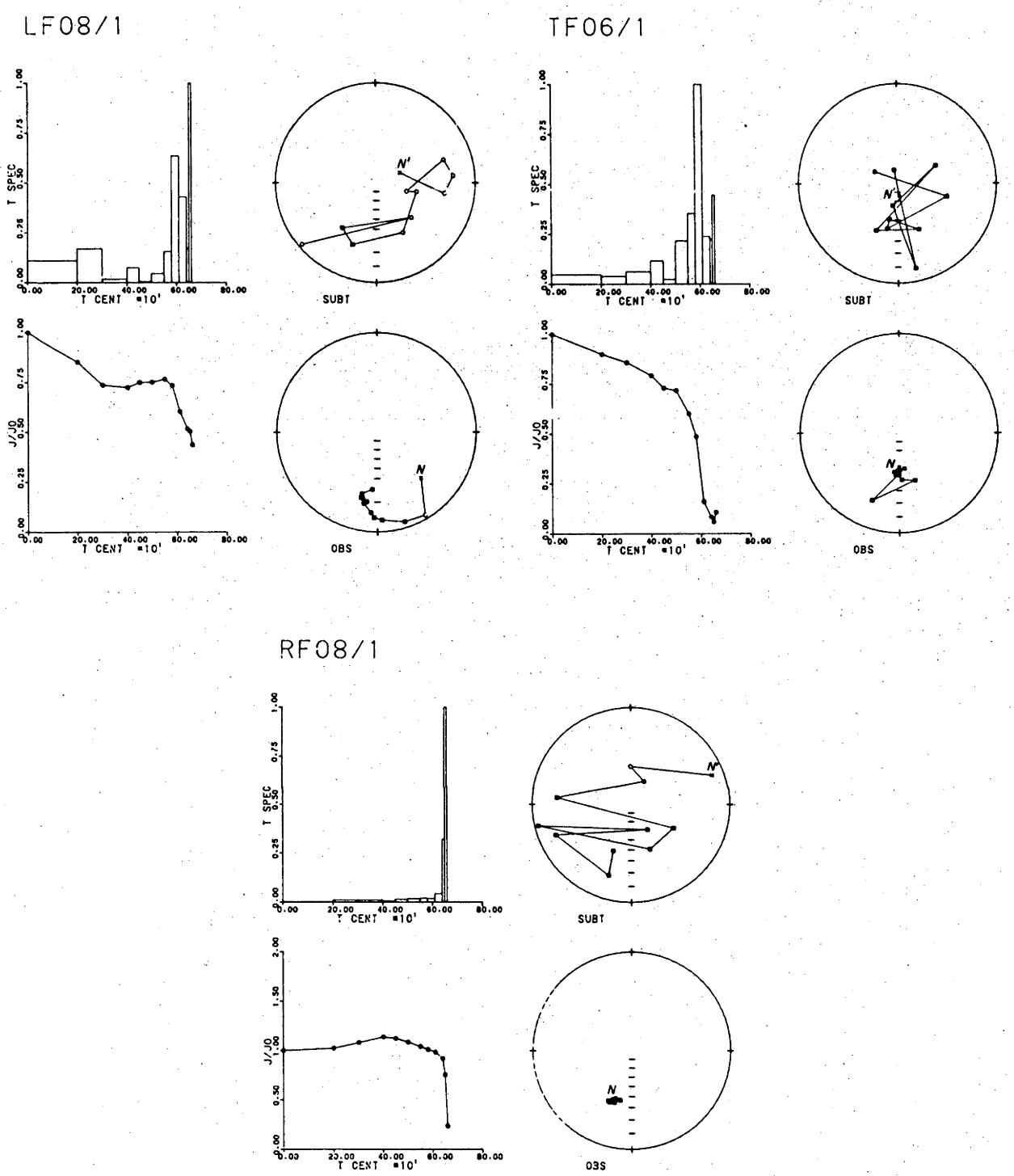

Figure 3.16(A) : Thermal demagnetization, Lubbock Formation, Tean Formation and Ranford Formation.

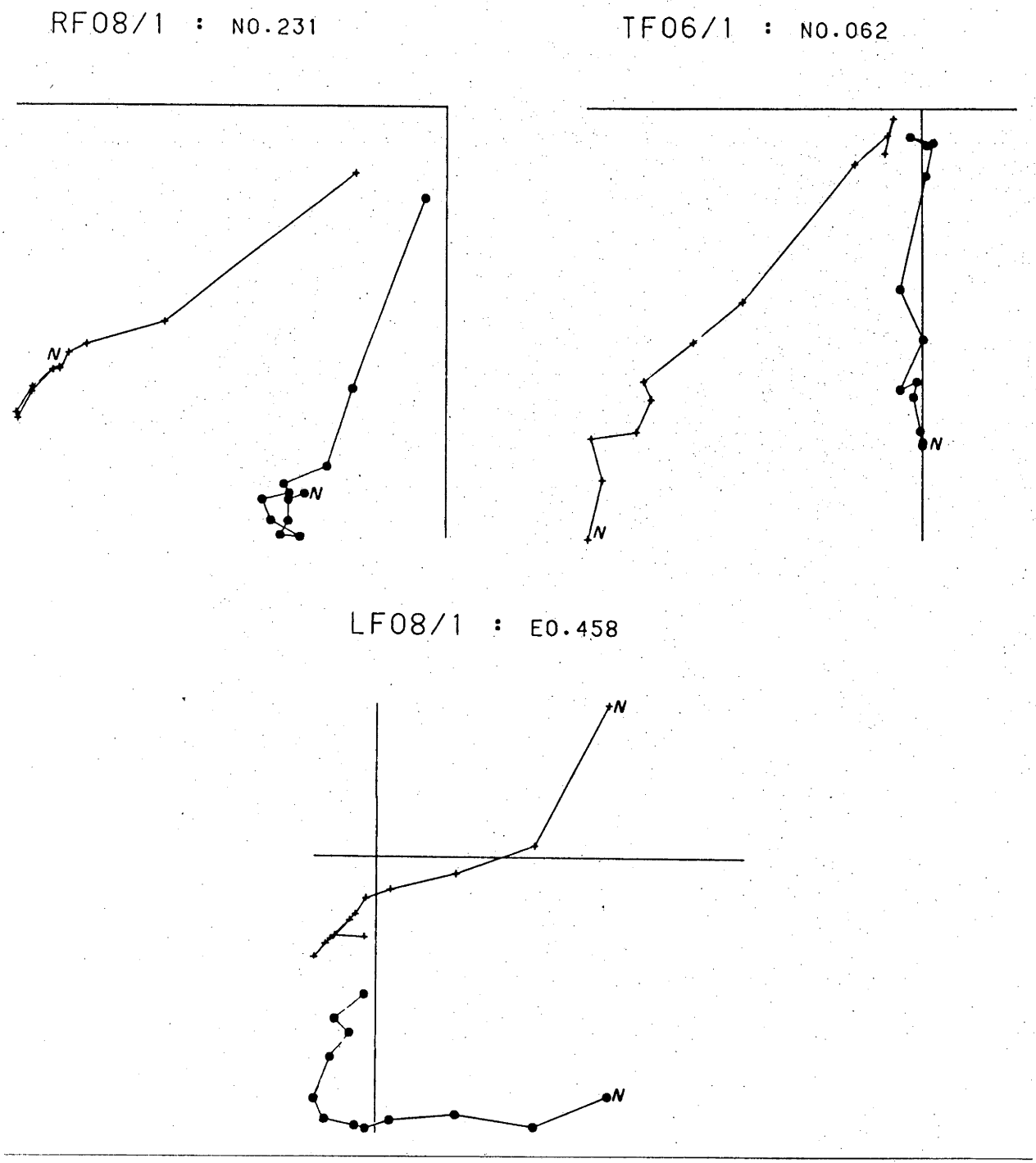

Figure 3.16(B) : Thermal demagnetization, Lubbock Formation, Tean Formation and Ranford Formation (continued).

TABLE 3.6

LUBBOCK FORMATION : Site mean directions after thermal demagnetization (580°- 650°)

SITE	N,R	D,I	D',I'
1	3,2.645	185,- 04	185,- 04
2	3,2.655	196,+19	197,- 02
4	3,2.948	178,+18	178,+08
Mean :		186,+11 ($R=2.925, \alpha_{95}=24°$)	187,+01 ($R=2.959, \alpha_{95}=18°$)
Pole position:		75S,332E dp,dm=13,25	71S,328E dp,dm= 09,18

TEAN FORMATION : Sample mean directions after thermal demagnetization (400°- 600°)

SAMPLE	D,I	D',I'
1	183,+69	147,+38
2	213,+53	175,+38
3	199,+64	158,+39
4	179,+58	153,+28
5	170,+37	175,+37
6	180,+45	184,+37
8	181,+49	186,+40
Mean :	185,+54 ($R=6.819, \alpha_{95}=11°$)	168,+38 ($R=6.846, \alpha_{95}=10°$)
Pole position:	74S,112E dp,dm=11,15	79S,202E dp,dm=07,12

TABLE 3.6 (continued)

RANFORD FORMATION : Sample mean directions after thermal demagnetization (650°)

SAMPLE	D,I	D',I'
7	201,+30	202,+36
8	199,+36	200,+42
9	249,+14	250,+16
10	205,+32	207,+37
11	201,+22	202,+27
12	192,+25	192,+31
Mean:	208,+28 ($R=5.688, \alpha_{95}=17°$)	209,+33 ($R=5.688, \alpha_{95}=17°$)
Pole position:	63S,036E dp,dm=10,19	62S,043E dp,dm=11,20

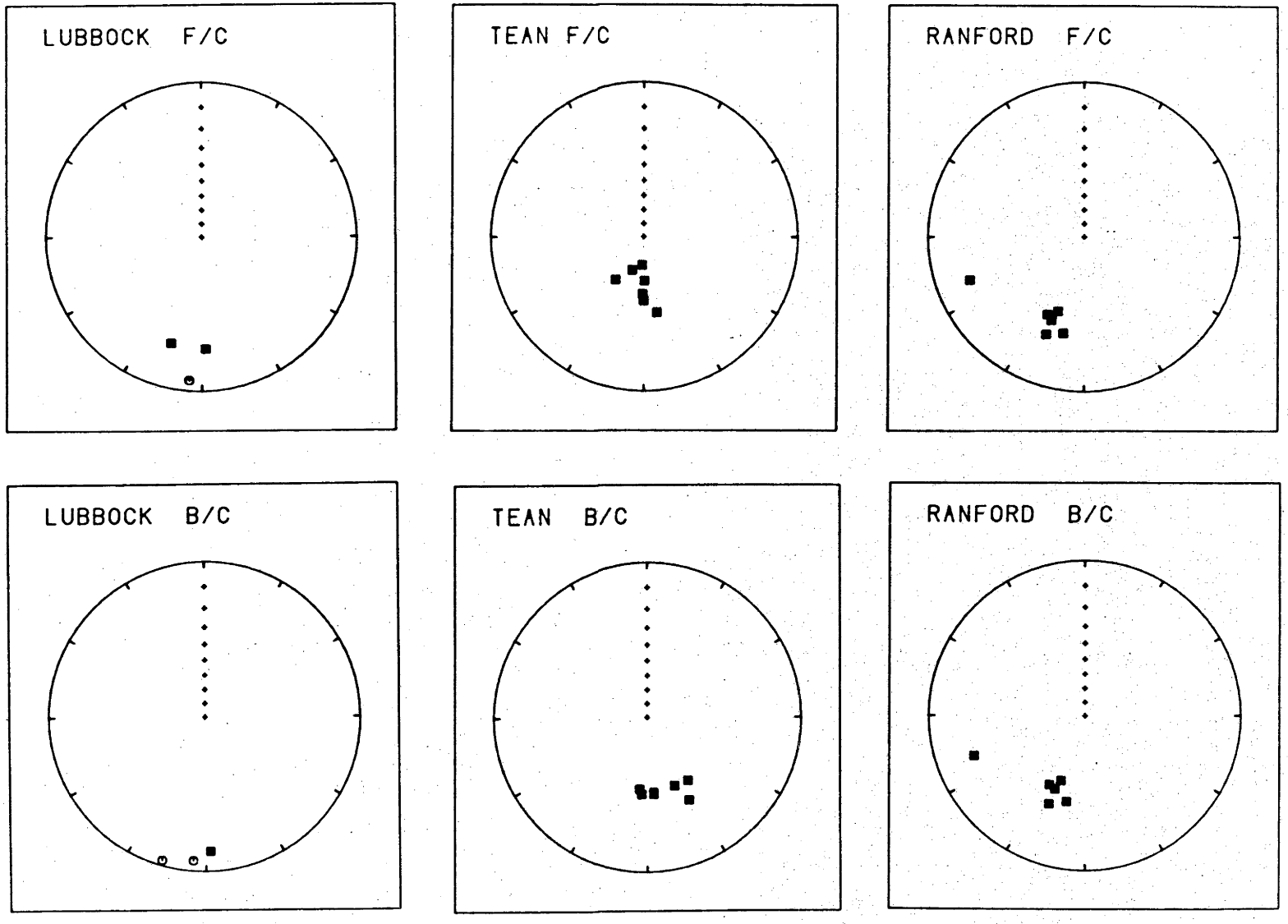

Figure 3.17 : Cleaned (site, sample) mean directions, (Lubbock, Tean, Ranford) Formations; equal angle projection. Open (closed) symbols refer to negative (positive) inclinations.

(k'/k=1.84, 95% significance point ≅5.05). The pole position from the structurally corrected mean direction lies between the PR1 pole position from the Pertatataka Formation and the AR2 pole from the Arumbera Sandstone (Figure 3.34). If the correlation of glacial successions between the Amadeus and Kimberley Basins is correct, the position of the Lubbock Formation pole combined with the increase in precision upon unfolding of the beds suggests an original Precambrian age of magnetization.

Tean Formation

NRM directions from samples of the Tean Formation were well grouped and reversed with respect to the PEF direction. Thermal demagnetization studies showed that of the 8 samples collected, 7 had directionally stable magnetizations in the 200°-580° heating range. After heating above 580° the onset of directional instability was marked by a sharp decrease in intensity (Figure 3.16). Directional scatter between the 7 stable samples is reduced after making structural corrections, but the increase in precision is not significant at the 95% level (k'/k=1.18, 95% significance point ≅2.58). The pole position calculated from the structurally uncorrected mean direction is very near the mean Upper Devonian-Lower Carboniferous and Tertiary poles for Australia (Schmidt, 1976), while the pole from the corrected direction is displaced about 30° eastwards from that of the underlying Lubbock Formation. A secondary rather than primary Precambrian age of magnetization is favoured.

§3.3.5 Duerdin Group (lower glacial succession): Ranford Formation

One formation in the Duerdin Group was sampled east of the Halls Creek Mobile Zone, the Ranford Formation. Samples of red and brown shales were taken at two localities in the Moonlight Valley. The Johnny Cake Shale Member of the Ranford Formation has been dated at 671±44*my using the whole-rock Rb/Sr isochron method (Bofinger, 1967).

NRM directions from one sampling locality were characterized by streaked shallow southwesterly directions; samples from the second locality had NRM directions with northerly declinations and steep negative inclinations. During thermal demagnetization, the former group of samples underwent systematic directional changes in the 20°-200° and 200°-300° steps as a PEF component was removed, stabilizing at the 400° and higher heating steps (Figure 3.16). Samples from the latter group generally remained stable up to the 650° heating but were collectively never significantly different from the PEF direction.

The six samples from the first locality which were different from the PEF direction are reasonably well grouped (Table 3.6 and Figure 3.17). No fold test was possible. The pole positions calculated from both the uncorrected and corrected mean directions are probably not different from the mean Upper Silurian-Lower Devonian or Middle Devonian-Lower Carboniferous poles from Australia (Schmidt, 1976; Figure 3.34). Athough the age of magnetization could be Precambrian (RF is similar to other late Precambrian poles), in the absence of evidence to the contrary, a secondary Palaeozoic age of magnetization is favoured as the more prudent assumption.

§3.4 Officer Basin: Chambers Bluff Volcanics, Table Hill Volcanics

Adelaidean strata outcrop in the Officer Basin of central and western South Australia and southeastern Western Australia (Figure 3.1). Little is known in detail of the stratigraphy and structure in this region, largely as a result of incomplete mapping due to poor exposure and inaccessibility. Two isolated igneous units from the Officer Basin were selected for palaeomagnetic study, with the hope that pole positions combined with available and potential isotopic age data might help to 'calibrate' the late Precambrian polar tracks for Australia derived from other stratigraphic sections which are devoid of igneous rocks. No previous palaeomagnetic studies have been reported from the Officer Basin.

§3.4.1 Chambers Bluff Volcanics

At Chambers Bluff in the Indulkana Ranges, a (?) Sturtian tillite is overlain, possibly conformably, by basalt and melaphyre (Figure 3.18; Thomson, 1969). The Adelaidean sequence dips to the southeast and unconformably underlies shallowly dipping Ordovician sediments. Samples of the volcanics (called herein the Chambers Bluff Volcanics for want of an official name) were taken at 11 sites through a thickness of 0.5 km of flows.

Site mean NRM directions were widely scattered with negative inclinations. Pilot AF demagnetization studies (Figure 3.19) suggested that, like the Wooltana Volcanics (§2.7.2), at least part of the total NRM was carried by high coercive force minerals of the hematite-ilmenite solid solution

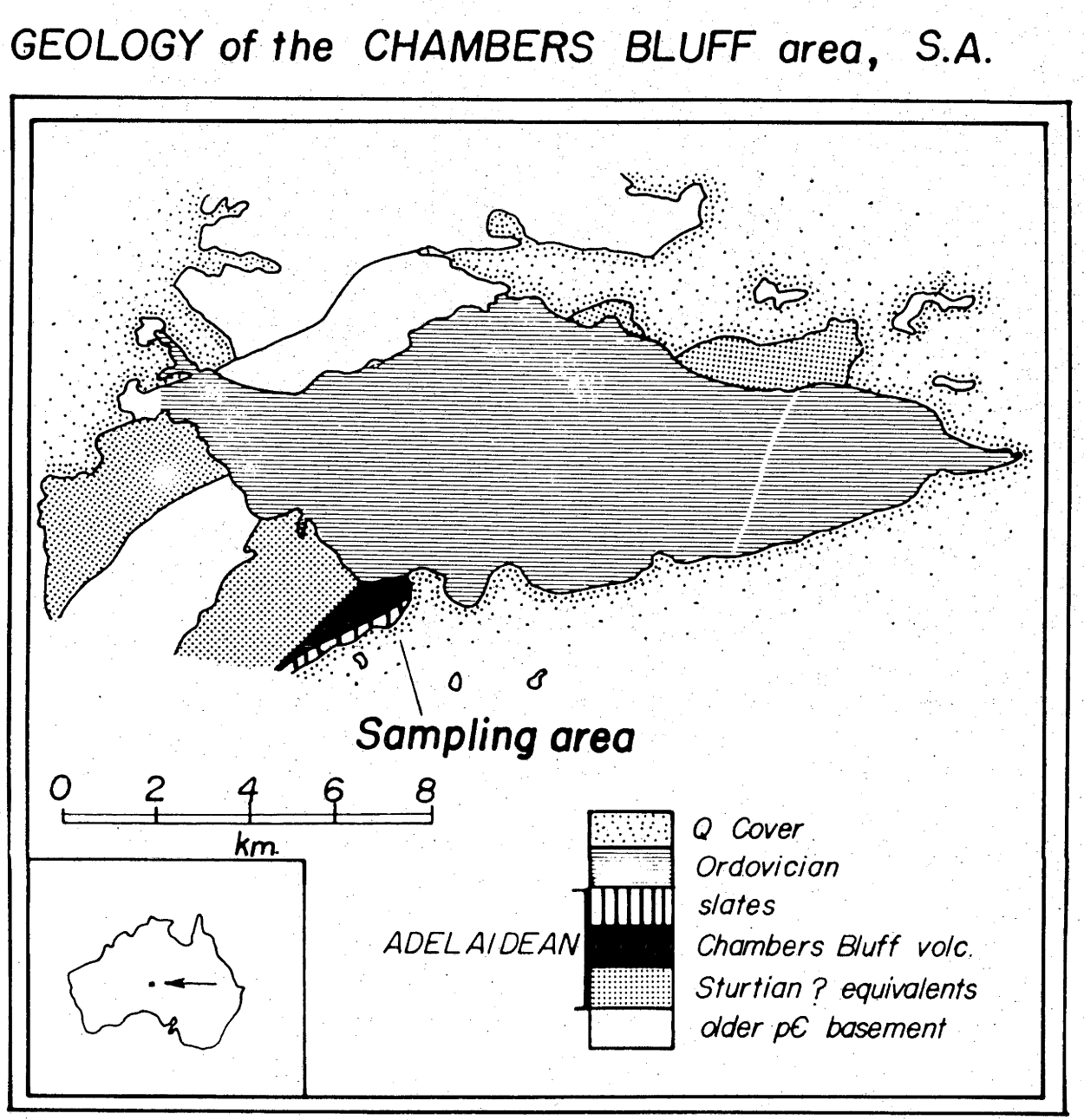

Figure 3.18 : Geological sketch of the Chambers Bluff area, Indulkana Ranges, South Australia, showing outcrop area of Chambers Bluff Volcanics. Map centred approximately upon 133°09'E, 27°00'S.

series. Inspection of polished sections of the volcanics in reflected light confirmed a moderate to high oxidation state for the lavas, with magnetite having been altered to hematite and ilmenite lamellae partially replaced by pseudobrookite. The original lamellar structure is almost completely obscured in some examples. Thermal demagnetization studies were conducted in attempt to demagnetize fully the high coercive force minerals, and to discover whether multicomponent magnetizations might be present.

Three general types of directional behaviour were observed during thermal demagnetization:

(1) Magnetizations initially with southwest (northeast) trending declinations and shallow to moderate negative (positive) inclinations which remained directionally stable during stepwise heating,

(2) Magnetizations with directional stability similar to (1) above, however declinations were northwest (southeast) trending with shallow to moderate negative (positive) inclinations, and

(3) Magnetizations with directions initially similar to (2) above, which upon progressive demagnetization systematically swing to the south, becoming aligned with directions like (1) above, reaching directional stability in the 300°-400° range. During the directional swing, a magnetization similar in direction to (1) above was removed.

The observed stable magnetizations of (1) and (2) above and the subtracted component of (3) have been respectively designated the WP1, WP2 and WP3 magnetizations in Table 3.7 and in Figure 3.2.1. An F-ratio test (Table 3.7) indicates

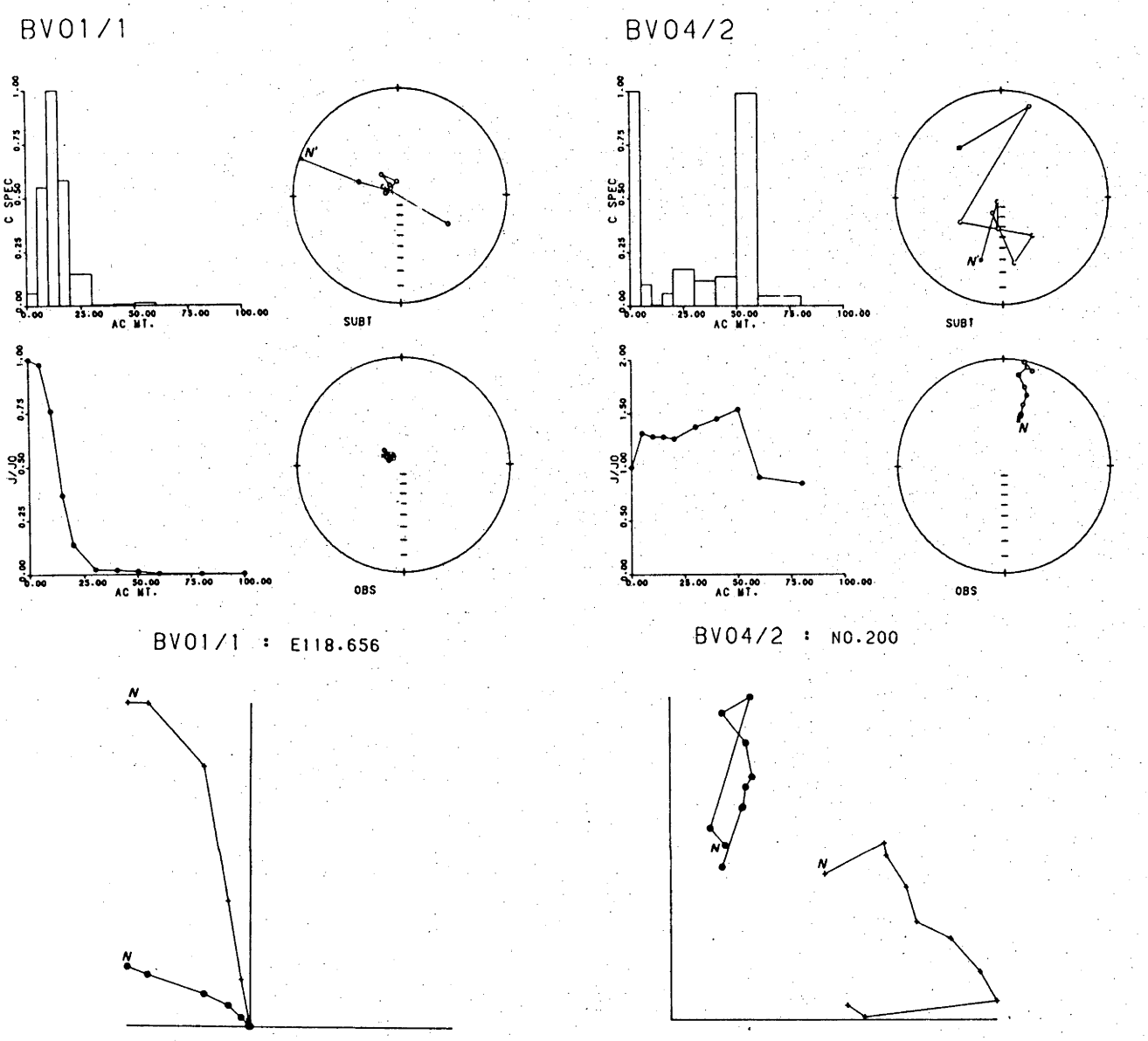

Figure 3.19 : AF demagnetization, Chambers Bluff Volcanics.

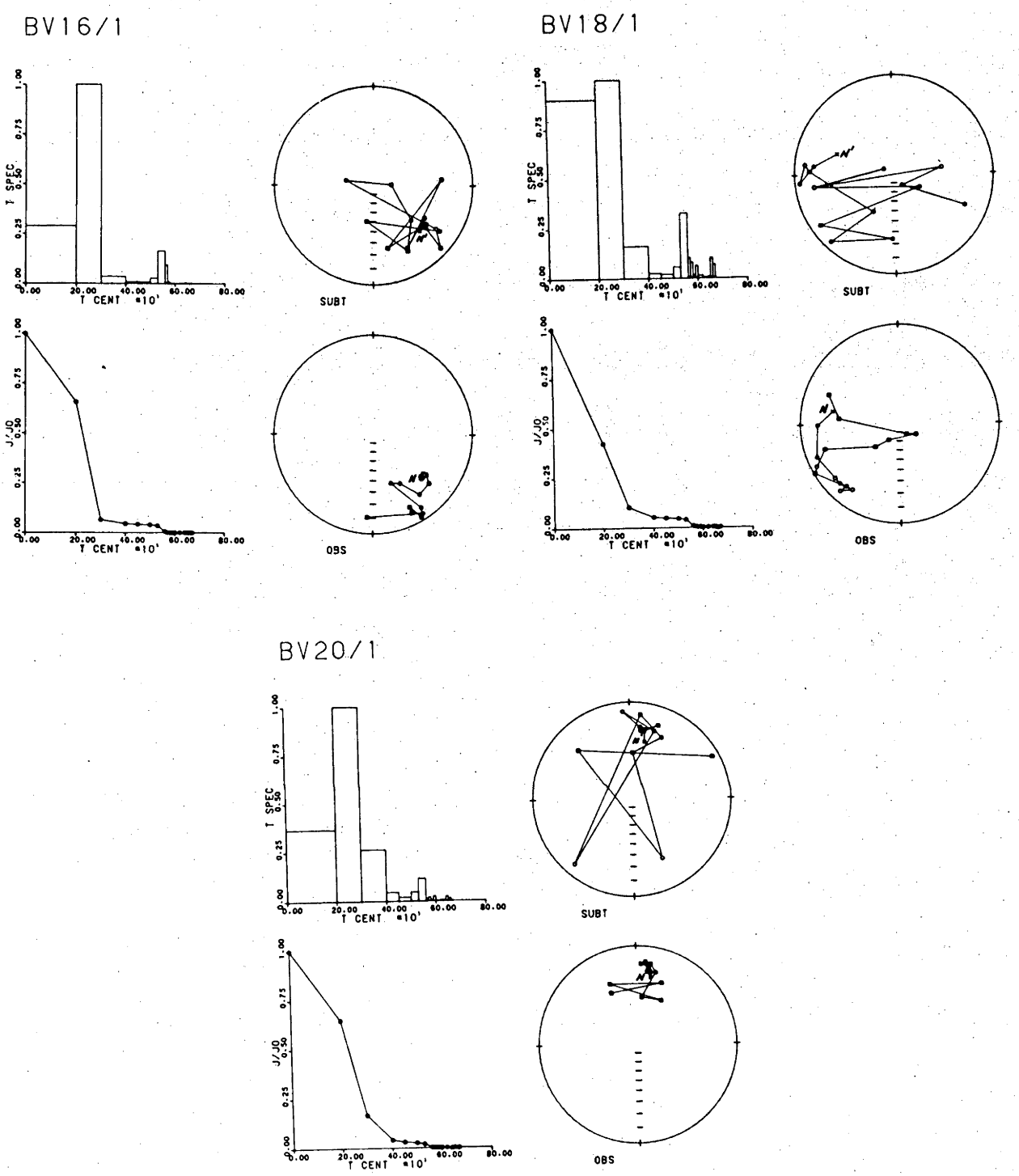

Figure 3.20(A) : Thermal demagnetization, Chambers Bluff Volcanics.

BV16/1 : E1340.714

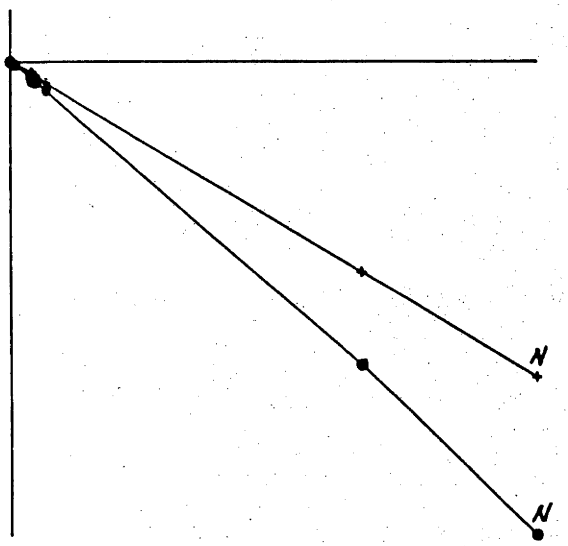

BV18/1 : E23.273

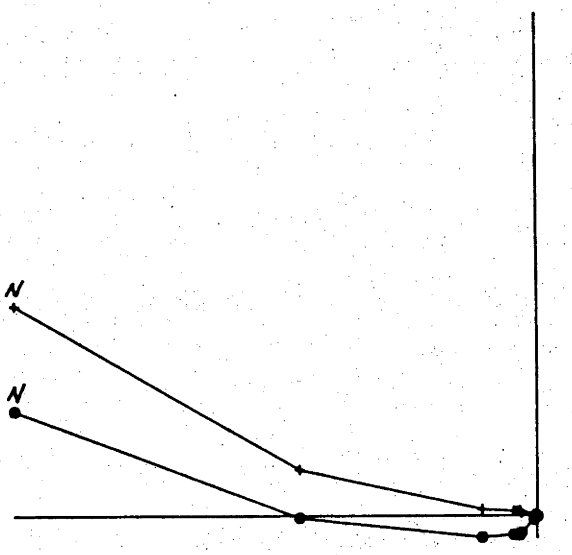

BV20/1 : N245.086

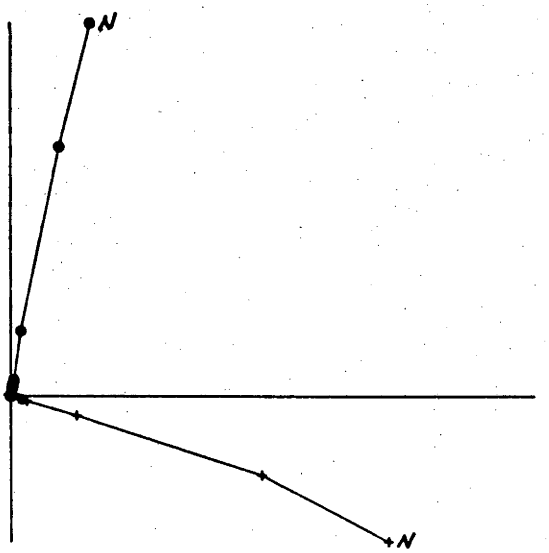

Figure 3.20(B) : Thermal demagnetization, Chambers Bluff Volcanics (continued).

TABLE 3.7 (A)

CHAMBERS BLUFF VOLCANICS : Site mean directions before and after thermal demagnetization

MAGNETIZATION	SITE	Before structural correction N	R	D	I	After structural correction D'	I'	T°C
NRM	1	4	2.516	059	-77			
	2	3	2.893	013	-32			
	3	3	2.914	288	-23			
	4	3	1.189	343	-61			
	5	3	1.512	180	-11			
	6	4	2.930	339	-33			
	7	3	2.416	266	-53			
	8	3	1.785	156	-51			
	9	3	2.452	267	-72			
	10	3	2.260	302	-61			
	11	3	1.996	084	-24			
WP1	2	3	2.978	023	20	037	31	500
	3	1	-	227	-27	242	-25	500
	4	2	1.982	196	-35	221	-47	500
	5	2	1.917	213	-19	225	-25	500
	6	2	1.905	212	-20	225	-27	500
	7	3	2.982	209	-39	236	-44	500
	8	2	1.955	190	-53	238	-63	500
	9	2	1.888	195	-47	233	-56	500
	10	1	-	190	-25	207	-41	500
WP2	1	2	1.929	253	-69	291	-48	500
	3	2	1.916	292	-18	293	09	500
	4	1	-	155	29	153	00	500
	5	1	-	130	23	131	-07	500
	8	1	-	162	21	161	-07	500
	10	2	1.876	290	-43	298	-16	500
	11	2	1.821	291	-42	298	-15	500
WP3	1	1	-	265	-63	291	-40	300-450
(subtracted directions from WP1 vectors)	2	1	-	350	-57	339	-29	300-450
	3	1	-	296	-22	298	05	300-400
	6	1	-	283	-20	285	04	300-450
	7	3	2.992	331	-30	330	00	300-400
	8	1	-	336	-63	329	-33	300-450
	9	3	2.877	328	-49	326	-19	300-450

TABLE 3.7 (B)

CHAMBERS BLUFF VOLCANICS : Mean directions before and after structural correction

	Before structural correction						pole			After structural correction				pole		
MAGNETIZATION	N	n	R	k	D_m	I_m	lat	long	dp,dm	R	k	D_m'	I_m'	lat	long	dp,dm
WP1	9	18	8.678	24.9	205	-32	39S	345E	07,12	8.678	24.9	227	-40	23S	360E	08,13
WP2	7	11	6.296	8.5	307	-37	41N	039E	15,26	6.287	8.4	310	-08	37N	060E	11,22
WP3	7	11	6.302	8.6	311	-47	47N	030E	18,28	6.299	8.6	314	-17	43N	057E	12,23
WP2+WP3	14	22	12.553	9.0	309	-42	44N	035E	11,17	12.541	8.9	312	-13	40N	058E	07,14

TABLE 3.7 (C)

CHAMBERS BLUFF VOLCANICS : F-ratio test; WP2 and WP3 magnetizations

N	R_1	R_2	R	$F_{2,24}$	Significance point (95%)
14	6.302	6.296	12.553	0.39	3.40

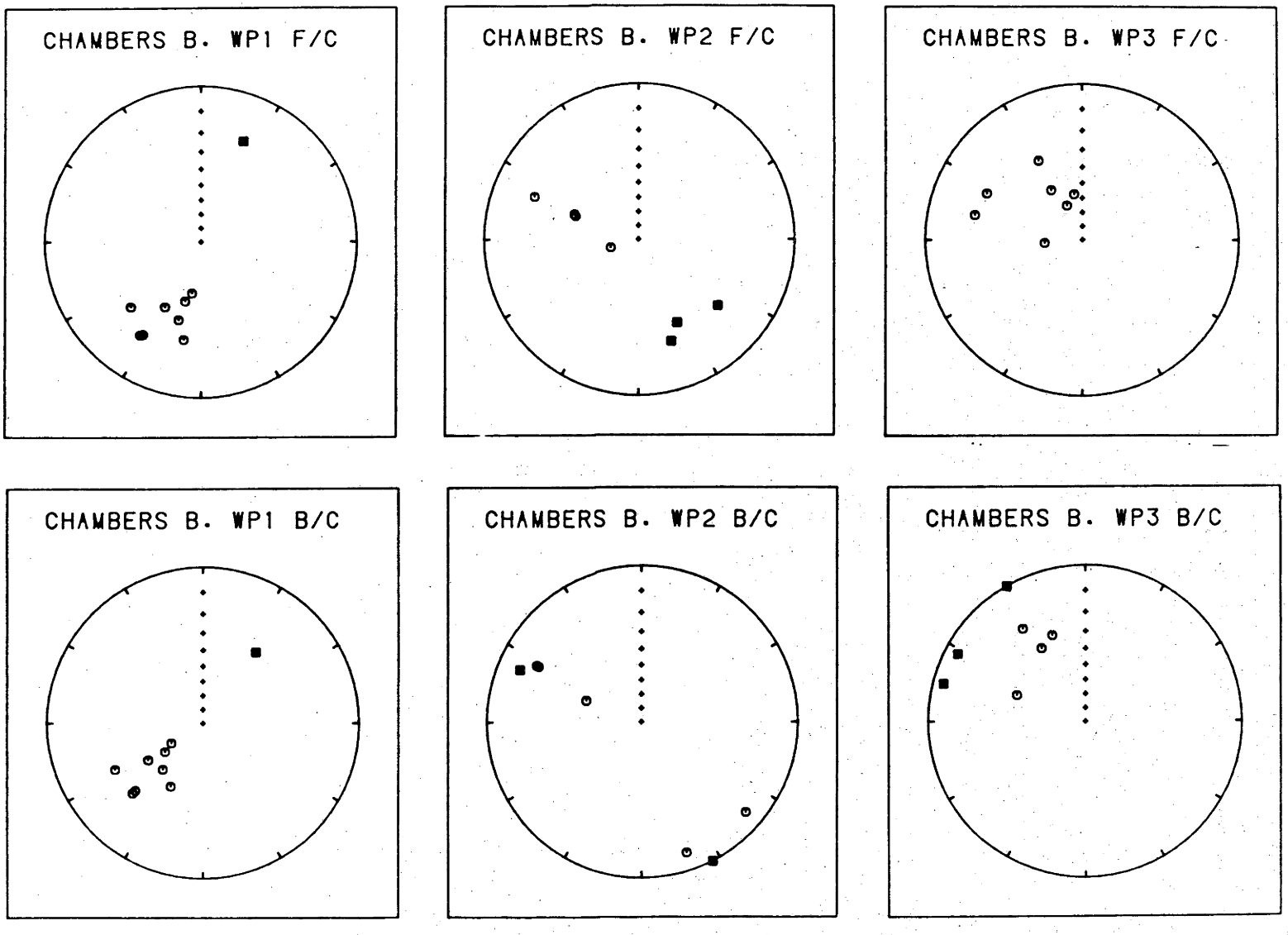

Figure 3.21 : Cleaned site mean magnetization directions, Chambers Bluff Volcanics WP1, WP2 and WP3 components; equal-angle projection. Open (closed) symbols refer to negative (positive) inclination.

that the (observed) WP2 and (subtracted) WP3 mean directions are not significantly different at the 95% confidence level. Therefore two magnetizations are present, and a particular sample may exhibit either the WP1 magnetization, the WP2 magnetization or both. The WP1 component has a higher T_b than the WP2 component in samples which exhibit both magnetizations.

Unlike the Pertatataka Formation (§3.2.4), an assessment of the relative ages of the WP1 and WP2 (+WP3) components cannot be based on a fold test, as the volcanics only outcrop in one locality with a nearly constant structural orientation. Again invoking the simple T_b-age relationship, the WP2 (+WP3) component is possibly the younger. This simple picture accords with the pole positions calculated from the two mean directions, as the WP1 pole is near other Adelaidean poles, while the WP2 (+WP3) poles are similar to Cambrian and Ordovician poles from elsewhere in Australia (Figure 3.34). Further discussion concerning the relative ages of the two components is deferred until §3.7. No isotopic age information is available for the Chambers Bluff Volcanics, however samples have been collected for U-Pb zircon studies, and a result may be forthcoming.

§3.4.2 Table Hill Volcanics

Outcrops of altered basaltic rocks with petrological affinities occur at widely scattered localities around the western part of the Officer Basin of South Australia and Western Australia (Figure 3.22). Peers (1969) originally interpreted the separate outcrops as contemporaneous and comagmatic and discussed discordant K/Ar ages from the

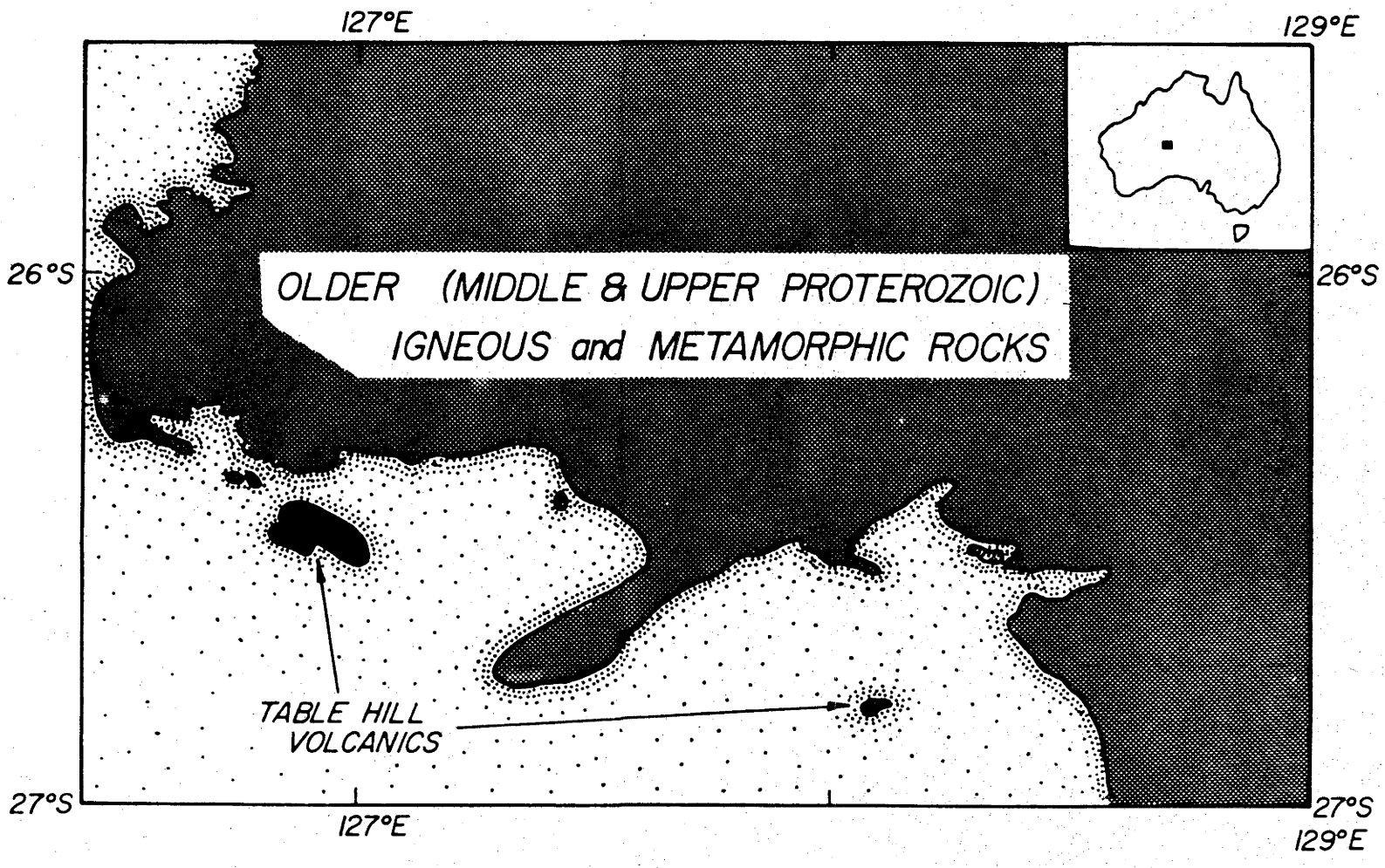

Figure 3.22 : Geological sketch of part of the Officer Basin, W.A., showing scattered surface outcrops of Table Hill Volcanics.

volcanics which suggested an Ordovician age of extrusion. Subsequent geological mapping and seismic studies have given support to Peers' original conclusion of contemporeneity (Lowry *et al.*, 1972), and indicate that a continuous widespread subsurface occurrence of the basalts may be present. Jackson (in Compston, 1974) has recommended the name *Table Hill Volcanics* for the basalts.

Although their exact stratigraphic position is uncertain, the following indirect information (summarized from Compston, 1974) is available:

(1) The Table Hill Volcanics are younger than the Townsend Quartzite, which unconformably overlies the Table Volcanics dated at 1060±110 my (Compston and Nesbitt, 1967).

(2) The Table Hill Volcanics are probably equivalent to the Kulyong Volcanics (Lowry *et al.*, 1972) and therefore stratigraphically above the Punkerri Sandstone. Major (1968) described a possible Ediacara fauna trace fossil in the Punkerri Sandstone which was subsequently confirmed as *Rangea* (Glaessner, 1971).

(3) The volcanics unconformably overlie probable Precambrian glacial beds and are in turn unconformably overlain by Permian glacial strata.

A model Rb/Sr age of about 1100 my has been calculated for the volcanics (Bofinger; in Jackson, 1966), however the above evidence would suggest a late Precambrian or early Palaeozoic age of extrusion. In a more recent study, Compston (1974) suggested that the initial $^{87}Sr/^{86}Sr$ ratio used in the model calculation might be too low, and in conjunction with new Rb/Sr

TABLE 3.8

TABLE HILL VOLCANICS : Calculation of mean inclination by method of Briden and Ward (1960)

Sample	Depth (m)	$\lvert\bar{I}_i\rvert$ (20mT)	θ_i	Sin θ_i	Cos θ_i
1	7	20.0	70.0	0.9397	0.3420
4	21	6.1	83.9	0.9943	0.1063
5	22	10.6	79.4	0.9829	0.1840
6	30	19.2	70.8	0.9444	0.3289
7	35	15.5	74.5	0.9636	0.2672
8	41	17.3	72.7	0.9548	0.2974
9	49	4.5	85.5	0.9969	0.0785
10	60	24.9	65.1	0.9070	0.4210
12	45	9.0	81.0	0.9877	0.1564

$\bar{C} = \frac{1}{N} \Sigma \text{ Cos } \theta_i = 0.2424$

$\bar{S} = \frac{1}{N} \Sigma \text{ Sin } \theta_i = 0.9635$

$\Lambda = [1 - (\bar{C}^2 + \bar{S}^2)^{-\frac{1}{2}}]^{-1} = 153.4$

$\theta = \tan^{-1} (\frac{\bar{S}}{\bar{C}}) = 75.9$

$\hat{I}_o = 14.8°$ $\hat{k} \cong 77$, dp $\cong 3°$

Arithmetic mean : $(\frac{1}{N} \Sigma |I_i| = 14.1°)$

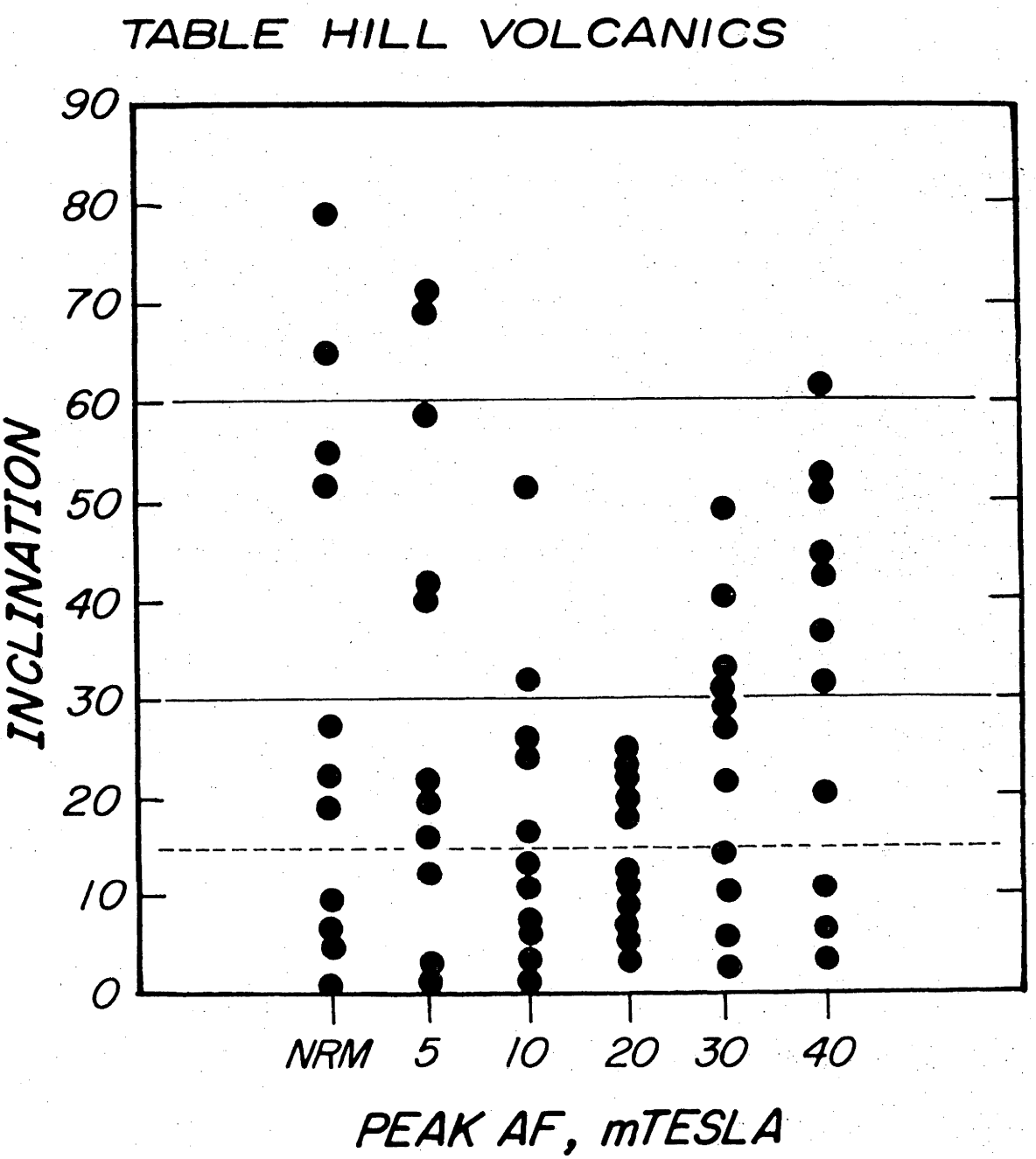

Figure 3.23 : AF demagnetization, Table Hill Volcanics. Individual specimen inclinations plotted versus peak alternating field.

analyses reached the conclusion that "... the Rb/Sr data are best interpreted as signifying an original extrusion of the basalts at 575±40 my ...".

Although it was not possible to directly sample the volcanics, core samples from the Yowalga No. 2 bore were available. Twelve samples were cut from vertically drilled borecore material taken at depths ranging from 7 to 60 m through a number of flows. The flows are flat lying at the drilling site (M.J. Jackson, pers. comm.) and therefore no tectonic correction is applied to the inclination results.

Progressive AF demagnetization studies showed that 9 of the 12 samples had magnetically 'soft' but stable remanence vectors; dispersion in inclination was minimized after the 20 mT demagnetization step (Figure 3.23). Inspection of polished sections in reflected light showed that much of the original lamellar magnetite-ilmenite structure was still present, although some high temperature oxidation had taken place. The basalts are probably best described as Class 3 in oxidation state (Wilson and Watkins, 1967).

Following the procedure for estimation of mean inclination in azimuthally unoriented borecore samples outlined by Briden and Ward (1960), a mean value of 14.8° was calculated for the Table Hill Volcanics samples (Table 3.8). The inclinations are well grouped; the uncertainty in mean inclination gives rise to a 'polar' error dp of 3°. The locus of poles described by the mean inclination intersects the Amadeus Polar Track at approximately the AR2 Arumbera Sandstone position (Precambrian-Cambrian boundary, Figure 3.34). In conjunction with the stratigraphic and fossil evidence, and with the new Rb/Sr age information, the results are very

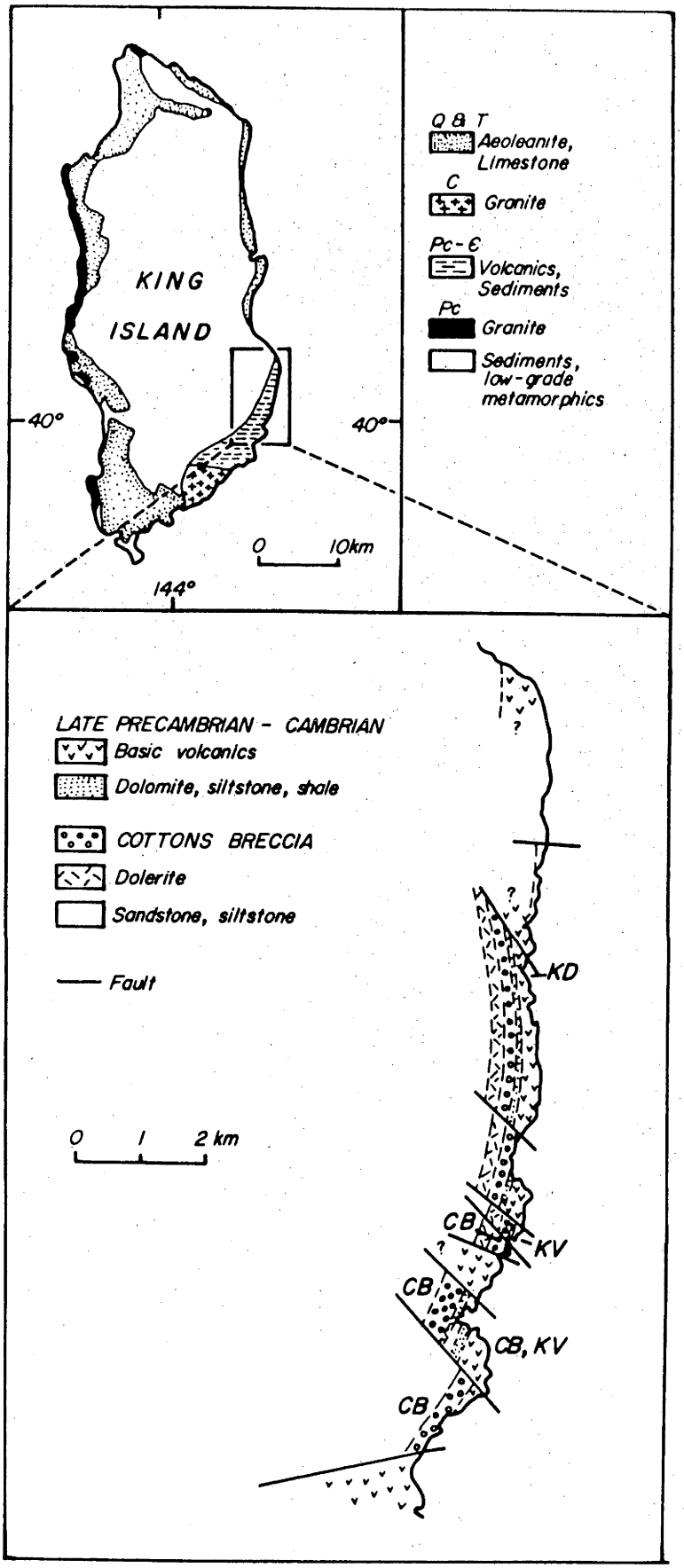

Figure 3.24 : Geological sketch of King Island, Tasmania, showing outcrops of King Island Volcanics and dykes, and Cottons Breccia. Sampling sites indicated CB (Cottons Breccia). KV (King Is. Volcanics), KD (King Is. Dykes). After Jago (1974b).

sediments between the breccia and the volcanics, however Solomon (1969) and Jago (1974b) consider the lavas to be Lower Cambrian on the basis of a correlation with petrologically similar volcanics on the west coast of Tasmania which underlie Middle Cambrian sediments. The age of the base of the volcanic section in mainland Tasmania is unknown however, and could be late Precambrian. A late Precambrian age for the Cottons Breccia is thus suggested.

Samples from the Cottons Breccia (? tillite and siltstones), the overlying volcanics (herein informally called the King Island Volcanics) and associated dykes were collected at a number of localities (Figure 3.24). Schmidt (1976) collected samples from dykes on King Island originally thought to be Mesozoic in age; it was later discovered that these were in fact associated with the (?) Cambrian Volcanics. These data are included with the data from the King Island Volcanics.

§3.5.1 Cottons Breccia

NRM directions from samples of the Cottons Breccia were somewhat scattered but had dominantly steep negative inclinations with northwest trending declinations, much like the cleaned directions from the overlying volcanic unit. A second, smaller group of NRM directions was characterized by shallow, southwesterly trending remanence vectors. Considering the locally cleaved nature of the breccia, thermal overprinting seemed a distinct possibility, and detailed thermal demagnetization studies were conducted on pilot specimens from each sample.

Three types of directional behaviour were observed during thermal demagnetization, similar to the Pertatataka

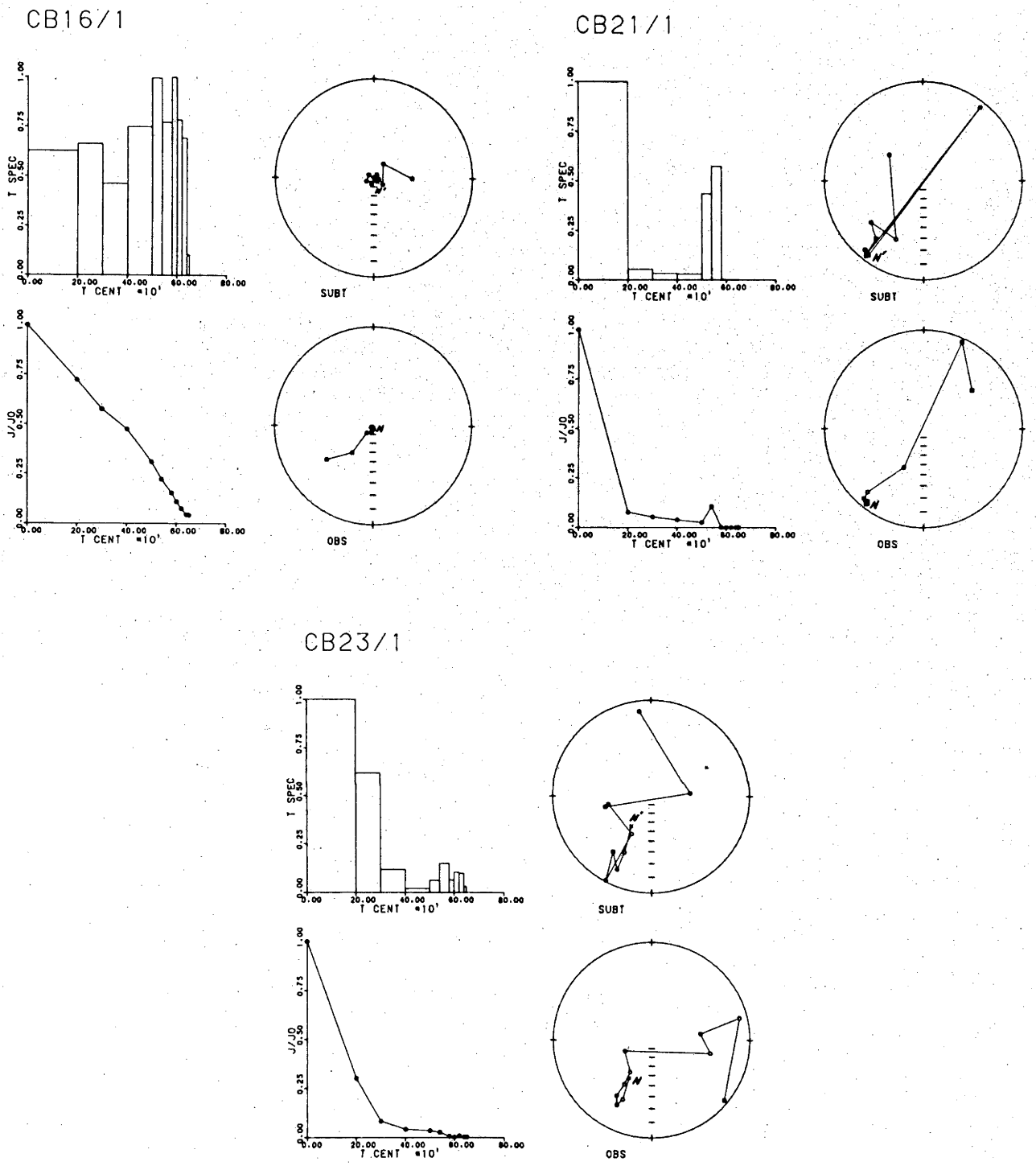

Figure 3.25(A) : Thermal demagnetization, Cottons Breccia.

CB16/1 : N1.253

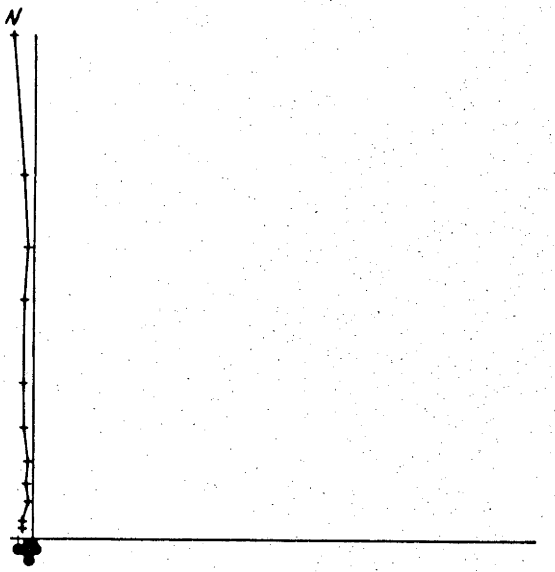

CB21/1 : N3499.529

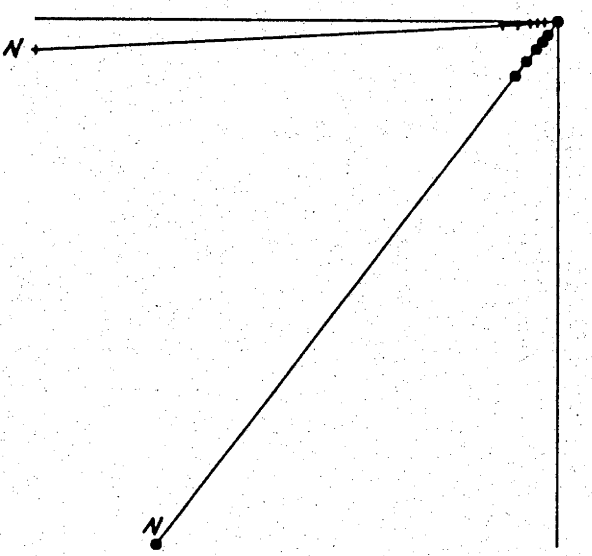

CB23/1 : N32.029

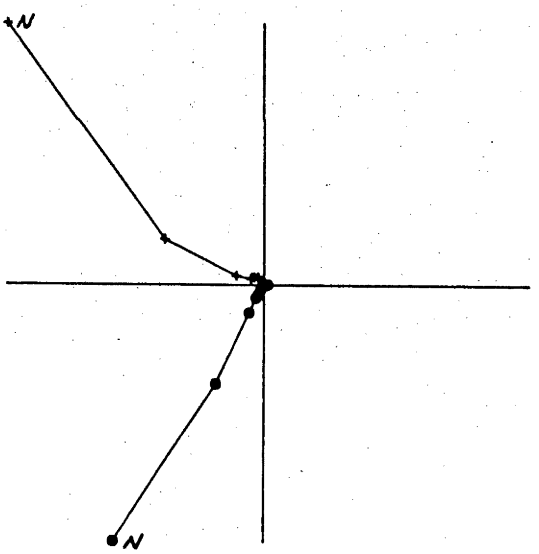

Figure 3.25(B) : Thermal demagnetization, Cottons Breccia (continued).

TABLE 3.9 (A)

COTTONS BRECCIA : Site mean directions before and after 500°C thermal demagnetization

		Before structural correction				After structural correction		
MAGNETIZATION	SITE	N	R	D	I	D'	I'	T°C
NRM	1	3	2.736	316	21			
	2	3	2.963	294	-77			
	3	3	2.938	316	-76			
	4	3	2.990	013	-79			
	5	3	2.943	030	-78			
	6	2	1.995	015	-86			
	7	3	2.991	283	61			
	8	3	2.733	208	-13			
	9	3	2.877	253	-55			
	10	3	2.146	244	-06			
	11	3	2.359	226	-21			
	12	3	2.887	226	-53			
	13	3	2.797	303	-61			
	14	3	2.495	311	-46			
	15	3	2.899	300	-70			
CB1	8	3	2.917	210	-04	215	-07	
	9	2	1.975	203	-23	221	-29	
	10	2	1.876	224	06	217	06	
	11	2	1.946	241	08	232	12	
	13	2	1.902	355	-04	178	-14	
	15	1	-	208	-07	214	-08	
CB2	2	3	2.907	261	-77	287	-13	
	3	3	2.941	304	-71	292	-14	
	4	3	2.992	360	-82	293	-31	
	5	3	2.950	015	-84	292	-33	
	6	2	1.996	050	-87	298	-38	
	7	3	2.997	270	62	159	60	
	9	1	-	284	-36	289	-01	
	10	1	-	262	55	197	62	
	11	1	-	176	-56	281	-61	
	12	2	1.996	203	-50	268	-46	
	13	1	-	245	-62	270	-34	
	14	2	1.909	140	-74	278	-68	
	15	2	1.974	133	61	308	-14	
CB3	8	1	-	206	-50	255	-36	20-300
(directions	9	2	1.958	258	-66	287	-36	20-300
subtracted from	10	1	-	168	-45	218	-65	20-300
CB1 vectors)	11	1	-	240	-20	253	-06	20-300
	12	1	-	251	-37	272	-09	20-300
	13	2	1.989	332	-54	318	-23	20-300

TABLE 3.9 (B)

COTTONS BRECCIA : Mean directions before and after structural correction

	Before structural correction									After structural correction						
							pole							pole		
MAGNETIZATION	N	n	R	k	D_m	I_m	lat	long	dp,dm	R	k	D_m'	I_m'	lat	long	dp,dm
CB1	6	12	5.541	10.9	210	-03	40S	005E	11,21	5.601	12.5	213	-07	37S	007E	10,20
CB2	13	27	11.562	8.3	242	-84	34N	337E	30,30	11.530	8.2	294	-39	32N	051E	11,18
CB3	6	8	5.023	5.1	237	-55	02N	007E	33,47	5.156	5.9	272	-32	13N	042E	19,34
CB2+CB3	19	35	16.141	6.3	238	-76	23N	348E	25,27	16.484	7.2	287	-37	25N	047E	09,16

TABLE 3.9 (C)

COTTONS BRECCIA : F-ratio test; CB2 and CB3 magnetizations

N	R_1	R_2	R	$F_{2,36}$	Significance point (95%)
19	11.562	5.156	16.484	1.74	3.26

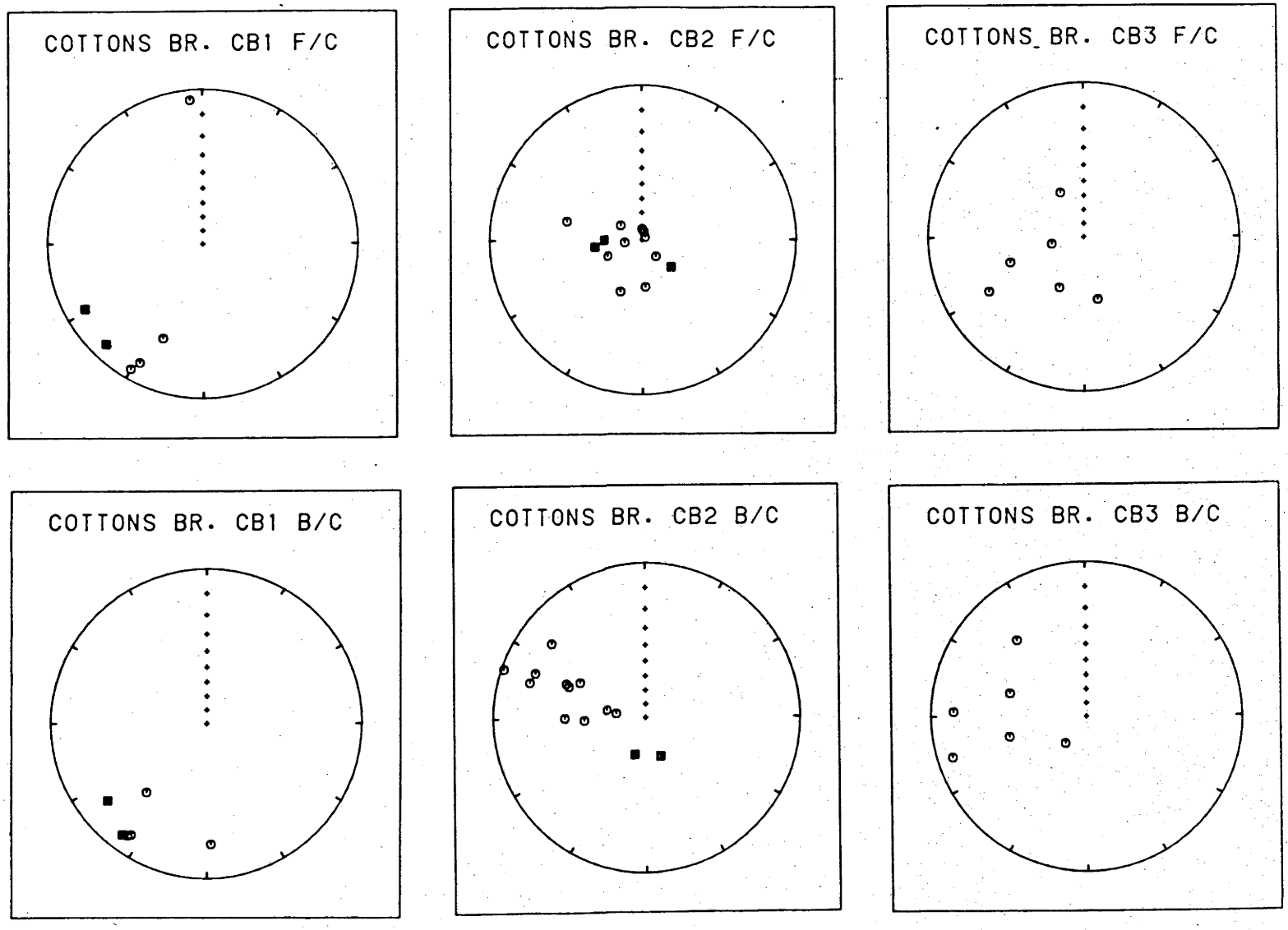

Figure 3.26 : Cleaned site mean magnetization directions, Cottons Breccia CB1, CB2 and CB3 components; equal-angle projection. Open (closed) symbols refer to negative (positive) inclination.

Formation (§3.2.4) and Chambers Bluff Volcanics (§3.4.1). In the first type (Figure 3.25), initially shallow southwesterly (northeasterly) directions remained very steady in direction during the demagnetization process, generally becoming directionally unstable after the 660° or 665° heating step. The second and more common type of behaviour was characterized by stable remanence vectors which remained aligned with the northwest trending steep negative NRM direction during demagnetization. A third class of samples exhibited systematic changes in direction upon demagnetization, with the remanence vector swinging away from the steeply inclined northwest direction to become directionally stable and aligned with the more shallow southwesterly direction. During the demagnetization process a magnetization with a steep negative inclination and northwest trending declination was consistently removed from the third class of samples in the 20°-200° and 200°-300° heating steps. These three magnetizations are summarized in Table 3.9. The first two magnetizations have been labeled the CB1 and CB2 components respectively.

The pole position calculated from the CB1 mean direction is similar to other late Precambrian glacial poles from the Adelaide 'Geosyncline', and the CB2 and CB3 poles are not inconsistent with a Cambrian age (Figure 3.34). However the palaeoposition of King Island is somewhat uncertain in the context of possible megashears along the southern coast of Australia as discussed in §2.8. Further discussion is reserved until later in this chapter.

§3.5.2 King Island Volcanics

NRM directions from the (?) Cambrian King Island

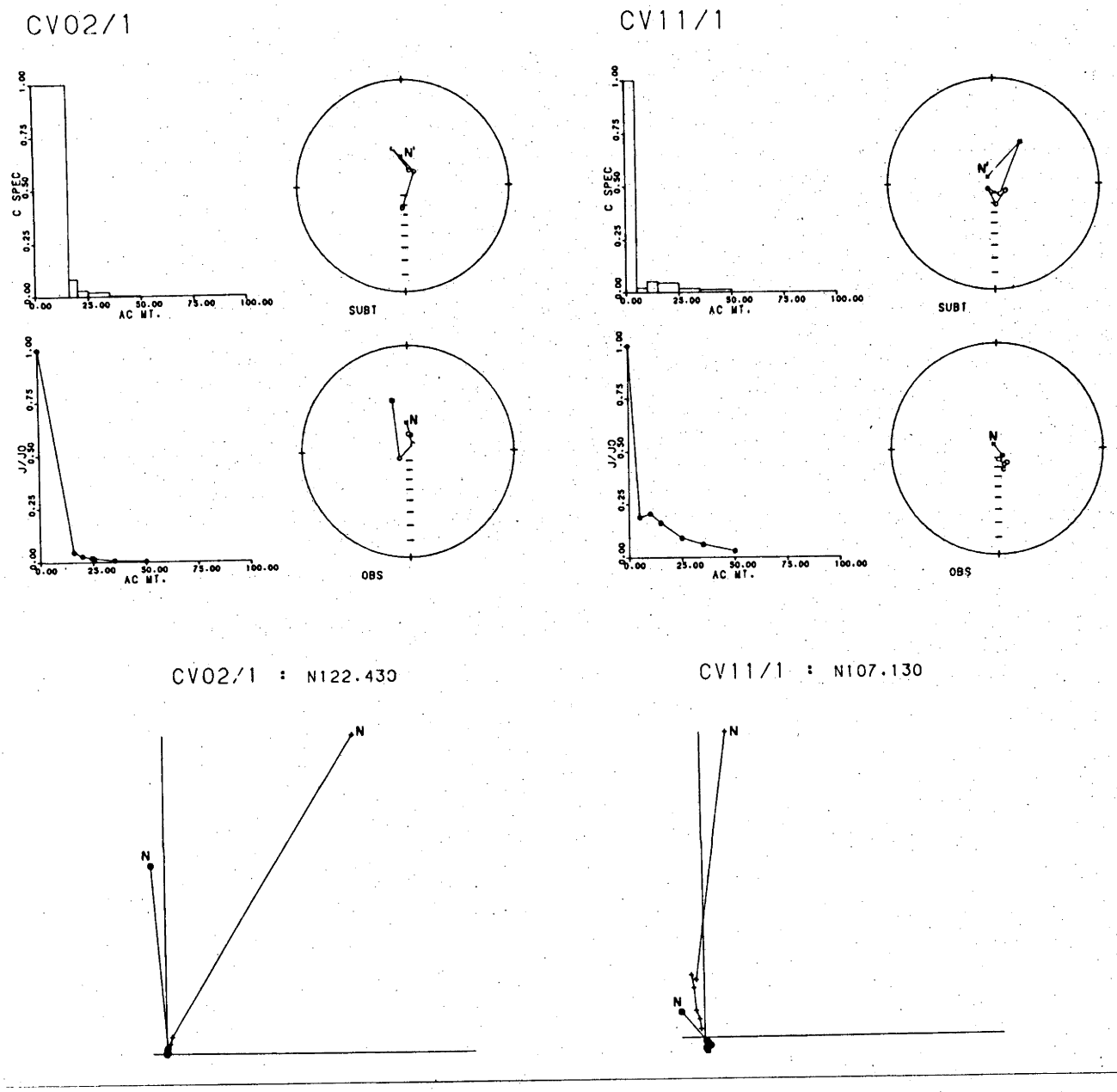

Figure 3.27 : AF demagnetization, King Island Volcanics.

TABLE 3.10 (A)

KING ISLAND VOLCANICS AND DYKES : Site and dyke mean directions before and after AF demagnetization

		NRM				After AF demagnetization						
MAGNETIZATION	SITE	N	R	D	I	N	R	D	I	D'	I'	AF mt.
KV (flows)	1	3	2.915	347	-56	3	2.874	356	-63	314	-15	20
	2	3	2.796	001	-80	3	2.835	335	-81	295	-21	20
	3	3	2.929	046	-82	3	2.959	068	-86	292	-31	15-25
	4	3	2.916	228	-82	3	2.989	203	-78	275	-25	15
	5	4	3.498	341	-69	2	1.987	329	-74	299	-15	10-35
	6	2	1.845	342	-72		(random)					
	7	4	3.681	315	-81	3	2.881	003	-67	325	-32	35
	8	3	2.754	321	-61	2	1.964	239	-80	292	-20	35
	9	2	1.723	253	13		(random)					
KD (dykes)	1*	(no data available)				3	2.975	049	-73	299	-44	20
	2*					4	3.787	021	-75	302	-35	20
	3*					2	1.907	031	-77	301	-37	20
	4*					5	4.839	029	-70	309	-37	20

TABLE 3.10 (B)

KING ISLAND VOLCANICS AND DYKES : Mean directions after AF demagnetization

	Before structural correction									After structural correction						
UNIT	N	n	R	k	D_m	I_m	pole lat	pole long	dp,dm	R	k	D_m'	I_m'	pole lat	pole long	dp,dm
Flows	7	19	6.800	30.0	339	-81	56N	335E	21,22	6.760	25.0	299	-23	30N	064E	07,13
Dykes	4	14	3.991	331.0	033	-74	61N	290E	08,09	3.988	242.0	303	-38	39N	057E	04,07

* data from Schmidt (1976)

TABLE 3.11

COTTONS BRECCIA and KING ISLAND VOLCANICS : F-ratio tests between volcanics and overprinted breccia

MAGNETIZATION COMPONENTS	N	R_1	R_2	R	$F_{2,N-2}$	SIGNIFICANCE POINT (95%)
KV-CB2	20	6.760	11.530	18.125	1.74	3.26
KV-CB3	13	6.760	5.156	11.629	2.91	3.40
KV-(CB2+CB3)	26	6.760	16.484	23.027	1.89	3.19

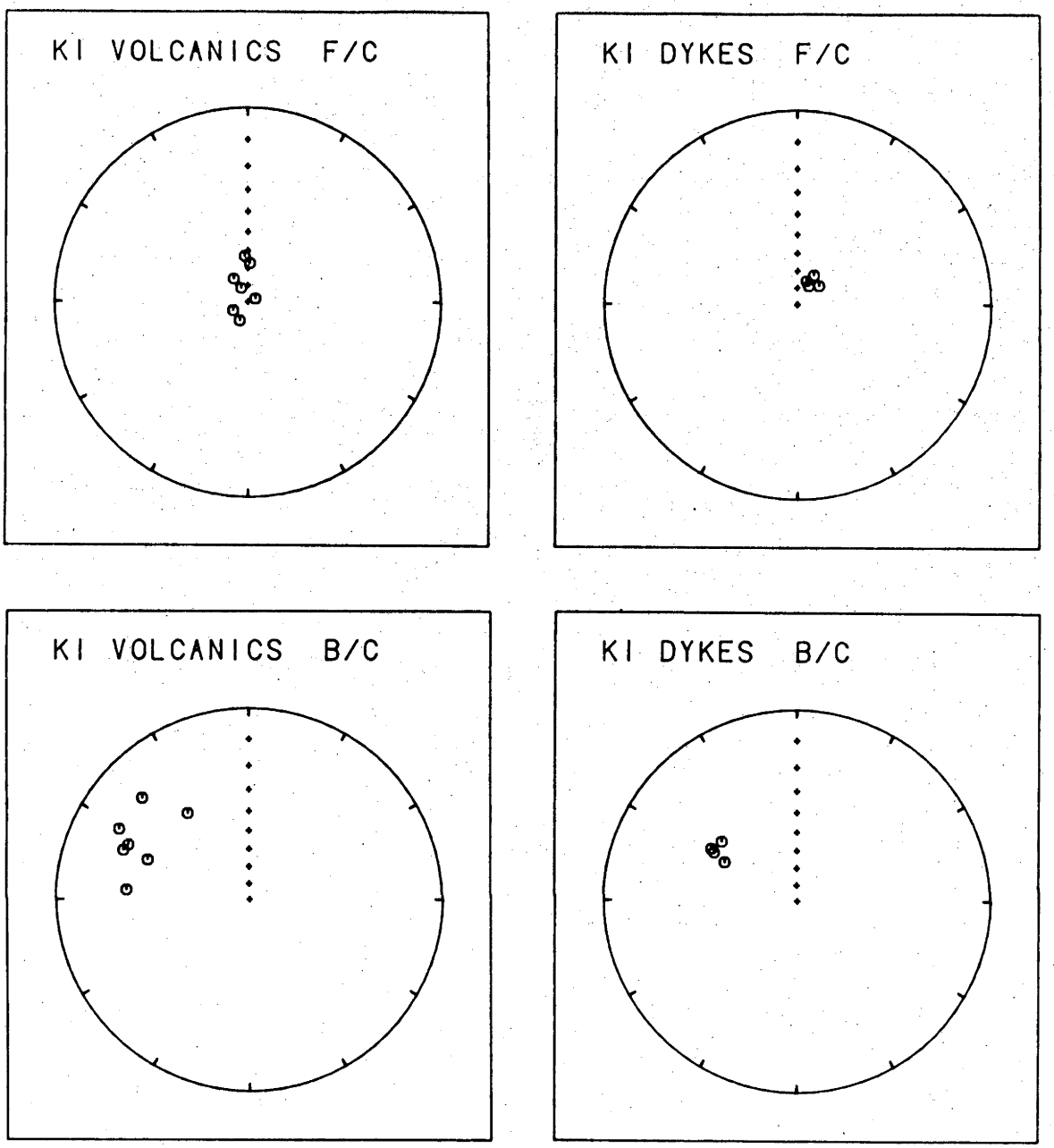

Figure 3.28 : Cleaned site mean magnetization directions, King Island Volcanics and dykes; equal angle projection. Open symbols refer to negative inclination.

Volcanics were reasonably well grouped and very near the PEF direction. During progressive AF demagnetization a large PEF component with a low coercive force was removed, and pilot specimens generally attained directional stability in the 15-35 mT range (Figure 3.27). Inspection of polished sections in reflected light shows that the visible magnetic grains are dominantly of a very low oxidation state, with small well-preserved skeletal titanomagnetite grains predominating, although some of the larger euhedral grains appear to be partially altered to titanomaghemite. The cleaned site mean directions (Figure 3.28 and Table 3.10) are well grouped and significantly different from the PEF direction at the 95% level. Comparison of the mean directions of the volcanics and the dykes studied by Schmidt (1976) is not directly possible by an F-ratio test. However, the distance between the KV and KD mean directions exceeds by 0.5° the square root of the sum of the variances $(\alpha_{KD}^2+\alpha_{KV}^2)^{\frac{1}{2}}$, suggesting that the two mean directions are just different. An F-ratio test (Table 3.11) indicates that the mean directions from the volcanics and the overprint mean direction from the underlying sediments are not significantly different. This suggests that heating of the underlying sediments during emplacement and cooling of the lavas probably resulted in low grade metamorphism and concomitant remagnetization. The pole positions for both the volcanics and the dykes are consistent with a Cambrian age of magnetization as discussed in §3.7.

§3.6 Northwest Queensland: Mount Birnie Beds, Devoncourt Limestone

The late Precambrian Mount Birnie Beds outcrop in the

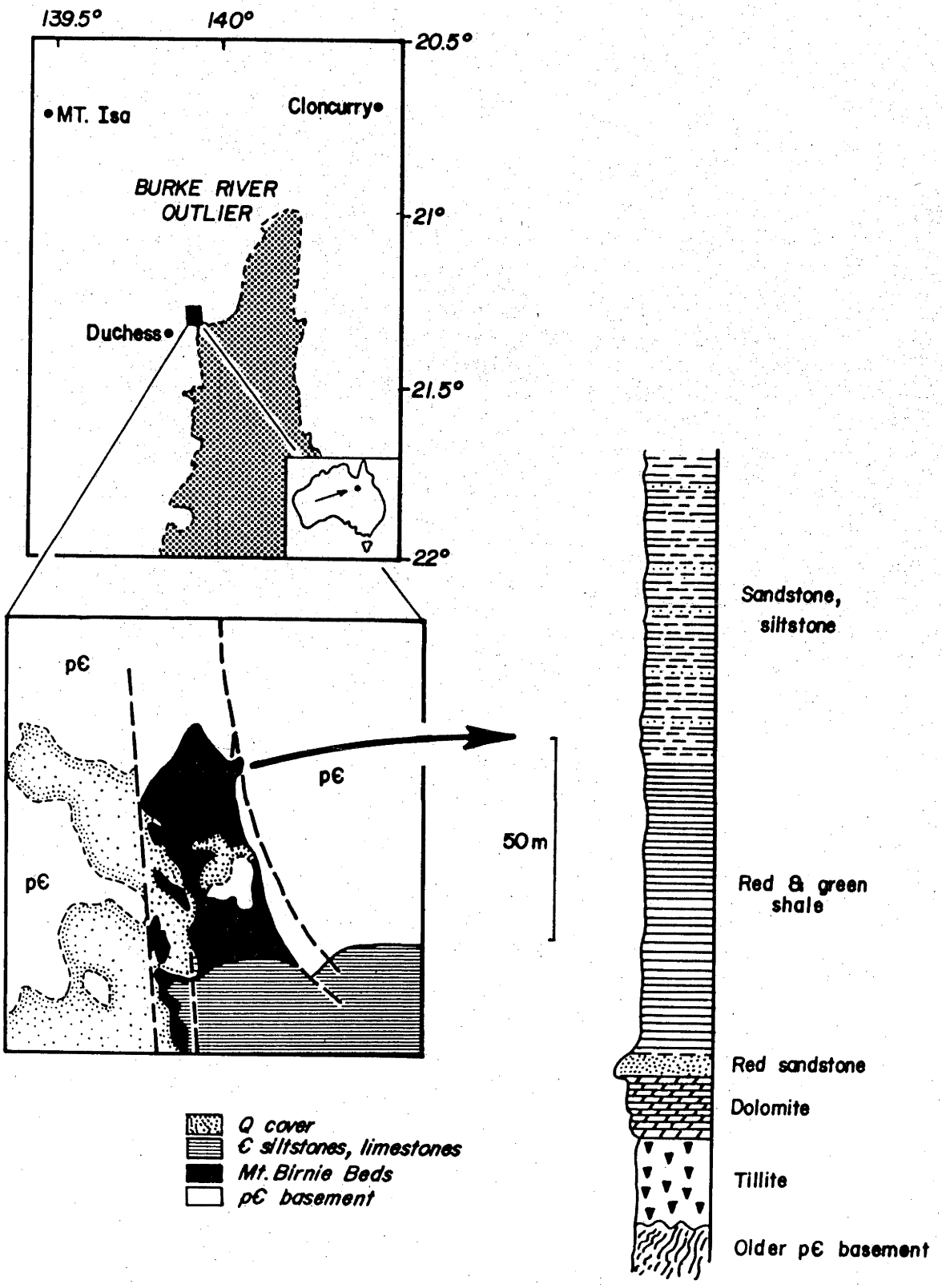

Figure 3.29 : Geological sketch of the area of outcrop of the Mt. Birnie Beds, Queensland (after de Keyser, 1972).

Duchess area (Figure 3.29), and lie with angular unconformity upon folded and metamorphosed Proterozoic rocks (de Keyser, 1969). They are overlain by fossiliferous Cambrian strata. The basal member of the Mount Birnie Beds is a glacial unit called the Little Burke Tillite, a boulder clay containing an unsorted heterogeneous assemblage of erratic clasts set in a ferruginous silty matrix (Plate 7). The clasts, which are highly polished and often facetted, range in size from sand particles to 1.5 m in diameter. De Keyser cites evidence which he feels confirms a glacial origin for this lower member of the Mount Birnie Beds. The Little Burke Tillite is immediately overlain by a red dolomitic layer followed by a micaceous and ferruginous red sandstone (Figure 3.29). Samples were taken from three units through about 40 m of section. Samples were also taken from the Cambrian Devoncourt Limestone which overlies the Mount Birnie Beds but is separated from them by a considerable thickness of intervening sediment.

NRM directions of the Little Burke Tillite were widely scattered and were random at the 95% confidence level. Detailed AF and thermal demagnetization studies failed to isolate a consistent direction of magnetization. Although many specimens exhibited directionally stable magnetizations during demagnetization, within-sample and/or within-site scatter was always too great to be meaningful. Chemical demagnetization was not attempted due to the friable nature of the rock and the presence of a considerable proportion of calcareous material binding the tillite together.

The immediately overlying red dolomites responded well to thermal demagnetization and initially exhibited a highly stable magnetization of probable recent origin at low

Plate 7 - tillite in Mount Birnie Beds

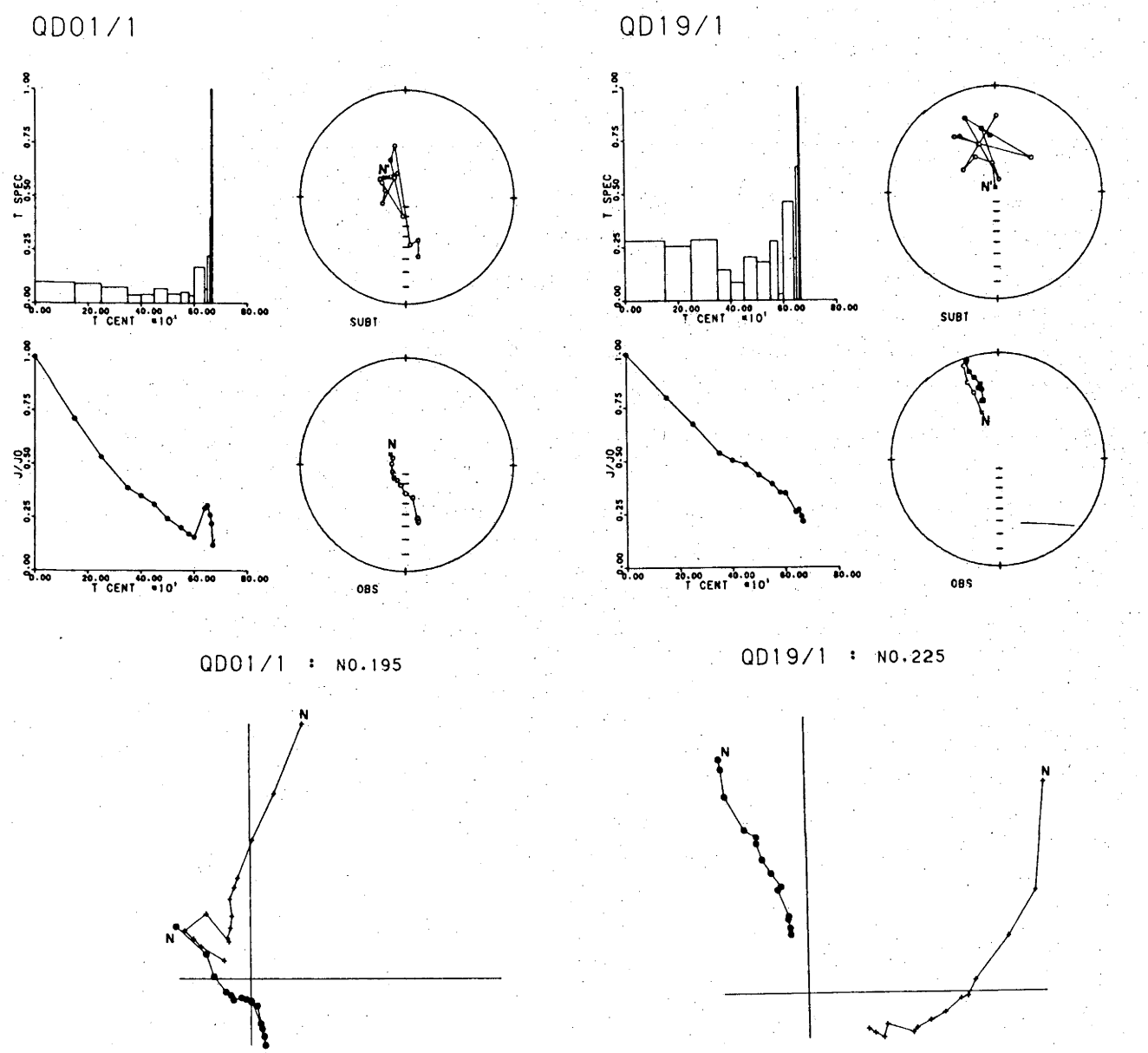

Figure 3.30 : Thermal demagnetization, Mt. Birnie dolomite.

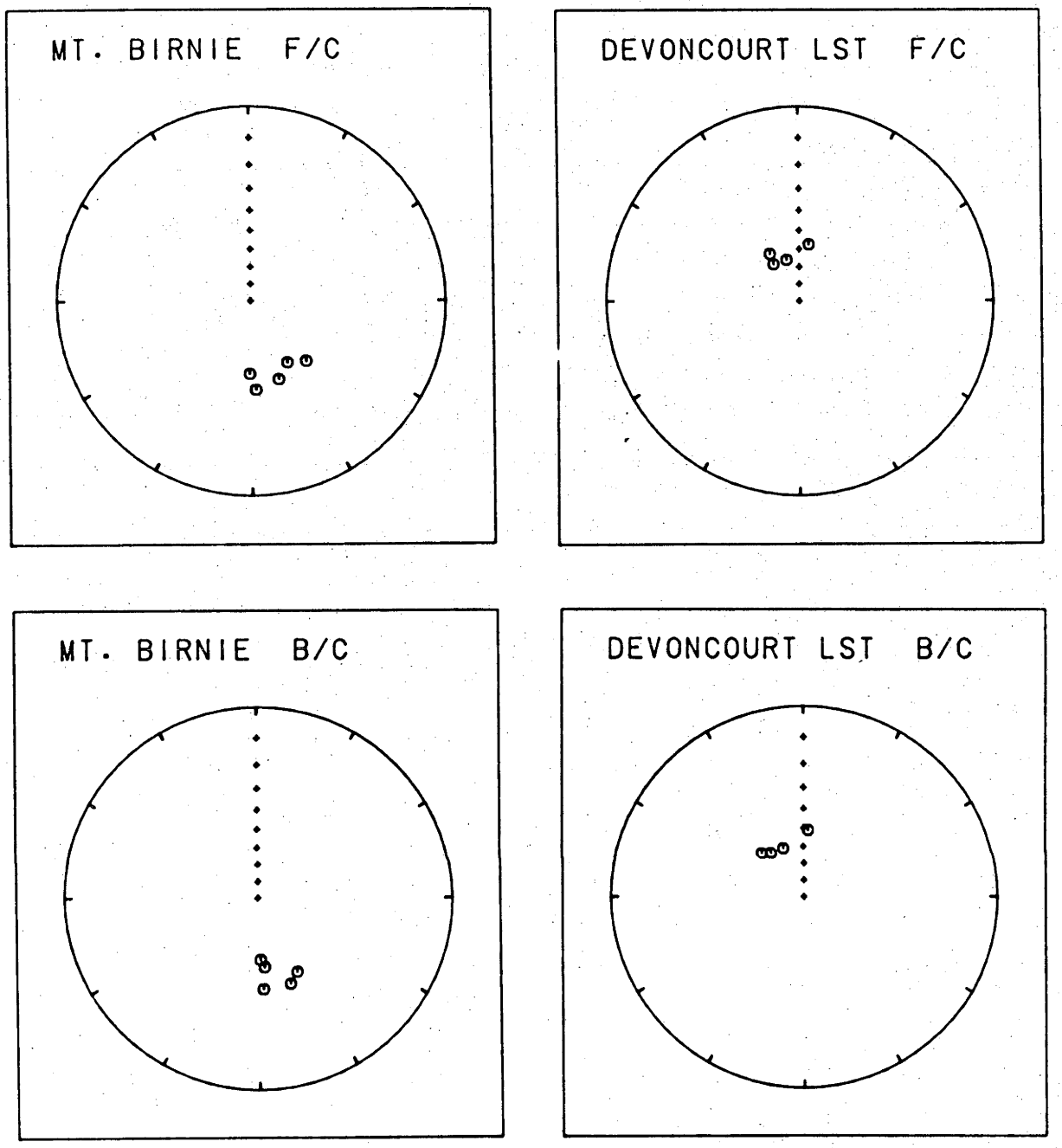

Figure 3.31 : Cleaned site mean magnetization directions, Mt. Birnie dolomite; equal-angle projection. Open symbols refer to negative inclination.

Figure 3.33 : Cleaned site mean magnetization directions, Devoncourt Limestone; equal-angle projection. Open symbols refer to negative inclination.

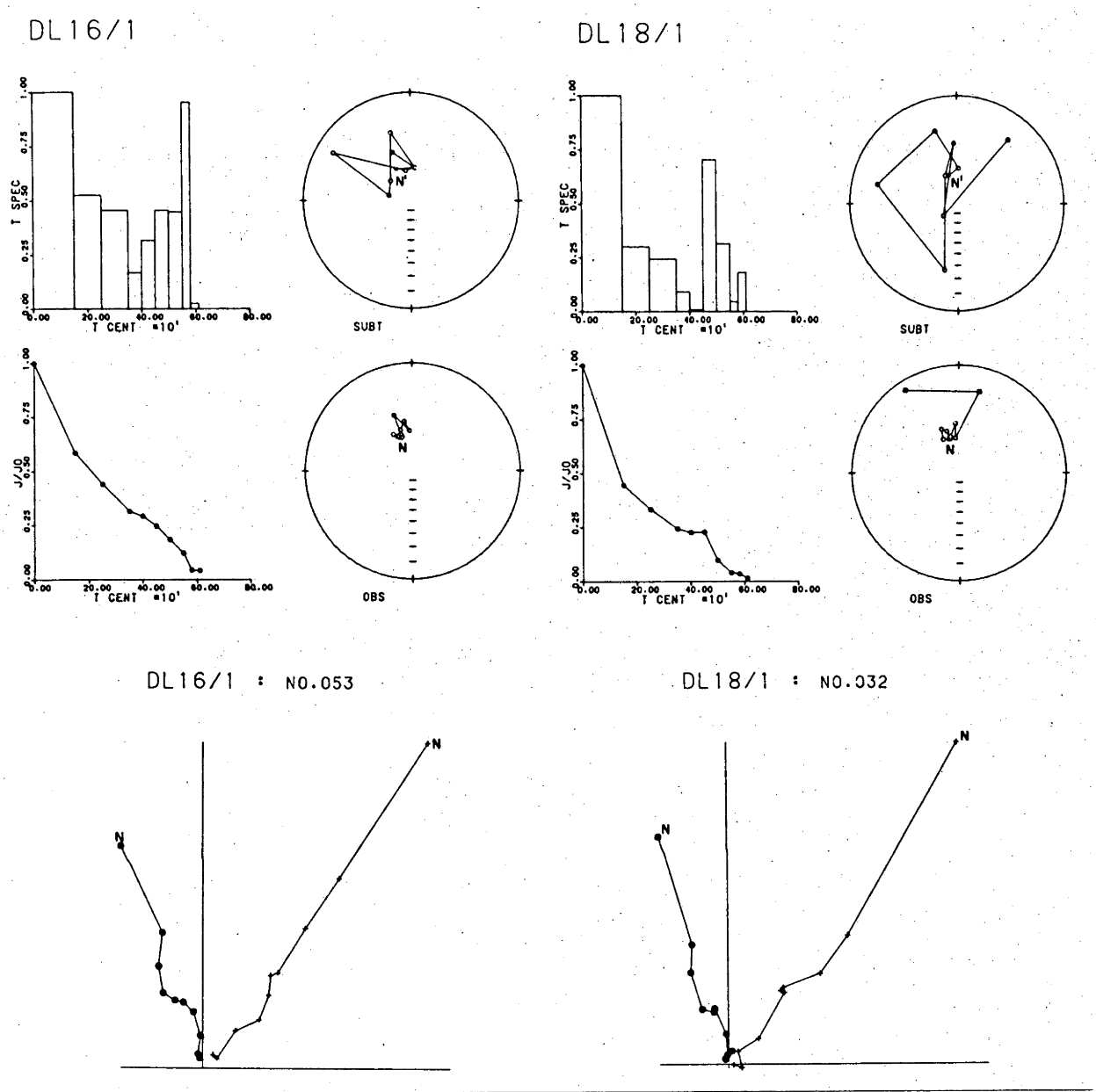

Figure 3.32 : Thermal demagnetization, Devoncourt Limestone.

TABLE 3.12 (A)

MT. BIRNIE DOLOMITE : Site mean directions before and after thermal demagnetization

	NRM				665°C					
SITE	N	R	D	I	N	R	D	I	D'	I'
1	3	2.973	330	-72		(random)				
2	3	2.990	309	-73	3	2.935	181	-49	178	-54
3	3	2.958	344	-61	2	1.880	177	-41	175	-50
4	3	2.818	345	-64	3	2.822	150	-50	160	-39
5	4	3.971	003	-68	3	2.957	138	-45	153	-43
6	4	3.527	344	-70	4	3.899	161	-44	177	-39

TABLE 3.12 (B)

MT. BIRNIE DOLOMITE : Mean directions after thermal demagnetization

		Before structural correction							After structural correction						
N	(n)	R	k	D_m	I_m	pole lat	pole	dp,dm	R	k	D_m'	I_m'	pole lat	pole	dp,dm
5	15	4.897	39.0	162	-47	38S	300E	10,16	4.933	59.7	168	-45	41S	306E	08,13

TABLE 3.13 (A)

DEVONCOURT LIMESTONE : Site mean directions before and after thermal demagnetization

	NRM				250°					
SITE	N	R	D	I	N	R	D	I	D'	I'
1	3	2.927	353	-66		(random)				
2	4	3.827	355	-68	4	3.622	325	-64	324	-58
3	5	4.835	024	-77	3	2.737	010	-57	004	-51
4	3	2.849	342	-69	3	2.821	343	-65	338	-59
5	5	3.190	332	-72	3	2.855	328	-58	317	-55

TABLE 3.13 (B)

DEVONCOURT LIMESTONE : Mean directions after thermal demagnetization

		Before structural correction							After structural correction						
						pole							pole		
N	(n)	R	k	D_m	I_m	lat	long	dp,dm	R	k	D_m'	I_m'	lat	long	dp,dm
4	13	3.946	55.0	342	-62	64S	171E	15,19	3.929	42.6	336	-57	64S	187E	15,21

to moderate temperatures. At higher temperatures a systematic shift towards a southerly more shallow negative direction occurred (Figure 3.30). High temperature directional stability was generally attained in the 660°-665° range. Cleaned mean directions from the 5 Sites with non-random grouping increases in precision upon making structural corrections, although the improvement is not significant at the 95% level (k'/k=1.53, 95% significance point ≅3.18). Although the age of folding is not known, the pole position calculated from the corrected mean direction is quite removed from the Phanerozoic APWP for Australia, suggesting an original age of magnetization.

Problems similar to those encountered with the Little Burke Tillite described above made determination of a reliable direction from the red micaceous sandstone unit impossible. Although many specimens had directionally stable magnetizations, the only consistent non-random direction observed was not significantly different from the PEF direction.

Samples of the Devoncourt Limestone had well grouped weak NRM's with north trending negative inclinations. The mean NRM direction is significantly different from the PEF direction but could possibly be a Tertiary direction. During thermal demagnetization, samples became too weak to accurately measure on the cryogenic magnetometer after heating to 400°. The steep negative direction persisted up to this point (Figure 3.32), but the dispersion of the cleaned directions is much greater than that of the NRM directions. Structural correction increases the dispersion, although the change is small due to the shallow bedding dips. The structurally uncorrected NRM and thermally cleaned mean directions yield poles which are both similar to Mesozoic and Tertiary poles from Australia (Figure 3.34).

§3.7 Summary of late Precambrian palaeomagnetism of Australia : Adelaidean correlation and tectonic implications

Late Precambrian palaeomagnetic data from Australia exclusive of the Adelaide 'Geosyncline' and Amadeus Basin are listed in Table 3.14. The data from Tables 3.3 and 3.14 are plotted in Figure 3.34, and form a moderately consistent APWP segment from the PR1 pole (Ringwood Member, Pertatataka Formation) through Cambrian and Ordovician poles to the Devonian. However, a number of poles appear to be seriously out of sequence, for example the Lubbock Formation and Cottons Breccia (?) primary poles (LF and CB1 respectively). This apparent inconsistency becomes much worse when poles from the Adelaide 'Geosyncline' are added (Figure 3.35 : open symbols from Adelaide 'Geosyncline'). Close inspection of Figure 3.35 reveals that all the poles from the Adelaide 'Geosyncline' and from King Island tend to be systematically displaced with respect to poles of (?) similar age from elsewhere in Australia. The sense of the displacement is such that Adelaide 'Geosyncline' poles tend to lie in apparently younger positions when referred to their probable time equivalents from the Amadeus and Kimberley Basins. For example, the MT1 pole from the Sturtian Merinjina Tillite is very near and not significantly different from poles from the (?) Precambrian-Cambrian Arumbera Sandstone (AR2, PRJ, TAE). Similar systematic displacements are possibly present in the late Cambrian and early Ordovician segment of Figure 3.35, where (?) Lower Cambrian poles KD, KV, CB2 and CB3 and (?) Ordovician overprint poles WV3 and MT3 appear to be different from their probable counterparts from the rest of Australia.

TABLE 3.14 (A)

Late Precambrian (Adelaidean) and lower Palaeozoic palaeomagnetic poles, excluding Adelaide 'Geosyncline' and Amadeus Basin poles

Symbol	Rock Unit	Probable Magnetization Age	Pole Position	dp,dm	Reference
Possible Primary Poles					
LF	Lubbock Formation	ℰPC	71S 328E	09,18	this study
EF	Estaughs Formation	ℰPC	23S 280E	17,21	this study
YB	Yilgarn 'B' dykes	?750 my	20S 282E	22,31	Giddings (1974)
MBD	Mount Birnie dolomite	ℰPC	41S 306E	08,13	this study
CB1	Cottons Breccia	ℰPC(>KD,KV)	37S 007E	10,20	this study
WP1	Chambers Bluff Volcanics	ℰPC	23S 360E	08,13	this study
TH+	Table Hill Volcanics (+inc)	575±40	mean incl 15°	03	this study
AV	Antrim Plateau Volcanics	ℰPC-C	09S 340E	17,21	McElhinny & Luck (1970)
HF	Hudson Formation	Cℰ	18N 019E	10,16	Luck (1972)
KD	King Island Dykes	?Cℰ-m	39N 057E	04,07	this study
KV	King Island Volcanics	?Cℰ-m	30N 064E	07,13	this study
TS	Tumblagooda Sandstone	O	30S 031E	09,10	Embleton & Giddings (1974)
Possible Secondary Poles					
WP2	Chambers Bluff Volcanics (obs)	?Cℰ	41N 039E	15,26	this study
WP3	Chambers Bluff Volcanics (subt)	?Cℰ	47N 030E	18,28	this study
EG	Egan Tillite (subt)	?C	23N 051E	13,25	this study
CB2	Cottons Breccia (obs)	?Cℰ-m	34N 337E	30,30	this study
CB3	Cottons Breccia (subt)	?Cℰ-m	02N 007E	33,47	this study
RF	Ranford Formation	?S-D	63S 036E	10,19	this study
TF	Tean Formation	?T	74S 112E	11,15	this study
DL	Devoncourt Limestone	?T	64S 171E	15,19	this study

Table 3.14 (B)

Summary of new Adelaidean palaeomagnetic results from Australia, exclusive of the Adelaide 'Geosyncline' and Amadeus Basin

Symbol	Rock Unit	Interpretation[1]
EF	Estaughs Formation	primary
RF	Ranford Formation	secondary, ℓ-m Pz
EG	Egan Formation	secondary, ~~Є~~-O(?)
TF	Tean Formation	secondary, T
LF	Lubbock Formation	primary (?)
MBD	Mount Birnie dolomite	primary
DL	Devoncourt Limestone	secondary, T
WP1	Chambers Bluff Volcanics	primary
WP2	Chambers Bluff Volcanics	secondary, ~~Є~~(?)
WP3	Chambers Bluff Volcanics	secondary, ~~Є~~(?)
TH+	Table Hill Volcanics	primary
CB1	Cottons Breccia	primary
CB2	Cottons Breccia	secondary, ~~Є~~
CB3	Cottons Breccia	secondary, ~~Є~~
KV	King Island Volcanics	primary
KD	King Island Dykes	primary

[1] age abbreviations as in Table 2.11 (b)

There are basically two possible explanations for these apparent displacements. Either (1) the ages of magnetization of the Adelaide 'Geosyncline' sediments are systematically younger than their stratigraphic "equivalents" in the Amadeus and Kimberley Basins and elsewhere, or (2) the ages of magnetization are essentially the same and the discordance results from a later relative tectonic movement.

Probably the most conclusive evidence which tends to refute the first possibility is the apparent discordant positions of the Precambrian-Cambrian boundaries in the Amadeus and Adelaide Tracks. The Precambrian-Cambrian boundary in the Adelaide Track probably lies in the region of poles BU and LFL, while in the Amadeus Track the Precambrian-Cambrian boundary is thought to lie within the Arumbera Sandstone; yet these poles are separated by an angular distance of at least 40°. Although this boundary is almost certainly not a worldwide universal time equivalent, it is highly unlikely that the fossiliferous parts of the Amadeus Basin sequence (for example the *archaeocyathid* bearing Todd River Dolomite, included in pole TAE) are the time equivalents of the Sturtian and Marinoan sediments in the Adelaide 'Geosyncline' which are separated from similar *archaeocyathid* limestones by thousands of metres of intervening sediments, as the apparent positions of the palaeomagnetic poles in Figure 3.35 would suggest. Similar arguments could be based upon the discordance between the poles from glacial horizons, but such a comparison would constitute circular reasoning, as the synchroneity of these glacial deposits is in question. It is instructive however to note that even if the glacial deposits are non-synchronous, the displacement of poles from the Adelaide 'Geosyncline'

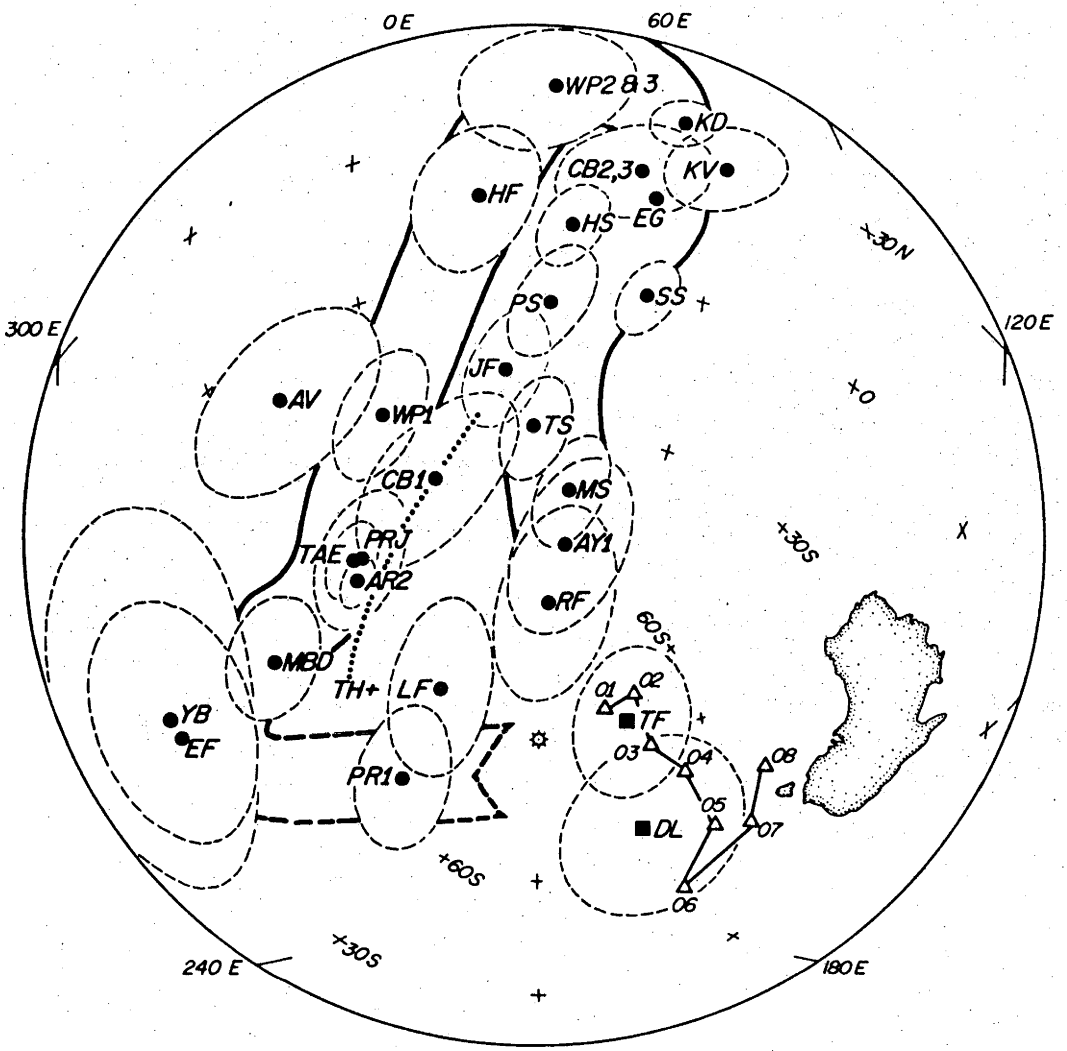

Figure 3.34 : Proposed Adelaidean and early Palaeozoic APWP segment derived from rocks outside the Adelaide 'Geosyncline'. Projection and APWP details as in Figure 2.27 or 3.9. Symbols as in Table 3.14 and 3.3. JF : Jinduckin Formation (Luck, 1972). Dotted line : locus of poles generated from inclination value obtained from Table Hill Volcanics; positive inclination used. Open triangles : Phanerozoic means as in Figure 2.27(B) and 3.9(B).

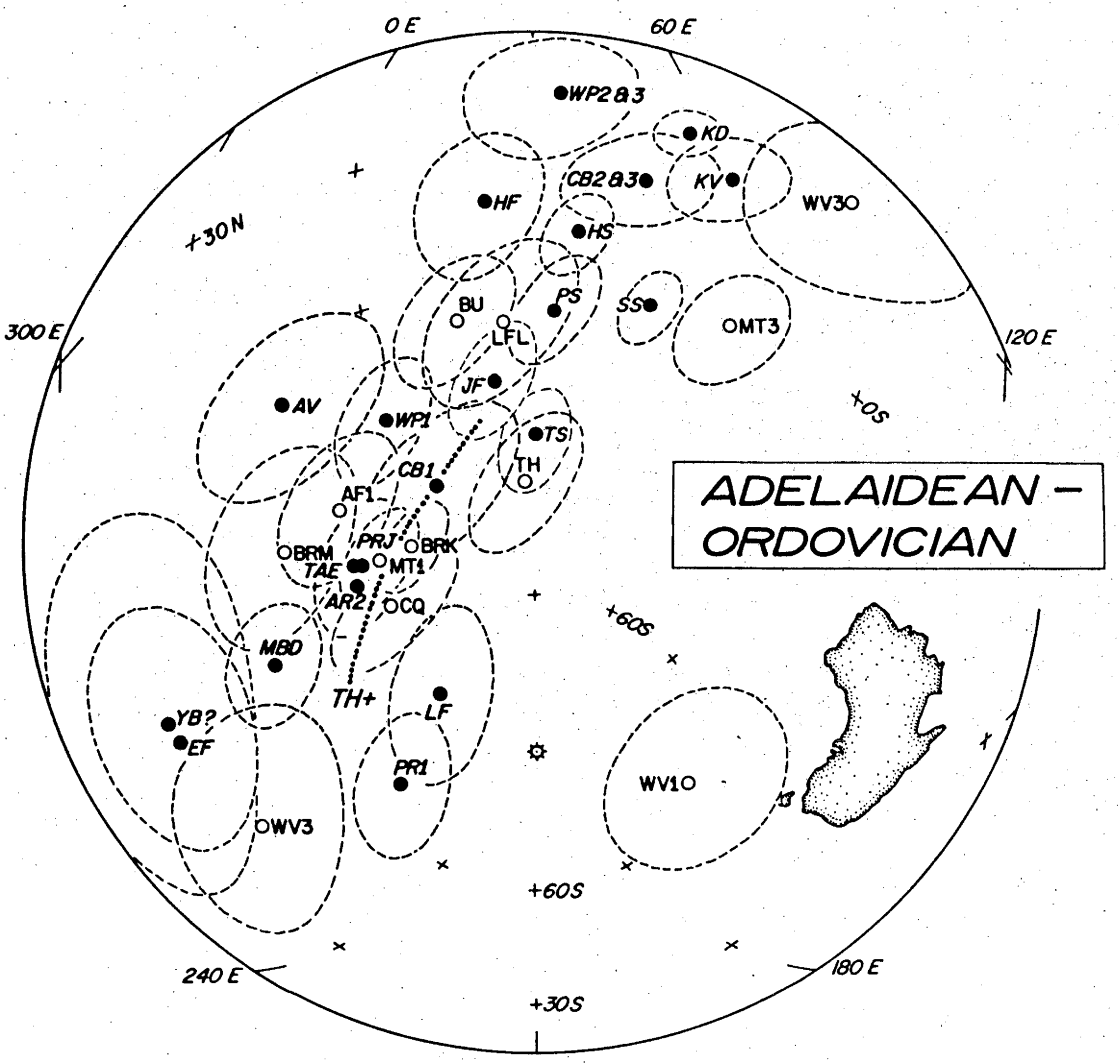

Figure 3.35 : Adelaidean and Cambro-Ordovician data of Figure 3.34 (solid symbols) plotted with Adelaidean and Cambro-Ordovician data from the Adelaide 'Geosyncline' (open symbols). Adelaide 'Geosyncline' symbols as in Table 2.11.

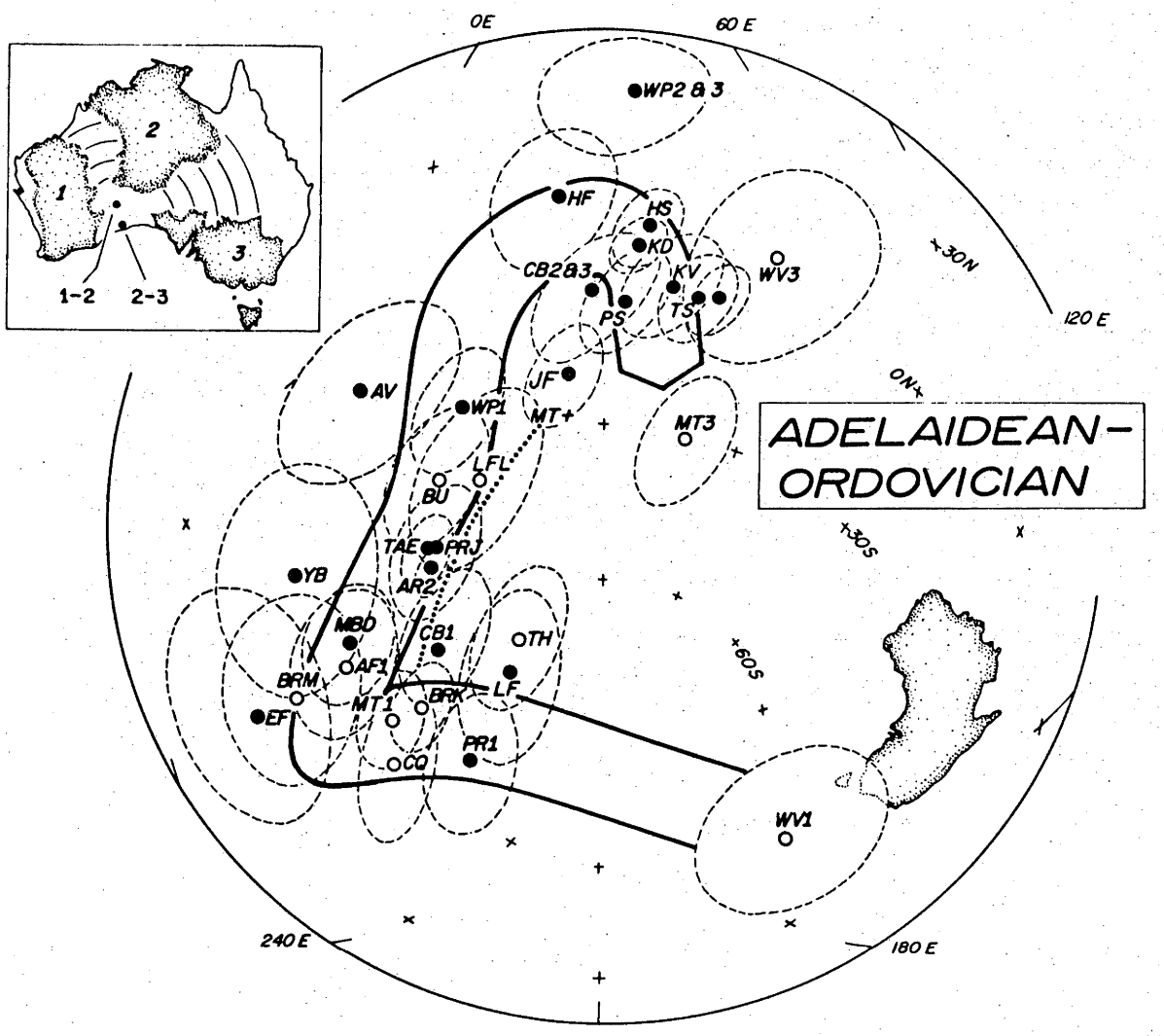

Figure 3.36 : Data of Figure 3.35 plotted after rotation of subplates 1, 2 and 3 according to the hypothesis of Harrington *et al.* (1973); such a rotation improves the agreement between Adelaidean and early Palaeozoic poles from the three units.

and Amadeus Basin would represent a time span of about 90(45,30) my between glaciations in these areas at an apparent polar motion rate of 5(10,15) cm yr^{-1}. Such a gap, while indeed not impossible, seems unlikely in two regions separated by only 600-700 km.

Considering possibility (2) above, Harrington *et al.* (1973) have suggested that in the early Palaeozoic, an originally intact Australian 'plate' broke into a number of sub-plates, and that these subplates rotated apart about Euler poles in the Eucla and Officer Basins (see inset of Figure 3.36). Such a rotation appears to resolve the discordance of the late Precambrian palaeomagnetic data as shown in Figure 3.36. After a 38° anticlockwise rotation of the block (3) containing the Adelaide 'Geosyncline' and King Island sampling sites about a pole at 32S,126E there is a marked improvement both in the grouping and relative positions of Adelaidean and Cambro-Ordovician poles. The (?) 750 my Yilgarn 'B' dykes pole and the Tumblagooda Sandstone pole have been rotated 32° clockwise about an Euler pole at 29S,125E. Although the data do not have a regular distribution, the improvement in precision can be tested by means of an F-ratio test

	k'/k*	95% significance point
All Adelaidean poles (N=17)	1.51	≅1.72
Adelaidean poles excluding WP1 (N=16)	1.70	≅1.75

* Ratio of mean pole precision before (k') and after (k) rotation.

Although the improvement is not quite significant at

the 95% level, there is nevertheless the strong suggestion that a tectonic rotation may explain the systematic differences in the Adelaidean and early Palaeozoic data. One of the obvious implications of the model is that such fragmentation would be expected to produce tensional features such as graben structures and major volcanism. The older geology of the areas where evidence of such rifts might be found is not well enough known to make a definitive judgement, as the older rocks are overlain by thick Mesozoic and Cenozoic basin deposits. Although some definite gravity patterns are apparent which delineate the cratonic margins, deep structure in the possible rift areas is probably masked by these thick younger deposits. It is worth noting however that recent magnetic variometer array studies in the eastern Amadeus Basin - Simpson Desert area and in the Northern Flinders area have suggested the presence of a region of anomalously high electrical conductivity which could possibly reflect a rift structure. Similar conductivity anomalies are observed in younger rifted areas such as the Rhine graben and east African rift system. It is important to emphasize that the improved agreement of palaeomagnetic data by means of the simple rotation outlined above does not constitute definitive proof of the continental fission hypothesis of Harrington *et al.* (1973), as other hypotheses could be invoked to create equally favourable rearrangements of the Adelaidean poles, such as a simple rotation of the Adelaide 'Geosyncline' data about a local vertical axis. However the hypothesis of Harrington *et al.* (1973) has the advantage that the rearrangement of both the Adelaide 'Geosyncline' and King Island data can be accommodated with a single movement irrespective of the position of King Island as discussed below, without the neccessity of two separate special movements to

explain each body of data.

Crawford and Campbell (1973) suggested that a 300 km dextral strike-slip movement occurred between a mainland Australia structural block and a block to the south containing Tasmania and King Island. This megashear was to have taken place along a fracture zone parallel to the present south coast of Australia in early Ordovician times. Daily *et al.* (1973) rejected this hypothesis on geological grounds, and as discussed in §2.8 Embleton and Giddings (1974) showed that the bend at the foot of Yorke Peninsula was probably original and was not due to such dextral movement as suggested by Crawford and Campbell. Subsequently Harrington *et al.* (1973) suggested that sinistral rather than dextral movement had taken place along similar fracture lines, this time with a displacement of over 1000 km. The relative arrangement of palaeomagnetic poles and Euler poles for either the dextral or sinistral movement preclude a palaeomagnetic test. The displacement of Tasmania and King Island according to either of these hypotheses does not change the palaeomagnetic pole positions enough to warrant speculation. However, regardless of the possible translational movements along southern fracture zones, this southern block appears to have moved with the Adelaide 'Geosyncline' block to produce the 40° angular discordance in Adelaidean and Cambrian data discussed above.

A further consideration in any such hypothetical rotation is that the relative agreements of older Precambrian (lower Proterozoic and Archean) palaeomagnetic data from the rotated blocks must be assessed before and after the rotation. In this case the data are so sparse that again a definite judgement is impossible. In some time spans such as 1600-1400 my

the proposed rotations bring poles into marginally better agreement, whereas in the 1800-1700 my range, poles are moved apart slightly. In the 2500-2300 my range the data come from one of the rotated blocks and therefore no judgement can be made.

If the rotated arrangements of poles of Figure 3.36 is tentatively adopted, it is surprising that the Adelaidean poles form such a tight group. The problem basically centres around the actual time interval recorded by Adelaidean sedimentation. If the base of the Adelaide System is taken to be the commonly accepted age of 1400-1300 my, the average rate of apparent polar motion defined by the proposed path is low, of the order 1.0-1.5 cm yr^{-1}. Motion as slow as this might be difficult to accept considering that the immediately adjoining Cambro-Ordovician segment of the path appears to indicate more rapid rates ($\sim$8-9 cm yr^{-1}), requiring a very abrupt increase in APW rate at approximately the Proterozoic-Phanerozoic boundary. Further, APW rates from other reasonably well documented continents indicate significantly higher rates of at least the order 6-10 cm yr^{-1} (Africa: Chapter 4; North America: McWilliams and Dunlop (1975, 1977), Morris and Roy, 1977). At the other extreme, the ca. 625 my age suggested for the Wooltana Volcanics (§2.5) leads to probably unacceptable rates of 16-20 cm yr^{-1}. A further complication in accepting such a young age is that the Rb/Sr shale isochrons must be discounted, as must the admittedly very approximate 750 my age for the Yilgarn YB dykes. Similar discontinuities in APW rate must be proposed as well, this time a decrease rather than an increase. Although the 16-20 cm yr^{-1} rates outwardly appear to be much too high, it must be remembered that the relative arrangement of poles and cratons allows for very rapid apparent

polar motion with only minimal actual motion of the lithosphere relative to the mantle.

The intermediate 900-800 my age for the base of the Adelaide System leads to possibly more acceptable average APW rates of 4-5 cm yr^{-1}. Considering all the available palaeomagnetic and geochronologic evidence, acceptance of this age generates fewer inconsistencies and requires fewer questionable assumptions than do the alternatives and it is therefore tentatively adopted. The problem is discussed in more detail in Chapter 5 with respect to late Precambrian and Palaeozoic palaeomagnetic data from Africa, India, South America and Antarctica.

Chapter 4

Late Precambrian Palaeomagnetism in Southern Africa : The Nama, Mulden and Nosib Groups and Tsumeb Subgroup of Namibia

§4.1 Introduction

This Chapter describes the results to date of a continuing project on the palaeomagnetism of late Precambrian rocks from southern Africa conducted jointly with A. Kröner, Johannes Gutenberg Universitat, Mainz FRG. Sampling was conducted by Kröner with G.J.B. Germs (Geological Survey of Namibia, Windhoek) and A.B. Reid (Department of Physics, University of Rhodesia, Salisbury). Sample preparation, palaeomagnetic measurements and interpretation are the sole responsibility of the author.

As in the study of late Precambrian palaeomagnetism in Australia, this study has a twofold approach. One aim is to test palaeomagnetically the structural integrity of the two cratonic units which dominate the Precambrian shield areas of southern Africa, the Congo and Kalahari cratons (Figure 4.1). The two are separated by a prominent and well documented zone of crustal mobility (the Pan-African Damara Mobile Belt) which has been variously interpreted as being a result of cratonic collision and suturing or as a result of *in situ* ensialic processes. By obtaining palaeomagnetic results from time equivalent formations on both sides of the mobile belt, it is possible to test for the absence or presence of large relative lithospheric displacements and thereby test a possible collisional model for the belt.

A second equally important aim of the project is to obtain more information concerning the depositional palaeolatitudes

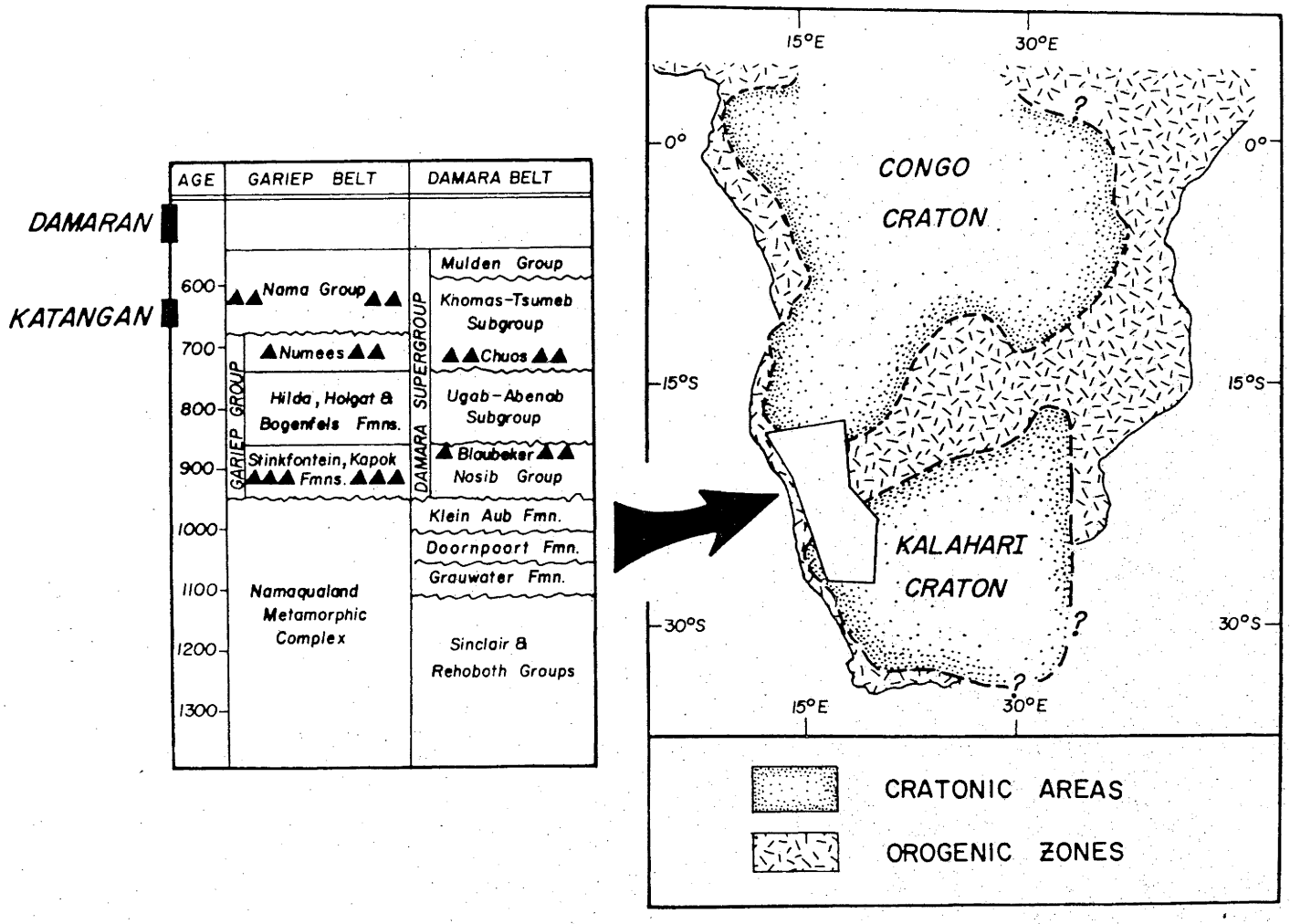

Figure 4.1 : Generalized structural sketch of southern Africa illustrating relationship between Congo and Kalahari cratons and intervening Damara mobile belt. Irregular polygon contains sampling sites for the Nama/Damara study.

Figure 4.2 : Stratigraphic relationships between Upper Proterozoic units in the Damara and Gariep belts, southern Africa. Triangles denote possible glacial horizons. Approximate timing of the Katangan and Damaran phases of the Pan-African orogenesis shown as bars at left.

of late Precambrian glacial deposits in southern Africa and possibly to relate these data to those from other late Precambrian glacial deposits. As outlined in Chapter 1, two general models for late Precambrian glaciations are prevalent, synchronous and nonsynchronous events. It is hoped that a broader base in terms of spatial distribution of the palaeomagnetic sampling sites for these data will aid in discovering the true nature of these deposits and the processes which formed them.

§4.2 Nama Group

§4.2.1 Stratigraphy and age

Nama Group sediments cover much of the older Precambrian complexes of southern Namibia and adjacent parts of the Cape Province of South Africa. Originally subdivided by Range (1912) into four units, the Nama Group has more recently been subdivided into three units : the Kuibis Subgroup, Schwarzrand Subgroup and Fish River Subgroup (Germs, 1972 and in preparation). The Kuibis Subgroup unconformably overlies a basement complex consisting of older sedimentary and metamorphic rocks of the Tsumis, Numees, Sinclair and Auborous Formations and the Gariep Group (Figure 4.2). Three units comprise the Kuibis Subgroup, the basal Dabis Formation, overlain by the Schwarzkalk Formation and the Urikos Member (Figure 4.4). Two distinct clastic carbonate sedimentary cycles are apparent, however the complete Kuibis Subgroup is not everywhere present due to tectonic sedimentation control. Excellent examples of Precambrian trace and macrofossils are present, including *Pteridinium, Namalia, Ernietta, Cloudina* as well as columnar

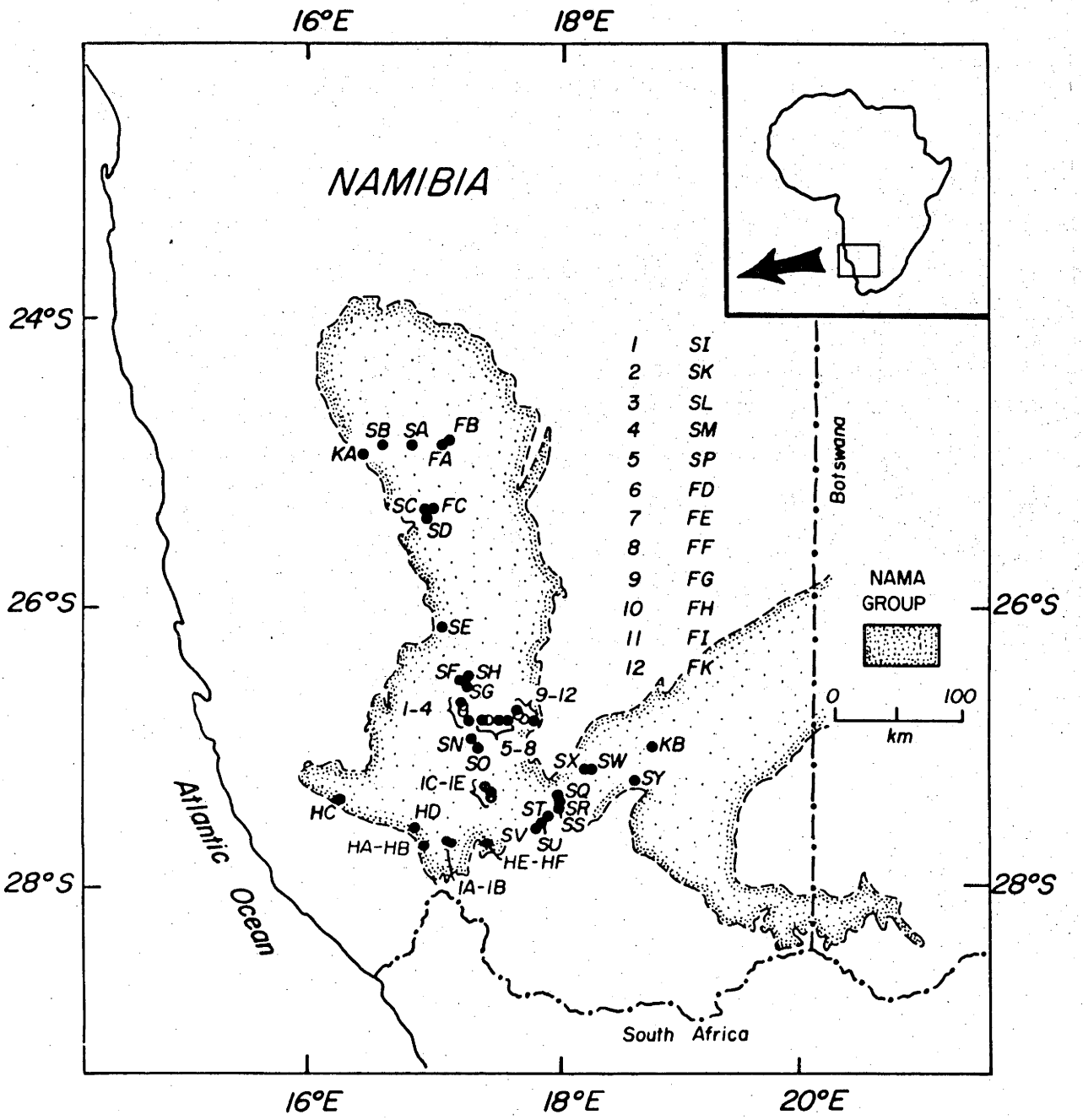

Figure 4.3 : Location of Nama Group sites in southern Namibia. Prefixes : F (Fish River Subgroup), S (Schwarzrand Subgroup), K (Kuibis Subgroup), H (Kuibis Subgroup), I (Schwarzrand Subgroup). Thus FC=NFC, SB=NSB, IA=GIA, HE=GHE etc.

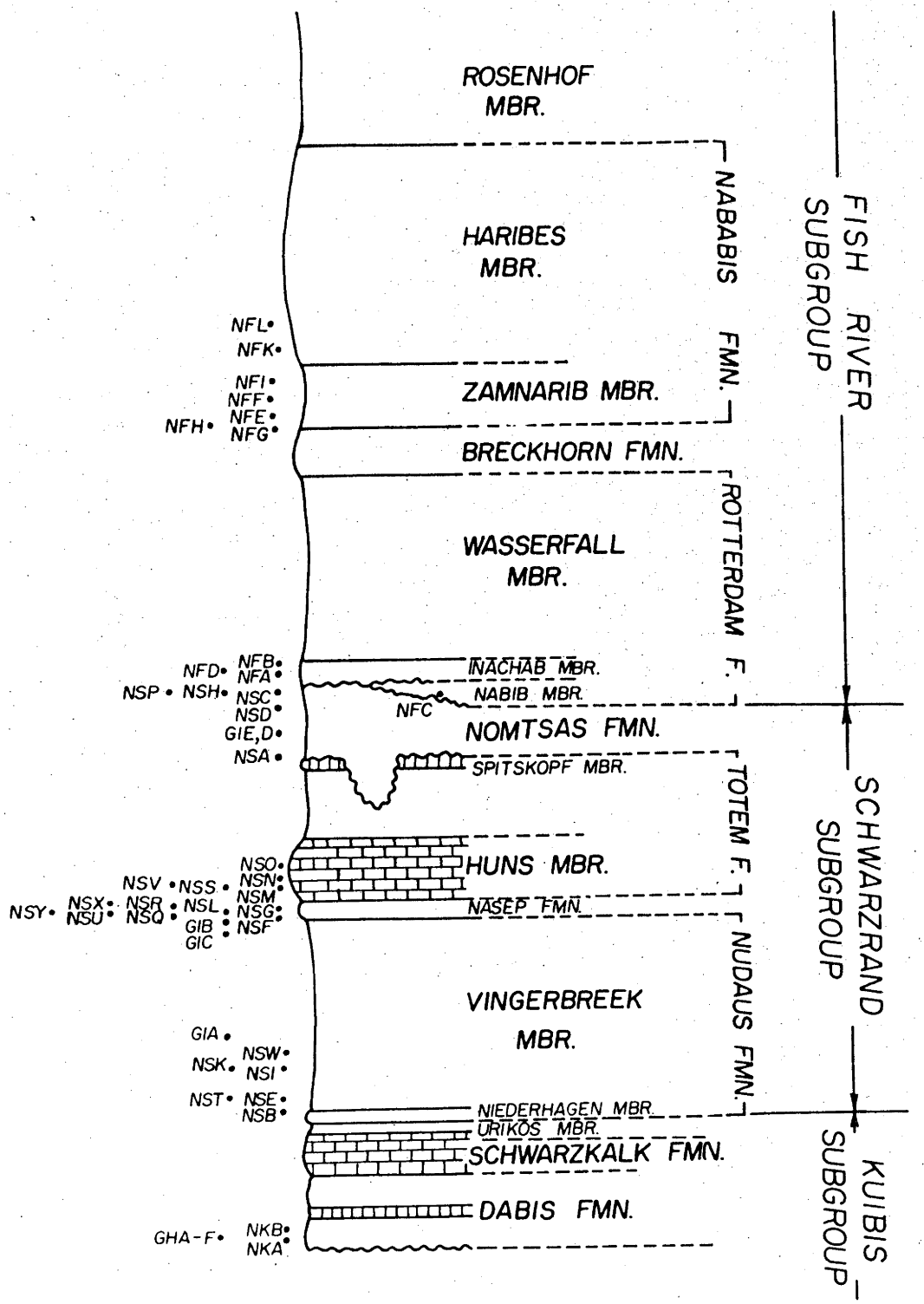

Figure 4.4 : Stratigraphic distribution of Nama Group sites, symbols as in Figure 4.3.

stromatolites.

The Schwarzrand Subgroup conformably overlies the Kuibis Subgroup and consists of four formations, the Nudaus Formation, Nasep Formation, Totem Formation and Nomtsas Formation in order of decreasing age (Figure 4.4). Again, not all members are everywhere present due to palaeotopographic and tectonic control of sedimentation. At least three unconformities appear to be present in the Schwarzrand Subgroup, within the Nudaus Formation, between the Totem and Nasep Formations, and between the Totem and Nomtsas Formation (Germs, 1972). It has been suggested (Kröner and Germs, 1971; Kröner and Rankama, 1973) that the unconformity within the Nudaus Formation is a result of glacial action, as it is overlain by a possible tillite. Another unconformity resulting from an episode of glaciation may be recorded between the Nomtsas and Totem Formations (Germs, 1972). Body fossils (*Rangea, Pteridinium, Paramedusium, Nasepia, Cloudina, Cyclomedusa*) are found in the lower parts of the Subgroup, as are columnar stromatolites (*Conophyton* (?), *Gymnosolen* (?), *Acadiella* (?), *Kulparia* (?)).

The Fish River Subgroup is separated from the underlying Schwarzrand Subgroup by a major unconformity, and consists of lithologies very different from the underlying formations. The older Kuibis and Schwarzrand Subgroups contain thick shale and limestone sequences; in contrast, the Fish River Subgroup consists mainly of crossbedded sandstones with intercalated shale lenses. Limestones are absent. The Fish River Subgroup is divided into the basal Rotterdam Formation overlain by the Breckhorn and Nababis Formations. No body fossils have been found. Sedimentary features possibly indicative of cold climate have been described by Hälbich (1964). Karroo (Upper Palaeozoic)

sediments overlie the Fish River Subgroup with prominent unconformity.

The precise age of the Nama Group is uncertain although considerable indirect evidence is available which contrains the age of the Nama within not unreasonable limits. In southern Namibia, the Kuibis Subgroup lies unconformably upon an older Precambrian sequence containing acid volcanics dated at 690±32* my. To the east, the Nama Group is intruded by granitic rocks of the Bremen Complex dated at 513* my. Preliminary Rb/Sr results from Kuibis Subgroup shales indicate a diagenetic age in the 620*-630* my range (Kröner, pers. comm.). Germs (1974) assigned an age of 700-600 my to the Nama Group as the Kuibis Subgroup contains *Ediacara*-type fossils. The upper Fish River Subgroup contains an occurrence of the trace fossil *Phycodes Pedum* and may therefore be lowermost Cambrian in part.

§4.2.2 Tectonic history

The Nama Group sediments were deposited on a stable continental platform (the Naukluft shelf) and have suffered only very localized deformation and metamorphism during Pan-African tectonism. The beds are predominantly flat lying or are slightly folded into broad synclinoria and monoclinoria with dips generally less than 10°. Peripheral to the Pan-African mobile belts, Nama sediments have been intensely folded and metamorphosed. Palaeomagnetic sampling was confined to undeformed and unmetamorphosed regions only.

---

* ^{87}Rb decay constant $1.42 \times 10^{-11} yr^{-1}$ used.

§4.2.3 Previous palaeomagnetic work

Piper (1975b) reported pole positions from red sandstones at 9 sites in the Fish River Subgroup. His results were based upon site mean directions calculated after high-field (∿100 mT) AF demagnetization. The cleaned sample mean directions were scattered and appeared to define a streaked distribution from a PEF direction to an east-southeast steep negative direction (Figure 13 of Piper, 1975b). No thermal demagnetization was attempted. Despite the facts that the mean formation direction was not significantly different from the PEF direction and that no fold test was employed, Piper implied that the dispersed directions are primary and record a period of rapid apparent polar motion suggested by McElhinny *et al.* (1974). As is shown in the next section, several components of magnetization may be present in the Fish River Subgroup which have been isolated by thermal demagnetization, suggesting that Piper's original conclusions may have been incorrect.

No other palaeomagnetic results from Nama Group sediments have been published to date.

§4.2.4 Palaeomagnetic results

Nama Group samples of widely varying lithology were collected at 47 sites through southern Namibia (Figure 4.2). Four samples were taken at each site. Seven formations in the three Subgroups were sampled, giving a good overall stratigraphic distribution of the sites (Figure 4.3). Sampling locality details are given in Appendix A. The orientation used for collection of all the samples from southern Africa reported

here is similar to that used in collection of the Australian samples, the accuracy of orientation (azimuth and dip) is estimated to be $\pm 1°$, as for the Australian samples.

Fish River Subgroup

Site mean NRM directions from the Rotterdam and Nababis Formations were loosely grouped and not significantly different from the PEF direction at the sampling site. Pilot thermal demagnetization revealed several characteristic magnetization types in the Fish River Subgroup samples. Some pilot specimens had directions which remained aligned with the PEF direction during most of the 16 demagnetization steps, with the onset of directional instability occurring in the 660°-670° range. Other specimens underwent systematic directional changes during the lower temperature demagnetization steps, generally reaching stable endpoints in the 450°-630° range. Two general groups of stable endpoints different from PEF directions were seen in the Fish River Subgroup; these have been labelled the N2 and N3 magnetizations in Table 4.1 and Figure 4.5 and 4.6. After bulk thermal demagnetization of remaining specimens, each site displayed only one of these magnetizations. The N2 component was observed in 15 samples at 4 sites and is characterized by an easterly declination and a shallow to moderate positive inclination. The N3 magnetization was observed at 4 different sites and had a south-southeast declination with a steep negative inclination. No consistent subtracted directions other than PEF vectors were observed during demagnetization, suggesting that either the N2 or N3 magnetizations (but not both) are present in any particular sample, although overlapping T_b spectra may have complicated the analysis. A

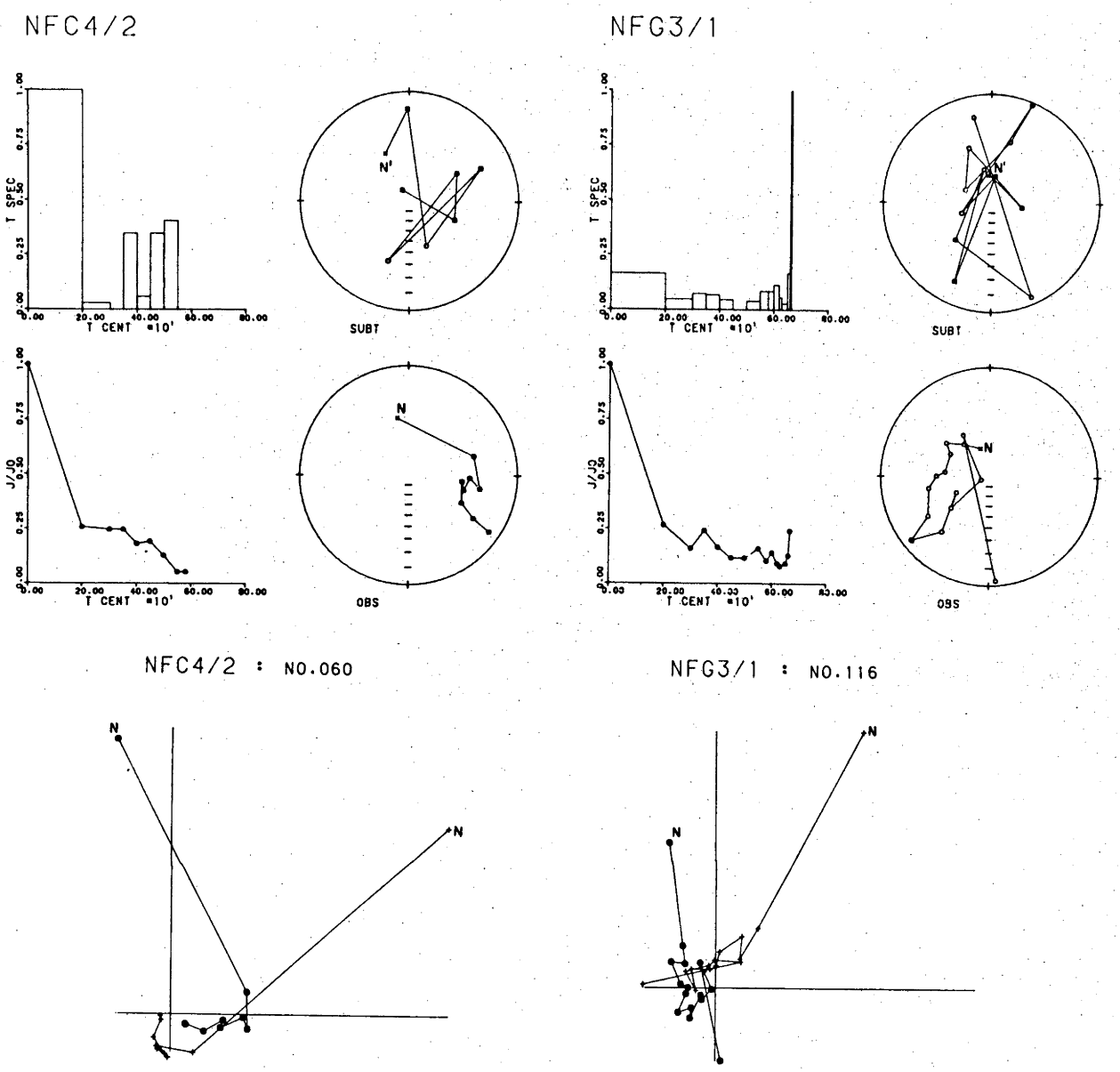

Figure 4.5 : Thermal demagnetization, Fish River Subgroup.

TABLE 4.1

NAMA GROUP : Site mean directions

(A) FISH RIVER SUBGROUP : Site mean directions before and after thermal demagnetization

		NRM				After thermal demagnetization							
FORMATION	SITE	N	R	D	I	N	R	D	I	T°C	D'	I'	MAGNETIZATION
	NFA	4	2.125	003	-01	3	2.924	321	67	500	331	70	N3
ROTTERDAM	NFB	4	3.464	354	-68			(random)					
FORMATION	NFC	4	3.333	067	-47	4	3.891	087	35	350	086	39	N2
	NFD	4	3.832	338	-59	4	3.989	348	-53	500	346	-51	PEF
	NFE	4	3.091	009	-75	4	3.674	256	-41	550	255	-39	N2
	NFF	4	3.967	060	-87	4	3.991	162	-61	500	161	-62	N3
NABABIS	NFG	4	3.700	295	-54	4	3.892	095	-72	640	094	-76	N3
FORMATION	NFH	4	3.846	306	-75	4	3.894	277	-18	500	277	-19	N2
	NFI	4	3.974	079	-43	4	3.991	105	-14	600	105	-15	?
	NFK	4	3.423	353	-43	3	2.836	139	-73	630	141	-77	N3
	NFL	4	3.634	359	-44	3	2.949	035	48	500	089	25	N2

(B) SCHWARZRAND SUBGROUP : Site mean directions before and after thermal demagnetization

		NRM				After thermal demagnetization							
FORMATION	SITE	N	R	D	I	N	R	D	I	T°C	D'	I'	MAGNETIZATION
	NSA	4	2.996	178	45			(random)					
	NSC	4	3.965	019	-05	4	3.836	016	17	360	017	11	N1
	NSD	4	2.022	076	53			(random)					
NOMTSAS	NSH	4	2.503	067	-14	4	3.550	179	-12	320	181	-09	N1
FORMATION	NSP	4	3.253	049	-08	4	3.799	051	-01	360	050	01	N1
	GID	4	3.712	214	-69	4	3.968	239	-20	320	236	-22	N1
	GIE	4	3.973	082	-48	4	3.976	085	-47	500	085	-47	N3
	NSM	4	3.993	169	41	4	3.997	171	46	450	171	46	N1
TOTEM	NSN	4	3.783	168	-70	4	3.841	126	-62	360	114	-57	N3
FORMATION	NSO	4	3.695	337	-47	4	3.954	023	-03	360	023	02	N1
	NSS	4	3.929	315	-71			(random)					
	NSV	4	3.755	249	-82	3	2.792	193	-12	360	193	-07	N1
	NSG	4	3.720	343	-52	3	2.989	045	-23	500	041	-30	N1
	NSL	4	3.979	001	-31	4	3.991	356	-47	cd*	354	-49	PEF
	NSQ	4	3.824	009	-70	4	3.808	023	-05	360	019	-03	N1
NASEP	NSR	4	3.899	325	-58			(random)					
FORMATION	NSU	4	3.947	337	-70	4	3.868	194	-12	360	193	-11	N1
	NSY	4	3.682	198	03	2	1.969	153	-28	cd*	151	32	N1
	GIB	4	3.879	341	-65	4	3.919	285	-71	500	293	-68	?
	GIC	4	3.859	087	-54	4	3.799	024	-28	320	025	-23	N1
	NSB	4	3.699	014	00	4	3.781	005	-34	360	002	-34	N1
	NSE	4	3.318	282	-33	4	3.757	282	-18	400	282	-18	?
	NSF	4	3.345	346	-62	4	3.585	039	-53	400	037	-54	PEF
NUDAUS	NSI	4	2.180	106	-61			(random)					
FORMATION	NSK	4	2.979	082	42	4	3.655	027	16	450	031	22	N1
	NST	4	3.921	009	-63	4	3.832	023	-17	360	023	-10	N1
	NSW	4	3.974	002	-56	4	3.939	002	-52	cd*	012	-53	PEF
	NSX	4	3.770	021	-47	4	3.994	008	-32	450	006	-28	N1
	GIA	4	3.794	214	-01	4	3.897	241	21	320	241	21	N1

(C) KUIBIS SUBGROUP : Site mean directions before and after thermal demagnetization

		NRM				After thermal demagnetization							
FORMATION	SITE	N	R	D	I	N	R	D	I	T C	D'	I'	MAGNETIZATION
	NKA	4	3.577	008	39	3	2.812	021	-42	400	024	-45	N1
	GHA	4	3.993	176	-04	4	3.992	174	-06	500	175	13	N1
	GHB	4	2.943	313	-09			(random)					
DABIS	GHC	4	3.984	349	54			(random)					
FORMATION	GHD	4	3.125	315	25			(random)					
	GHE	4	3.932	166	-26			(random)					
	GHF	4	3.343	200	-02	4	3.381	200	01	500	200	01	N1

TABLE 4.1

(D) NAMA GROUP : Mean directions and palaeomagnetic poles after thermal and chemical demagnetization

		Before structural correction									After structural correction						
MAGNETIZATION	FORMATION	N	n	R	k	D_m	I_m	pole lat	pole long	dp,dm	R	k	D_m'	I_m'	pole lat	pole long	dp,dm
N1	NOMTSAS	4	16	3.618	7.8	031	13	45S	244E	18,36	3.669	9.1	031	12	46S	245E	17,33
N1	TOTEM	3	11	2.667	6.0	011	-12	67S	226E	29,56	2.682	6.3	011	-12	67S	226E	28,55
N1	NASEP	5	17	4.300	5.7	017	-04	60S	234E	18,35	4.460	7.4	015	-17	67S	239E	16,31
N1	NUDAUS	5	20	4.506	8.1	025	-19	61S	257E	15,30	4.422	6.9	025	-16	60S	254E	17,32
N1	DABIS	3	11	2.733	7.5	191	12	67S	226E	25,49	2.781	9.1	192	20	70S	234E	24,45
N1:																	
unit weight sites:		20	75	17.318	7.1	020	-07	60S	241E	07,13	17.510	7.6	020	-11	61S	243E	06,13
unit weight formations:		5	75	4.863	29.2	019	-07	61S	239E	07,14	4.854	27.4	019	-11	62S	241E	08,15
N2	ROTTERDAM	1	4	-	-	087	35	06N	269E	-	-	-	086	39	06N	266E	-
N2	NABABIS	3	11	2.746	7.9	253	-39	04S	260E	33,56	2.940	33.3	268	-28	05N	273E	13,24
N2:																	
unit weight sites:		4	15	3.731	11.2	077	38	01S	263E	20,34	3.926	40.5	087	31	05N	271E	09,16
unit weight formations:		2	15	1.989	93.4	080	37	01N	265E	-	1.991	106.2	087	33	05N	270E	-
N3	ROTTERDAM	1	3	-	-	321	67	07N	353E	-	-	-	331	70	06N	001E	-
N3	NABABIS	3	11	2.943	35.3	137	-71	00N	355E	32,37	2.947	37.9	140	-74	02S	359E	33,36
N3	NOMTSAS	1	4	-	-	085	-47	16S	311E	-	-	-	085	-47	16S	311E	-
N3	TOTEM	1	4	-	-	126	-62	05N	341E	-	-	-	114	-57	01N	331E	-
N3[1]	FISH RIVER FORMATION	4	20	3.954	65.5	102	-53	20S	317E	11,16	3.954	65.5	099	-60	27S	321E	12,16
N3:																	
unit weight sites[2]:		6	22	5.796	24.6	122	-67	02S	344E	19,23	5.579	11.9	108	-73	14S	347E	32,36
unit weight sites[3]:		10	42	9.655	26.1	112	-61	03S	334E	11,15	9.646	25.4	110	-65	07S	337E	13,16
unit weight formations[2]:		4	22	3.875	24.1	116	-64	03S	339E	24,30	3.848	19.8	114	-64	04S	338E	27,34
unit weight formations[3]:		5	42	4.855	27.5	113	-62	03S	335E	18,23	4.840	25.0	110	-64	06S	336E	20,25

[1] N3 data from Table 4.2.
[2] excluding Piper's data.
[3] including Piper's data.
[4] PEF data from Table 4.2

NAMA GROUP : Mean directions and palaeomagnetic poles

		Before structural correction									After structural correction						
MAGNETIZATION	N	n	R	k	D_m	I_m	pole lat	pole long	dp,dm	R	k	D_m'	I_m'	pole lat	pole long	dp,dm
PEF	4	16	3.911	33.8	005	-53	82S	347E	15,22	3.913	34.5	006	-53	81S	343E	15,22
PEF[4]	4	19	3.894	28.4	007	-49	83S	318E	15,23	3.894	28.4	359	-42	88S	175E	13,21
PEF: unit weight sites[3]	8	35	7.801	35.2	007	-51	82S	329E	09,13	7.764	29.6	002	-48	87S	343E	09,13

TABLE 4.2

FISH RIVER SUBGROUP: Data of Piper (1975), AF demagnetization to 100 mT, not corrected for bedding

SITE	n	D_m	I_m	α95	MAGNETIZATION
94	5	002	-16	07	?
95	5	008	-54	24	PEF
96	6	037	-52	12	PEF
97	5	350	-37	21	PEF
98	4	101	-51	24	N3
99	6	091	-52	13	N3
100	3	002	-49	33	PEF
101	6	091	-56	38	N3
102	4	125	-51	20	N3

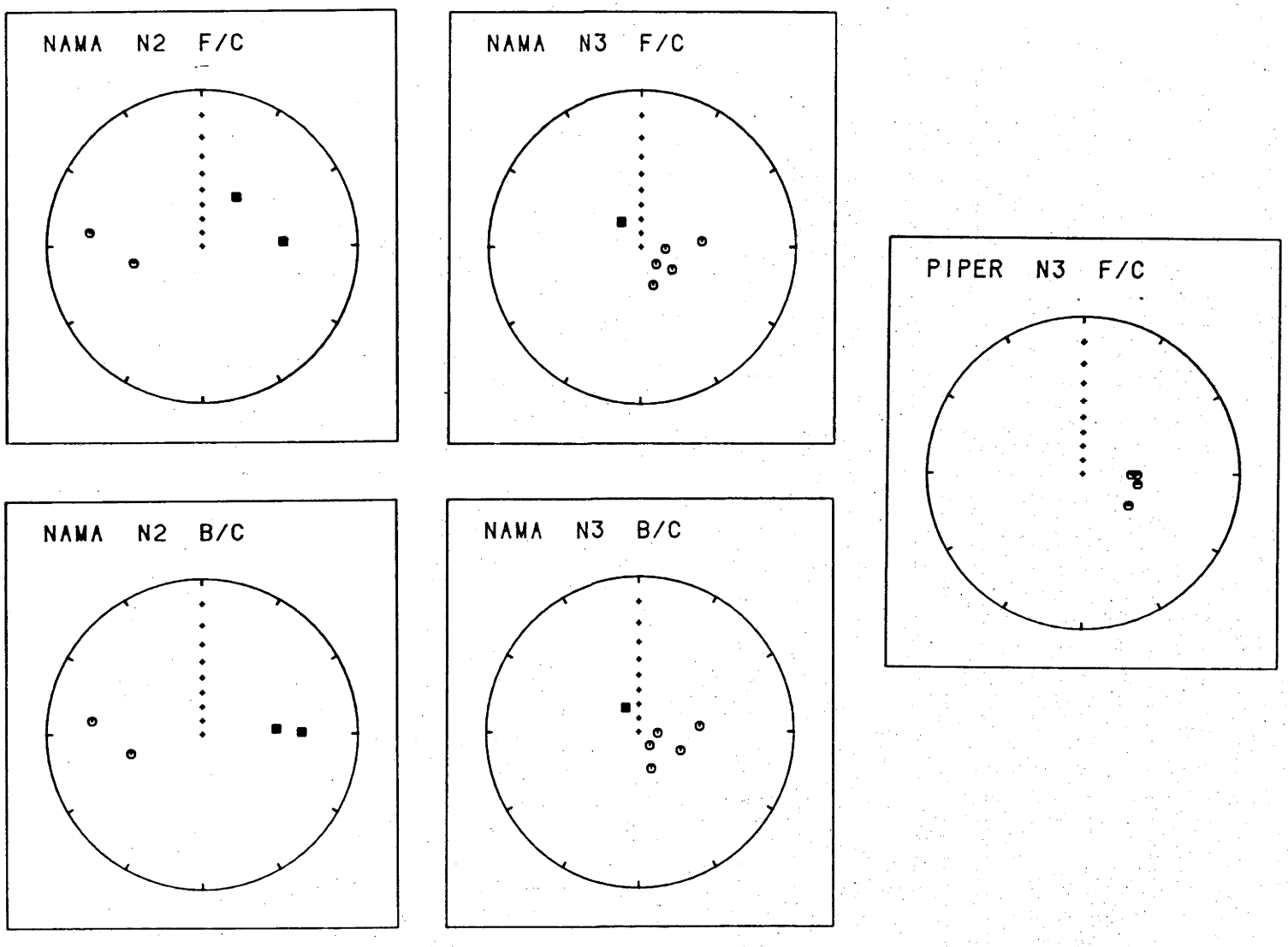

Figure 4.6 : Cleaned site mean magnetization directions, Fish River Subgroup N2 and N3 components; equal-angle projection. Open (closed) symbols refer to negative (positive) inclination.

direct comparison of the relative T_b's of the N2 and N3 magnetizations was therefore not possible. However, a fold test indicates that the N2 component was probably acquired before folding of the Fish River Subgroup occurred (probably in a Pan-African event ca. 500-550 my), while the N3 magnetization might have been acquired either before or after folding:

Magnetization	k'/k	95% significance point
N2	3.62	3.79
N3	1.05	3.79

A magnetization age sequence N2→N3 is favoured.

AF demagnetization experiments conducted on a number of pilot specimens showed that high coercive forces are exhibited by the mineral grains carrying the PEF and N3 magnetizations, and that thermal demagnetization was a much more suitable tool for isolating the various components. With this in mind, a reexamination of the palaeomagnetic data from the Fish River Subgroup presented in Piper (1975b) suggests that the apparently streaked distribution of sample and site mean directions may be due to incomplete removal of a PEF component coexisting with an N3-type component in some sites. The non-PEF endpoint of the distribution of Piper's data is very similar indeed to the N3 direction from the Fish River Sbugroup described above. By rejecting 4 sites (95,96,97 and 100) whose mean directions are not significantly different from the PEF direction and a fifth with an indeterminate mean direction (94), the remaining 4 sites define a mean direction similar to but significantly

different from the N3 mean direction:

Magnetization	N	R	D_m	I_m
N3 (Fish River Subgroup)	4	3.941	139	-70
Piper (Fish River Subgroup)	4	3.954	102	-53
combined	8	7.733	115	-63

$F_{2,12}=9.31$ 95% significance point = 3.89

As similar magnetizations are found in the underlying Schwarzrand Subgroup, it seems possible that these southeasterly and steep negative directions may be the result of a post-diagenetic overprinting of preexisting (?) primary magnetizations in the Nama Group. If this is indeed the case, the palaeomagnetic results presented in Piper (1975b) probably have more relevance to secondary overprinting than to an original primary magnetization.

The NFI site mean direction is somewhat problematic, as it is distinct from both the N2 and N3 mean directions. As this direction lies near the great circle segment connecting the N2 and N3 directions, there are two probable interpretations. Either it represents an intermediate magnetization acquired in the time interval between times of acquisition of the N2 and N3 components, or coexisting N2 and N3 magnetizations are present in the NFI samples and have not been separated during demagnetization. Unfortunately, high temperature instability problems prevented more detailed investigation. However, considering the exceptionally stable directional behaviour at lower temperatures (<650°) and the tight grouping of the site mean direction, the former interpretation is favoured and the NFI

site mean pole is considered to be a VGP intermediate in age between N2 and N3.

Schwarzrand and Kuibis Subgroup

Site mean NRM directions from the 5 formations sampled in the Schwarzrand and Kuibis Subgroups were widely scattered, again with a PEF trend. Like the Fish River Subgroup sites, variable behaviour during thermal and chemical demagnetization was noted (Figure 4.6). Three sites exhibited very stable PEF magnetizations, while two others reached stable endpoints very similar to the N3 mean direction described above. These latter sites have been grouped with the Fish River Subgroup N3 sites to form the N3 mean direction in Table 4.1. In two sites (NSE,G1B), well grouped cleaned mean directions were observed which did not seem to be related to any of the other observed magnetizations. These mean directions have not been included in any of the mean magnetization directions.

In the majority of sites, a significant PEF component was removed in the initial heating steps, with remanence vectors stabilizing to a consistent shallow north-northeast (south-southwest) direction, generally in the 350°-500° range (Figure 4.6). This stable characteristic shallow magnetization has been designated the N1 component, and was observed in 75 samples from 20 sites in 5 formations (Table 4.1, Figure 4.7). An F-ratio test indicates that the 5 formation mean directions are not significantly different:

S	N	R	ΣR_i	$\Sigma N_i - R_i$	F
5	20	17.510	17.824	2.176	0.541 (95% significance point = 2.27)

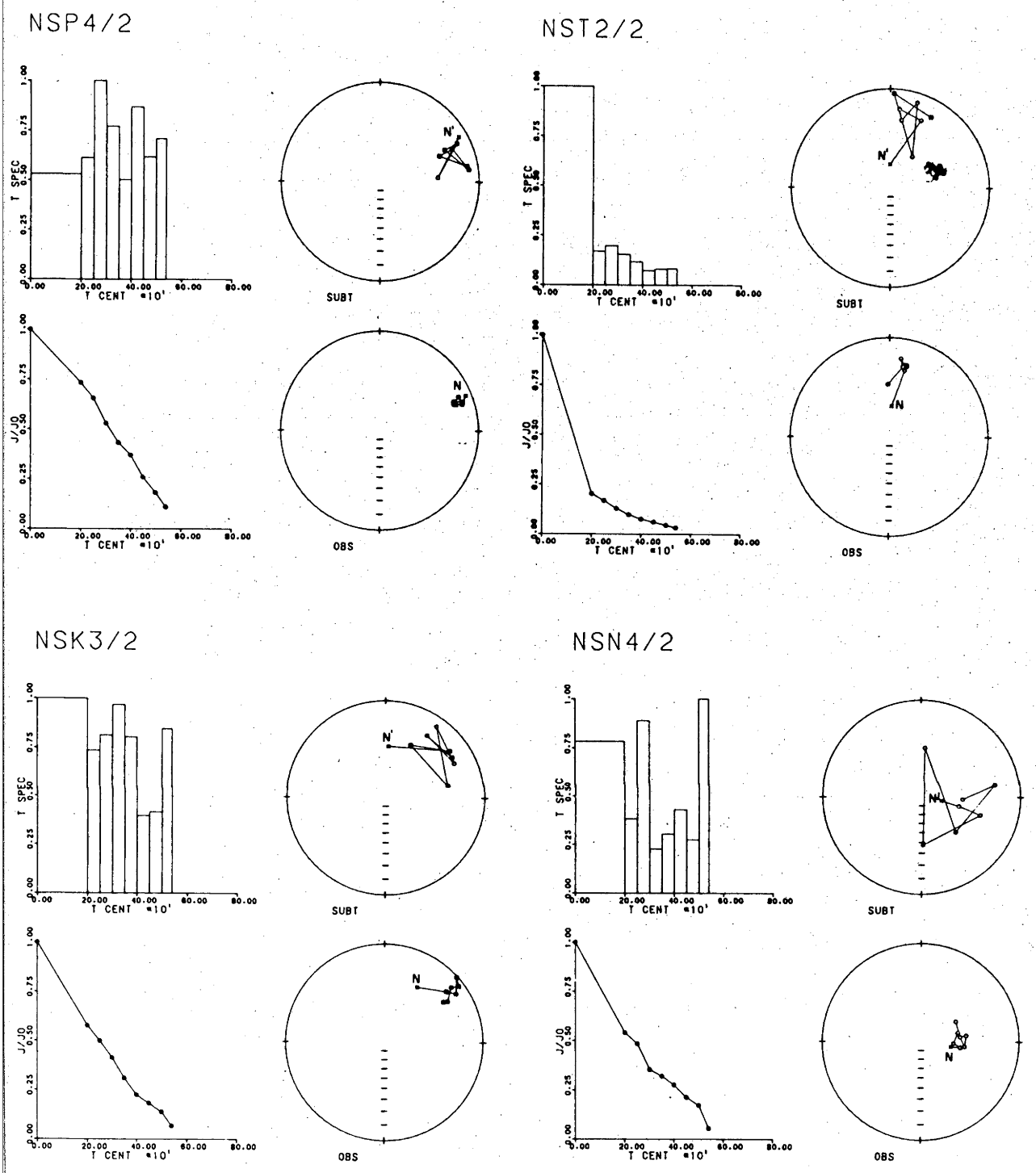

Figure 4.7(A) : Thermal demagnetization, Schwarzrand Subgroup.

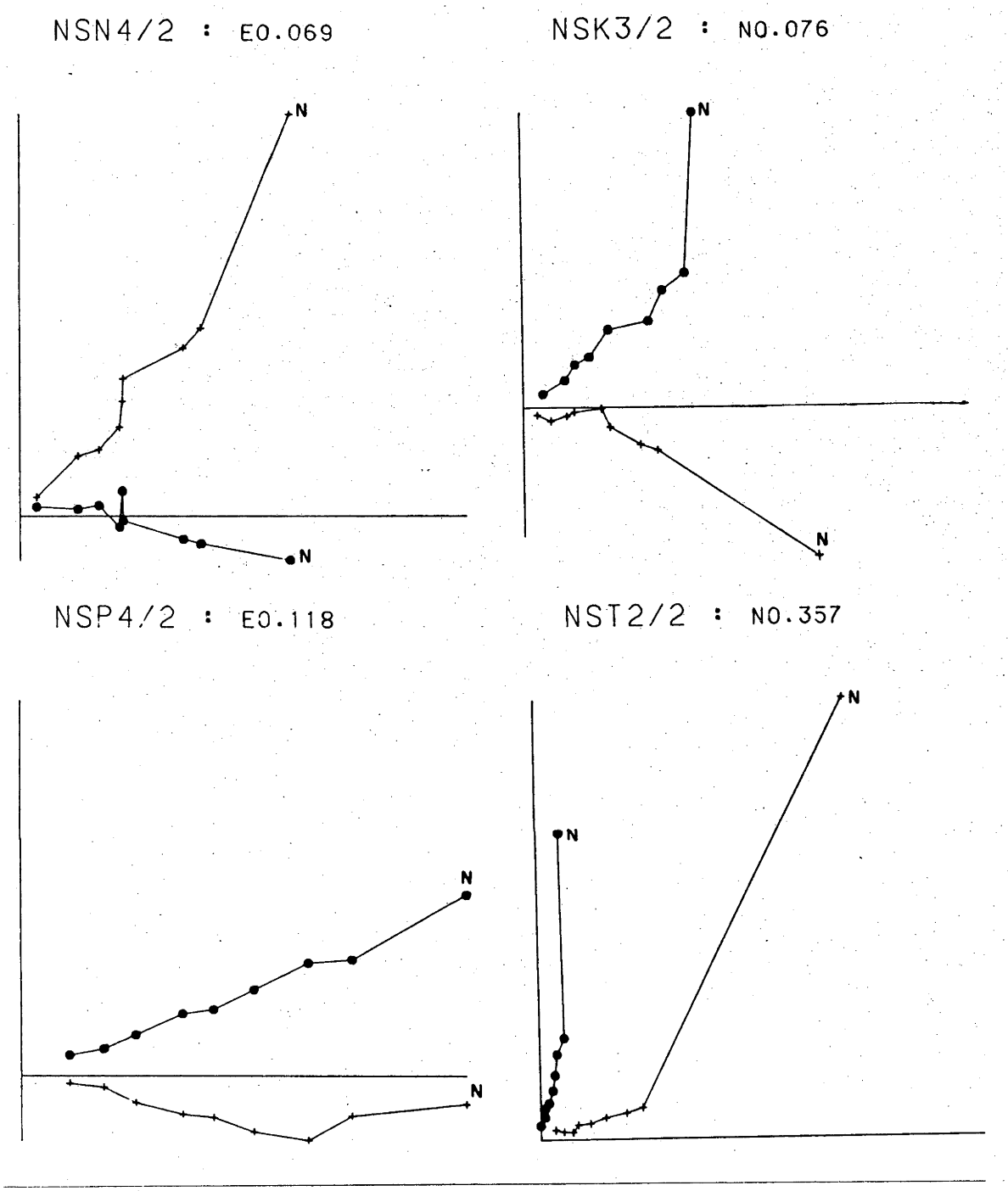

Figure 4.7(B) : Thermal demagnetization, Schwarzrand Subgroup (continued).

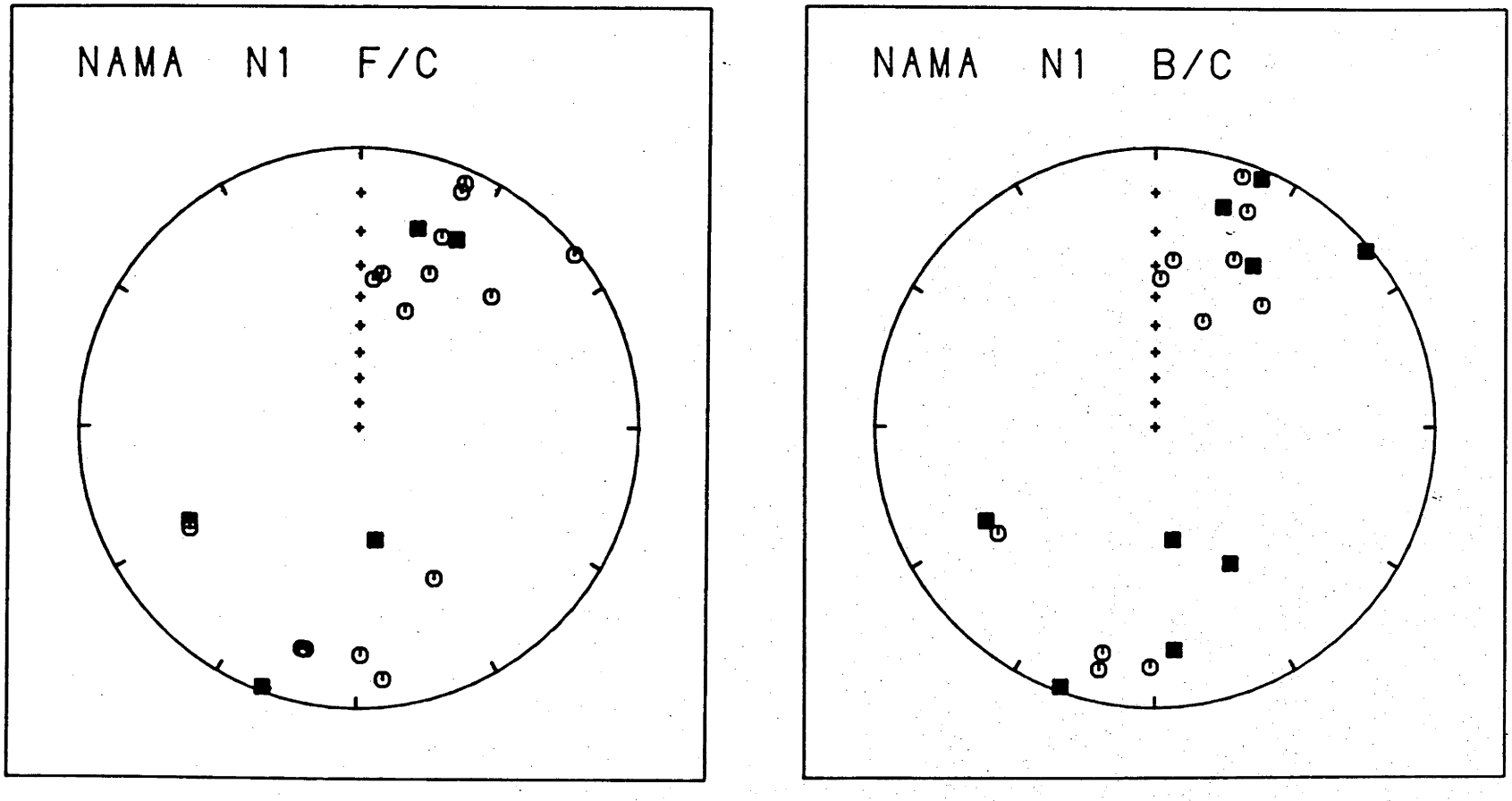

Figure 4.8 : Cleaned site mean magnetization directions, Schwarzrand and Kuibis Subgroup N1 component; equal-angle projection. Open (closed) symbols refer to negative (positive) inclination.

The 5 formation mean directions and 20 site mean directions have been grouped to define the N1 mean direction in Table 4.1.

Upon tectonic correction, overall precision of the N1 magnetization increases slightly when unit weight is given to site mean directions and decreases slightly when unit weight is given to formation mean directions:

Magnetization	k'/k	95% significance point
N1 : (sites)	1.07	1.56
N1 : (formations)	0.94	3.45

Neither of the changes are significant at the 95% level, due to the nearly flat lying nature of the beds. As the fold test is inconclusive, the only evidence which can be cited in support of a primary magnetization age is that the pole position calculated from the N1 mean direction is markedly distinct from most of the younger Phanerozoic APWP, although it is admittedly in the general vicinity of, but removed from, Cambro-Ordovician poles. The N1 pole is near poles from pre-Nama formations whose ages are just older than the ages obtained from the basal Nama sediments (Figure 4.18).

Interpretation of the Nama results in the framework of other African late Precambrian poles is deferred until §4.4.

§4.3 Damara Supergroup

§4.3.1 Stratigraphy and age

Martin (1965) and Kröner (1971, 1977b) have suggested that the Damara Supergroup of central and northern Namibia is the stratigraphic equivalent of the Nama and Gariep Groups to

the south. Although different facies are apparent, the differences between the two are attributable to differing depositional environments, the Nama and Gariep sediments having been deposited in a shelf environment, while the Damara Supergroup was deposited in a geosynclinal environment (the Nosib-Damara Geosyncline of Martin, 1965). No direct contact between the Damara and Nama/Gariep exists, and the various correlations made between them have been necessarily indirect and the subject of much debate.

The Damara Supergroup rests unconformably on older Precambrian sediments and intrusives, and is divided into four major units separated by unconformities (Figure 4.2) : the basal Nosib Group, followed by the Ugab/Abenab Subgroup, the Khomas/Tsumeb Subgroup and terminated by the Mulden Group. Sediments of possible glacial origin are found in the lower part of the Khomas/Tsumeb Subgroup (the Chuos Tillite) and in the upper part of the Nosib Group (the Blaubeker and Varianto Formations).

The Mulden Group is thought to be an equivalent of the upper Nama Group (Fish River Subgroup); preliminary Rb/Sr ages from Mulden Group shales indicate a depositional age of about 570-590 my (Kröner, pers. comm.). The Chuos Tillite at the base of the Khomas/Tsumeb Subgroup is correlated with the Numees Tillite of the Gariep Group, which overlies felsite lavas with Rb/Sr ages of 709±28*my (de Villiers, 1969) and 706±12*my (Alsopp, in Kröner, 1977b). Underlying the felsites, the Stinkfontein Formation unconformably overlies

---

*^{87}Rb decay constant $1.42 \times 10^{-11} yr^{-1}$.

a crystalline basement complex, and is intruded by granites dated at 810±35 my (Pb-Pb zircon age, Alsop, in Kröner, 1977b). On the northern side of the Damara Mobile Belt, the Nosib Group is correlated with the Stinkfontein and Kapok Formations and is intruded by a syenite with a provisional minimum age of 760 my (Pb-Pb zircon age, Kröner and Burger in Kröner, 1977b). The age of the Damara Supergroup would thus appear to be bracketed between about 600 my and the age of the basement complex upon which it rests, currently thought to be about 950-1050 my.

§4.3.2 Tectonic history

The Damara Supergroup sediments were probably deposited in a subsiding trough of appreciable size, and are divided into a eugeo- and miogeosynclinal facies. To a large degree, basement topography is responsible for depositional control. However, unconformities between the various groups may reflect as well phases of Pan-African tectonism. Clifford (1967) has demonstrated that at least two phases are recognizable during Pan-African orogenesis in southern Africa, the Katangan (*ca.* 660-610 my) and Damaran (*ca.* 550-450 my) episodes. Both phases are significant in an understanding of multicomponent magnetizations in Damara Supergroup rocks.

The Nosib-Damara Geosyncline was deformed and metamorphosed during the Katangan episode before deposition of the upper part of the Damara Supergroup. Later, the entire Supergroup was affected by the Damaran episode. This polyphase tectonism and metamorphism had highly variable effects upon Damara Supergroup rocks, ranging from open folding with little or no visible metamorphic effects, to complex tight folding

with medium to high grade metamorphism. Although palaeomagnetic sampling was confined to areas with minimal visible metamorphic effects, the palaeomagnetic results clearly reflect Pan-African thermal events, as demonstrated in the next sections.

§4.3.3 Mulden Group

Samples of the Mulden Group were collected at 8 sites in northern Namibia dispersed through a thickness of several hundred metres. The dominant lithology sampled was a thickly bedded and finely laminated maroon to grey siltstone. Although no metamorphic effects were outwardly visible, the development of minor chlorite flakes seen in thin section suggested that some samples may have suffered a very low grade (low pressure, 250°-350°) metamorphism. This possible heating is reflected in the Rb/Sr data from Mulden Group shales and probably occurred at 526±15*my (Kröner, pers. comm.).

NRM directions were quite scattered, but a trend of shallow westerly (easterly) directions was apparent. During pilot thermal demagnetization, remanence vectors at 6 sites converged upon a common shallow westerly (easterly) direction at temperatures of 570°-620°, confirming the trend observed in the NRM directions (Figure 4.9). After bulk thermal treatment, a significant improvement in precision over the NRM directions was realized at these sites, which define the DM magnetization (Table 4.3). Precision of the DM magnetization improves markedly upon structural correction, although the improvement is not significant at the 95% confidence level

---

*^{87}Rb decay constant $1.42 \times 10^{-11} yr^{-1}$.

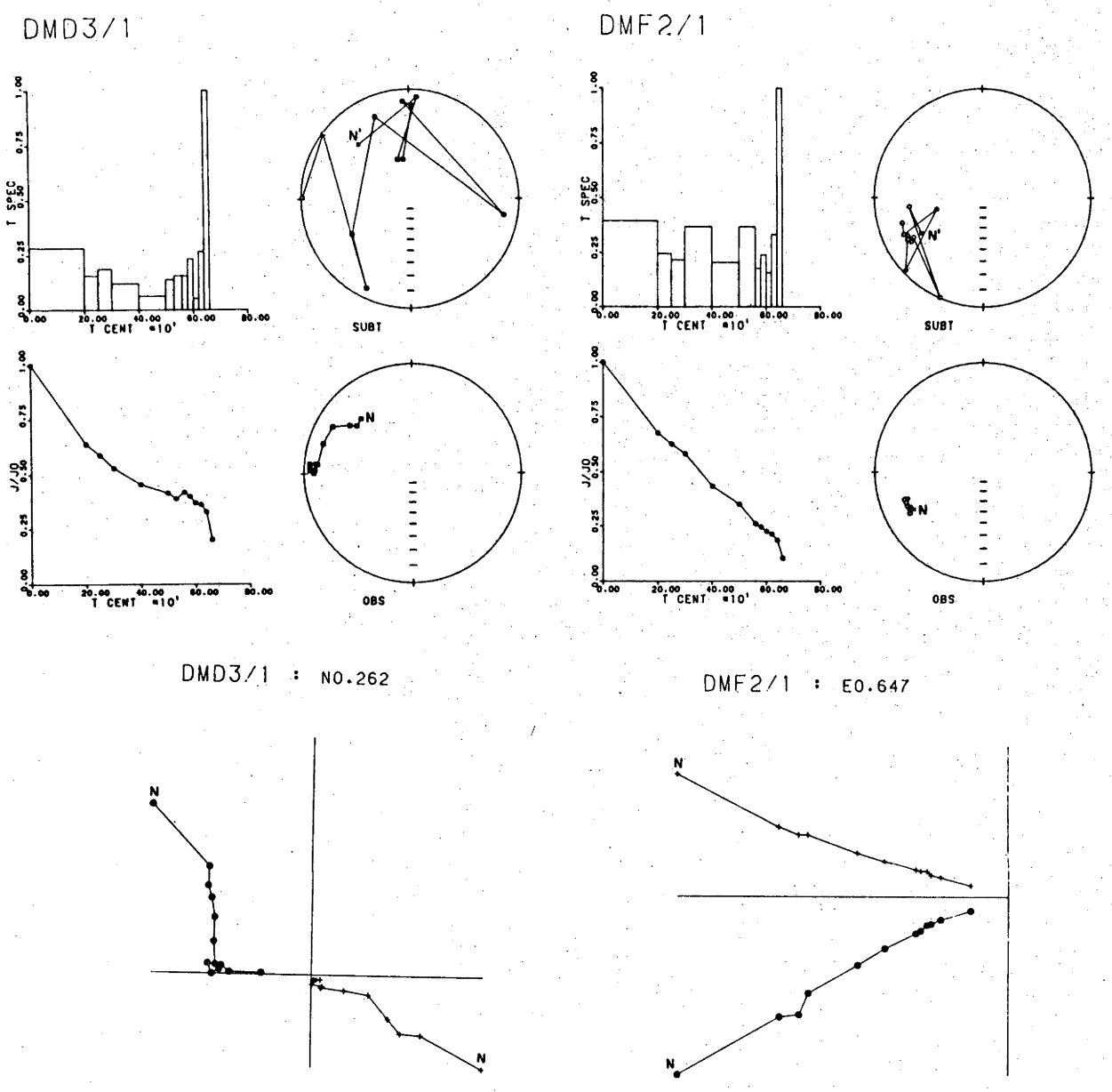

Figure 4.9 : Thermal demagnetization, Mulden Group.

TABLE 4.3 (A)

MULDEN GROUP : Site mean directions before and after thermal demagnetization

	NRM				After thermal demagnetization							
SITE	N	R	D	I	N	R	D	I	T°C	D'	I'	MAGNETIZATION
DMA	4	3.994	086	-70	4	3.971	093	-55	580	107	-41	N3
DMB	4	3.865	317	-64	4	3.845	286	-34	580	275	-38	DM
DMC	4	3.998	280	-01	4	3.989	275	-11	580	262	-28	DM
DMD	4	3.557	149	17	4	3.604	125	05	580	124	23	DM
DME	4	3.921	236	16	4	3.963	270	-11	620	267	-34	DM
DMF	4	3.689	076	-05	4	3.893	076	03	620	074	33	DM
DMG	4	3.844	135	15	4	3.838	129	14	620	126	36	DM
DMH	4	3.983	163	-30	4	3.984	241	-61	620	213	-31	?

TABLE 4.3 (B)

MULDEN GROUP : Mean direction and palaeomagnetic pole after thermal demagnetization (Sites DMB-DMG)

	Before structural correction									After structural correction						
							pole							pole		
	N	n	R		D_m	I_m	lat	long	dp,dm	R		D_m'	I_m'	lat	long	dp,dm
DM	6	24	5.600	12.5	283	-14	15N	283E	10,20	5.715	17.6	278	-34	13N	270E	11,19

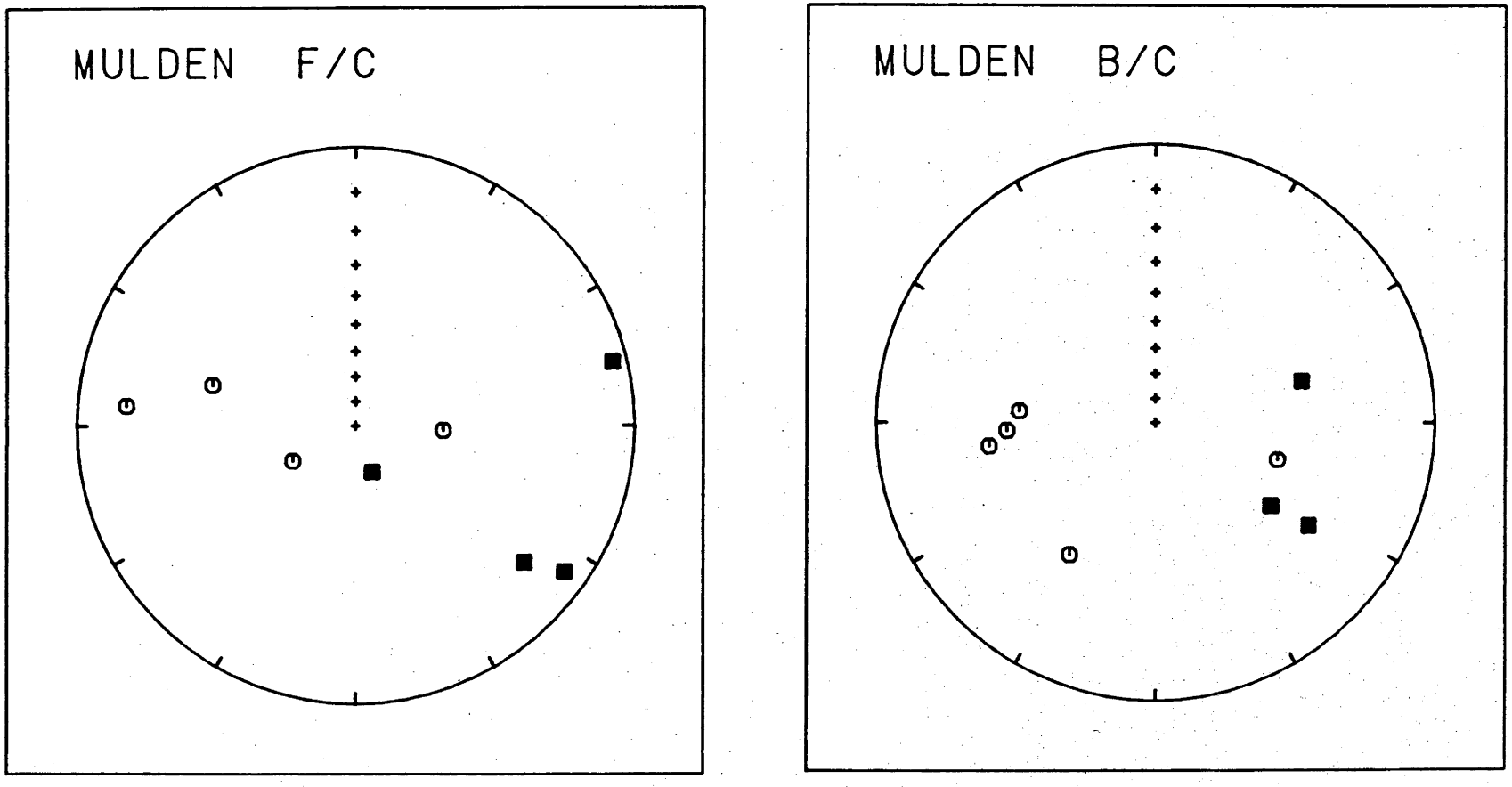

Figure 4.10 : Cleaned site mean magnetization directions, Mulden Group; equal-angle projection. Open (closed) symbols refer to negative (positive) inclination.

(k'/k=1.41, 95% significance point = 2.98). Although the vectors substracted during the early demagnetization steps were generally well grouped within each site, the mean site subtracted vectors were widely scattered and random at the 95% confidence level. No systematic overprint direction could be isolated.

Magnetization vectors at two other sites (DMA and DMH) reached stable endpoints during pilot demagnetization, however these directions were widely displaced from the DM direction and from each other. After bulk thermal treatment, site DMA had a mean direction (093,-55) very much like the N3 (?) secondary component observed in the Nama sediments. The VGP calculated from the cleaned DMA site mean direction is essentially identical to the N3 pole (Figure 4.18). As is discussed later in this chapter, a widespread early Cambrian or late Precambrian thermal event may have produced the N3-type overprinting. The DMA mean direction is tentatively grouped with the other N3 magnetization directions.

The cleaned DMH site mean direction is unlike any magnetization observed in Damara or Nama rocks, and is also unlike a younger Phanerozoic magnetization. No explanation is obvious, and the direction remains problematic.

§4.3.4 Tsumeb Subgroup : Chuos Formation, Maieberg Formation

Massive iron rich mixtites and glacial marine sediments of the Chuos Formation and Maieberg Formation outcrop in central and northern Namibia (Kröner and Rankama, 1973). Typically the boulder beds consist of a wide variety of striated and facetted clasts ranging in size from grit to 2.5 m in diameter, set in an argillaceous matrix. Some laminated shale bands are

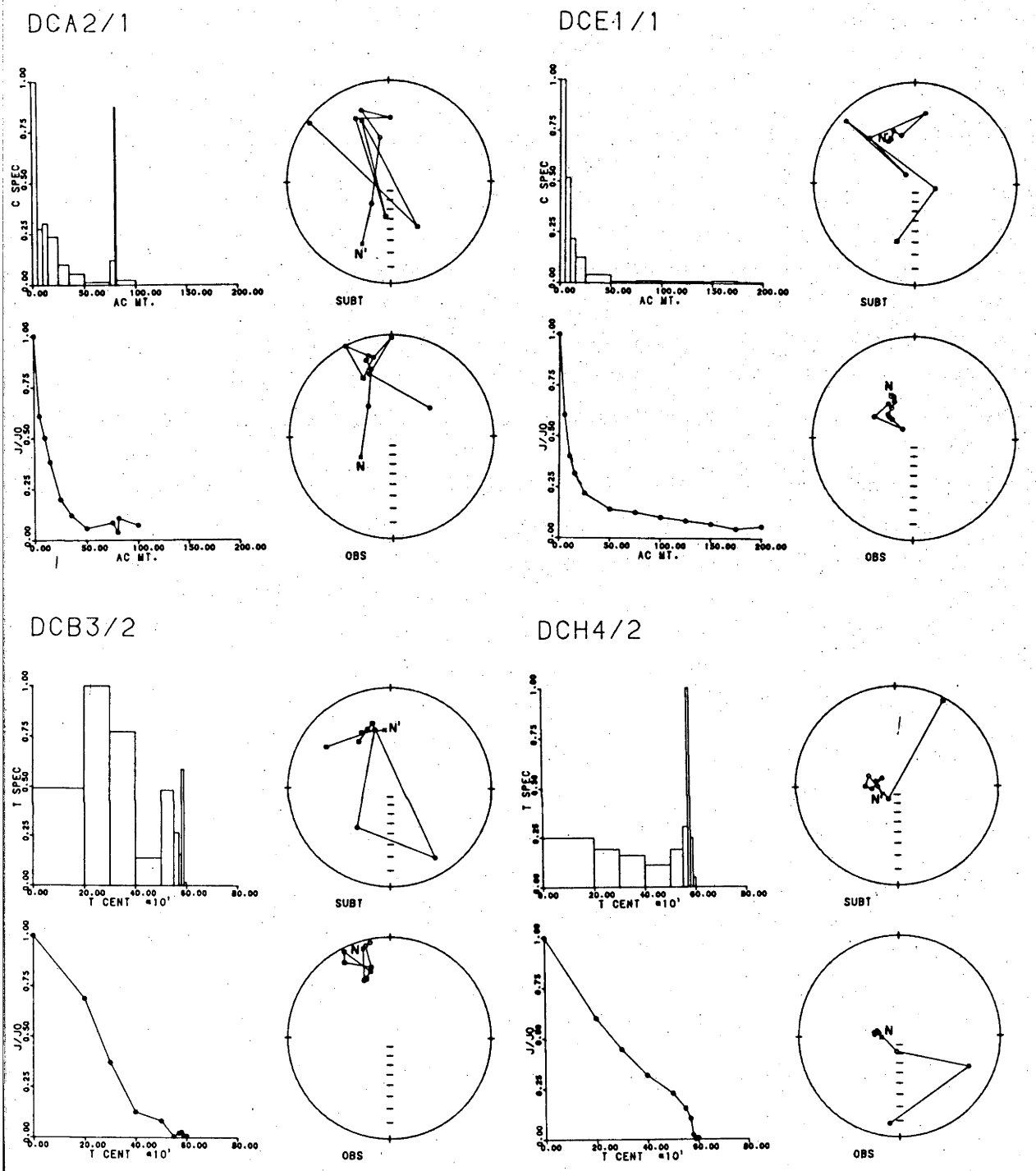

Figure 4.11(A) : Thermal and AF demagnetization, Chuos Formation (Tsumeb Subgroup).

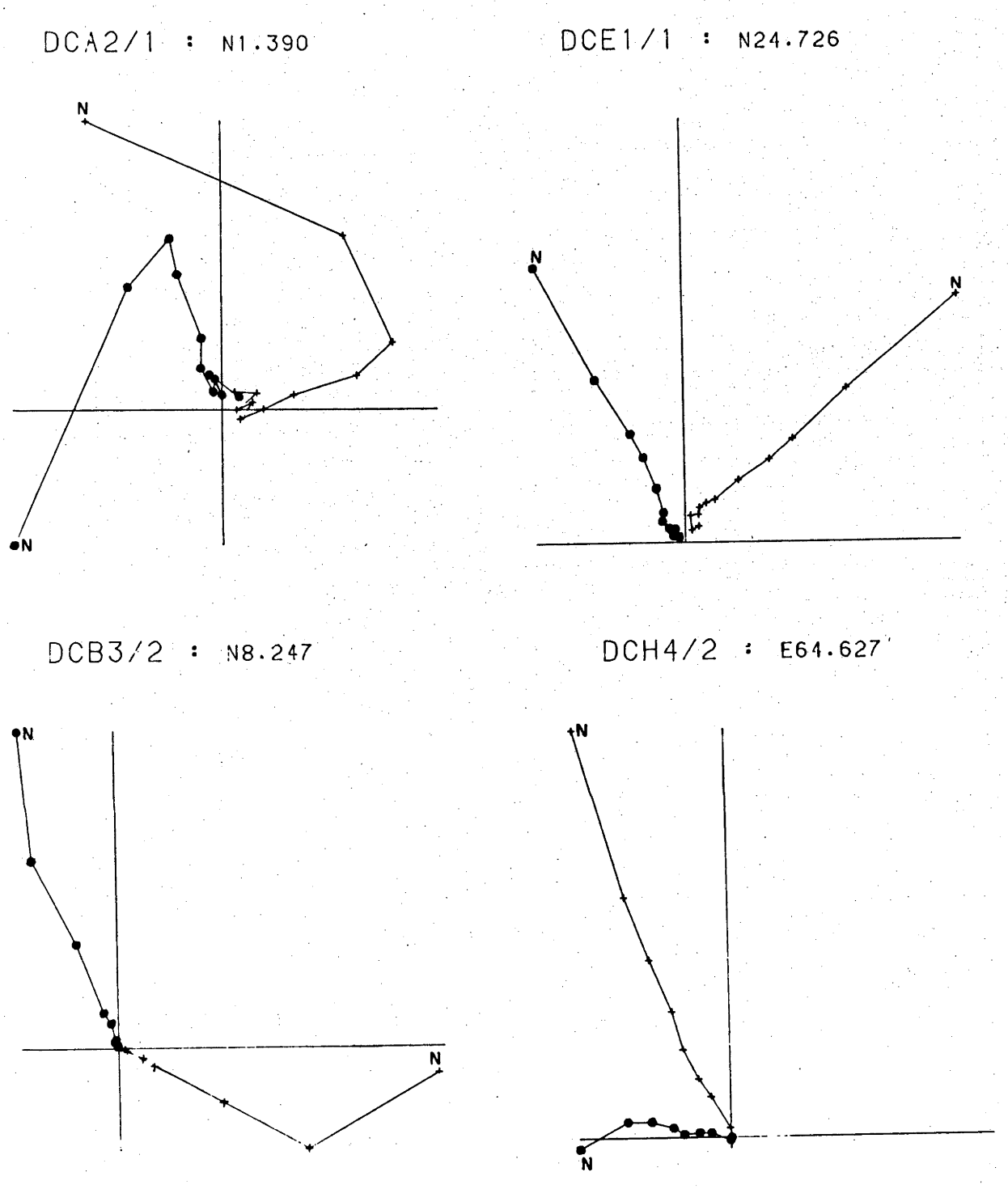

Figure 4.11(B) : Thermal and AF demagnetization, Chuos Formation (Tsumeb Subgroup, continued).

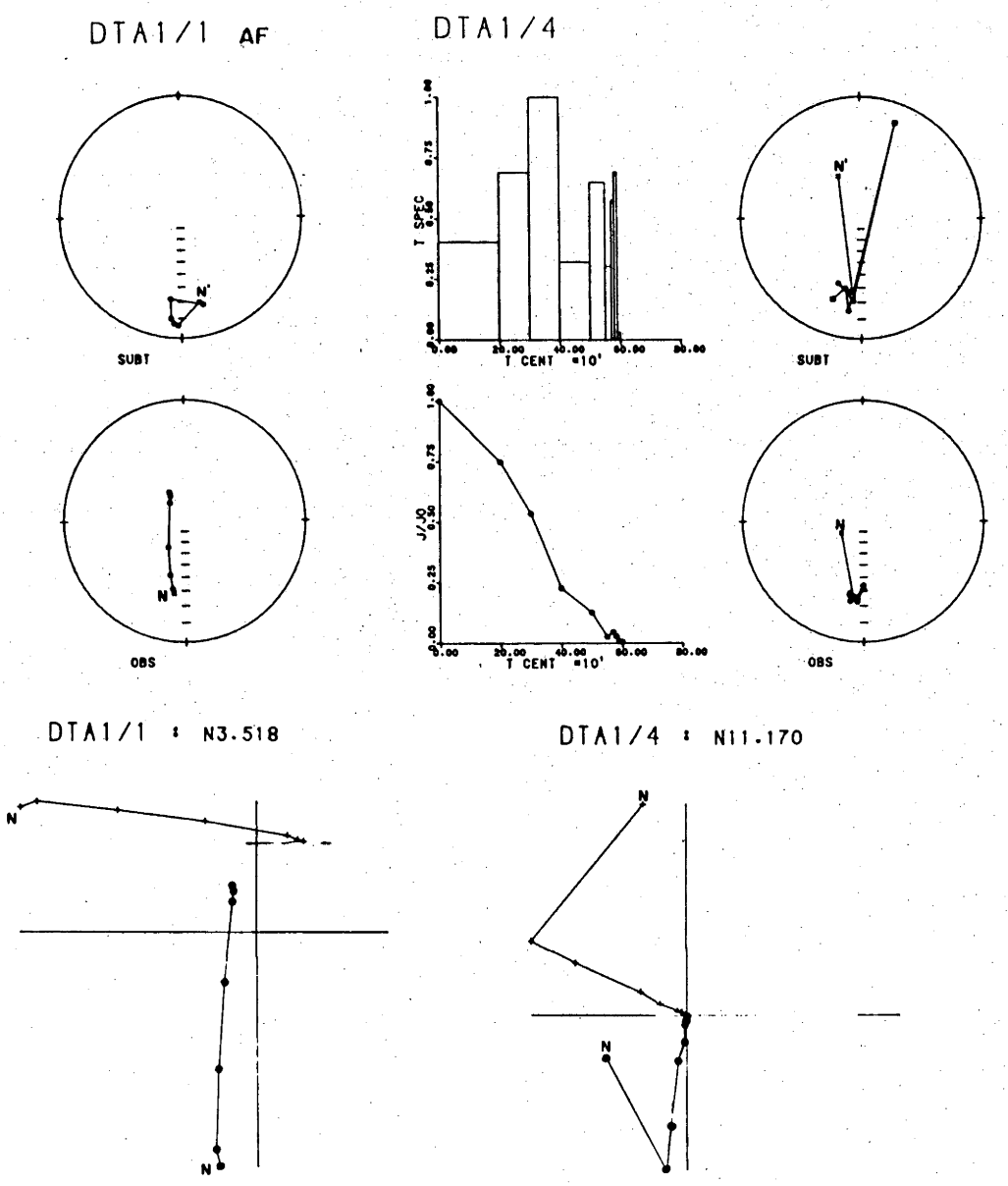

Figure 4.12 : Thermal and AF demagnetization, Maieberg Limestone (Tsumeb Subgroup).

present; in places the mixtites are overlain by calcic sediments. No striated pavements have been found underlying the Chuos Formation. In many areas, the mixtites and associated sediments have been strongly metamorphosed, so much so that the rock has been described as a "pebbly schist".

Samples of the Chuos mixtite and of an overlying gritty limestone of the Maieberg Formation were taken at 8 sites in northern Namibia (Figure 4.1). The rocks have a definite cleavage although the metamorphic grade appears to be low. The age of metamorphism of the Chuos Formation in the sampling region appears to be approximately 640-630 my (Kröner, unpublished results).

Pilot AF and thermal demagnetization revealed several distinctly different magnetizations (Figure 4.12). During AF demagnetization, the Chuos specimens exhibited stable northwest trending directions with negative inclinations in the 15-50 mT range after (in some cases) removal of a significant low H_c component. The Maieberg limestone samples also showed similar endpoints during AF demagnetization, however examination of orthogonal vector plots (Figure 4.12) showed clearly that a second magnetization with a higher H_c is present. Upon thermal demagnetization, this high H_c component is seen to have a very low T_b and is completely removed in the initial heating steps. After removal of the low T_b component, the magnetization vector is seen to converge upon the origin. In the Chuos samples however the T_b of both components are similar and resolution of both components is difficult. Three magnetizations have been identified and have been labelled the DC1, DC2 and DC3 components (Table 4.4):

TABLE 4.4 (A)

CHUOS TILLITE, MAIEBERG FORMATION : Site mean directions before and after thermal and AF demagnetization

		NRM				After demagnetization							
MAGNETIZATION	SITE	N	R	D	I	N	R	D	I	AF, T°C	D'	I'	RANGE; AF,T°C
DC1	DCA	4	3.552	312	-77	3	2.927	305	33	420°	316	42	
	DCB	4	3.951	335	-05	4	3.989	323	26	400°	333	30	
	DTA	4	3.124	193	-17	4	3.923	188	-14	400°	198	-18	
	DTB	4	3.988	360	-83	4	3.938	141	-64	500°	202	-32	
DC2	DCC	4	3.813	315	-21	2	1.988	337	-36	25	323	-34	
	DCD	4	3.882	250	-82	2	1.995	064	-60	100	061	-76	
	DCE	4	3.544	141	-39	2	1.999	311	-53	125	283	-27	
	DCF	4	3.919	118	47	4	3.757	109	59	560°	113	33	
	DCG	4	3.991	110	-69	4	3.959	313	-71	560°	261	-36	
	DCH	4	3.976	095	-79	4	3.830	193	-83	560°	229	-26	
DC3	DCA					2	1.947	359	-63		325	-63	10-35 mT
(subtracted	DCB					2	1.988	349	-35		336	-36	10-35 mT
directions from	DTA					2	1.970	336	-57		322	-36	200-400°C
DC1 vectors)	DTB					2	1.999	328	-83		243	-35	200-400°C

TABLE 4.4 (B)

CHUOS TILLITE, MAIEBERG FORMATION :

							pole						pole		
MAGNETIZATION	N	n	R	k	D_m	I_m	lat	long	dp,dm	R	k	D_m'	I_m'	lat	long	dp,dm
DC1	4	15	2.869	2.7	331	07	54S	139E	36,71	3.620	7.9	354	34	52S	185E	23,40
DC2	6	18	5.412	8.5	327	-69	48S	044E	35,41	4.957	4.8	280	-46	17S	080E	28,44
DC3	4	8	3.816	16.3	344	-60	64S	042E	27,35	3.488	5.9	307	-49	41S	080E	36,55
DC2+DC3	10	26	9.180	11.0	335	-65	55S	044E	20,25	8.338	5.4	291	-48	27S	080E	19,30

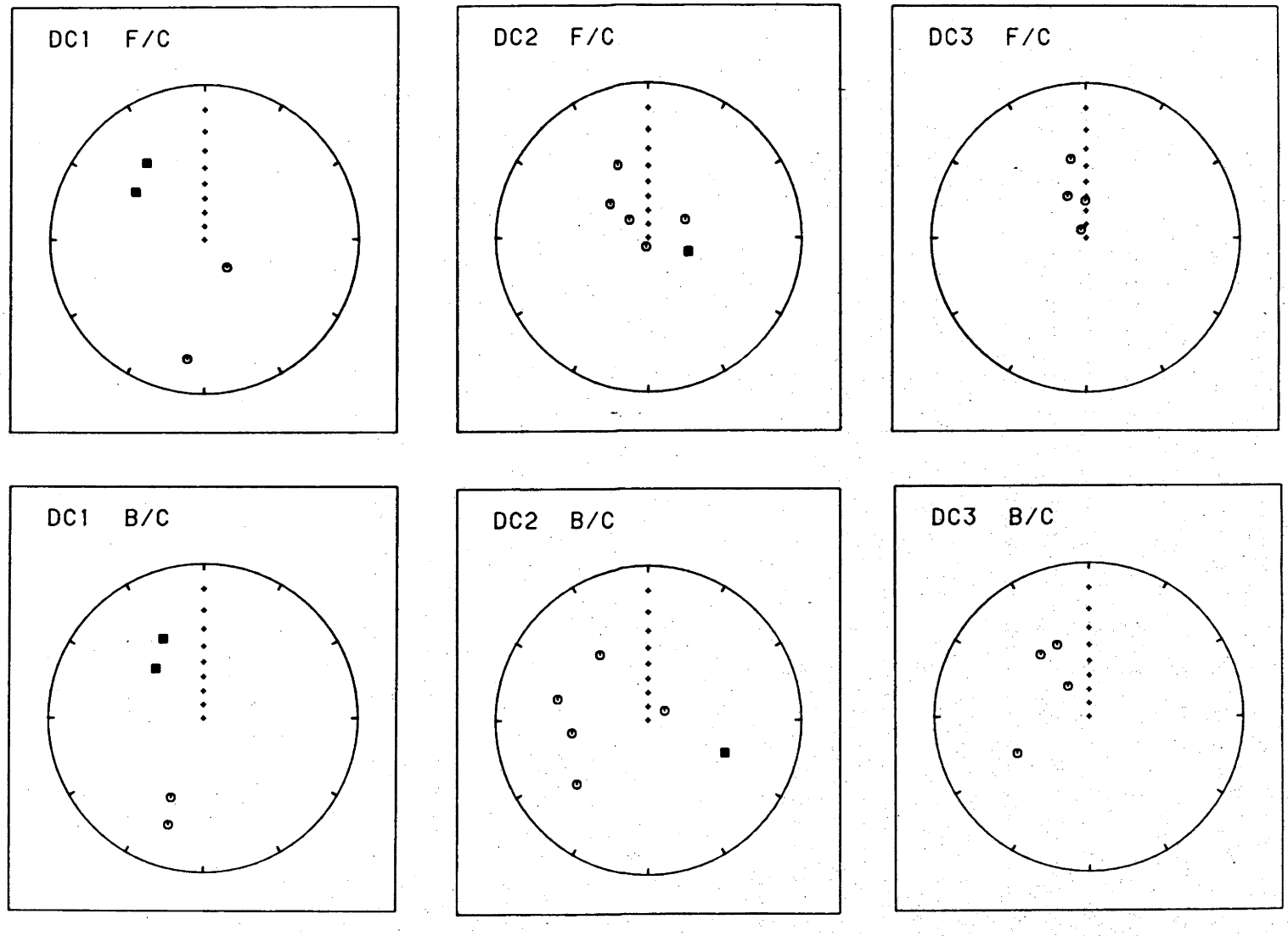

Figure 4.13 : Cleaned site mean magnetization directions, Tsumeb Subgroup DC1, DC2 and DC3 components; equal-angle projection. Open (closed) symbols refer to negative (positive) inclination.

DC1: This shallow northwesterly (southeasterly) component was directly observed in 15 samples at four sites and only after thermal demagnetization. In the case of the Chuos Formation sites (DCA,DCB) significant (?) secondary magnetizations were present which had similar H_c but low T_b compared to the (?) primary magnetization, rendering isolation by AF demagnetization difficult but not impossible. During thermal demagnetization, these secondary components were completely removed and directions converged upon the DC1 direction. Blocking temperatures of the DC1 magnetization were generally in the 500°-570° range. A high degree of scatter is apparent in the uncorrected final mean direction, which is essentially random at the 95% confidence level. Upon structural correction, a very pronounced increase in precision is realized (k'/k=2.93, 95% significance point - 3.79). Although not significant at the 95% confidence level, the increase in precision is in fact significant if samples, rather than sites are given unit weighting in the mean direction, suggesting that the DC1 magnetization was acquired before the (?) Katangan folding and metamorphism.

DC2: The majority of samples (6 sites) exhibited this magnetization, whether during AF or thermal demagnetization. The DC2 component is characterized by a northwesterly (southeasterly) steep negative (positive) magnetization vector and generally has a high H_c and T_b's in the 570°-580° range. The sites directly exhibiting this component are reasonably well grouped; precision of the DC2 component decreases upon structural correction, although again the

change is not significant (k'/k=0.56, 95% significance point ≅ 0.34).

DC3: This is the component removed from the DC1 sites in the early (low peak AF and T) demagnetization steps. In the Chuos sites, the DC3 magnetization has a slightly lower H_c than the DC1 magnetization and is preferentially removed from some specimens in the 10-35 mT range. The DC3 component in the Maieberg sites has a much higher H_c but lower T_b than DC1 and is removed in the 200°-400° heating steps. The DC3 component also suffers a marked decrease in precision upon structural correction (k'/k=0.36, 95% significance point ≅ 0.26).

A comparison of the DC2 and DC3 mean directions by an F-ratio test indicates that they are not significantly different at the 95% level:

N	R_1	R_2	R	$F_{2,2(N-1)}$	95% significance point
10	5.4112	3.816	9.180	0.50	3.55

A fold test on the combined DC2 and DC3 magnetizations is negative and very nearly significant at the 95% confidence level (k'/k=0.49, 95% significance point = 0.45), strongly suggesting that the DC2 and DC3 magnetizations were acquired after folding occurred.

§4.3.5 Nosib Group : Blaubeker Formation

The Blaubeker Formation is one of the uppermost units in the Nosib Group and outcrops along the southern margin of the Nosib-Damara Geosyncline (Figure 4.1). It unconformably

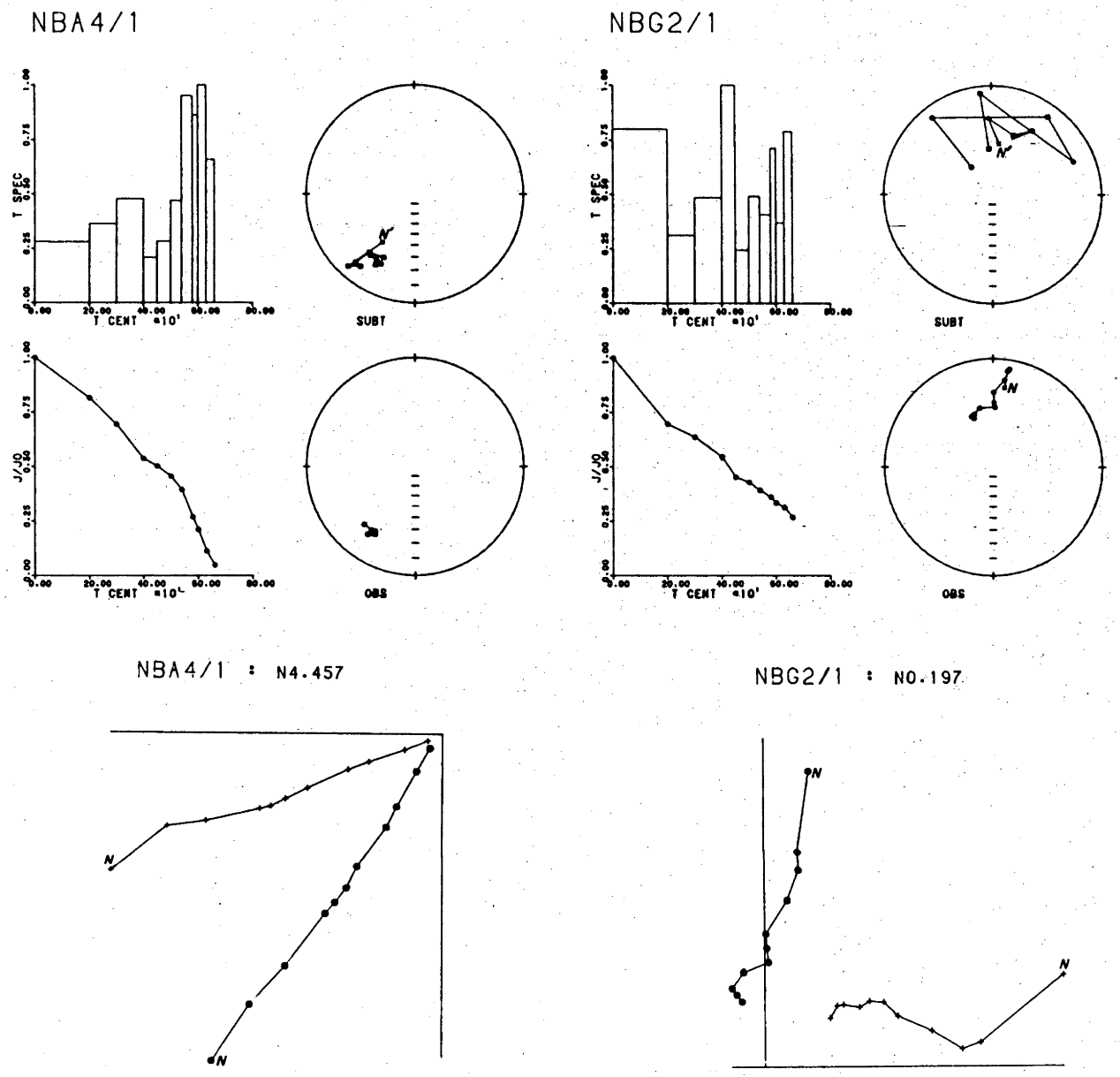

Figure 4.14 : Thermal demagnetization, Blaubeker Formation (Nosib Group).

TABLE 4.5 (A)

BLAUBEKER FORMATION : Site mean directions before and after thermal demagnetization

	NRM				After thermal demagnetization						
SITE	N	R	D	I	N	R	D	I	T°C	D'	I'
NBA	4	2.829	197	-03	3	2.688	208	14	600	211	09
NBB	4	3.828	019	-26			(random)				
NBC	4	3.637	008	-48	3	2.960	191	31	650	200	33
NBD	4	3.889	326	-71	3	2.883	079	-08	650	087	-13
NBE	4	2.470	056	-51	4	3.356	349	31	650	342	33
NBF	3	2.755	325	-30	3	2.858	341	10	500	344	-24
NBG	3	2.813	357	05	2	1.973	036	41	500	055	45
NBH	4	3.648	043	-45	4	3.606	344	29	650	341	17

TABLE 4.5 (B)

BLAUBEKER FORMATION :

						pole							pole		
N	n	R	k	D_m	I_m	lat	long	dp,dm	R	k	D_m'	I_m'	lat	long	dp,dm
6	19	5.049	5.3	004	12	60S	204E	16,33	4.674	3.8	007	05	63S	212E	20,40

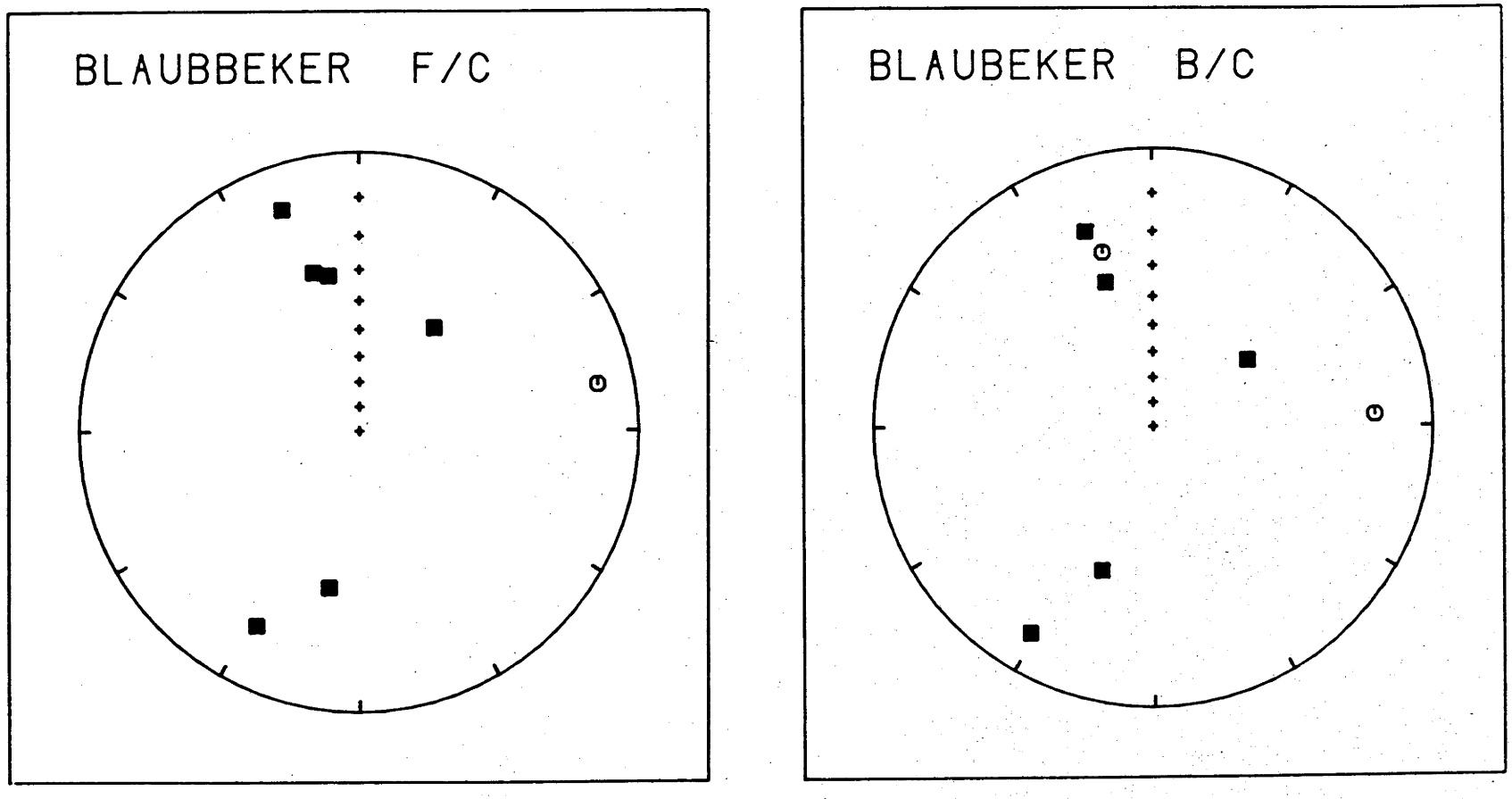

Figure 4.15 : Cleaned site mean magnetization directions, Blaubeker Formation (Nosib Group); equal-angle projection. Open (closed) symbols refer to negative (positive) inclination.

overlies lower Nosib Group rocks and is in turn unconformably overlain by Nama Group sediments (Figure 4.2). Kröner and Rankama (1973) cite evidence in support of a glaciogenic origin for parts of the Blaubeker Formation. Kröner (1977b) has correlated the Blaubeker Formation with the Stinkfontein and Kapok (?) glacial beds in the lower Gariep Group.

Samples of red quartzites from the lower Blaubeker Formation were collected at 8 sites in central Namibia (Figure 4.1). A low grade metamorphism is apparent in the rocks, which show signs of incipient cleavage. The metamorphism could be a result of either the Katangan or Damaran episode of the Pan-African orogeny. Radiometric ages in the immediate area have a simple mean value 484±34 (±1s.d. : Rb/Sr, K/Ar and U/Pb ages of Clifford, 1967; Burger and Coertze, 1973; Kröner and Hawkesworth, 1977), suggesting that the Damaran episode might have been the most recent significant heating event.

NRM site mean directions were loosely grouped with a northerly, shallow negative trend. During thermal demagnetization, specimens from most sites exhibited rather poor directional stability, but at high temperatures tended to group around a direction with a shallow to moderate positive (negative) inclination and northerly (southerly) declination. Apart from PEF components subtracted during demagnetization, this was the only consistently observed magnetization. Temperatures for bulk thermal treatment of remaining specimens were chosen by examination of stability ranges of individual pilot specimens; these ranged from 500° to 650°. The final cleaned direction (after omission of one random site mean direction) has a rather low precision. Upon structural correction however, the already low precision markedly decreases,

suggesting a post folding magnetization age. As discussed in §4.4, the pole position calculated from the uncorrected mean direction from the Blaubeker Formation is near other Cambro-Ordovician poles, which suggests that magnetization age of 485 my might possibly be correct. Alternatively, the post folding magnetization of the Blaubeker Formation could date from Katangan times, as the NB pole position is not unlike 650-630 my poles (Figure 4.18).

§4.3.6 Nosib Group - lower quartzites, sandstones

Quartzites and sandstones of the lower Nosib Group were collected at seven sites in northern Namibia (Figure 4.1). These samples are probable stratigraphic equivalents of the Chela Group of southern Angola and are thought to have been deposited approximately in the 900-1000 my range. It was originally hoped that a comparison of palaeomagnetic results from Nosib rocks of the northern (these samples) and southern (Blaubeker) parts of the Nosib-Damara Geosyncline would facilitate a test of plate collision in the Damara Mobile Belt using direct stratigraphic equivalents in the Damara Supergroup. As described in the previous section, the Blaubeker results appear to be of a post folding age, and thus the direct test was not possible. Indirect tests are still possible, and the problem is discussed in more detail in §4.4.

As with the other Damara Supergroup rocks of central and northern Namibia, there exists the possibility that these rocks have been subjected to low grade metamorphism. In this case, although the quartzites and sandstones show no outward metamorphic effects, the palaeomagnetic results suggest (possibly multiple) low temperature metamorphic overprinting.

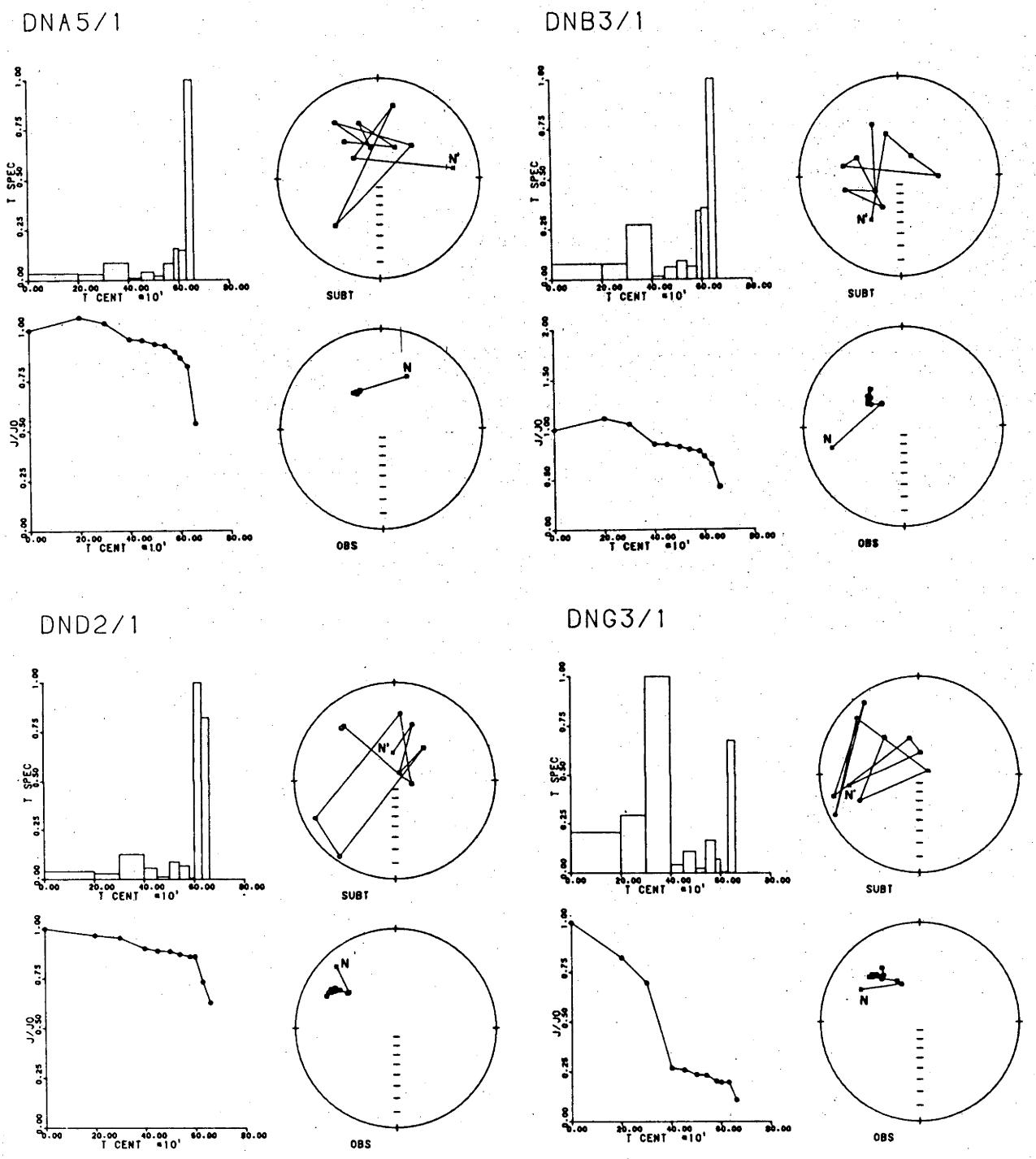

Figure 4.16(A) : Thermal demagnetization, Nosib Group Quartzites.

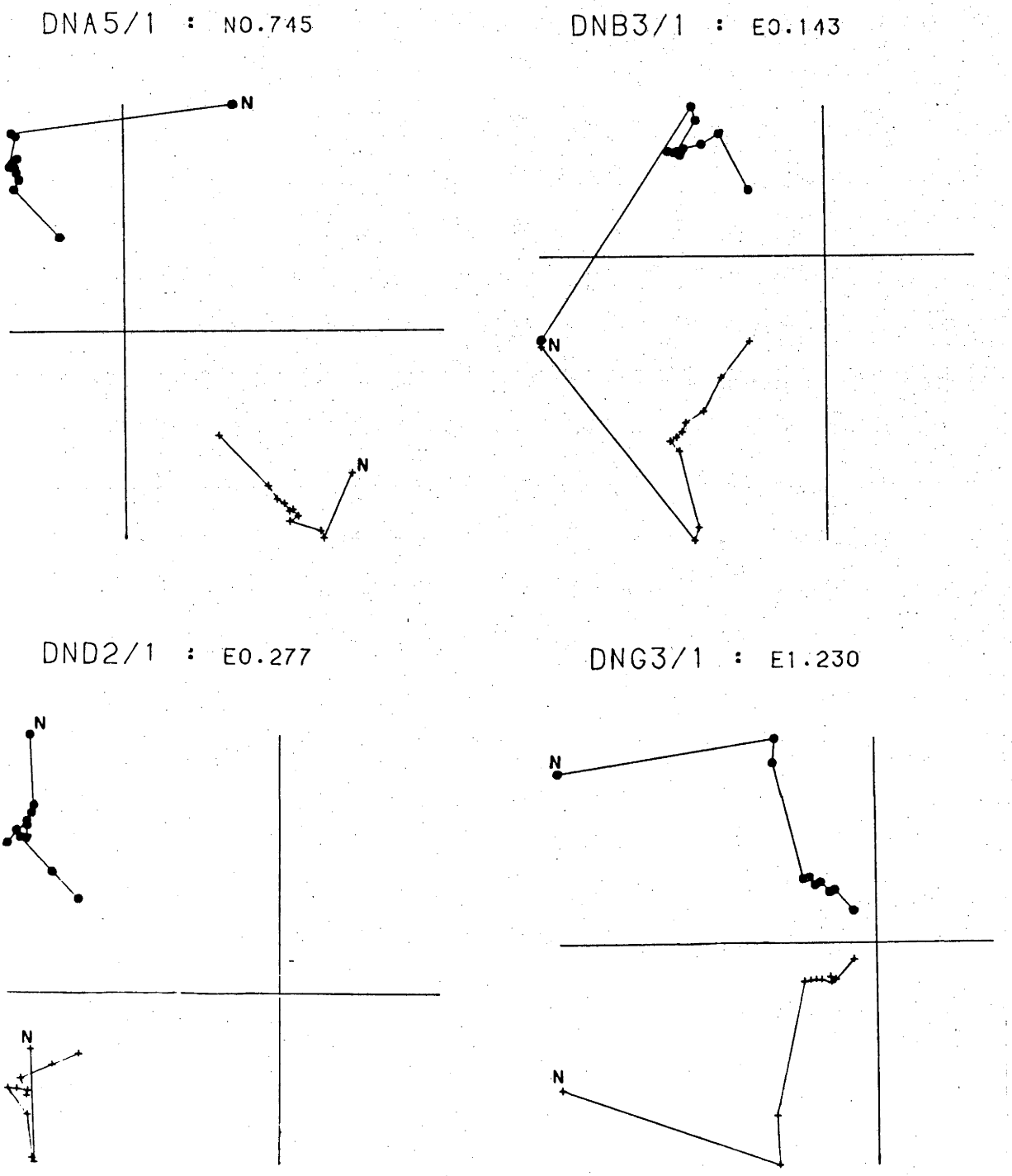

Figure 4.16(B) : Thermal demagnetization, Nosib Group Quartzites (continued).

TABLE 4.6 (A)

NOSIB GROUP : Site mean directions before and after thermal demagnetization

		NRM				After thermal demagnetization							
MAGNETIZATION	SITE	N	R	D	I	N	R	S	I	T°C	D'	I	T RANGE, °C
	DNA	5	4.691	047	25	5	4.868	330	43	500	337	43	
	DNB	4	3.947	263	07	4	3.743	324	34	500	327	35	
	DNC	4	3.965	100	01	4	3.969	320	39	500	307	44	
NQ1	DND	4	3.661	328	03	4	3.972	293	22	500	289	27	
	DNE	4	3.984	293	-04	4	3.961	264	30	350	289	52	
	DNF	4	3.983	136	-58	4	3.981	137	-53	500	201	-24	
	DNG	4	3.975	306	18	4	3.928	318	18	500	320	32	
	DNA					5	4.833	006	29		009	25	300-450
	DNB					4	3.857	019	33		021	29	300-450
NQ2	DNC					4	3.735	017	10		016	25	300-500
(substracted	DND					3	2.966	359	41		001	52	200-500
directions from	DNE					4	3.971	342	50		005	27	200-350
NQ1 vectors)	DNG					4	3.985	352	51		009	59	300-450

TABLE 4.6 (B)

NOSIB GROUP : Mean directions and palaeomagnetic poles after thermal demagnetization

	Before structural correction									After structural correction					
							pole						pole		
MAGNETIZATION	N	n	R		D_m	I_m	lat	long	dp,dm	R		D_m'	I_m'	lat	long	dp,dm
NQ1	6	25	5.597	12.4	308	33	27N	317E	13,23	5.761	20.9	312	40	28N	323E	11,18
NQ2	6	24	5.727	18.3	004	36	52S	200E	11,19	5.799	24.9	011	36	51S	211E	09,16
NQ2+DNF	7	28	6.557	13.5	359	40	49S	193E	12,21	6.770	26.1	012	35	51S	213E	08,14
NQ3	3	13	2.705	6.8	104	-05	13N	291E	26,52	2.826	11.5	103	-12	10N	294E	20,39
NQ3*	-	13	11.473	7.9	102	-07	10N	292E	08,16	11.925	11.2	102	-13	09N	295E	07,13

*unit weight to samples

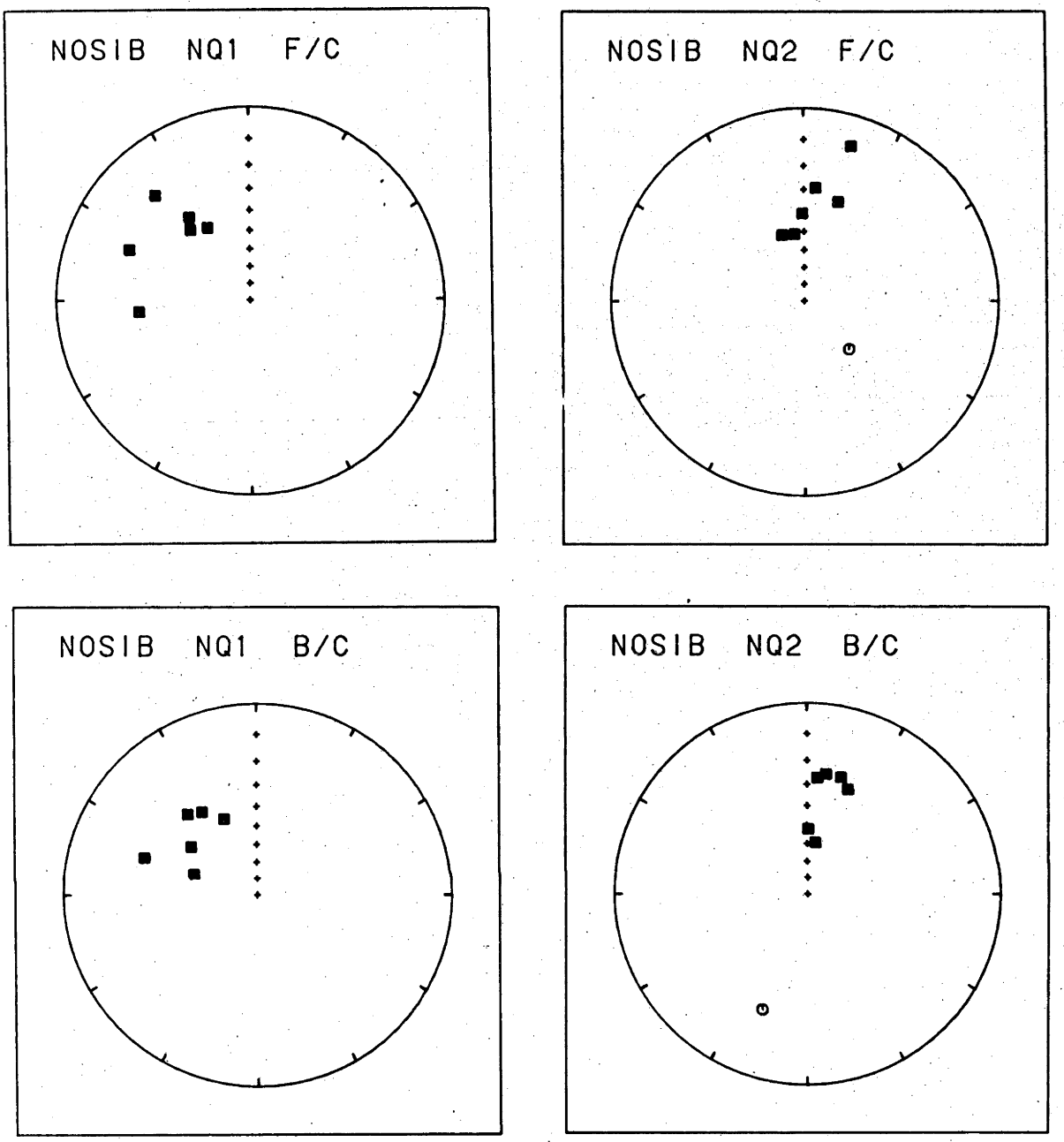

Figure 17 : Cleaned site mean magnetization directions, Nosib Group Quartzites NQ1 and NQ2 components; equal-angle projection. Open (closed) symbols refer to negative (positive) inclination.

The NRM site mean directions are scattered but have a roughly defined east-west trend. In the initial 20°-200° thermal demagnetization step, a large component (the NQ3 component) with a very shallow inclination and easterly (westerly) declination was removed from 13 samples at 3 sites. In the higher 300°-450° range, an intermediate magnetization with a northerly declination and moderate positive inclination was consistently removed from the majority of the samples. Twenty-four samples from 6 sites exhibited this subtracted vector, called here the NQ2 component. Mean directions from these same 6 sites became directionally stable at somewhat higher temperatures, converging to a northeasterly direction with a moderate positive inclination. This final high T_b magnetization is called the NQ1 component. Resolution of the various components by AF demagnetization was not possible due to overlapping H_c spectra although in many cases it was possible to isolate the final high T_b NQ1 magnetization. The remaining site (DNF) exhibited a very stable magnetization which was quite different in direction to the NQ1 magnetization, but was reversed with respect to the NQ2 magnetization.

The precision of each of the NQ1, NQ2 and NQ3 magnetizations markedly increases upon structural correction, though none of the improvements are significant at the 95% confidence level:

Magnetization	k'/k	95% significance point
NQ1	1.69	2.98
NQ2	1.36	2.98
NQ2+DNF	1.93	2.69
NQ3(sites)	1.69	6.39
NQ3(samples)	1.42	1.98

There is therefore the suggestion that each of the magnetizations was acquired before folding of the rocks occurred. However, the fold test information cannot be employed to infer the relative age sequence. Assuming again the simple blocking temperature-age model (which is probably quite realistic in the case of purely thermal effects in a polymetamorphic terrane), the preferred magnetization sequence in order of decreasing age would be NQ1,→NQ2→NQ3. As discussed in the next section this simple picture fits the available data quite well.

§4.4 Summary and tectonic implications of the late Precambrian palaeomagnetism of Africa

All published palaeomagnetic results from Africa in approximately the 1100 my to Ordovician interval are listed in Table 4.7 and plotted in three parts in Figure 4.18. Results from the Congo craton are plotted as open circles, closed circles are poles from the Kalahari craton. Solid triangles represent poles from northern Africa (mainly from Morocco but one result, SR, is from Sudan). A cross represents the only result available from Arabia in this interval. The pole from the Ntonya ring structure is plotted as a diamond; the sampling site for this pole lies in the Pan-African Mozambique belt and thus cannot be definitively assigned to either the Congo or Kalahari cratons. A single apparent polar wander path can be constructed which incorporates all of the available palaeomagnetic results in this interval, irrespective of the craton from which the data are derived, without violating any of the age constraints, as discussed below:

<u>1100-700 my</u> - Palaeomagnetic data in this interval come from the Congo and Kalahari cratons only. This APWP segment is

essentially identical to that presented in McElhinny and McWilliams (1977) except that the polarity with respect to Cambro-Ordovician data has been reversed. At about 1050 my there is good agreement between Kalahari poles AU and OK and Congo poles CG, NQ1 and KS. A minimum age of 930 my is suggested for the Kisii lavas (KS), however the magnetization age is somewhat uncertain. More recent $^{40}Ar/^{39}Ar$ dating of the Kisii lavas has indicated an age of about 1200 my (Charlton, 1973), thus pole KS could be part of an older APWP segment. With or without pole KS, palaeomagnetic results on both sides of the Damara Mobile Belt are in agreement at about 1050-1000 my.

Somewhat later at about 900 my, the pole from the Klein Karas dykes (KK) in the Kalahari craton is in reasonably good agreement with Congo craton poles of a similar age from the Bukoban System, although the KK error ellipse is rather large. The younger pole path is defined only by results from the Congo craton to about 700 my.

800-600 my - The first phase (the Katangan episode) of the Pan-African orogeny occurs in this interval. A more complicated APWP than that of McElhinny and McWilliams (1977) is required to fit the data in the correct order. The complication arises from the similarity of the 650-630 my APWP segment with the Cambro-Ordovician segment, and from difficulty in deciding whether the various overprint components result from the Katangan episode (and thus should be incorporated in this segment) or the Damaran episode (and therefore should be incorporated in the 600 my - Ordovician segment).

At about 750-650 my, pole positions from the Mbozi complex and Lower Buanji Group of the Congo craton (MBZ and LBG) are in agreement with the Kalahari PND pole from the

TABLE 4.7 (A)

African Palaeomagnetic Poles, *ca.* 1100-500 my

Symbol	Rock Unit	Probable Magnetization Age	Pole Position	dp,dm	Reference
PWD	Post Waterberg dolerites	1115	65S 231E	04,08	McElhinny (1966)
UDL	Umkondo dolerites and lavas	1140	63S 207E	04,08	Jones and McElhinny (1966)
AU	Auborous Formation	<1250	43S 174E	07,13	Piper (1975b)
KIS	Kisii Series	?960	06S 168E	12,16	Brock *et al.* (1972)
OK	O'okiep intrusives	1070±20	16S 186E	13,19	Piper, (1975b)
CG	Chela Group	1050-1100	30S 184E	13,20	Reid (in Kröner, 1975)
NQ1	Nosib Group		28S 143E	11,18	this study
BS	Bukoba Sandstone	<1200,>1000	40S 137E	11,21	Piper (1972)
AS	Abercorn Sandstone	≥940±40	49S 120E	08,16	Piper (1975a)
IG	Ikorongo Group		35S 084E	19,27	Piper (1975a)
KK	Klein Karas dykes	878±41	20S 114E	18,35	Piper (1975b)
KF	Kigonero Flags	>GL	12S 093E	22,35	Piper (1972)
MD	Mbala dolerites	<AS	09N 100E	13,22	Piper (1975a)
MS	Malagarasi Sandstone	>GL,<BS	07N 112E	13,26	Piper (1972)
BD	Bukoban dolerites	806±30,<BS	11N 101E	12,22	Piper (1972)
GL	Gagwe lavas	813±30,<BS,MS,KF	29N 103E	08,14	Piper (1972)
MR	Manyovu redbeds	<813±30,<BS,MS,KF	24N 118E	20,40	Piper (1972)
MBZ	Mbozi complex	743±30	72N 068E	09,19	Piper (1975a)
LBG	Lower Buanji Group		87N 263E	05,09	Piper (1975a)
PND	Pre-Nama dykes	653±70	85N 228E	21,30	Piper (1975b)
DC1	Chuos/Maieberg Formation		52N 005E	23,40	this study
NTR	Ntonya Ring Structure	630±24	27N 345E	01,02	Briden (1968)
NB	Nosib Group, Blaubeker Formation	<NQ1	60N 024E	16,33	this study
NQ2	Nosib Group	<NQ1	51N 033E	08,14	this study
N1	Lower Nama Group	630-640	62N 061E	06,13	this study
SR	Sabaloka Ring Structure	<540	83N 339E	08,15	Briden (1973)
DC2,3	Chuos/Maieberg Formation	<DC1	55N 224E	20,25	this study
OUV	Ourzazate Volcanics	578±15	30N 237E	17*	Hailwood (1972)
AT	Amouslek Tuffs	?Є	41N 250E	10*	Hailwood (1972)
N2	Upper Nama Group	Pc/Є,<N1	05N 271E	09,16	this study
DM	Mulden Group	590-570	13N 270E	11,19	this study
NQ3	Nosib Group	<NQ1	09N 295E	07,13	this study
N3	Nama Group	<N2,N1	07S 337E	13,16	this study
SJ	Sijarira Group	Pc/Є	02N 352E	26,30	Reid (1968)
KLH	Klipheuval Formation	Pc/Є	16N 316E	03,05	Creer (1973)
HI	Hook Intrusives	500±17	14N 336E	29,43	Brock (1967)
JRB	Jordanian redbeds	Є(?Є-O)	37N 323E	07,10	Burek (1969)
ML	Moroccan lavas	?Єm	53N 034E	-	Helsley (1965)
TLI	Tassili sediments	Є-O	53N 026E	-	Ileana (1971)
HMS	Hasi-Messaud sediments	Є-O	53N 026E	05,06	Bucur (1971)
TM	Table Mountain Series	O	50N 349E	03,05	Graham and Hales (1961)
AAR	Anti-Atlas rocks	532±18	47N 042E	09,11	Daly and Pozzi (1977)
DP	Doornpoort Formation	?550-500	22N 045E	07,10	Piper (1975b)

*A_{95} circle only

Table 4.7 (B)

Summary of new late Precambrian results from southern Africa

Symbol	Rock Unit	Interpretation
NQ1	Nosib Group	primary
DC1	Chuos/Maieberg Formation	primary
NB	Nosib Group, Blaubeker	secondary, Katangan
NQ2	Nosib Group	secondary, Katangan
N1	Lower Nama Group	primary
DC2	Chuos/Maieberg Formation	secondary, Pc-$\mathcal{C}$
DC3	Chuos/Maieberg Formation	secondary, Pc-$\mathcal{C}$
N2	Upper Nama Group	primary
DM	Mulden Group	primary
NQ3	Nosib Group	secondary, Damaran

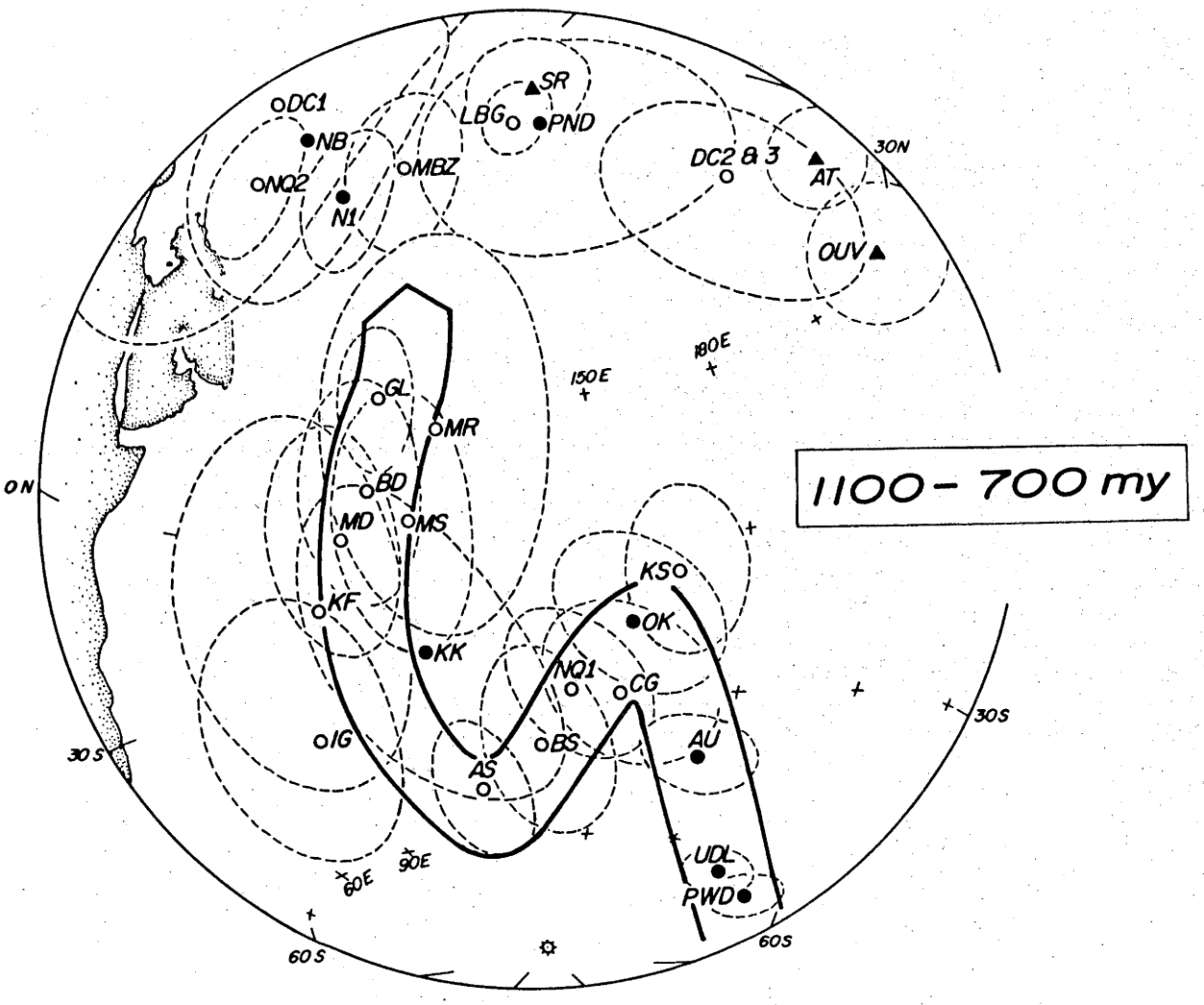

Figure 4.18(A) : Proposed APWP segment for southern Africa, 1.1-0.7 by. Projection and APWP details as in Figure 2.27 or 3.9. Symbols as in Table 4.7. Open circles : Congo craton, closed circles : Kalahari craton, triangles : northern Africa.

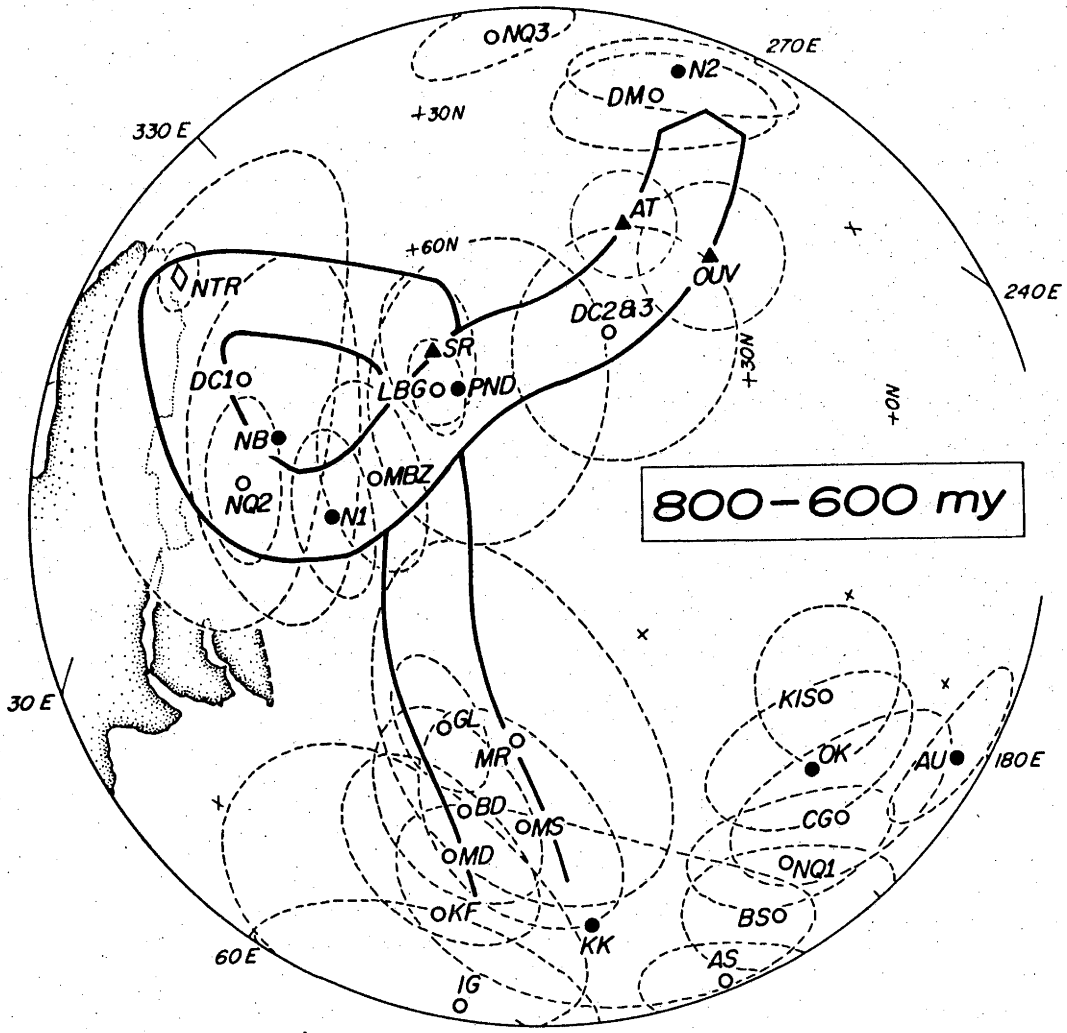

Figure 4.18(B) : Continuation of 4.18(A) for the 0.8-0.6 by interval. Diamond: pole from Ntonya Ring Structure, Mozambique belt.

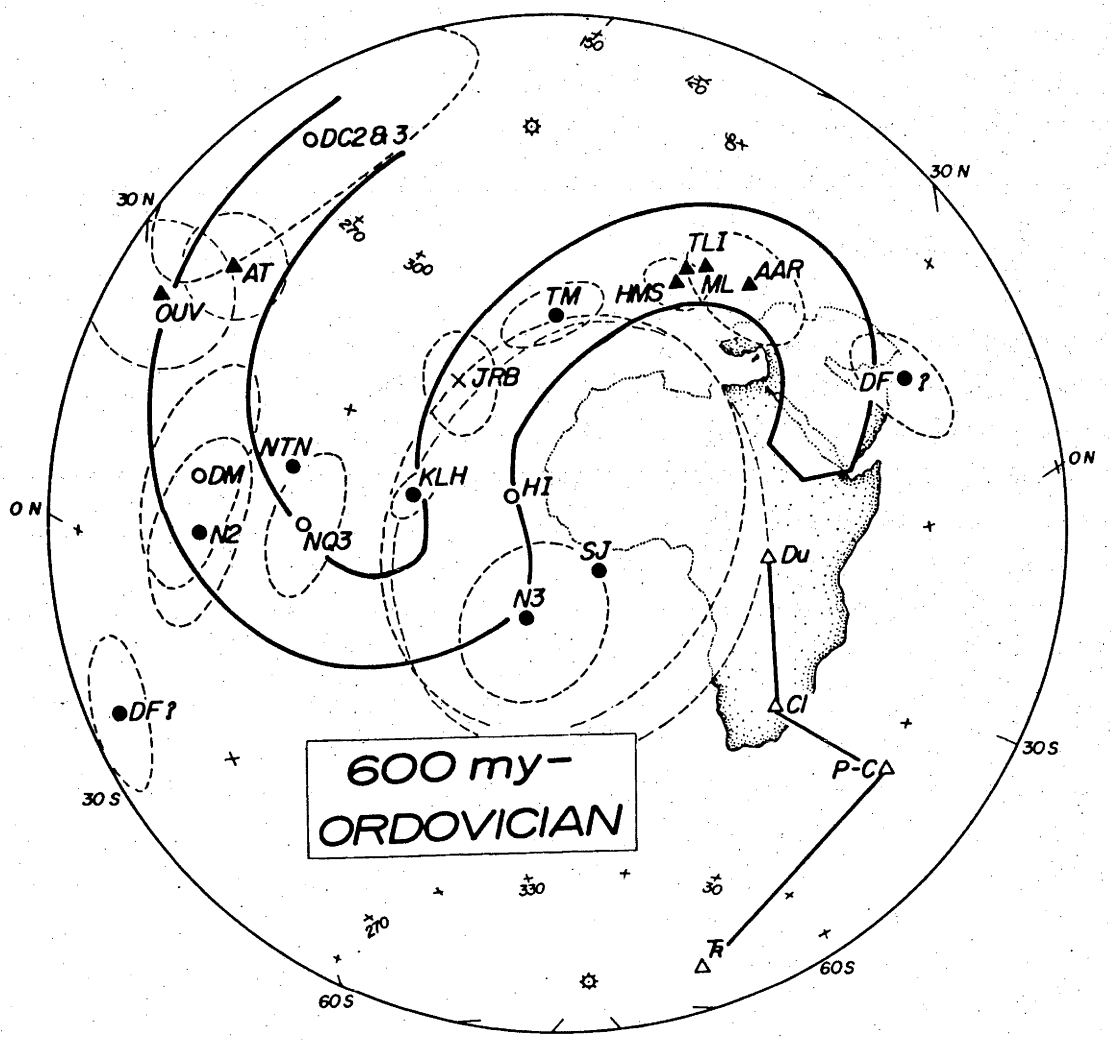

Figure 4.18(C) : Continuation of 4.18(B) for the 0.6 by - Ordovician interval.

Pre-Nama dykes. The SR pole from the Sabaloka ring structure can also be incorporated into the pole path at this point, although its age of magnetization is in question and is only known to be greater than about 540 my (quoted by Almond, 1967) but less than basement ages of about 900 my (Briden, 1973). Again, if the doubtable SR pole is not included from the APWP at this point, the agreement between the Congo and Kalahari cratons is unaffected.

A tight anticlockwise loop in the pole path is required to incorporate the next 5 poles in a possibly correct sequence. Poles NTR, DC1 and N1 probably represent primary magnetizations with estimated ages of 630±24, (?) 640-630 and 630-620 my respectively. Poles NQ2 and NB probably represent magnetizations acquired after either the Katangan or Damaran episodes, however the positive fold test on the NQ2 component would tend to suggest a Katangan (*ca.* 660-610 my) age. One problem here is the proximity of these poles to the Cambro-Ordovician APWP. As an alternative, poles NTR through NQ2 (and possibly N1) might date from the Damaran episode and thus might not be incorporated in the 800-600 my APWP. The fold test on NQ2 and the fact that (?) Damaran overprints appear to be clustered around a much different segment of the 600 my - Ordovician APWP tend to refute this argument.

The suggested pole path passes through these (?) Katangan secondary poles from both cratons, and crosses back over itself. The Sabaloka SR pole could possibly be incorporated in this section of the APWP, considering its loose age constraints.

<u>600 my</u> - <u>Ordovician</u> - After completing the *ca.* 650 my loop, the proposed APWP passes through the probable secondary overprint poles DC2 and DC3, continuing through to poles DM and N2 from

either side of the Damara Mobile Belt. Also incorporated into this APWP segment are the poles from the Ourzazate Volcanics and Amouslek Tuffs of Morocco. The Ourzazate Volcanics have recently been dated at 578±15 my (Juery *et al.* 1974); the Mulden Group pole DM predates a 526±15 my (Damaran) event and has a probable age of about 590-570 my. The path then passes through a number of primary and secondary poles possibly attributable to the Damaran episode, turning northwards in a clockwise loop similar to that proposed by McElhinny *et al.* (1974), ending in the Ordovician. A VGP from one site (NTN) excluded from the Ntonya ring structure result lies quite near the proposed path. In the original result, Briden (1967) concluded that the mean direction (represented by pole NTR) was primary in age and post-metamorphic, *i.e.* post-Katangan. The discordant site could possibly reflect a younger (?) Damaran re-heating, rather than a structural problem as originally suggested.

It is important to emphasize that although a pre-600 my age is favoured for the overprint components in the loop of the 800-600 my APWP, it is possible that these poles could possibly represent a Damaran, rather than Katangan reheating. In this case, the *ca.* 650-630 my loop would disappear (leaving PND and N1 in an inconsistent relative position) and these poles would be incorporated in an alternative form of the Cambro-Ordovician segment of the APWP as illustrated in Figure 4.19. The proximity of the 650-630 my and lower Palaeozoic poles makes a definitive interpretation difficult, however the palaeomagnetic and geochronologic evidence would tend to favour the arrangement of Figure 4.18. The Cambro-Ordovician APWP in either case connects with the younger Phanerozoic pole path as represented by the open

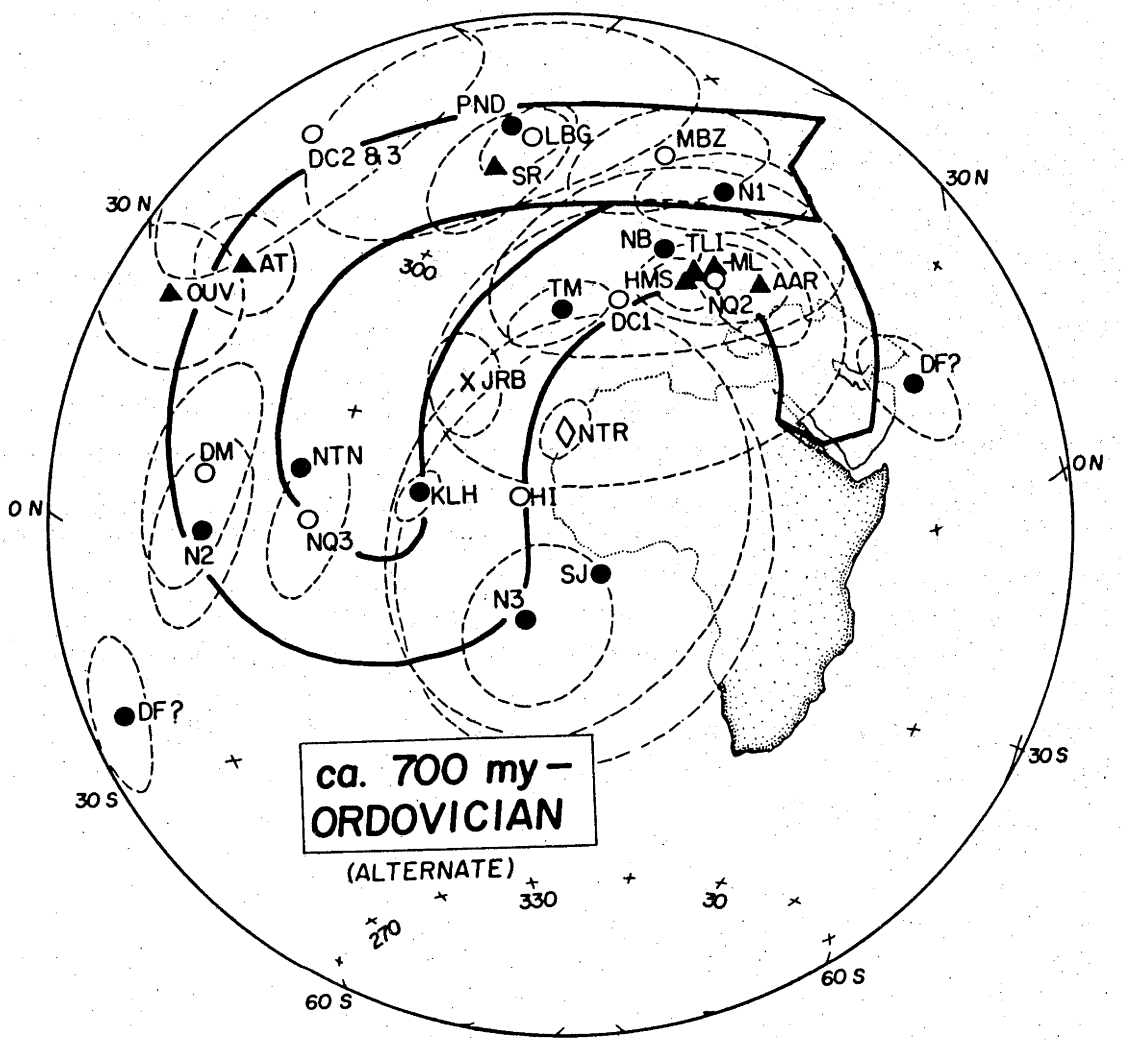

Figure 4.19 : Possible alternative to 4.18 (B & C); such an arrangement might be possible if some overprints are Damaran rather than Katangan (see text for details).

triangles of Figure 4.18 and 4.19.

The Damara Mobile Belt - an ensialic or collisional feature?

As discussed above, a single APWP can be constructed which incorporated the palaeomagnetic data available from the Congo and Kalahari cratons. Poles from both structural units are in quite reasonable agreement at *ca*. 1050, 900, 650-630 and 600-500 my, a time span which encompasses both the Katangan and Damaran phases of Pan-African orogenesis in southern Africa.

McElhinny and McWilliams (1977) point out that if the Damara Mobile Belt were a result of tectonic processes like those presently operative on a global scale (cratonic displacement with subsequent collision and suturing), APWPs for each craton would be expected to be dissimilar but convergent up until the time of collision, after which a common path would be apparent. This is clearly not the case with respect to the African palaeomagnetic data. The obvious conclusion is that the Congo and Kalahari cratons have maintained approximately their present relative positions since at least 1100 my. This implies that the Damara Mobile Belt did not result from cratonic collision following large scale displacement. However, the geometric arrangements of palaeomagnetic poles and possible cratonic displacement (Euler) poles does not preclude the creation and destruction of small intercratonic oceans with concomitant formation of suture-like structures. This would be a much more restricted tectonic form compared to modern plate tectonics. A direct uniformitarian application of plate tectonics to the Damara Mobile Belt is not supported by the palaeomagnetic data.

Chapter 5

Late Precambrian palaeomagnetism of Australia and Africa : some implications

§5.1 On the existence of Gondwanaland in the Late Precambrian

Upon adopting a Mesozoic reconstruction (such as that of Smith and Hallam, 1970) the good agreement of middle and late Palaeozoic to Mesozoic palaeomagnetic data from Australia, Africa, South America, India, Antarctica and Madagascar (*cf.* McElhinny, 1973) has demonstrated that the supercontinent Gondwanaland existed as a unit from at least early Palaeozoic times up until its dispersal in Mesozoic times. A common apparent polar wander path can be constructed in this interval for all the Gondwana continents utilizing one or another of the possible reconstructions available. Each of the reconstructions has a particular palaeogeographical or geological advantage; adoption of a particular reconstruction generally results in minor relative adjustments of the continents and palaeomagnetic poles, but the gross configuration of the supercontinent remains unchanged. The breakup of Gondwanaland in the later Mesozoic is marked by the divergence of APW paths for each continent from a coincident path relative to a chosen reconstruction. Subsequent plate motion and sea-floor spreading has resulted in the present distribution of the continents.

While the existence and dispersal of Gondwanaland in one or another of its possible Phanerozoic reconstructions now appears to be beyond reasonable doubt, its older history and that of other continental reconstructions has been the subject of considerable debate. The concept in question is the

relevance to the earth's older history of plate tectonics and continental drift, mechanisms which for almost certainly the last 200 my have been responsible for the relative displacement, creation, destruction and modification of the earth's lithosphere. Fundamentally, the debate centres about the uniformitarian application of plate tectonics to explain older geologic features within the present continents. As outlined in Chapter 1, essentially two diametrically opposed schools of thought prevail. The uniformitarian school proposes that plate tectonics has been the dominant tectonic mechanism on the earth's surface since at least Archaean times, and that geologic structures such as mobile (orogenic) belts between and within present day cratonic assemblages (continents) are a direct result of these mechanisms. The other school, 'dynamic', for want of a better name, proposes that tectonic mechanisms have gradually evolved through geologic time, and that present day plate tectonics may be only the most recent tectonic form to have been developed. The dynamicists would suggest that the older orogenic domains between cratons were possibly formed *in situ* and resulted from very different and not well understood mechanisms.

It was the study of palaeomagnetism which provided conclusive evidence of relative continental displacement in the Phanerozoic, leading to the now widely accepted theories of continental drift and plate tectonics. Similarly, palaeomagnetism will almost certainly supply solutions to the problem of deciphering Precambrian global tectonic regimes. At present, good quality Precambrian palaeomagnetic data from most continents are not so numerous so as to make absolutely confident judgment about the history and possible evolution of

crustal displacements possible. The palaeomagnetic studies described in Chapters 2,3 and 4 in conjunction with previously published data allow a number of definitive statements concerning the existence of Gondwanaland in late Precambrian times. These statements, outlined below, have direct relevance to only the continents which made up Gondwanaland, but the general tectonic picture has a more global context.

Any interpretation of younger Precambrian tectonic mechanisms based upon palaeomagnetic data must inevitably be a two-stage process. In the first stage, palaeomagnetic results from each of the older cratonic nucleii which make up each continent must be carefully compared to discover whether or not relative movements between cratons have taken place. If no significant movements have occurred or if any movements which occur can be compensated for, the second stage may be considered, in which the APWP swathes from each cratonic assemblage may be compared to test whether or not relative continental movements have occurred. The second stage is of course exactly analogous to the palaeomagnetic study of Phanerozoic plate tectonics.

A number of workers have recently discussed the problem of the structural integrity of Gondwanaland as interpreted by palaeomagnetic data. Piper *et al.* (1973) discussed palaeomagnetic results from the 3 African cratons, suggesting that these units had maintained approximately their present relative position since about 2.2 by. By comparison with sparse data from South America, these authors proposed that Africa and South America had remained together as a single continental mass until their Mesozoic breakup. A further suggestion based upon palaeomagnetic data was that North America may have been

joined to the Africa-South America continental assemblage until about 1.0 by.

McElhinny *et al.* (1974) and McElhinny and Embleton (1976) discussed Australian palaeomagnetic data in the 2500-400 my interval and suggested that Precambrian and Palaeozoic orogenic belts within that continent did not result from large scale displacement/collision mechanisms. By comparison with palaeomagnetic data from Africa, South America, India and Antarctica, these authors proposed a common Gondwanaland APWP since at least 750 my. Implicit in such a common path was an *in situ*, rather than collisional, origin for the widespread *ca.* 500 my Pan-African orogenic belts.

Piper (1976), reinforcing earlier work (Piper *et al.* 1974), subsequently suggested that Precambrian data from all continents could be accommodated in a single APWP and proposed that the bulk of the Precambrian cratonic nucleii were assembled in a single supercontinent from at least 2.0 by (2.7 by for North America and Africa) to late Precambrian times. Taking the diametrically opposed view, Burke *et al.* (1976) analysed Precambrian palaeomagnetic data and constructed widely divergent APW paths for 'suture' bounded cratonic assemblages. They infer that the data accord equally with a model of large scale relative movement and collision or with a fixist, *in situ* model of orogenesis. The opposing views of Piper (1976) and of Burke *et al.* (1976) highlight the problem of interpreting Precambrian palaeomagnetism : using (potentially) the same bank of palaeomagnetic data, the respective authors reached completely different conclusions.

The studies outlined in Chapters 2,3 and 4 significantly increase the amount of late Precambrian palaeomagnetic information

available from Gondwanaland, warranting a re-examination of the problem of its older history. Australian data are summarized in Tables 2.11, 3.3 and 3.14 and African data in Table 4.7. Sparse data from India, Antarctica and South America are listed in Table 5.1 and plotted in Figure 5.1 with the African and Australian data on a modified Smith-Hallam reconstruction.

The proposed rifting of a proto-Australian plate into 3 smaller subplates (§3.5) must be considered when making a reconstruction of Gondwanaland on the basis of present continental morphology. While the younger Palaeozoic and Mesozoic palaeomagnetic data agree well on a Smith-Hallam reconstruction, if subplates 1,2 and 3 of Figure 3.36 are rotated back together as suggested, the relative positions of Australia and Antarctica on a fit of Gondwanaland must be altered. Two possibilities are apparent if such a rotation is adopted. The western subplate (1) could be rotated to the central subplate (2) and the two together then rotated in a clockwise fashion to the southeastern block, with the Australia-Antarctica fit based upon the match between subplate (3) and the Antarctic continental outline. Alternatively, the western subplate (1) can be regarded as fixed with respect to Antarctica and subplates (2) and (3) rotated anticlockwise to fit with subplate (1). The latter possibility appears to be more favourable, as the scatter between late Cambrian and early Ordovician palaeomagnetic data from Australia and the remainder of Gondwanaland is markedly reduced in this reconstruction. As discussed below, such a pre-500-450 my reconstruction is in accord with the proposed Precambrian/Palaeozoic evolution of Australia and Antarctica suggested

Late Precambrian and early Palaeozoic palaeomagnetic poles from India, Antarctica and South America

Symbol	Rock Unit	Probable Magnetization Age	Unrotated Pole Position	dp,dm	Reference
INDIA					
MR1	Malani rhyolites	745±10	78S,225E	10,14	Athavale *et al.*, (1963)
MR2	Malani rhyolites	745±10	81S,224E	08,11	Klootwijk, (1975)
RW1	Rewa series	Pc-$\bar{\mathbb{C}}$	36S,041E	09,16[1]	Athavale *et al.*, (1972)
RW2	Rewa series	Pc-$\mathbb{C}$	45S,011E	12,24[1]	McElhinny *et al.*, (in press)
BH1	Bhander series	Pc-$\mathbb{C}$	32S,019E	03,06	Athavale *et al*, (1972)
BH2	Bhander series	Pc-$\mathbb{C}$	49S,033E	03,06	Klootwijk (1973)
BH3	Bhander series	Pc-$\mathbb{C}$	51S,043E	08,15	McElhinny *et al.*, (in press)
KHE	Khewra Sandstone[2]	Pc-$\mathbb{C}$	28S,031E	10,17	McElhinny (1970)
BAG	Baghanwala Sandstone[3]	Pc-$\mathbb{C}$	22S,032E	07,11	Wensink (1972)
ANTARCTICA					
CHA	Charnockites, Mirnyy Station	$\mathbb{C}$u	02N,208E	08,16	McQueen *et al.*, (1972)
SOR	Sor Rondane intrusives	Oℓ	28N,190E	05,06	Zijderveld, (1968)
SOUTH AMERICA					
PMV	Purmamarca Village	$\mathbb{C}$	61N,293E	16,32	Thompson (1973)
STL	South Tilcara	$\mathbb{C}$	52N,027E	15,26	Thompson (1973)
NTL	North Tilcara	$\mathbb{C}$	49N,023E	20,27	Thompson (1973)
PMM	Purmamarca	$\mathbb{C}$	05N,039E	11,15	Thompson (1973)
ABR	Abra de Cajas	$\mathbb{C}$	02N,028E	25,50	Thompson (1973)
SLJ	Salta and Jujuy	$\mathbb{C}$-O	12N,329E	26,38	Creer (1970)
SAL	Salta	O	31N,013E	23,45	Thompson (1973)
URM	Urucum Formation	O-S	17N,347E		Creer (1967)

[1] unit weight to samples
[2] formerly Purple Sandstone
[3] formerly Salt Pseudomorph beds

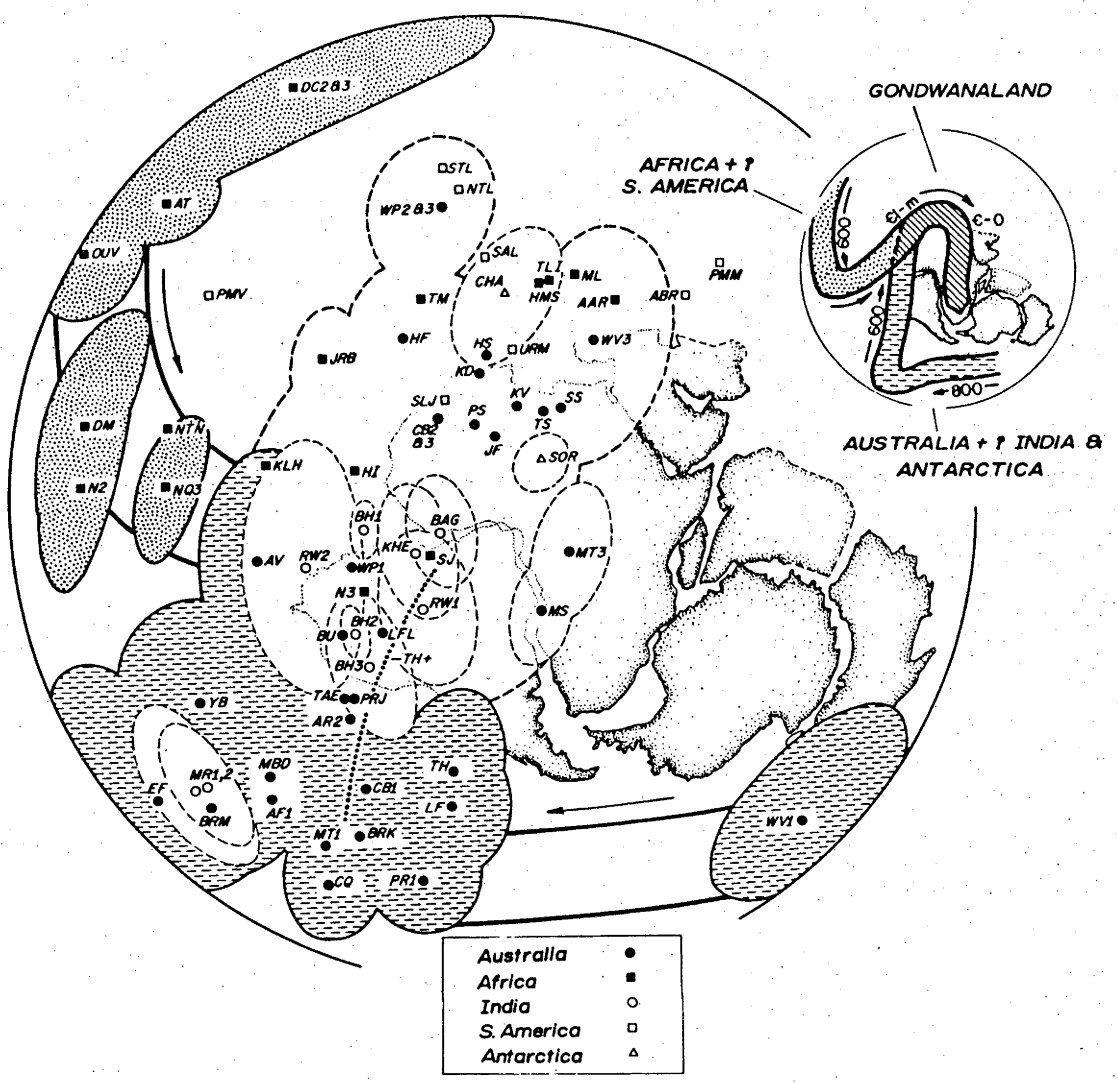

Figure 5.1 : Late Precambrian APWP for the Gondwana continents. Inset shows generalized trend for eastern and western assemblages. Dashed ovals enclose area of common path for east and west Gondwanaland. Reconstruction of Smith and Hallam (1970) modified to include the subplate model discussed in Chapter 3. Equal-area projection, radius 115°. Symbols for India, Antarctica and South America listed in Table 5.1; African symbols as in Figure 4.18; Australian symbols as in Figure 3.36. Swathe width 15° at equator.

solely on geological grounds and has probable significance to the tectonic history of Gondwanaland as a whole.

Irrespective of the Australian reconstruction used (unchanged Smith-Hallam, rotated to subplate 1, or to subplate 3, the late Precambrian APW paths of Africa and Australia are distinctly different, converging to form a single path in (probably) early Cambrian times (Figure 5.1). The few Indian Precambrian and early Cambrian data tend to suggest that India and Australia might have moved as a unit since at least ∿750 my; however no definitive conclusions can be made about the late Precambrian palaeopositions of South America and Antarctica. The convergent pole paths strongly suggest that Africa and Australia (+ India?) were separate entities in the late Precambrian, and that Gondwanaland as represented by Smith-Hallam or closely related reconstructions did not exist before about 550 my. This conclusion is in direct opposition to the concept of an intact Gondwanaland in the late Precambrian suggested by McElhinny *et al.* (1974), McElhinny and Embleton (1976) and Piper (1976). It is instructive to recall that only 3 palaeomagnetic results were available for Australia in the 1000 my - Cambrian interval at the time these earlier conclusions were reached, and as discussed in Chapter 2, two of these three probably do not reflect an original primary magnetization.

The observation of convergent pole paths discussed above has relevance to the origin of the 550-450 my Pan-African orogenic belts (Figure 5.2). If separate eastern and western Gondwana blocks (represented by Australia-India (?) and Africa in part, respectively) did indeed collide in early Cambrian times, some of these belts may have directly resulted from

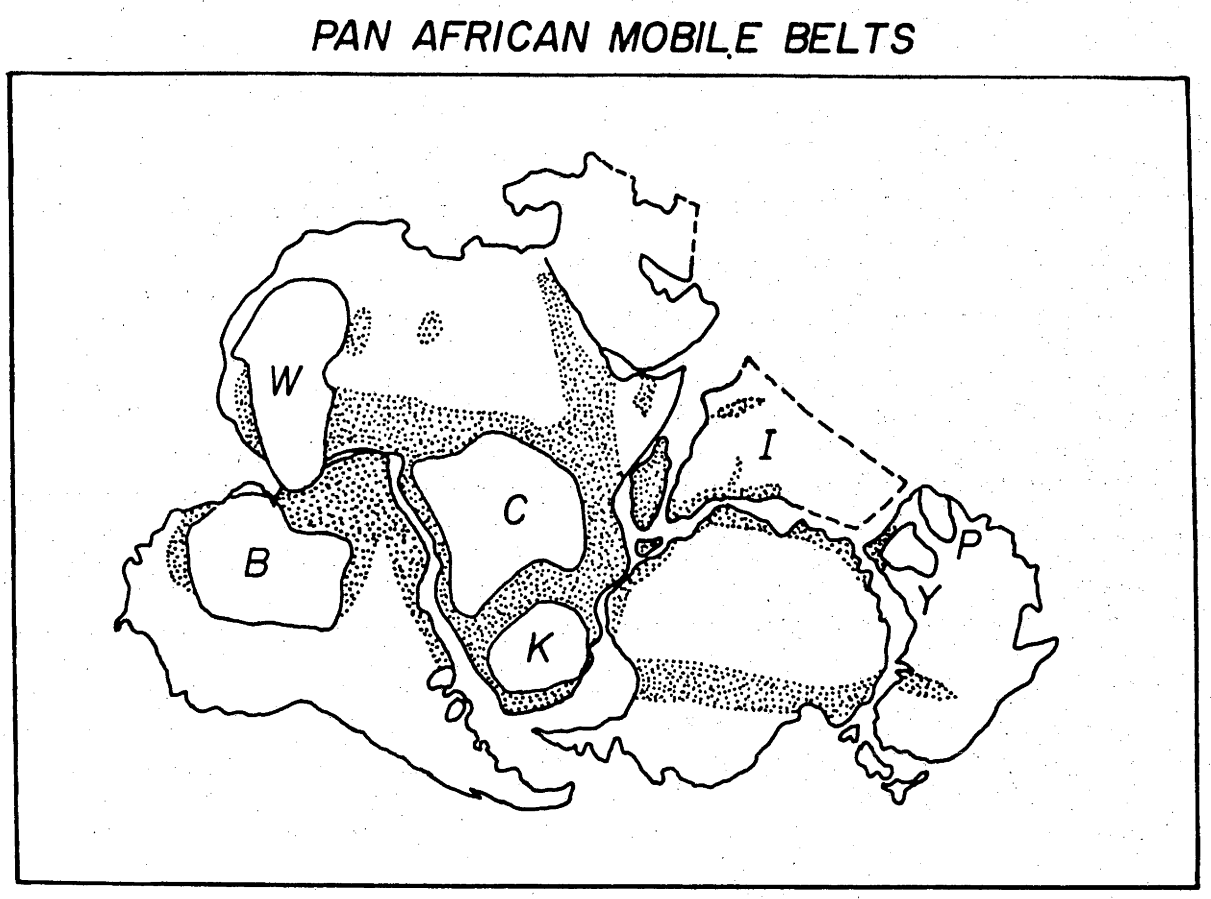

Figure 5.2 : Pan-African mobile belts (stippled) after McElhinny (1973); isotopic ages range from 650 my to 450 my.

collisional (plate-tectonic) type mechanisms similar to those suggested by Hurley (1972) or Burke and Dewey (1972). However, the palaeomagnetic studies described in Chapter 4, in conjunction with published data, suggest that at least one of the Pan-African belts (the Damara mobile belt) did not originate from plate collision but probably from an *in situ* ensialic mechanism (Shackleton, 1969, 1973; Kröner, 1977a). This apparent contradiction illustrates both the palaeomagnetic (mentioned above) and geological dilemma which has faced earth scientists attempting to interpret Precambrian tectonic mechanisms : in the case of some orogenic zones, evidence can be cited which strongly supports a collisional origin, while in others, ensialic orogenesis is seen as dominant. Commonly an ensialic (or collisional) mechanism is indicated for a particular mobile belt or belts and an author then proceeds with a uniformitarian, inductive approach, concluding that all mobile belts of this age are therefore of ensialic (or collisional) origin. The interpretations presented in this work imply that straightforward inductive reasoning may not be correct in assessing the earth's tectonic history.

The apparent paradox can be resolved by speculatively allowing both ensialic and collisional orogenesis to occur simultaneously, but at different places, during at least late Proterozoic times. As summarized by Hargraves (1976), the earth's thermal history has been complicated, but a pattern of decreasing thermal flux is apparent. The dominant form of global tectonics at a given time might be expected to change in response to such heat flux changes, leading to an evolution of tectonic mechanisms. Archaean tectonics may therefore have been dominantly of a more mobile form, reflecting the relatively

high heat flux and elevated crustal temperatures, while lower temperature Phanerozoic tectonics was and continues to be dominated by much more rigid plate tectonics. The intervening Proterozoic eon may have been the transitional period between ductile and brittle crustal behaviour, with the particular mode dependent to first order upon temperature and strain rate.

Finally, it is instructive to consider the model of evolution of the Australian-Antarctic platform (Veevers, 1976; Veevers and McElhinny, 1976) in light of the observation of convergent pole paths for Africa and Australia. These authors have adopted a modified version of the Harrington *et al.* (1973) model, which postulates a major Cambro-Ordovician sinistral strikeslip movement along a fracture zone to the south of Australia. Such movement implies a relative movement of the Australian and Antarctic plates as illustrated in Figure 5.3. The mechanisms which produced this movement may have also caused the fission of a proto-Australian plate into 3 subplates as suggested by palaeomagnetic data in Chapter 3, with major attendant volcanism in the rifted zones. Various authors have suggested that the *ca.* 600-550 my volcanic episodes (including the Antrim, Table Hill and (?) Chambers Bluff volcanics) are attributable to rifting which subsequently produced the younger basins which separate subplates (Warris, 1973; Laws and Kraus, 1974). Although Veevers (1976) and Veevers and McElhinny (1976) argued that these events may have occurred within the framework of an intact Gondwanaland, the palaeomagnetically suggested plate convergence is entirely consistent with the hypothesis; indeed the existence of plate tectonic mechanisms at about this time would tend to make the model even more tenable.

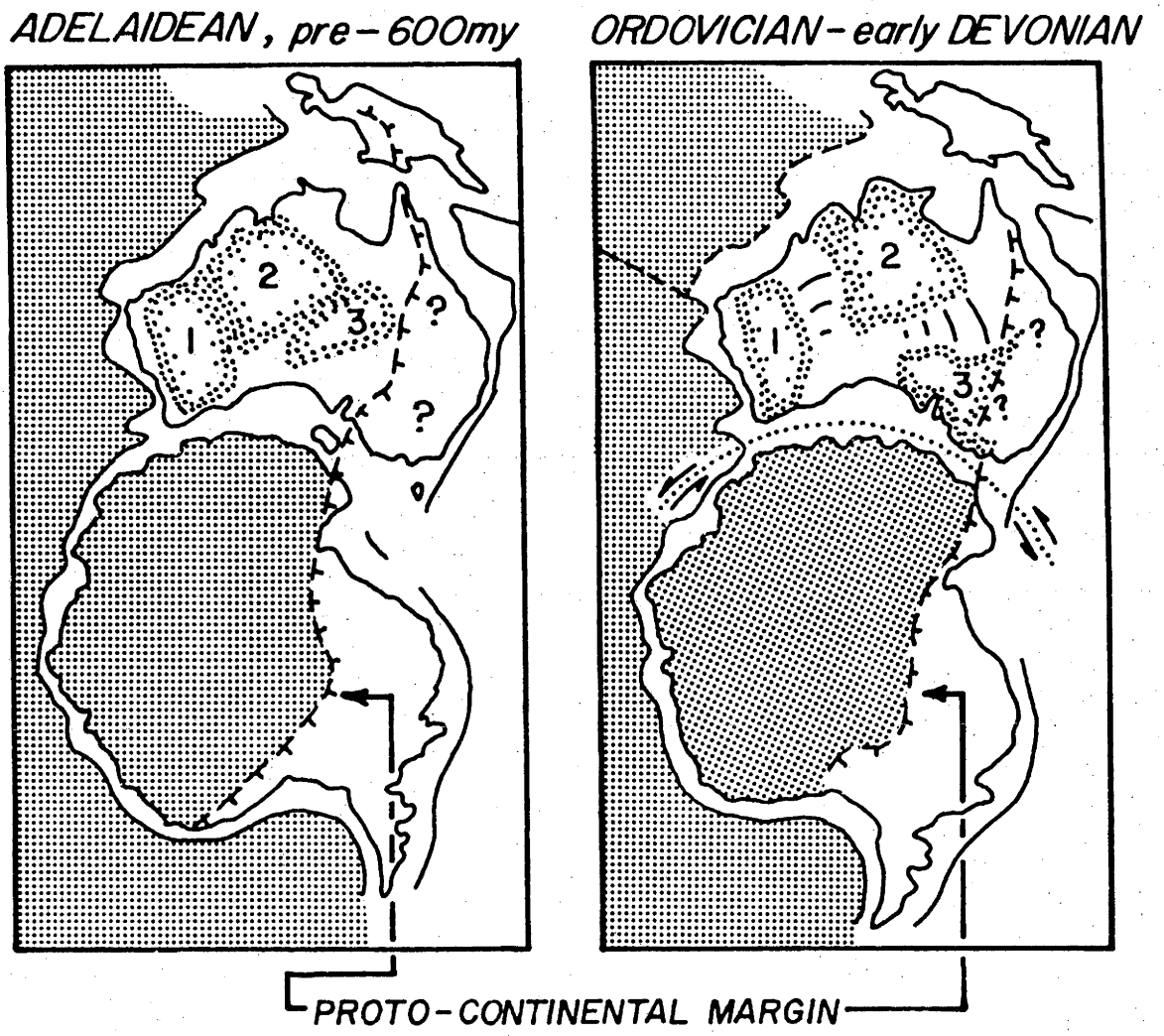

Figure 5.3 : Clockwise rotation of Antarctica with respect to Australia as suggested by Veevers (1976) and Veevers and McElhinny (1976). The mechanisms causing such a movement may have also resulted in the rifting and fragmentation of a proto-Australian shield.

To summarize, the palaeomagnetic results described in Chapters 2,3 and 4 together with published data suggest that Gondwanaland did not exist before about 550 my ago, and that some of the 550-450 my Pan-African orogenic domains may have resulted from plate convergence and collision. The good agreement of palaeomagnetic data from the Congo and Kalahari cratons of southern Africa indicates however that the Damara mobile belt did not directly result from plate collision and it is therefore clear that not all of the Pan-African belts are of plate tectonic origin. Many of the Precambrian and early Palaeozoic tectonic and thermal events can perhaps be directly or indirectly related to the early Cambrian formation of Gondwanaland, during which time both plate tectonic and ensialic orogenesis may have occurred. Such a "hybrid" tectonic form may be the best explanation for the apparent geological and palaeomagnetic paradox which results from uniform acceptance of only one of the mechanisms at any one point in the earth's earlier history.

§5.2 Palaeolatitude of late Precambrian glacial deposits

Harland (1964) originally advanced a hypothesis of a globally synchronous late Precambrian refrigeration to explain the widespread occurrence of glacial deposits underlying Cambrian sediments in many continents. This event was to have been severe enough to have been responsible for simultaneous deposition of glacial and glacially related sediments from polar to equatorial palaeolatitudes, as compared to the more latitudinally restricted Phanerozoic glaciations. The obvious potential of deposits so produced as intra- and intercontinental chronostratigraphic marker

horizons has prompted a great deal of study and debate, the salient points of which are reviewed here.

At the fundamental level, two opposing viewpoints exist. On one side there is the belief that the 'tillites' and related sediments are indeed of glacial origin (e.g. Harland, 1964; Young, 1976a,b; Kröner and Rankama, 1973; Deynoux and Trompette, 1976). The opposing minority view (Schermerhorn 1974, 1975, 1976) holds that the 'tillites' were not directly formed by glacial action, but resulted from tectonic or secondary glacial mechanisms. The prolific terminology arising from this debate has been reviewed by Kröner and Rankama (1973) and by Jago (1974a). It is not intended to enter the fundamental argument except to state that the bulk of the evidence certainly favours a glacial origin.

Having accepted late Precambrian glaciation as a probable reality, opinion is again divided regarding the mode of occurrence of these widespread deposits. In the original hypothesis, Harland (1964) cited palaeomagnetic evidence which suggested a very low (average <10°) depositional palaeolatitude for late Precambrian glacial deposits from Scandinavia and Greenland, inferring that ice caps existed from high down to very low latitudes. This view was adopted by Dunn *et al.* (1971), who proposed that the glacial horizons be used as chronostratigraphic reference markers. Roberts (1976) suggested that such a synchronous global event was possibly triggered by a locking up of CO_2 in dolomites which stratigraphically precede glacial sediments in some localities.

Crawford and Daily (1971) rejected the concept of a synchronous global event, alternatively suggesting that the

late Precambrian glaciation, like the Ordovician, Permian and Pleistocene events, was essentially a high latitude circumpolar feature. The relatively small polar area ensures that a small proportion of the surface is glaciated; continents would then be glaciated at different times as they drift into higher latitudes. As an alternative to synchronous global and nonsynchronous circumpolar glaciation, Williams (1974, 1975) has suggested that the obliquity of the earth's ecliptic was much higher (between approximately 54°-126°) during the late Precambrian glaciation; as a result, climatic zonation would be reversed and glacial sedimentation would occur only in low to moderate palaeolatitudes. In this model, nonsynchroneity is tacitly assumed and continents would be glaciated as they drift through the low, rather than high palaeolatitude zone. A synchronous glaciation could be invoked in the special case where all the continents which contain late Precambrian tillites were arranged in low palaeolatitudes. In such a case, it might be difficult to tell the difference between a 'dynamic obliquity' glaciation and a synchronous global glaciation.

The palaeomagnetic consequences of the three models are vastly different when considered on a global scale, as illustrated in Figure 5.4. The synchronous global model would predict that palaeomagnetic data from glacial deposits on all continents would be distributed throughout the entire inclination spectrum, and that coincident pole positions would be observed provided that the correct relative palaeogeographical reconstruction was known (for example a Gondwana or Pangaea reconstruction). The nonsynchronous circumpolar model would predict only high inclinations from the glacial deposits, as in this mode, continents would be glaciated only in high

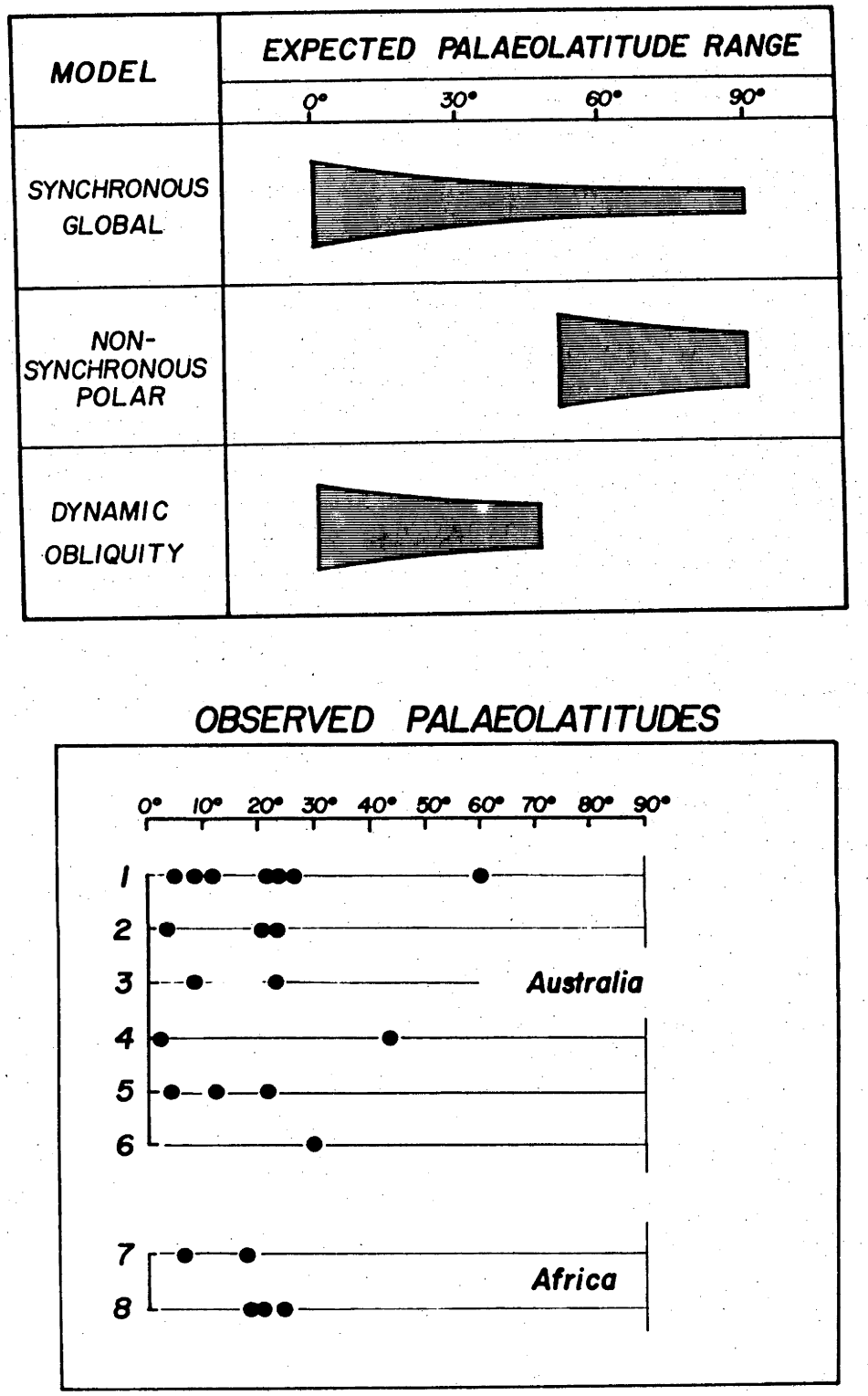

Figure 5.4 : Expected and observed palaeolatitude spectra for late Precambrian glacial deposits according to the various models discussed in the text. Width of bar proportional to expected frequency of occurrence.

latitudes. Pole positions from different continents on a known reconstruction would be dissimilar, reflecting the differing depositional ages. The dynamic obliquity model is inversely analogous to the nonsynchronous circumpolar model in that the reversed climatic zonation would predict observation of only low to moderate inclinations from the glacial deposits. Again, pole positions would be dissimilar, except in the special case mentioned above.

Much of the palaeomagnetic speculation regarding the three models has been centred not around palaeolatitude information directly obtained from the glacial deposits themselves, but indirectly inferred from various proposed APW paths. Piper (1973) constructed an APWP for the 900-500 my interval which suggested that Africa lay in low palaeolatitudes during a presumably synchronous glaciation. A later analysis by McElhinny *et al.* (1974) resulted in the opposite conclusion, that the APWP for an intact Gondwanaland rapidly passed over the supercontinent during the interval of glaciation, with tillites deposited nonsynchronously in high latitudes only.

Until the present study, direct palaeomagnetic studies of late Precambrian glacial and related sediments were few. Harland (1964) supported his original hypothesis on low inclinations from tillites from Norway and Greenland (Harland and Bidgood, 1959; Bidgood and Harland, 1961). In retrospect, Harland's conclusion appears to be rather questionably founded, considering the reliability of these palaeomagnetic observations, made before magnetic cleaning techniques were routine procedure. Tarling (1974) reported low (<10°) apparent palaeolatitudes from late Precambrian tillites from Scotland, and also demonstrated the questionable reliability of the original

results quoted by Harland (1964). Tarling's result was in doubt also, as the samples were taken from regions which had suffered low grade metamorphism during a Caledonian orogenic event. However, Abouzakhm and Tarling (1975) showed in a subsequent study that the heating did not affect the primary remanence of these rocks, and that the original conclusion of a low depositional palaeolatitude was still valid. Recently Morris (1977) reported a study of the glaciogenic upper Rapitan Group from the Northwest Territories of Canada; detailed analysis revealed three components of magnetization, two of which were regarded as being possibly of late Precambrian age. Knowledge of the relative age of these two components was critical to the determination of depositional palaeolatitude of these rocks; thermal and chemical demagnetization experiments suggested that the primary (depositional) magnetization was acquired in low ($\sim$14°) palaeolatitudes.

The palaeomagnetic studies described in Chapters 2,3 and 4 similarly indicate low palaeolatitudes late Precambrian glacial sequences in Australia and in southern Africa. Together with the North American, European and Greenland data, a dominant picture of low latitude glaciation emerges, effectively eliminating the nonsynchronous circumpolar model. Before making any further conclusions, it is important to consider again the predictions implicit in each of the remaining possibilities with respect to the distribution of the sampling sites.

Taken at face value, the data could support a low latitude only glaciation (*i.e.* the dynamic obliquity model). Alternatively, the data could be taken to represent a non-random

sampling of a broad spectrum of depositional palaeolatitudes resulting from a synchronous global event. While this possibility may initially seem remote, it must be remembered that the probability of randomly selecting an arbitrary point on the earth's surface whose latitude is 60°(45°) or greater is 0.13(0.29). A third possible explanation is that either synchronous global or dynamic obliquity (it would be very difficult to tell which) glaciation occurred during a time when all the glaciated continents were lying in low palaeolatitudes. This is actually an extension of the previous non-random sampling argument; this time the sampling would be regarded as uniform but not the distribution of continents. Considering the possible non-existence of Gondwanaland in the late Precambrian as discussed in §5.1, such a special distribution is indeed possible. A synchronous glaciation is implied in this and the previously discussed possibility.

In development of the dynamic obliquity model of glaciation, Williams (1975) cites a number of geological arguments which he feels support the concept of pronounced climatic seasonality and thus a much higher obliquity of the earth's ecliptic in the late Precambrian compared to the present value. The arguments are generally based upon apparently paradoxical coexisting warm/cold palaeoclimatological indicators in the glacial horizons; for example evaporites, dolomites, stromatolites and iron formations found in intimate association above and with late Precambrian glacial sediments. These curious associations have also been cited in an attempt to refute a glacial origin altogether (e.g. Schermerhorn, 1974, 1976). As discussed in the following paragraphs, few of the features necessarily support the concept of an increased

obliquity, and most can be explained at least as convincingly without invoking dramatic changes in the dynamics of the earth's rotation and orbit.

Evaporites: Consider a large, extensively glaciated continent in low palaeolatitudes. Upon deglaciation, land areas below sea level will be covered by sea water. Being a much slower process than deglaciation, isostatic rebound and uplift will slowly and gradually lower sea level relative to the land. As the seas recede, sea water may become trapped in relatively shallow inland basins, at the bottom of which moraine-type deposits might have been deposited. Provided that net evaporative conditions prevail in the basin, evaporites might be precipitated out of the more concentrated and layered brine solution at a time when concentration and temperature conditions permit (Sloss, 1969; Schmalz, 1969). In this manner, the commonly reported association of tillites and evaporites could be created.

It is fundamental to note however that such features are not necessarily indicative of a warm climate. For example, Dort and Dort (1970) review recent evaporites in Antarctica formed by the process outlined above. Ferrar (1905) noted well formed sodium sulfate deposits up to 45 cm thick among Antarctic moraines during Scott's first expedition, terming the occurrences "freaks of nature". Wellman and Wilson (1963) observed long windrows of accumulated salts lying directly on sea ice and estimated that as much as 10^6 tons of this salt might accumulate on the ice of McMurdo Sound each year. The occurrence of evaporites need not necessarily be unquestionably assumed to reflect warm climate.

Stromatolites: Again the Antarctic analogy serves to show

that the occurrence of stromatolites does not necessarily reflect warm conditions. The blue-green algae which form stromatolites are known to exist in Antarctica, and benthonic algal mats occur in L. Bonney (77°S). Although it is not yet clear, all the available evidence suggests that carbonate stromatolites are forming in the lake (Walter, pers. comm.). At first glance, the occurrence of high concentrations of dissolved salts in the confined basins might be expected to be toxic to algal life, however Weand *et al.* (1976) and Brock (1977) have pointed out that besides their extreme temperature adaptability (0°-70°), cyanophytes and eucaryotes can exist under the extremely inhospitable pH and salinity conditions which would be present.

Sedimentary iron formation: Williams (1975) adopts the view that the high concentration of iron in late Precambrian tillites and related iron formations was derived from lateritic weathering and their presence therefore indicates warm climate. Young (1976a) has succinctly summarized the status of the theory of sedimentary iron formation genesis: "Iron formations have been the subject of many papers and have been interpreted as products of almost every conceivable depositional environment". Cold climate alternatives to production of an iron-rich regolith in a warm climate might be an increased seawater iron content due either to lower atmospheric O_2 content (Cloud, 1973) or to freezing of seawater (Young, 1976a). As in the case of evaporites, the presence of iron-enriched sediments is not necessarily a reliable indicator of warm climate.

Laminae in glacially related sediments, cryoturbation structures: Laminae (often interpreted as varves) are commonly observed

in late Precambrian glacial sequences and probably reflect seasonal changes in depositional conditions. Some glacial sequences also exhibit cryoturbation (freeze/thaw) structures which suggest seasonality. Consider again a glaciated continent in low palaeolatitudes during a synchronous global event. The laminae and cryoturbation features would in fact be predicted; low latitude regions would be expected to have dramatic response to seasonal changes, not because of changes in local insolation, but in direct response to shifts in the small near-equatorial regions of warmer climate from one hemisphere to the other. The evidence for seasonality cited by Williams (1975) as supporting a higher obliquity could therefore equally support a synchronous global glaciation.

Dolomite in the glacial environment: The coexistence of dolomites with tillites remains problematic. Some dolomites could form by the method outlined above for evaporite deposition, *i.e.* concentration of dissolved Ca and Mg to a precipitation point in a layered, closed basin, or alternatively by the locking up of great quantities of fresh water in continental ice sheets. However, the consensus regarding dolomite formation is that temperatures greater than 20° are required; the presence of glacial dropstones within dolomites would seem to be contradictory. Kröner's (1977) observation that in Africa (and Australia), carbonates generally postdate rather than predate glacial rocks might again be what would be expected during and just after a global event in low latitudes with the earth's obliquity at its present value. Consider once more the glaciated continent at low latitudes. Following deglaciation, an overall warming could result in carbonate deposition in the lower latitudes, conformably above the glacial sediments.

Dropstones in the overlying carbonates could reflect a return to glacial conditions, although this is certainly questionable.

The purpose of the preceding paragraphs has been to suggest that a major change in obliquity of the earth's ecliptic is not necessary to explain many of the geological features and palaeolatitude of late Precambrian glacial sediments. The hypothesis of a synchronous global glaciation similar to that first suggested by Harland (1964) is viewed as equally tenable. At this stage, the decision between the two possible mechanisms rests fundamentally upon which 'special' condition is regarded as less acceptable: changing obliquity or a late Precambrian equatorial arrangement of the continents for which palaeomagnetic data are available. Although the problem is not discussed here, a major change in obliquity does require serious dynamic considerations centred around mechanisms of conservation and transferral of angular momentum. Considering the fact that Gondwanaland may not have existed in the late Precambrian, the latter possibility of a synchronous global glaciation appears to be the better choice.

REFERENCES

Abouzakhm, A.G. and Tarling, D.H. (1975) Magnetic anisotropy and susceptibility of late Precambrian tillites from northwestern Scotland. *J. geol. Soc. Lond., 131*, 647-652.

Almond, D.C. (1967) Discovery of a tin-tungsten mineralization in northern Kartoum Province, Sudan. *Geol. Mag., 104*, 1-12.

Athavale, R.N., Radhakrishnamurthy, C. and Sahasrabudhe, P.W. (1963) Palaeomagnetism of some Indian rocks. *Geophys. J. R. astr. Soc., 7*, 304-313.

Athavale, R.N., Hansraj, A. and Verma, R.K. (1972) Palaeomagnetism and age of Bhander and Rewa Sandstones from India. *Geophys. J. R. astr. Soc., 28*, 499-509.

Beck, M.E. (1970) Palaeomagnetism of Keeweenawan intrusive rocks, Minnesota. *J. geophys. Res., 75*, 4895-4996.

Bennett, R. and Gellatly, D.C. (1970) Rb-Sr age determinations of some rocks from the West Kimberley region, Western Australia. *Bur. Min. Resources Aust. Rec.* 1970/20 (unpublished).

Bidgood, D.E.T. and Harland, W.B. (1961) Palaeomagnetism in some east Greenland sedimentary rocks. *Nature, 189*, 633-634.

Bofinger, V.M. (1967) Geochronology in the East Kimberley area of Western Australia. Unpublished Ph.D. thesis, Australian National University, Canberra.

Briden, J.C. (1967) Preliminary palaeomagnetic results from the Adelaide System of South Australia. *Trans. Roy. Soc. S.Aust., 91*, 17-25.

Briden, J.C. (1968) Palaeomagnetism of the Ntonya Ring Structure, Malawi. *J. geophys. Res., 73*, 725-733.

Briden, J.C. (1973) Palaeomagnetic estimate of the age of the Sabaloka Complex, Sudan, *in* 17th Annual Report, Institute of African Geology, University Leeds, p. 39.

Briden, J.C. and Ward, M.A. (1960) Analysis of magnetic inclination in borecores. *Pure and Appl. Geophys., 63*, 133-152.

Brock, A. (1967) Palaeomagnetic Result from the Hook Intrusives of Zambia. *Nature, 216*, 359-360.

Brock, A. Raja, P.K.S. and Vise, J.B. (1972) The palaeomagnetism of the Kisii Series, (western) Kenya. *Geophys. J. R. astr. Soc., 28*, 129-137.

Brock, T.D. (1977) Environmental microbiology of living stromatolites, *in* M.R. Walter (ed.) *Stromatolites*, Elsevier (Amsterdam).

Brooks, C., James, D.E., Hart, S.R. and Hofmann, A.W. (1976) Rb-Sr mantle isochrons, *in* Annual Report of the Director, Carnegie Institution, Dept. of Terrestrial Magnetism.

Buchan, K.L. and Dunlop, D.J. (1976) Palaeomagnetism of the Haliburton intrusions : superimposed magnetizations, metamorphism and tectonics in the late Precambrian. *J. geophys. Res., 81,* 2951-2967.

Bucur, I. (1971) Étude paléomagnetique d'une formation sédimentaire du Sahara algérien, d'âge Cambro-Ordovicien. *Ann. Geophys., 27,* 255-261.

Burek, P.J. (1969) Device for chemical demagnetization of redbeds. *J. geophys. Res., 74,* 6710-6712.

Burger, A.J. and Coertze, F.J. (1973) Radiometric age measurements on rocks from southern Africa to the end of 1971. *Bull. Geol. Surv. S. Afr., 58,* p. 46.

Burke, K.C.A. and Dewey, J.F. (1972) Orogeny in Africa, *in, African Geology,* (eds.) T.F.J. Dessauvagie and A.J. Whiteman, published by Geology Department, University of Ibadan, Nigeria.

Burke, K., Dewey, J.F. and Kidd, W.S.F. (1976) Precambrian palaeomagnetic results compatible with contemporary operation of the Wilson Cycle. *Tectonophysics, 33,* 287-299.

Charlton, S.R. (1973) Limitations of the Argon 39 method on Precambrian dolerites. 17th Annual Report Research Institute African Geology, Leeds, 45-47.

Clifford, T.N. (1967) The Damaran Episode in the Upper Proterozoic-Lower Palaeozoic structural history of Southern Africa. *Geol. Soc. Am. Spec. Paper, 92,* p. 100.

Cloud, P. (1973) Palaeoecological significance of the banded iron formations. *Econ. Geol., 68,* 1135-1145.

Coats, R.P. and Blissett, A.H. (1971) Regional and Economic Geology of the Mount Painter Province. *Bull. geol. Surv. S.Aust., 43,* Adelaide.

Compston, W. (1974) The Table Hill Volcanics of the Officer Basin - Precambrian or Palaeozoic? *J. geol. Soc. Aust., 21,* 403-412.

Compston, W., Crawford, A.R. and Bofinger, V.M. (1966) A radiometric estimate of the duration of sedimentation in the Adelaide Geosyncline, South Australia. *J. geol. Soc. Aust., 13,* 229-276.

Compston, W. and Nesbitt, R.W. (1967) Isotopic age of the Tollu Volcanics, Western Australia. *J. geol. Soc. Aust., 14,* 235-238.

Cooper, J.A. (1975) Isotopic datings of the basement-cover boundaries within the Adelaide Geosyncline (abstract). Geological Society of Australia, First Geological Convention on Proterozoic Geology, Adelaide.

Cooper, J.A. and Compston, W. (1971) Rb-Sr dating within the Houghton Inlier, South Australia. *J. geol. Soc. Aust., 17,* 213-219.

Crawford, A.R. (1963) The Wooltana volanic belt, South Australia. *Trans. R. Soc. S.Aust., 87,* 123-154.

Crawford, A.R. and Daily, B. (1971) Probable non-synchroneity of late Precambrian glaciations. *Nature, 230,* 111-112.

Crawford, A.R. and Campbell, K.W. (1973) Large-scale horizontal displacement within Australo-Antarctica in the Ordovician. *Nature, 241,* 11-14.

Creer, K.M. (1967) Palaeomagnetism of some lower Palaeozoic South American rocks. *Symposium on Continental Drift* (UNESCO/IUGS), Montevideo, Uruguay; *Trans. Amer. geophys. Un., 53,* 172.

Creer, K.M. (1970) A palaeomagnetic survey of South American rock formations. *Phil. Trans. R. Soc., A267,* 457-558.

Creer, K.M. (1973) A discussion of the arrangement of palaeomagnetic poles on the map of Pangaea for Epochs in the Phanerozoic, *in,* Tarling, D.H. and Runcorn, S.K. (eds.) *Implications of Continental Drift to the Earth Sciences,* Academic Press (London).

Cumming, G.L. and Richards, J.R. (1975) Ore lead isotope ratios in a continuously changing earth. *Earth Planet. Sci. Lett., 28,* 155-171.

Daily, B., Jago, J.B. and Milnes, A.R. (1973) Large-scale horizontal displacement within Australo-Antarctica in the Ordovician. *Nature, 244,* 61-64.

Daly, L. and Pozzi, J.P. (1977) Determination d'un noveau pole palaeomagnetique Africain sur des formations Cambriennes du Maroc. *Earth Planet. Sci. Lett., 34,* 264-272.

David, T.W.E. (1922) Occurrence of small crustacea in the Proterozoic (?) or Lower Cambrian rocks of Reynella, near Adelaide. *Trans. R. Soc. S.Aust., 46,* 6-8.

Deynoux, M. and Trompette, R. (1976) Late Precambrian mixtites : Glacial and/or nonglacial? Dealing especially with the mixtites of west Africa (discussion). *Amer. J. Sci., 276,* 1302-1315.

Dort, W. and Dort, D.S. (1970) Sodium sulfate deposits in Antarctica. *Modern Geology, 1,* 97-117.

Dow, D.B. and Gemuts, I. (1969) Geology of the Kimberley Region, Western Australia : The East Kimberley. *Bureau Mineral Resources Bulletin, 106.*

Duncan, R.A. and Compston, W. (1977) Sr isotopic evidence for an old mantle source region for French Polynesia. *Geology, 4,* 728-732.

Dunn, P.R., Thomson, B.P. and Rankama, K. (1971) Late Pre-Cambrian glaciation in Australia as a stratigraphic boundary. *Nature, 231,* 498-502.

Embleton, B.J.J. (1972a) The palaeomagnetism of some Proterozoic-Cambrian sediments from the Amadeus Basin, Central Australia. *Earth Planet. Sci. Lett., 17,* 217-226.

Embleton, B.J.J. (1972b) The palaeomagnetism of some Palaeozoic sediments from Central Australia. *J. and Proc. R. Soc. N.S.Wales, 105,* 86-93.

Embleton, B.J.J. and Giddings, J.W.G. (1974) Late Precambrian and Lower Palaeozoic palaeomagnetic results from South Australia and Western Australia. *Earth Planet. Sci. Lett., 22,* 355-365.

Evans, M.E. (1969) Precambrian palaeomagnetism of Australia and Africa. Unpublished Ph.D. Thesis, Australian National University, Canberra.

Fander, H.W. (1963) The Wooltana lavas. *Trans. R. Soc. S.Aust. 87,* 155-157.

Ferrar, H.T. (1905) Summary of the geological observations made during the cruise of the S.S. "Discovery", 1901-1904, *in,* R.F. Scott, *The voyage of the "Discovery"*, Smith, Elder, London, pp. 437-468.

Fisher, R.A. (1953) Dispersion on a sphere. *Proc. Roy. Soc. Lond. A217,* 295-305.

Forbes, B.G. (1971) Stratigraphic subdivision of the Pound Quartzite (Late Precambrian, South Australia). *Trans. R. Soc. Aust., 95,* 219-225.

Germs, G.J.B. (1972) The stratigraphy and palaeontology of the lower Nama Group, South West Africa. Precambrian Research Unit Bulletin 12, Department of Geology, University of Cape Town.

Germs, G.J.B. (1974) The Nama Group in south west Africa and its relationship to the Pan-African Geosyncline . *J. geol., 82,* 301-317.

Giddings, J.W.G. (1974) Precambrian Palaeomagnetism of Australia. Unpublished Ph.D. thesis, Australian National University, Canberra.

Glaessner, M.F. (1948) Stratigraphical nomenclature in Australia. *Aust. J. Sci., 11,* 7-9.

Glaessner, M.F. (1971) Geographic distribution and time range of the Ediacara Precambrian fauna. *Geol. Soc. Am. Bull., 82,* 509-514.

Glaessner, M.F. and Daily, B. (1959) The geology and Late Precambrian fauna of the Ediacara Fossil Reserve. *Rec. S. Aust. Mus., 13,* 369-401.

Glaessner, M.F., Preiss, W.V. and Walter, M.R. (1969) Precambrian Columnar Stromatolites in Australia : Morphological and Stratigraphic Analysis. *Science, 164,* 1056-1058.

Graham, J.W. (1949) The stability and significance of magnetism in sedimentary rocks. *J. geophys. Res., 5,* 131-167.

Graham, K.W.T. and Hales, A.L. (1961) Preliminary palaeomagnetic measurements on Silurian sediments from South Africa. *Geophys. J.R. astr. Soc., 5,* 318-325.

Haggerty, S.E. and Lindsley, D.H. (1969) Stability of the Pseudobrookite (Fe_2TiO_5) - Ferropseudobrookite ($FeTi_2O_5$) series. Annual Report Geophysical Laboratory, Carnegie Institution, 1968-69.

Hailwood, E.A. (1972) Palaeomagnetic studies on rock formations in the High Atlas and Anti-Atlas regions of Morocco. Unpublished Ph.D. thesis, University of Newcastle-upon-Tyne.

Hälbich, I.W. (1964) Observations on primary features in the Fish River Series and the Dwyka Series in south west Africa. *Trans. geol. Soc. S.Afr., 67,* 95-100.

Halls, H.C., (1976) A least-squares method to find a remanence direction from converging remagnetization circles. *Geophys. J. R. astr. Soc., 45,* 297-304.

Hargraves, R.B. (1976) Precambrian geologic history. *Science, 193,* 363-371.

Hargraves, R.B. and Burt, D.M. (1967) Palaeomagnetism of the Allard Lake anorthosite suite. *Can. J. Earth Sci., 4,* 357-369.

Harland, W.B. (1964) Critical evidence for a great infra-Cambrian glaciation. *Geol. Rundschau., 54,* 45-61.

Harland, W.B. and Bidgood, D.E.T. (1959) Palaeomagnetism in some Norwegian sparagmites and the late Precambrian Ice Age. *Nature, 184,* 1860-1862.

Harrington, H.J., Burns, K.L. and Thomson, B.P. (1973) Gambier-Beaconsfield and Gambier-Sorell Fracture zones and the movement of plates in the Australia-Antarctica-New Zealand region. *Nature, 245,* 109-112.

Helsley, C.E. (1965) Palaeomagnetic results from the Middle Cambrian of north west Africa (abstract). *Trans. Am. geop. Un., 46,* 67.

Hurley, P.M. (1972) Can the subduction process of mountain building be extended to Pan-African and similar ocogenic belts? *Earth Planet. Sci. Lett., 15,* 305-314.

Ileana, B. (1971) 1st European Earth Planet. Physics Colloquium, Reading (abstract).

Irving, E. (1964) Palaeomagnetism and its application to geological geophysical problems. *Wiley-Interscience,* New York, p. 399.

Irving, E. and Park, J.K. (1972) Hairpins and superintervals. *Can. J. Earth Sciences, 9,* 1318-1324.

Irving, E., Park, J.K. and Emslie, R.F. (1974) Palaeomagnetism of the Morin Complex. *J. geophys. Res., 79,* 5482-5490.

Irving, E. and McGlynn, J.C. (1976) Polyphase magnetization of the Big Spruce Complex, Northwest Territorries. *Can. J. Earth Sciences, 13,* 476-489.

Jackson, P.R. (1966) Hunt Oil-Planet Oil, well completion report No. 2, Yowalga. Hunt Oil Company Report (unpublished).

Jago, J.B. (1974a) The terminology and stratigraphic nomenclature of proven and possible glaciogenic sediments. *J. geol. Soc. Aust., 21,* 471-474.

Jago, J.B. (1974b) The origin of Cottons Breccia, King Island, Tasmania. *Trans. R. Soc. S.Aust., 98,* 13-28.

Jones, D.L. and McElhinny, M.W. (1966) Palaeomagnetic correlation of basic intrusions in the Pre-Cambrian of southern Africa. *J. geophys. Res., 71,* 543-552.

Juery, A., Lancelot, J.R., Hamet, J., Proust, F. and Allègre, C.J. (1974) L'âge des rhyolites du Précambrien III du Haut Atlas et le problème de la limite Précambrien-Cambrien. *2-éme Réun. Ann. des Sci. de la Terre, Nancy.*

Karner, G. (1975) Palaeomagnetism of the Brachina Formation at Hallett Cove. Unpublished M.Sc. thesis, Flinders University, Adelaide.

Keyser, F. de (1972) Proterozoic tillite at Duchess, Northwestern Queensland. *Bureau Mineral Resources Australian Bulletin, 125,* 1-6.

Klootwijk, C.T. (1973) Palaeomagnetism of Upper Bhander Sandstones from Central India and implications for a tentative Cambrian Gondwanaland reconstruction. *Tectonophysics, 18,* 123-145.

Klootwijk, C.T. (1975) A note on the palaeomagnetism of the late Precambrian Malani Rhyolites near Jodhpur, India. *J. geophys. Res., 41,* 189-200.

Krogh, T.E. (1973) A low-contamination method for hydrothermal decomposition of zircon and extraction of U and Pb for isotopic age determination. *Geochim. Cosmochim. Acta, 37,* 485-494.

Kröner, A. (1971) Late Precambrian correlation and the relationship between the Damara and Nama Systems of South West Africa. *Geol. Rundschau, 60,* 1513-1523.

Kröner, A. (1975) (Editor) Twelfth Annual Report 1974, Precambrian Research Unit, University of Cape Town, p. 60.

Kröner, A. (1977a) Non-synchroneity of late Precambrian glaciations in Africa. *J. geol. Res., 85,* 289-300.

Kröner, A. (1977b) Precambrian mobile belts of southern and eastern Africa - Ancient sutures or sites of ensialic mobility? A case for crustal evolution towards plate tectonics. *Tectonophysics, 40,* 101-135.

Kröner, A. and Germs, G.J.B. (1971) A re-interpretation of the Numees-Nama contact at Aussenkjer, South West Africa. *Trans. geol. Soc. S. Afr., 74,* 69-74.

Kröner, A. and Rakama, K. (1973) Late Precambrian glaciogenic rocks in southern Africa : a compilation with definitions and correlations. *Geol. Soc. Finland Bull., 45,* 79-102.

Kröner, A. and Hawkesworth, C. (1977) Late Pan-African emplacement ages for Rossing alaskitic granite (Damara belt) and Rooi Lepel bostonite (Gariep belt) in Namibia and their significance for the timing of metamorphic events. *20th Annual Report, Research Institute African Geology, Leeds, 1977.* p.14-17.

Laws, R.A. and Kraus, G.P. (1974) The regional geology of the Bonaparte Gulf Timor Sea area. *Aust. Pet. Expl. Assn. J., 14,* 77-84.

Lowry, D.C., Jackson, M.J., van der Graaff, W.J.E. and Kennerwell, P.J. (1972) Preliminary results of geological mapping in the Officer Basin, Western Australia. *Geol. Surv. W. Aust. Annual Report, 1972,* p.50-56.

Luck, G.R. (1970) The palaeomagnetism of some Cambrian and Ordovician sediments from the Northern Territory, Australia. *Geophys. J. R. astr. Soc., 20,* 31-39.

Luck, G.R. (1972) Palaeomagnetic results from Palaeozoic sediments of Northern Australia. *Geophys. J. R. astr. Soc., 28,* 475-487.

Major, R.B. (1968) Preliminary notes on the geology of the Birksgate 1:250,000 sheet area. *Geol. Surv. S.Aust. Report 66/122* (unpublished).

Martin, H. (1965) The Precambrian geology of South West Africa and Namaqualand. *Precambrian Research Unit, University of Cape Town,* p. 159.

McElhinny, M.W. (1964) Statistical significance of the fold test in palaeomagnetism. *Geophys. J. R. astr. Soc., 8,* 338-340.

McElhinny, M.W. (1966) The palaeomagnetism of the Umkondo lavas, eastern southern Rhodesia. *Geophys. J. R. astr. Soc., 10,* 375-381.

McElhinny, M.W. (1970) Palaeomagnetism of the Cambrian Purple Sandstones from the Salt Range, West Pakistan. *Earth Planet Sci. Lett., 15,* 218-219.

McElhinny, M.W. (1973) Palaeomagnetism and plate tectonics. Cambridge University Press, Cambridge, p. 358.

McElhinny, M.W. and Luck, G.R. (1970) The palaeomagnetism of the Antrim Plateau Volcanics of Northern Australia. *Geophys. J. R. astr. Soc., 20,* 191-205.

McElhinny, M.W., Luck, G.R. and Edwards, D.J. (1971) Large-volume magnetic field-free space for thermal demagnetization and other studies in palaeomagnetism. *Pure Appl. Geophys., 90,* 126-130.

McElhinny, M.W., Giddings, J.W.G. and Embleton, B.J.J. (1974) Palaeomagnetic results and late Precambrian glaciations. *Nature, 248,* 557-561.

McElhinny, M.W. and Evans, M.E. (1976) Palaeomagnetic results from the Hart Dolerite of the Kimberley Block, Australia. *Precambrian Res. 3,* 231-241.

McElhinny, M.W. and Embleton, B.J.J. (1976) Precambrian and Early Palaeozoic palaeomagnetism in Australia. *Phil. Trans. R. Soc. Lond., A280,* 417-431.

McElhinny, M.W. and McWilliams, M.O. (1977) Precambrian geodynamics : a palaeomagnetic view. *Tectonophysics, 40,* 137-159.

McElhinny, M.W., Cowley, J.A. and Edwards, D.J. (in press) Palaeomagnetism of some rocks from India and Kashmir. *Tectonophysics.*

McQueen, D.J., Scharnberger, C.K., Scharon, L. and Halpern, M. (1972) Cambro-Ordovician palaeomagnetic pole position and rubidium-strontium total rock isochron for charnokitic rocks from Mirnyy Station, east Antarctica. *Earth Planet. Sci. Lett., 16,* 433-438.

McWilliams, M.O. and Dunlop, D.J. (1975) Precambrian palaeomagnetism : magnetizations reset by the Grenville orogeny. *Science, 190,* 269-272.

McWilliams, M.O. and Dunlop, D.J. (1977) Grenville palaeomagnetism and tectonics. Submitted to *Can. J. Earth Sci.*

Mawson, D. and Sprigg, R.C. (1950) Subdivision of the Adelaide System. *Aust. J. Sci., 13,* 69-72.

Morris, W.A. (1977) Palaeolatitude of glaciogenic upper Precambrian Rapitan group and the use of tillites as chronostratigraphic marker horizons. *Geology, 5,* 85-88.

Morris, W.A. and Roy, J.L. (1977) Discovery of the Hadrynian Polar Track and the Grenville problem revisited. *Nature, 266,* 689-692.

Nagata, T. (1961) Rock Magnetism. *Maruzen, Tokyo, 2nd edition,* p. 350.

Peers, R. (1969) A comparison of some volcanic rocks of uncertain age in the Warburton Range area. *Geol. Surv. W. Aust. Ann. Rep. 1968,* pp, 57-61.

Piper, J.D.A. (1972) A palaeomagnetic study of the Bukoban System, Tanzania. *Geophys. J. R. astr. Soc., 28,* 111-127.

Piper, J.D.A. (1973) Latitudinal extent of late Precambrian glaciations. *Nature, 244,* 342-344.

Piper, J.D.A. (1975a) Palaeomagnetic correlations of Precambrian formations of east-central Africa and their tectonic implications. *Tectonophysics, 26,* 135-161.

Piper, J.D.A. (1975b) The palaeomangetism of Precambrian igneous and sedimentary rocks of the Orange River Belt in South Africa and South West Africa. *Geophys. J. R. astr. Soc., 40,* 313-344.

Piper, J.D.A. (1976) Palaeomagnetic evidence for a Proterozoic super-continent. *Phil. Trans. R. Soc. Lond., A280,* 469-490.

Piper, J.D.A., Briden, J.C. and Lomax, K. (1973) Precambrian Africa and South America as a single continent. *Nature, 245,* 244-248.

Prichard, C.E. and Quinlan, T. (1962) The geology of the southern half of the Hermannsburg 1:250,000 Sheet. *Bureau of Mineral Resources Australian Report 61.*

Pullaiah, G., Irving, E., Buchan, K.L. and Dunlop, D.J. (1975) Magnetization changes caused by burial and uplift. *Earth Planet. Sci. Lett., 28,* 133-143.

Raggatt, H.G. (1950) Stratigraphic nomenclature. *Aust. J. Sci., 12,* 170-173.

Range, P. (1912) Geologie des deutschen Namalandes. *Beitr. geol. Erdforsch. dt. Schutzgeb. II.*

Reid, A.B. (1968) A palaeomagnetic study of the Sijarira Group, Rhodesia. Unpublished M.Phil. thesis, University of London.

Roberts. J.D. (1976) Late Precambrian dolomites, Vendian glaciation, and synchroneity of Vendian glaciations. *J. geol. Res., 84,* 47-63.

Roy, J.L. and Park, J.K. (1974) The magnetization process of certain red beds. Vector analysis of chemical and thermal results. *Can. J. Earth Sci., 11,* 437-471.

Roy, J.L. and Lapointe, P.L. (1976) The palaeomagnetism of Huronian red beds and Nippising diabase; Post-Huronian igneous events and apparent polar wander path for the interval -2300 to -1500 Ma for Laurentia. *Can. J. Earth. Sci., 13,* 749-773.

Rutland, R.W.R. (1973) Tectonic evolution of the continental crust of Australia. *In:* Continental Drift, Sea Floor Spreading and Plate Tectonics : Implications to the Earth Sciences, (ed.) D.H. Tarling and S.K. Runcorn, Academic Press (London) 1973, 1003-1025.

Rutland, R.W.R. and Murrell, B. (1976) Tectonics of the Adelaide Fold Belt (abstract). *Geological Society of Australia, First Geological Convention on Proterozoic Geology, Adelaide.*

Scheibner, E. (1974) Fossil fracture zones, segmentation and correlation problems in the Tasman Fold Belt system. *In:* The Tasman Geosyncline : A Symposium. (eds.) A.K. Denmean, G.W. Tweedale and A.F. Wilson, Geol. Soc. Aust. Qld. Div. 1974.

Schermerhorn, L.J.G. (1974) Late Precambrian mixtites : glacial and/or nonglacial? *Amer. J. Sci., 274,* 673-824.

Schermerhorn, L.J.G. (1975) Tectonic framework of late Precambrian supposed glacials, in : Wright, A.E. and Moseley, F. (eds.) *Ice Ages Ancient and Modern : Geol. J. Special Issue, 6,* 241-274.

Schermerhorn, L.J.G. (1976) Reply to discussion by Deynoux and Trompette (1976) : Late Precambrian mixtites : glacial and/or nonglacial? Dealing especially with the mixtites of west Africa. *Amer. J. Sci., 276,* 1315-1324.

Schmalz, R.F. (1969) Deep water evaporite deposition : A genetic model. *Am. Assn. Pet. Geol. Bull., 53,* 798-823.

Schmidt, P.W. (1976) Late Palaeozoic and Mesozoic palaeomagnetism of Australia. Unpublished Ph.D. thesis, Australian National University, Canberra.

Schopf, J.W. (1968) Microflora of the Bitter Springs Formation, Late Precambrian, central Australia. *J. Paleont., 42,* 651-688.

Shackleton, R.M. (1969) Displacement within continents, *in: Time and Place in Orogeny, Geol. Soc. London Spec. Publ, 3,* 1-7.

Sloss, L.L. (1969) Evaporite deposition from layered solutions. *Am. Assn. Pet. Geol. Bull., 53,* 776-789.

Smith, A.G. and Hallam, A. (1970) The fit of the southern continents. *Nature, 255,* 139.

Solomon, M. (1969) The nature and possible origin of the pillow lavas and hyaloclastic breccias of King Island, Australia. *Q. J. Geol. Soc. Lond., 124,* 153-169.

Sprigg, R.C. (1952) Sedimentation in the Adelaide Geosyncline and the formation of the continental terrace. *In:* Sir Douglas Mawson Anniv. Volume, Ed. M.F. Glaessner and R.C. Sprigg, Univ. of Adelaide 1952, 153-159.

Stacey, F.D. and Bannerjee, S.K. (1974) *The physical principles of rock magnetism.* Elsevier, Amsterdam, p. 195.

Tarling, D.H. (1974) A palaeomagnetic study of Eocambrian tillites in Scotland. *J. geol. Soc. Lond., 130,* 163-177.

Thomson, B.P. (1969) Precambrian basement cover : The Adelaide System. *In:* Handbook of South Australian Geology, (ed.) L. Parkin. Geol. Surv. S. Aust., 1969.

Thompson, R. (1973) South American Palaeozoic palaeomagnetic results and the welding of Pangaea. *Earth Planet. Sci. Lett., 18,* 266-278.

Ueno, H. and Irving, E. (1976) Palaeomagnetism of the Chibougamau greenstone belt, Quebec, and the effects of Grenvillian post-orogenic uplift. *Precambrian Research, 3,* 303-315.

Veevers, J.J. (1976) Early Phanerozoic events on and alongside the Australasian - Antarctic platform. *J. Geol. Soc. Aust., 23,* 183-206.

Veevers, J.J. and McElhinny, M.W. (1976) The separation of Australia from other continents. *Earth-Science Reviews, 12,* 139-159.

Vincenz, S.A. and Bruckshaw, J. McG. (1960) Note on the probability distribution of a small number of vectors. *Proc. Camb. Phil. Soc., 56,* 21-26.

Walter, M.R. (1972) Stromatolites and Biostratigraphy of the Australian Precambrian and Cambrian. Special Papers in *Palaeontology, II,* The Palaeontological Association, London.

Warris, B.J. (1973) Plate tectonics and the evolution of the Timor Sea, northwest Australia. *Aust. Pet. Expl. Assn. J., 13,* 13-18.

Watson, G.S. (1956a) A test for randomness of directions. *Mon. Nat. Roy. Ast. Soc. Geophys. Suppl., 7,* 160-161.

Watson, G.S. (1956b) Analysis of dispersion on a sphere. *Mon. Nat. Roy. Ast. Soc. Geophys. Suppl., 7,* 153-159.

Weand, B.L., Hoehn, R.C. and Parker, B.C. (1976) Trace element distributions in an Antarctic meromictic lake. *Hydrobiological Bulletin, 10,* 104-114.

Wellman, H.W. and Wilson, A.T. (1963) Salts on sea ice in McMurdo Sound, Antarctica. *Nature, 200,* 462-463.

Wells, A.T., Stewart, A.J., Cook, P.J. and Shaw, R.D. (1967) The geology of the north-eastern part of the Amadeus Basin, Northern Territory. *Bureau Min. Resources Aust. Report, 113.*

Wells, A.T., Forman, D.J., Ranford, L.C. and Cook, P.J. (1970) Geology of the Amadeus Basin, central Australia. *Bureau Min. Resources Bulletin, 100,* Canberra, 1970.

Wensink, H. (1972) The palaeomagnetism of the Salt Psuedomorph beds of Middle Cambrian age from the Salt Range, West Pakistan. *Earth Planet. Sci. Lett., 16,* 189-194.

White, A.J.R., Compston, W. and Kleeman, A.W. (1967) The Palmer Granite - A study of a granite within a regional metamorphic environment. *J. Petrology, 8,* 29-50.

Williams, G.E. (1974) Discussion of late Precambrian glacial climate and the earth's obliquity. *J. Geol. Soc. Lond., 130,* 599-601.

Williams, G.E. (1975) Late Precambrian glacial climate and the earth's obliquity. *Geol. Mag., 112,* 441-465.

Wilson, R.L. and Haggerty, S.E. (1966) Reversals of the earth's magnetic field. *Endeavour, 25, (95),* 104-109.

Wilson, R.L. and Watkins, N.D. (1967) Correlation of magnetic polarity and petrological properities in Columbia Plateau basalts. *Geophys. J. R. astr. Soc., 12,* 405-424.

Young, G.M. (1976a) Iron formation and glaciogenic rocks of the Rapitan Group, Northwest Territories, Canada. *Precambrian Research, 3,* 137-158.

Young, G.M. (1976b) Late Precambrian mixtites : glacial and/or nonglacial? *Geol. Mag.*, *276*, 366-370.

Zijderveld, J.D.A. (1968) Natural remanent magnetizations of some intrusive rocks from the Sør Rondane Mountains, Queen Maud Land, Antarctica. *J. Geophys. Res.*, *73*, 3773-3785.

APPENDIX A

SITE LOCATIONS

ROCK UNIT	SITE(S)	LATITUDE(S) D	M	LONGITUDE (E) D	M
Wooltana Volcanic	1-20	30	22.1	139	26.7
	21-24	30	19.4	139	27.7
Copley Quartzite	1	30	35.7	138	20.8
	2	30	18.0	139	26.4
	3-7	30	26.9	138	12.7
Merinjina Tillite	1,2,18-21	30	18.4	139	24.3
	3,4	30	27.2	139	23.8
	5-11	30	21.8	139	25.3
	12-17	30	21.2	139	25.1
Tapley Hill Formation (samples)	4,6,7B				
	8-12	30	20.9	139	24.0
	27	30	27.0	139	23.3
	28,31,32	30	39.5	138	30.1
Angepena Formation	1-5	30	32.0	139	18.9
Yerelina Subgroup	1-5	30	06.1	139	09.6
	6,7	30	06.5	139	10.4
	8-10	30	13.1	139	11.3
	11-17	30	14.3	138	54.6
Brachina Formation	1-4	30	44.0	138	25.0
	5,6	30	32.2	138	46.8
	7,8	30	32.7	138	36.7
	9,10	30	07.6	138	31.3
	11,12	30	51.5	139	16.5
	13,14	30	51.5	139	15.7
Bunyeroo Formation	4-6	31	20.1	138	35.0
	7-9	30	51.7	139	12.6
	10,11	31	26.4	138	32.9
	12	31	33.1	138	38.4
Pound Quartzite	3-5	31	20.0	138	33.0
	6,7	31	31.6	138	35.1
Areyonga Formation	1-10	23	46.9	133	03.8
	11,12	23	50.2	135	15.8
Pertatataka Formation	1-4	23	50.3	135	16.1
	5-15	23	52.9	135	20.7
	16	24	02.9	135	05.8
	17	24	03.6	135	06.1
Estaughs Formation	1-6	17	06.0	125	38.1
Egan Formation (samples)	1-15	18	43.9	126	38.8

ROCK UNIT	SITE(S)	LATITUDE(S) D	M	LONGITUDE (E) D	M
Lubbock Formation	1	18	44.1	126	40.7
	2	18	46.8	126	52.0
	4	18	36.6	126	53.6
Tean Formation (samples)	1-4	18	44.1	126	46.3
	5-8	18	46.8	126	52.0
Ranford Formation (samples)	7-12	17	02.7	128	28.9
Mt Birnie Dolomite	1-6	21	16.3	139	56.3
Devoncourt Limestone	1-4	21	20.9	140	00.7
	5	21	22.3	140	02.2
Cottons Breccia	1-6	40	00.2	144	09.8
	7-12	40	02.0	144	09.1
	13-15	40	00.9	144	09.4
Cottons Volcanics	1-6	40	00.2	144	09.8
	7-9	40	00.9	144	09.4
Nama Group: Fish River Subgroup	NFA	24	49.9	17	00.4
	NFB	24	49.6	17	02.1
	NFC	25	18.2	16	54.5
	NFD	26	47.7	17	24.3
	NFE	26	46.9	17	33.0
	NFF	26	46.9	17	33.6
	NFG	26	45.0	17	40.0
	NFH	26	45.4	17	41.4
	NFI	26	45.7	17	43.2
	NFK	26	47.5	17	47.0
	NFL	26	44.7	17	45.4
Nama Group: Schwarzrand Subgroup	NSA	24	50.7	16	48.6
	NSB	24	49.1	16	33.1
	NSC	25	18.9	16	52.8
	NSD	25	18.9	16	52.9
	NSE	26	04.0	17	01.5
	NSF	26	29.6	17	13.6
	NSG	26	29.3	17	13.6
	NSH	26	29.1	17	15.2
	NSI	26	42.9	17	14.4
	NSK	26	45.4	17	14.1
	NSL	26	46.5	17	15.8
	NSM	26	47.3	17	17.5
	NSN	26	51.2	17	20.9
	NSO	26	51.5	17	20.8
	NSP	26	48.3	17	23.8
	NSQ	27	24.3	17	56.8
	NSR	27	24.3	17	56.9
	NSS	27	25.7	17	57.0
	NST	27	27.5	17	55.4
	NSU	27	30.8	17	49.6
	NSV	27	30.7	17	49.5
	NSW	27	08.0	18	12.1
	NSX	27	08.5	18	10.5
	NSY	27	10.9	18	37.5

ROCK UNITS	SITE(S)	LATITUDE(S) D	M	LONGITUDE (E) D	M
Nama Group: Kuibis Subgroup	NKA	26	58.0	18	45.1
Damara Supergroup: Mulden Group	DMA,B,C	19	13.7	15	05.5
	DMD,E,F	19	16.4	14	57.5
	DMG	19	15.9	14	57.6
	DMH	19	20.0	15	01.3
Damara Supergroup: Chuos Formation	DCA,B,C	18	40.0	14	00.7
	DCD	18	39.5	14	01.3
	DCE	18	29.8	13	55.0
	DCF	18	07.7	13	52.8
	DCG	19	05.9	14	31.0
	DCH	19	05.1	14	30.5
Damara Supergroup: Tsumeb Subgroup	DTA	18	07.7	13	52.8
	DTB	19	05.1	14	30.5
Damara Supergroup: Nosib Group Quartzites	DNA,B,C	17	25.1	14	18.5
	DND	17	25.1	14	18.5
	DNE	19	02.1	14	22.1
	DNF	19	09.5	14	32.4
Nosib Group: Blaubeker Formation	NBA,B,C	23	54.0	16	29.0
	NBD	23	55.0	16	28.3
	NBE,F,G	23	54.0	16	29.0
	NBH	23	54.3	16	29.1

APPENDIX B

An explanation of the two systems employed in presenting demagnetization data for thermal, alternating field and chemical demagnetization experiments. Refer to §1.2.4 for magnetization vector notation. Magnetization vector directions are always plotted with respect to present horizontal in demagnetization plots.

B.1 Stereographic projections and normalized intensity plots.

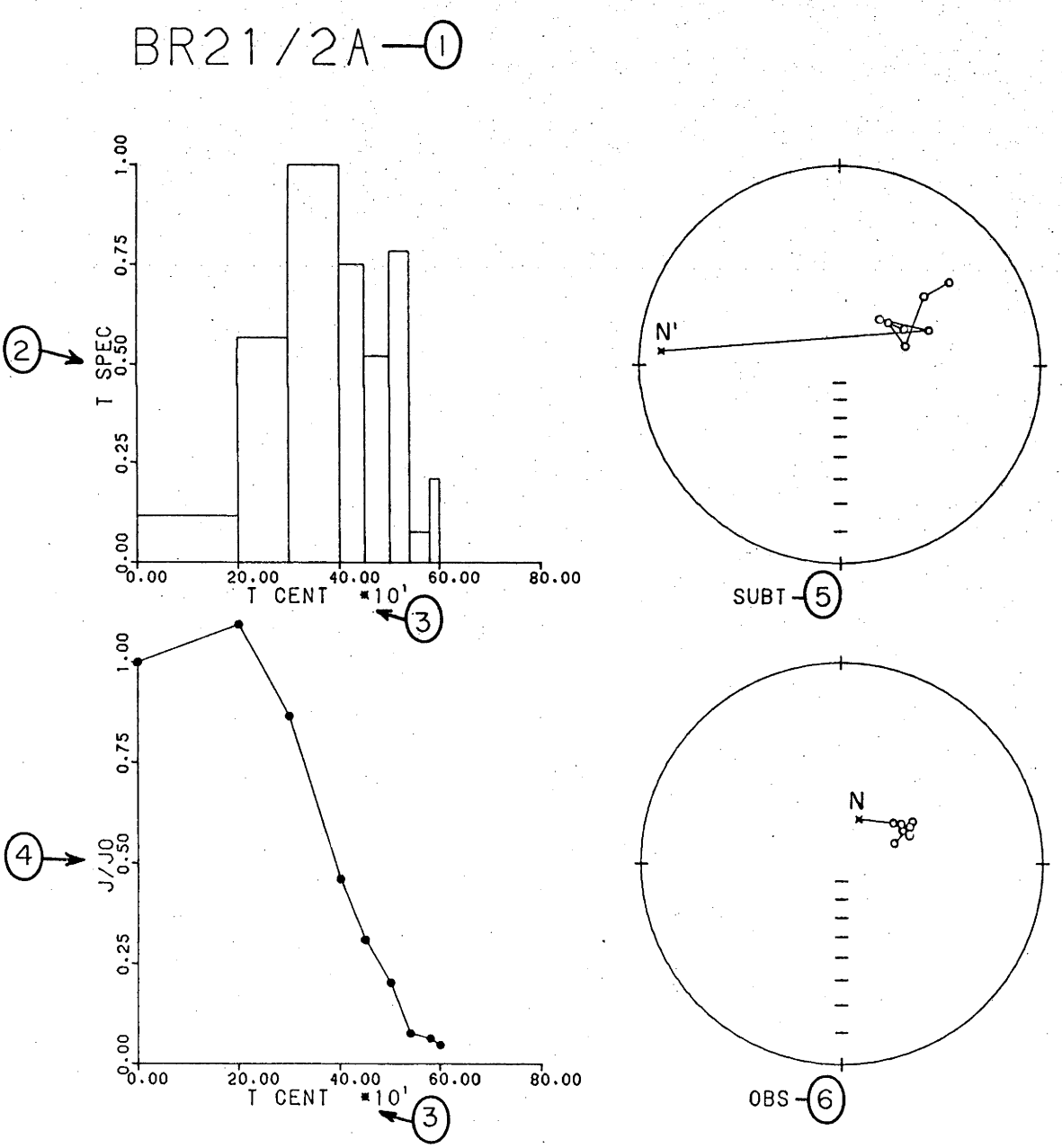

KEY:

1. Specimen identification.
2. Normalized blocking temperature spectrum : height of histogram bar is proportional to $(\Delta J/\Delta T)_i$ for the ith demagnetization step. Values are normalized to $(\Delta J/\Delta T)_{max}$ = 1.0. For AF demagnetization, normalized coercivity spectrum values $(\Delta J/\Delta \tilde{H})_i$ are plotted; for chemical demagnetization, chemical resistance spectrum values $(\Delta J/\Delta t)_i$ are plotted.
3. Demagnetization treatment : temperature (°C), peak AF intensity (mTesla), time in acid bath (hours).
4. Normalized intensity : values of the ratio $|\vec{J}(k)|/|\vec{J}(0)|$ are plotted versus demagnetization treatment value.
5. Equal angle (stereographic) projection of vectors subtracted between successive demagnetization steps : $\Delta\vec{J}(m-n)$, n=m+1. Open (closed) circles (squares) denote negative (positive) inclination; reference ticks 10° apart. North declination to top; east declination 90° clockwise from top; reference ticks 90° apart. Lines connect successive subtracted vector direction $\Delta\vec{J}(0\text{-}1)$ indicated by N'; plotted as 'x'('*') for negative (positive inclination.
6. Equal angle (stereographic) projection of observed vector directions $\vec{J}(k)$ after each successive demagnetization step. Conventions as in (5) above. Initial NRM direction $\vec{J}(0)$ indicated by N.

B.2 Orthogonal vector projections.

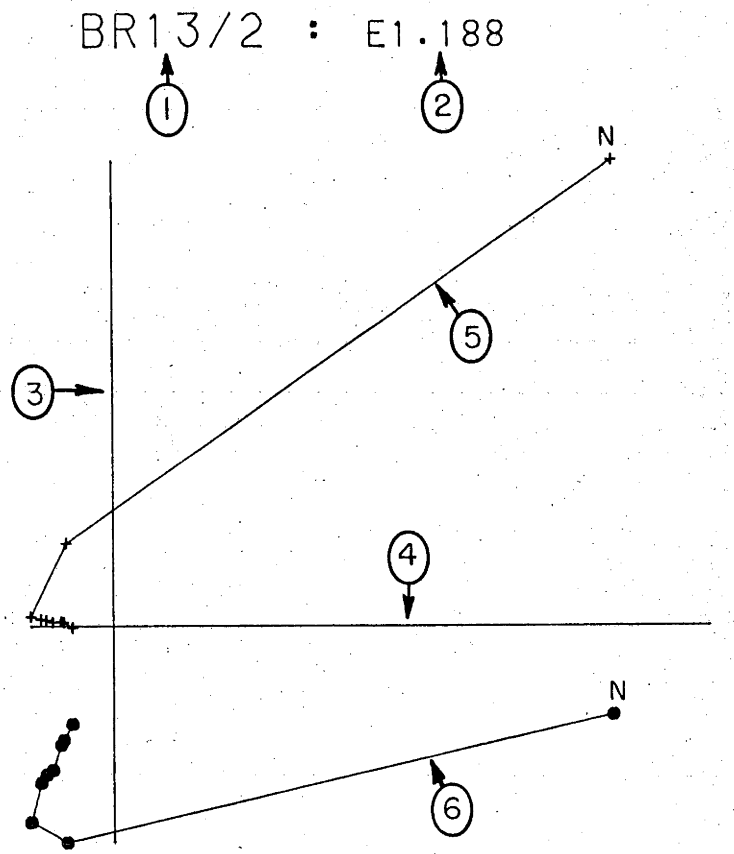

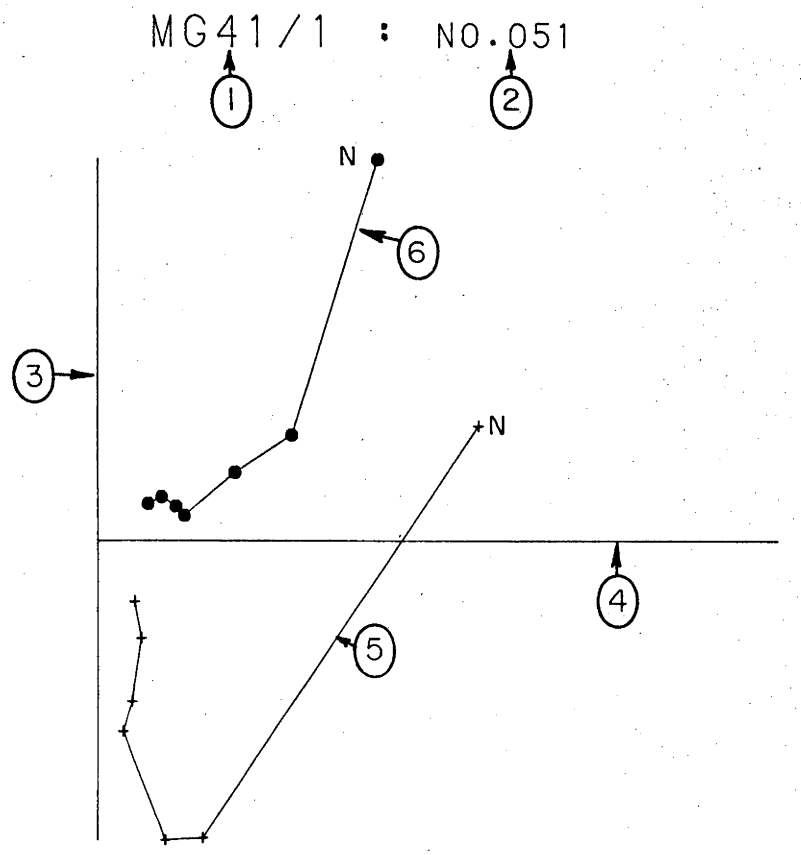

KEY:

1. Specimen identification.
2. Projection type and scale factor : the first letter denotes whether the projection is in the north-south vertical plane (N) or in the east-west vertical plane (E). the following axis conventions apply:

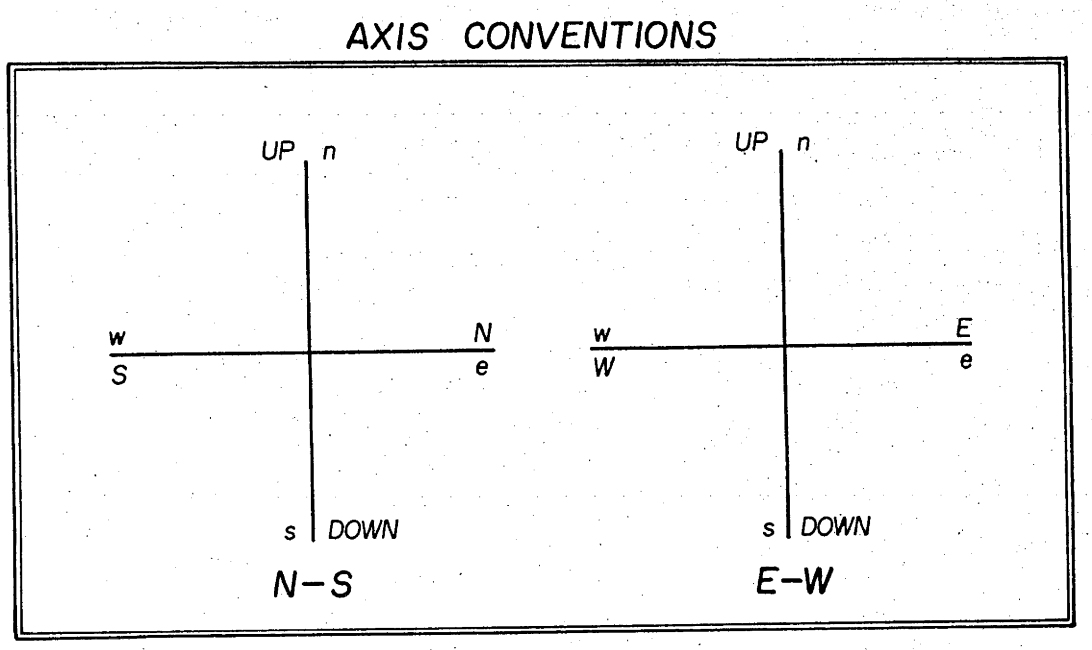

Upper case letters above refer to the projection of the vector on the vertical plane; lower case letters above refer to the horizontal plane.

The number immediately following the plane identification letter is a scaling factor. When multiplied by 4.0 this factor expresses the total length of either of the axes in mAm^{-1}; thus a scaling factor of 0.05 indicates that the full axis length represents a magnetization intensity of 0.2 mAm^{-1}.

3. Vertical axis for vertical plane projection; north-south axis for horizontal plane projection.
4. East-west axis for horizontal plane projection; north-south (east-west) axis for north-south (east-west) vertical plane projection.

5. Projection of endpoint of magnetization vector upon the north-south (or east-west) vertical plane after successive demagnetization steps. Endpoint of initial NRM vector indicated by N.
6. Projection of endpoint of magnetization vector upon the horizontal plane after successive demagnetization steps. Endpoint of initial NRM vector indicated by N.

Tectonophysics, 40 (1977) 137—159

PRECAMBRIAN GEODYNAMICS — A PALAEOMAGNETIC VIEW

M.W. McELHINNY and M.O. McWILLIAMS

Research School of Earth Sciences, Australian National University, Canberra, A.C.T. (Australia)

(Received November 2, 1976)

ABSTRACT

McElhinny, M.W. and McWilliams, M.O., 1977. Precambrian geodynamics — a palaeomagnetic view. In: M.W. McElhinny (editor), The Past Distribution of Continents. Tectonophysics, 40: 137—159.

The problem of the origin of the major Precambrian orogenic belts presently located within continents is examined using palaeomagnetic data for Africa, Australia and North America. For the period 2300—1900 m.y. data from the West African and Kaapvaal cratons form a coherent set with poles of similar age from each craton falling consistently on a combined apparent polar wander path constructed for this time interval. For the interval 1100—700 m.y. data from the Kalahari and Congo cratons likewise form a coherent set. The consistency of the data strongly suggests that these cratons were not previously widely separated and then converged to form the Pan African and older orogenic belts of Africa. New isotopic information drastically alters the shape of the African apparent polar wander path in the time interval 1250—1050 m.y. The evidence for a Precambrian supercontinent based on the matching of this section of the path with the Logan Loop of North America is no longer tenable.

Data from Australia for the time-interval 2500—1100 m.y. also form a coherent set irrespective of the craton from which they were derived. This consistency again suggests that the Ophthalmian, Musgrave and Albany—Frazer belts did not arise from the convergency of widely separated cratons. The extensive data from North America likewise form a coherent set in the time-interval 2600—1400 m.y. using data from the Superior, Churchill, Nain, Bear and Slave Provinces and from the Bear-Tooth uplift of Wyoming and Montana. The Hudsonian orogeny cannot therefore be the result of plate convergence in agreement with that found for the belts on other continents. Results from the Grenville Province are shown to have been derived during a period of post-orogenic uplift and cooling and can be related to thermochrons deduced from K—Ar dating of Grenville rocks. The apparent polar wander path in the interval 1100—700 m.y. derived from these results shows an extension of the Logan Loop into a Grenville Loop. Independent confirmation of this extension is seen in preliminary results reported from the Grand Canyon sequence.

Palaeomagnetic data preclude plate-tectonic models involving the convergence of previously widely separated cratons to explain all of the Precambrian orogenic belts examined. Uncertainties and inherent errors associated with the data do not, however, exclude models involving the opening and closing of small (500—1000 km) intercratonic oceans. The requirement, however, is that these oceans must always open and close so as to return the cratons to their same relative positions. Precambrian tectonic mechanisms thus cannot have been the same as present-day plate tectonics. Plate tectonics as seen in the Phaner-

ozoic may therefore have evolved gradually from a more primitive form operating during the Precambrian.

INTRODUCTION

Twenty years have passed since it was first seriously argued from palaeomagnetic data that the apparent polar wander paths for various continents differed in a systematic way (Runcorn, 1956; Irving, 1956) and that continental drift must have occurred at least during the Phanerozoic. Ten years passed before the theory of plate tectonics emerged as the geotectonic framework within which these horizontal displacements of the earth's crust could so readily be fitted (McKenzie and Parker, 1967; Morgan, 1968; Le Pichon, 1968). The general geological consequences have since been enumerated (Dewey and Bird, 1970a,b) and the theory has been widely and successfully applied to the interpretation of Phanerozoic orogenic belts such as the Appalachian—Caledonian belts (Dewey, 1969) and the Uralides (Hamilton, 1970). The introduction of the now widely used magnetic and thermal cleaning techniques (As and Zijderveld, 1958; Irving et al., 1961) to palaeomagnetic studies led to the rapid accumulation of data of good quality from many different parts of the world. These results have demonstrated that the geological interpretation of Phanerozoic orogenic belts in terms of plate-tectonic theory is essentially correct (McElhinny, 1973).

In spite of the successful application of plate-tectonic theory to Phanerozoic geology there has been a widespread feeling among those who study Precambrian geology that the nature of geological activity has changed during the earth's history (e.g. Sutton and Watson, 1974). For example, much controversy has centred about the older orogenic domains of Africa, which have been variously interpreted as having been formed either by internal deformation (ensialic belts; Clifford, 1968) or as marking the sites of continental collision in a plate-tectonic model (Burke and Dewey, 1972). The earliest apparent polar wander paths for North America (Du Bois, 1962) and Africa (McElhinny et al., 1968) both showed that relative motion between present continental blocks and the pole occurred throughout the Precambrian at least as far back as 2700 million years ago. In the past decade therefore, much activity has been concentrated on determining the pattern of these paths in relation to the distribution of ancient orogenic belts. Even so, the number of Precambrian palaeomagnetic results covering the 2700—600 m.y. interval is only about 200 compared with about 1500 for the past 600 m.y. (Briden, 1976).

The state of the art in Precambrian palaeomagnetism is thus not unlike that of 20 years ago with respect to Phanerozoic studies, when the first systematic differences between apparent polar wander paths could be seen. Just as those first Phanerozoic paths provided fundamental evidence relating to tectonics in the last 600 m.y., so too are the new Precambrian paths provid-

ing clues as to the nature of Precambrian tectonics. In this paper, we review palaeomagnetic results from the Precambrian of Africa, Australia and North America insofar as they relate to the origin of some of the major orogenic belts in those continents.

REPRESENTATION OF PRECAMBRIAN POLE PATHS

When considering Phanerozoic palaeomagnetic data, it is common to be able to assign results to a particular subdivision of a geological period either from stratigraphic evidence and fossil control or from radiometric dating. The accumulation of results from a single continental block for each of these periods enables overall means to be calculated period by period or subdivision. Whereas there may be some internal scatter of the order 10—15° between results from the same period for a particular block, the period means themselves can be determined with high precision and relatively small errors. The resulting pole paths can in many cases be defined fairly precisely (McElhinny, 1973). This is not the case in Precambrian studies, because one is forced to rely exclusively on radiometric ages; in the 10^9 year region, age uncertainties are often greater than the length of the Phanerozoic geological periods. Thus, it is not possible to average results period by period and it is necessary to plot all the data and determine the general trend (Spall, 1971) as representing the best estimate of the apparent polar wander path. The inability to determine sequentially averaged results amplifies the inherent inaccuracies present in individual palaeomagnetic results. These inaccuracies arise in a number of ways, they may be associated with sampling errors due to minor local tectonics or they may be due to laboratory problems associated with isolating and measuring a primary remanence. Also, periods of rapid apparent polar motion combined with frequent reversals of the earth's magnetic field can lead to difficulty in the interpretation of already sparse data. The result is that Precambrian apparent polar wander paths are not represented by period means as in the Phanerozoic, but must be represented by swathes of width 10—15° arising from the inherent inaccuracies in *individual* results. The concept of a swathe was first suggested by Beck (1970) and introduced by Piper et al. (1973).

There are other complications associated with Precambrian palaeomagnetism which are more serious than in Phanerozoic studies. The older the rock formation, the more likely it is to have been subjected to thermal or chemical overprinting of the original (primary) magnetization, with possible concomitant tectonic re-orientation. Laboratory studies using a variety of techniques such as alternating field demagnetization, high- and low-temperature thermal demagnetization, and chemical demagnetization coupled with detailed vector analysis of the various magnetic components (multicomponent analysis) can reveal the presence of magnetizations acquired at different times under different conditions (Roy and Park, 1974; Buchan and Dunlop, 1976). However, only field tests (baked contact or fold tests) can establish

the relative timing of such multicomponent magnetizations. Alternatively, it can be assumed that the magnetizations with the higher blocking temperatures are the oldest in any slowly cooled rock (Irving et al., 1974a); this is strictly true only if all the magnetic components are of thermal origin (TRM). This situation arises commonly in Precambrian terrains and is due either to slow initial cooling or to subsequent heating during burial and regional metamorphism and slow cooling during post-orogenic uplift. The magnetizations may be related to radiometric ages determined by different methods, whole-rock Rb—Sr ages to the higher blocking temperatures and mineral K—Ar ages to the lower blocking temperature magnetizations (Irving et al., 1974a). The uninitiated must tread warily in attempting to interpret Precambrian palaeomagnetic data; without a clear understanding of the evidence related to the timing of the various magnetizations which may be present in a particular rock unit, an interpretation could be completely incorrect.

On the assumption that the time-averaged field is that of an axial geocentric dipole, palaeomagnetic poles of the same general age from regions that have not suffered relative displacement should agree with one another. Extended to a time-sequence of poles represented by an apparent polar wander path, various situations arise according to the applicable tectonic model for intercratonic orogenesis as illustrated in Fig. 1. In the diagram we imagine

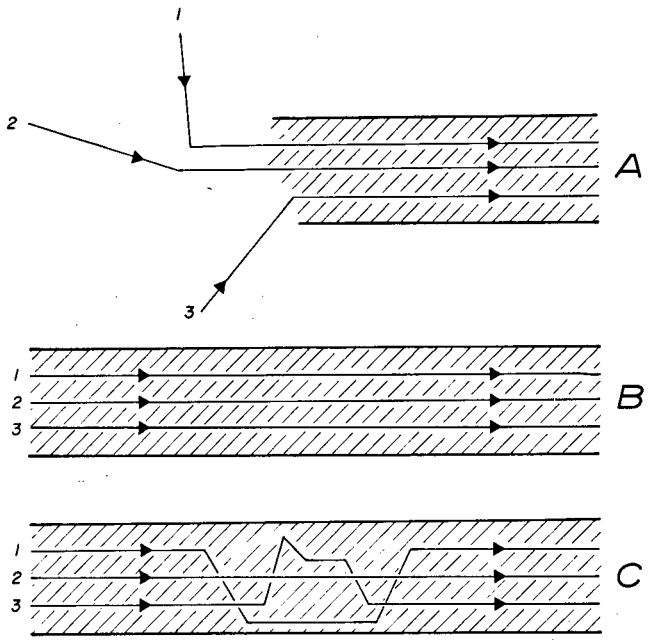

Fig. 1. Expected apparent polar wander paths for differing tectonic mechanisms (after Piper et al., 1973). A. Plate-tectonic model. B. Fixed plate model. C. Combination of A and B representing opening and closing of small intercratonic oceans.

three cratonic blocks each defined by its separate apparent polar wander path 1, 2 or 3. If the plate-tectonic model of convergence of widely separated blocks is valid to explain the orogenic belts then Fig. 1A should describe the apparent polar wander paths of each of the blocks. The three paths will diverge prior to the time of collision and after convergence of all three blocks, a unified common path results represented by the swathe. Generally speaking, the separate paths would be represented by a widening of the swathe beyond its normal limits coupled with an inability to contain all the data within a single swathe. If on the other hand the orogenic belts were formed by internal deformation without relative movement, the data from all three blocks can be constrained to a single common swathe, as illustrated in Fig. 1B. The width of the swathe is large enough to allow limited relative movement and/or the opening and closing of relatively small (500—1000 km) oceans, as illustrated in Fig. 1C. However, such openings and closings must be such that the blocks *always return to their original relative positions*, as we shall illustrate in the following sections. The "small-movement" model illustrated in Fig. 1C therefore cannot be distinguished from the static model, Fig. 1B.

AFRICA

The first palaeomagnetic results from the Precambrian of Africa suggested there might have been little apparent polar wander for long periods of the Precambrian (Gough et al., 1964). As subsequent data accumulated, it soon became apparent that the Precambrian polar wander path was similar in length and rates of polar movement to Phanerozoic paths (McElhinny et al., 1968; Piper et al., 1973). Although the African data are spread in age from about 2700 m.y. through to latest Precambrian, there is a concentration of results in the time ranges 2300—1900 and 1100—650 m.y., with sparse data in the intervening period. The distribution of sampling localities with respect to the African cratons in these two intervals is illustrated in Fig. 2.

2300—1900 m.y.: the older orogenic belts of Africa

In the older time interval (Fig. 2A) the data are derived largely from the West African and Kaapvaal cratons with only a single result from the Congo craton. To avoid repetition, the details of the individual results will not be given but readers may refer to Appendix I in Piper (1976). The apparent polar wander path derived from these data is illustrated in Fig. 3, after Piper et al. (1973). For this interval it is possible to construct an apparent polar wander path in the form of a swathe which contains all the data irrespective of craton, without violating any of the age constraints upon magnetization times. These data support the single continent model (Fig. 1B), and indicate that intervening orogenic belts created since 1900 m.y. could not have involved major relative movements.

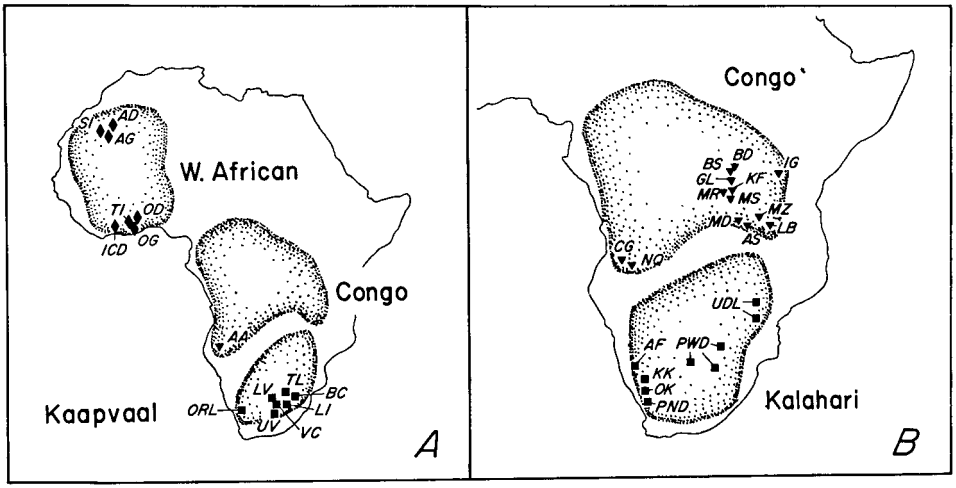

Fig. 2. Palaeomagnetic sampling localities for African Precambrian (details in summary by Piper, 1976). A. 2300—1900 m.y.: *AA* = Angola anorthosite, *AD* = Aftout dolerite, *AG* = Aftout gabbro, *BC* = Bushveld complex, *ICD* = Ivory Coast dolerites, *LI* = Losberg intrusion, *LV* = Lower Ventersdorp lavas, *OD* = Obuasi dolerite, *OG* = Obuasi greenstone body, *ORL* = Orange River lavas, *SI* = Syntectonic igneous rocks, *TI* = Tarkwaian intrusions, *TL* = Transvaal lavas, *UV* = Upper Ventersdorp lavas, *VS* = Vredefort ring complex. B. 1100—700 m.y.: *AF* = Auborous formation, *AS* = Abercorn sandstone, *BD* = Bukoban dolerites, *BS* = Bukoban sandstone, *CG* = Chela group, *IG* = Ikorongo group, *KF* = Kigonero flags, *KK* = Klein Karas dykes, *LB* = Lower Buanji series, *MD* = Mbala dolerites, *MR* = Manyovu redbeds, *MS* = Malagarasi sandstone, *MZ* = Mbozi complex, *NQ* = Nosib Group quartzites, *OK* = O'Okiep intrusives, *PND* = Pre-Nama dykes, *PWD* = Post-Waterberg dolerites, *UDL* = combined Umkondo dolerites and lavas.

1100—650 m.y.: The Pan-African events

For the younger time interval 1100—650 m.y., results are confined to the Congo and Kalahari cratons (Fig. 2B). These results are also listed in Piper (1976), but we include new results from the Chela Group of Southern Angola (data of Reid quoted in Kröner, 1975) and unpublished results from the Nosib Group of northern Southwest Africa, a correlative of the Chela Group. This correlation is evident in the palaeomagnetic data (Fig. 4) and confirms the previously suspected age of ca. 1050 m.y. These data, combined with new age data for the Sinclair Group of South-West Africa, drastically alter the interpretation of the apparent polar wander path in the time range 1250—1100 m.y. The Barby Formation lavas have been dated at 1265 ± 15 m.y. (Rb—Sr whole-rock isochron; A. Kröner, personal communication, 1976). The overlying Guperas lavas are intruded by a granitic body yielding U—Pb zircon ages of 1250 m.y. (data of Burger, quoted in Kröner, 1975). These results therefore predate those of the Umkondo dolerites and lavas (1140 m.y.) and post-Waterberg diabases (1115 m.y.), and thus do not

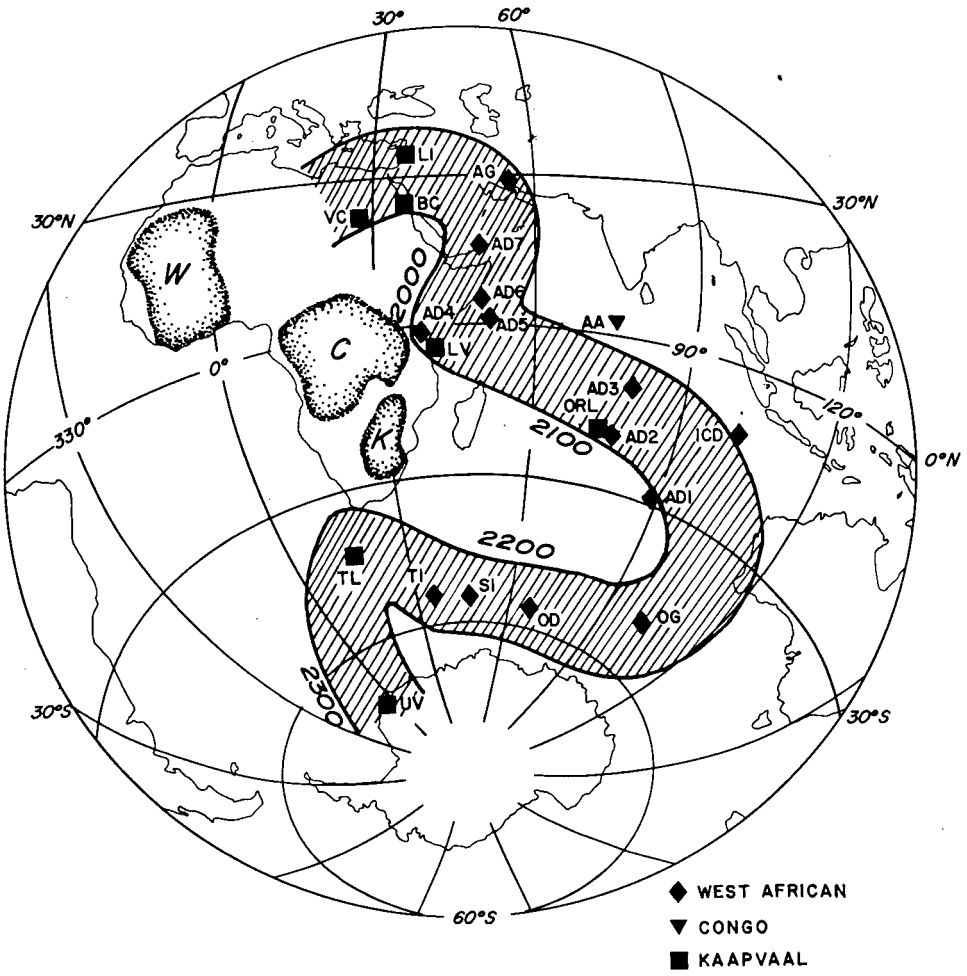

Fig. 3. Apparent polar wander path for African cratons (stippled), 2300—1900 m.y. Swathe width 15° at equator, approximate path ages in m.y. Symbols as in Fig. 2A.

lie on the apparent polar wander path in Fig. 4. This indicates that the pole path for Africa does not form a loop matching the North American Logan loop, as Piper et al. (1973) and Piper (1976) have proposed. Further support comes from recent U—Pb zircon ages for the O'Okiep intrusions of southern South-West Africa (1070 ± 20 m.y.; Stumpfl et al., 1976) previously thought to be similar in age to the Guperas and Barby results in the path proposed by Piper et al. (1973) and Piper (1976). The Auborus Formation in the upper part of the Sinclair Group lies unconformably on the 1250 m.y. granite intruding the Guperas lavas. Its pole (*AF* in Fig. 4) falls on the path at a point corresponding to an age of slightly less than 1100 m.y. The apparent polar wander path of Fig. 4 can be drawn irrespective of the craton from

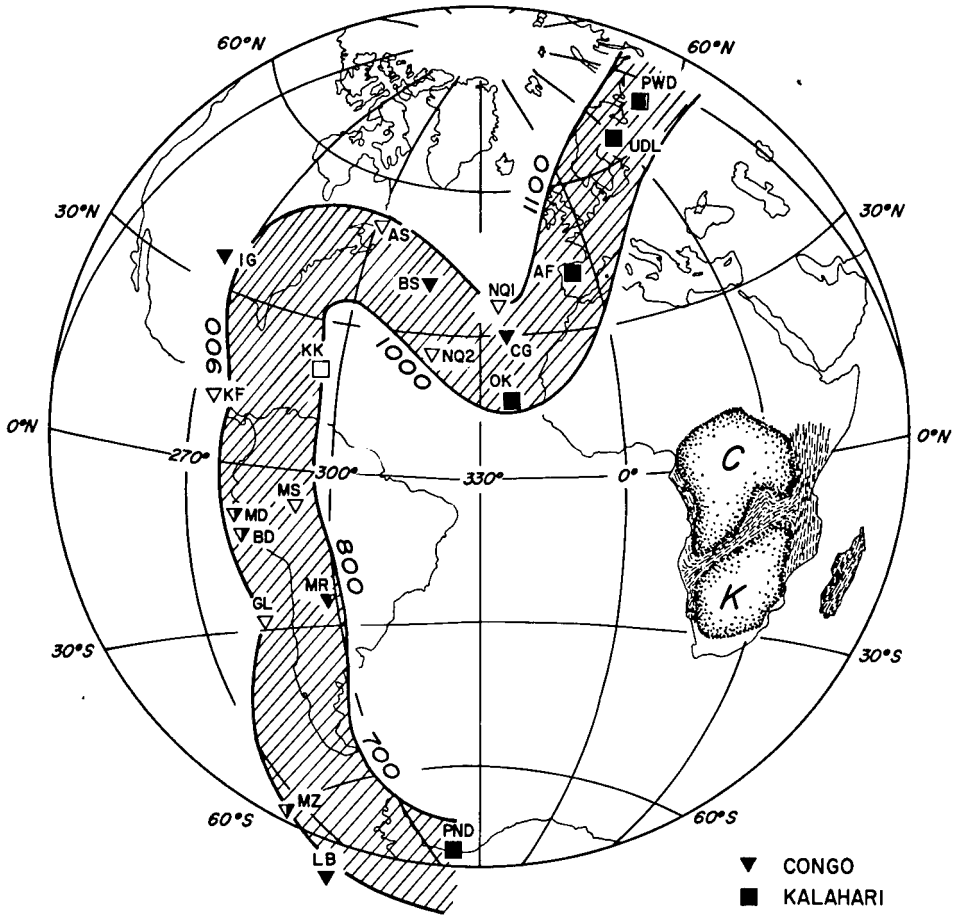

Fig. 4. Apparent polar wander path for African cratons (stippled), 1100—700 m.y. Solid symbols are poles, open symbols antipoles, mixed polarity indicated by partially solid symbols. Assignment of normal and reversed polarity awaits connection to Phanerozoic APWP. Pan-African mobile belts indicated by dashed lines. Swathe width 15° at equator, approximate path ages in m.y. Symbols as in Fig. 2B.

which the data were derived. Once again the model of no large-scale relative movements between the two cratons is given support; the intervening Damara belt cannot be explained in plate-tectonic terms, except in a constrained model.

AUSTRALIA

A simplified structural map of Australia showing the main Precambrian structural features is shown in Fig. 5. Sampling localities of palaeomagnetic studies are indicated and a review of the palaeomagnetic results is given else-

Fig. 5. Simplified structure map of Australia. Basement ages given in 10^9 years. Age of sedimentary basins indicated as *N* (Nullaginian, 2200—1800 m.y.), *C* (Carpentarian, 1800—1400 m.y.), *A* (Adelaidean, 1400—600 m.y.), *P* (Phanerozoic, <600 m.y.). Sampling sites for palaeomagnetic poles are indicated from McElhinny and Embleton (1976). *ERV* = Edith River volcanics, *G* = Giles complex, *GA*, *GB* = Gawler dykes A + B groups, *HD* = Hart dolerite, *IA* = Mt. Isa dykes, group A, *IB* = Lake View dolerite, *IM* = Iron Monarch deposit, *IP* = Iron Prince deposit, *KA* = Koolyanobbing "A" deposit, *KD* = Koolyanobbing Dowd's Hill deposit, *LC* = Lunch Creek lopolith, *MG* = Mt. Goldsworthy deposit, *ML* = Morawa lavas, *MN* = Mt. Newman deposit, *RD* = Ravensthorpe dykes, *TP* = Mt. Tom Price deposit, *WD* = Widgiemooltha dykes, *YA*, YC, YD, YE, YF = Yilgarn dykes group A, C, D, E, F. Solid symbols denote primary magnetization; open symbols denote secondary magnetizations.

where (McElhinny and Embleton, 1976). For a discussion of orogenic evolution in Australia readers are referred to Rutland (1976). The data are not so numerous as from Africa but even so it is again possible to draw a single common apparent polar wander path through all the data from 2500 to

1100 m.y. without violating age constraints (see caption Fig. 6 for discussion of pole *YA*).

2400—1700 m.y.: The Ophthalmian belt

Data for this interval come from the Yilgarn and Pilbara cratons, with a single result from the Kimberley block. As this latter result is of the same age

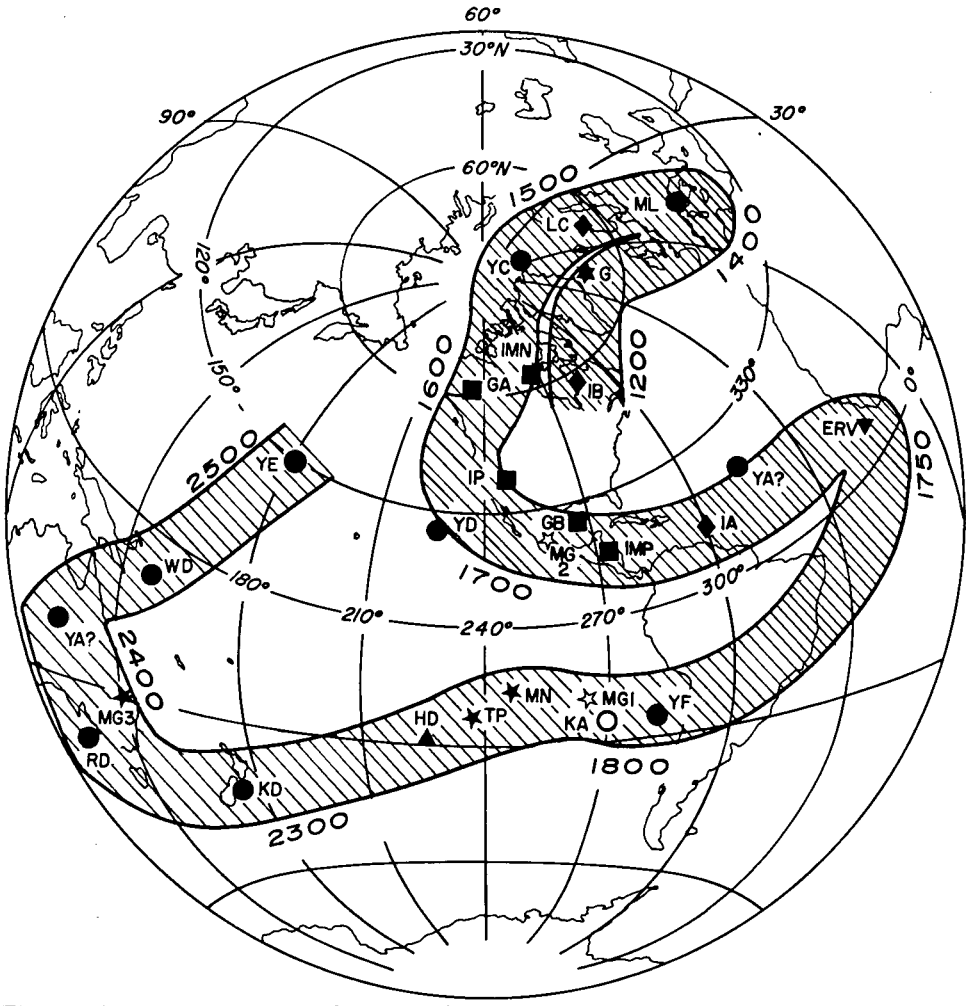

Fig. 6. Apparent polar wander path for Australian cratons 2500—1200 m.y., after McElhinny and Embleton (1976). Symbols as indicated in Fig. 5. *MG1, 2, 3*, are multi-components from the Mt. Goldsworthy deposit where *MG3* > *MG1* > *MG2* in age. *IMN* and *IMP* are the negative and positive magnetizations respectively from the Iron Monarch deposit. Both pole and antipole are plotted for the *YA* dykes due to equivocal Rb—Sr data. Swathe width 15° at equator; approximate path ages in m.y.

as the King Leopold mobile belt, its position can yield no information about the origin of that belt, but serves to verify the ages of similar poles from the Pilbara and Yilgarn. As can be seen, the apparent polar wander path deduced for each craton in this interval is identical within the previously described uncertainties. A single common path is constructed and large-scale relative motions are ruled out. Secondary magnetization *KA* falls on the path predetermined from primary magnetizations.

1700—1200 m.y.: The Albany—Frazer and Musgrave belts

Data for this younger interval come from the Yilgarn, Gawler and Mt. Isa blocks, with a single result from within the Musgrave mobile belt and a single (secondary) magnetization from the Pilbara. The good general agreement of data in the 1700 m.y. range indicate that the component cratonic blocks could not have been widely divergent before formation of the intervening Musgrave belt. Similarly, the agreement of poles in the 1700—1500 m.y. range demonstrates that the younger Albany—Frazer mobile belt was not the result of large-scale horizontal displacement.

NORTH AMERICA

We shall consider here the palaeomagnetic data for individual cratons in the interval 2600—1400 m.y. and discuss also the data from a single younger unit, the Grenville Province. The former is a discussion of intercratonic movements as in the previous sections; the latter considers the history of an orogenic belt itself, as interpreted from the palaeomagnetic data.

2600—1400 m.y.: The Hudsonian orogeny

An extensive review of palaeomagnetic data from the Precambrian of the Laurentian shield has recently been given by Irving and McGlynn (1976). More recently, new results from the Huronian have been presented by Roy and Lapointe (1976). These last authors provide a list of data in the time interval 2600—1400 m.y. The data are separated into those established as primary magnetization associated with the relevant isotopic age and those established as secondary magnetization but whose age is not defined except within broad limits. Figure 7 shows the main structural provinces of the Laurentian shield and gives the sampling localities of the palaeomagnetic data. Primary magnetization is indicated by an age and solid symbol, secondary magnetization by an open symbol and letter code.

The apparent polar wander path is defined from the primary magnetization and a single path can be drawn through the data irrespective of structural unit throughout the entire 2600—1400 m.y. interval, as shown in Fig. 8. Of particular interest is the excellent agreement of poles from the Superior, Slave and Nain provinces at ca. 2100 m.y. Each of these structural units

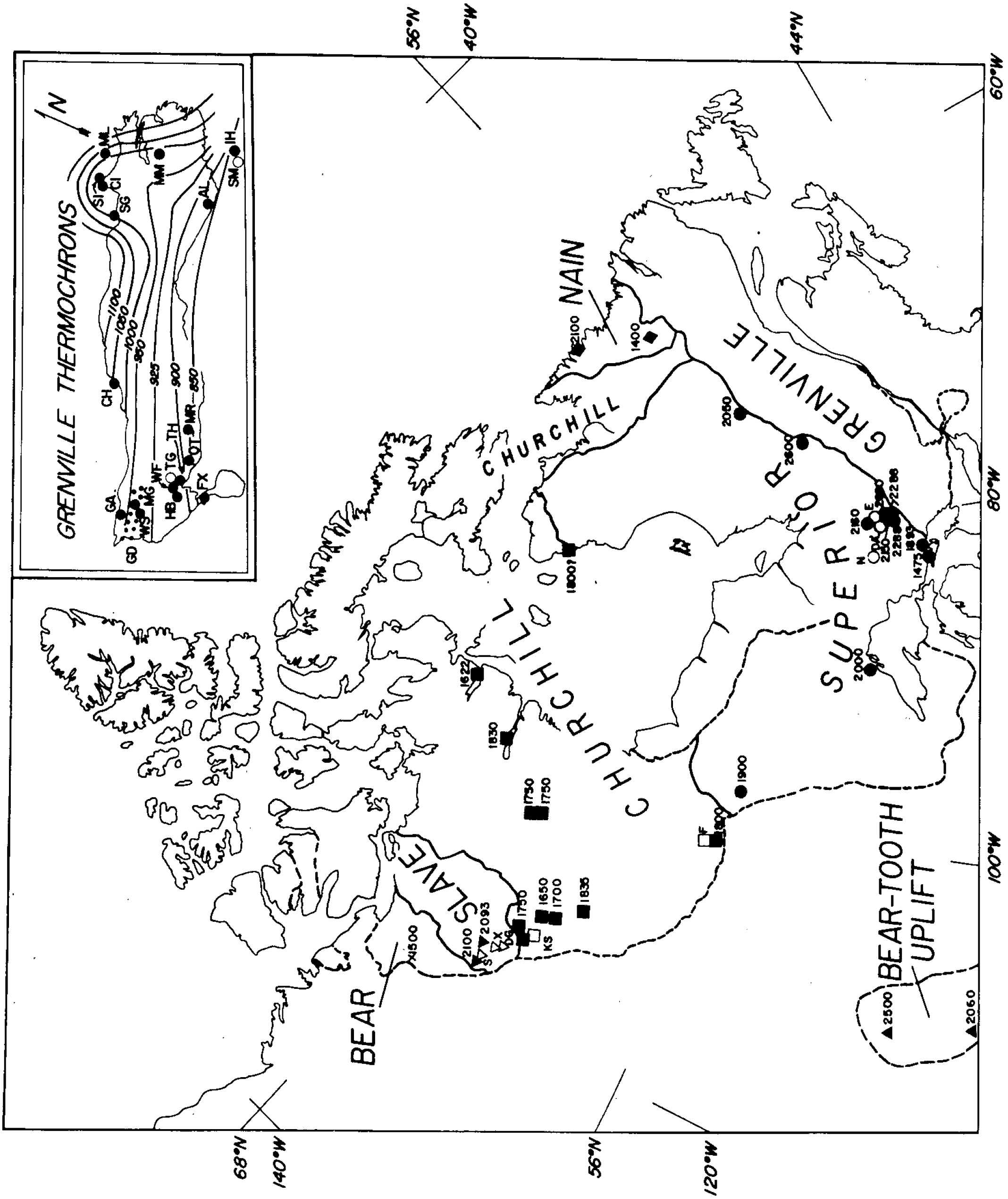
GRENVILLE THERMOCHRONS
N
CHURCHILL
NAIN
GRENVILLE
SUPERIOR
CHURCHILL
SLAVE
BEAR
BEAR-TOOTH UPLIFT
56°N
40°W
44°N
60°W
80°W
100°W
68°N
140°W
56°N
120°W

borders a Hudsonian belt so that if agreement between poles is maintained before and after the Hudsonian event it seems impossible that large-scale displacements were involved in their formation. Furthermore, the polar wander path predicts that all secondary magnetization palaeomagnetic poles should conform with it at positions corresponding to an age younger than the primary magnetization. This should occur irrespective of sampling location. Examination of Fig. 8 shows this to be the case. Therefore, the fixed continent model again prevails indicating that the Hudsonian orogeny must have occurred from internal deformation and not from large-scale horizontal displacement and plate collision.

1100—700 m.y.: The Grenville orogeny

Palaeomagnetic data from the younger 1000—700 m.y. interval come largely from within the Grenville Province, the type area for the ca. 1000 m.y. Grenville orogeny. These data form a discordant group removed from data of roughly similar age from elsewhere in North America. Interpretations of

---

Fig. 7. Simplified structural map of the North American part of the Laurentian shield. Sampling localities for poles in the range 2700—1400 m.y. are indicated from those listed by Roy and Lapointe (1976). Solid symbols with ages are primary magnetizations, open symbols with ages are secondary magnetizations. *2690* = Matachewan dykes, *2600* = Chibougamau greenstone belt, *2500* = Stillwater Complex, > *2288* = Coleman member Gowganda Formation, *2288* = Firstbook member Gowganda Formation, *2160* = Otto Stock, *2211* = Big Spruce Complex, *2100* = Mugford Basalt, *2150* = Nipissing diabase, Gowganda Formation, *2288* = Firstbrook member Gowganda Formation, *2160* = Otto Stock, *2111* = Big Spruce Complex, *2100* = Mugford Basalt, *2150* = Nipissing diabase, *2060* = Wind River dykes, *2050* = Otish Gabbro, *2093* = Indin dykes, *2000* = Gunflint Formation , *1900* = Molson dykes, *1893* = Spanish River Complex, *1873* = Kahocella Formation, *1830* = Dubawnt Group, *1835* = Martin Formation, *1800* = Flin Flon B magnetization, *1800?* = Cape Smith Basalts (Fujiwara and Schwarz, 1975), *1750* = Stark Formation, *1750* = Et-then Group, *1700* = Sparrow dykes, *1650* = Nonacho Group, *1622* = Melville Daly Bay metamorphics, *1500* = Western Channel diabase, *1475* = Croker Island Complex, *1400* = Michikamau Anorthosite. *N* = Gowganda secondary, *S* = Big Spruce secondary, *X* = *X* dykes, *DG* = Dogrib dykes, *F* = Flin-Flon secondary, *DA*, *E* = Nipissing secondary, *KS* = Kahocella secondary. *Inset.* Palaeomagnetic sampling sites within the Grenville Province. Details of palaeomagnetic results listed in Irving et al. (1974b) and Buchan and Dunlop (1976). Contours are biotite K—Ar "thermochrons", after Harper (1967); data in m.y. *AL* = Allard Lake anorthosite, *CH* = Chibougamau CH component, *CI* = Croteau igneous rocks, *FX* = Frontenac axis dykes, *GA* = Grenville anorthosites, *GD* = Grenville dykes, *HB* = Haliburton intrusives, *IH* = Indian Head anorthosite, *MG* = Magnetawan metasediments, *ML* = Michael gabbro, *MM* = Mealy Mt. anorthosite, *MR* = Morin anorthosite, *OT* = Ottawa intrusive rocks, *SI* = Seal Lake igneous rocks, *SG* = Shabogamo gabbro, *SM* = Steel Mt. anorthosite, *TG* = Tudor gabbro, *TH* = Thanet intrusives, *WF* = Wilberforce pyroxenite, *WS* = Whitestone anorthosite. Small dots denote areal extent of GD sites. Poles *TG* and *SM* are the only two results which do not fit the model outlined in the text; these are plotted as open symbols. Geochronological evidence suggests that *SM* may have a younger age of 415 m.y. (Leech et al., 1963), while *TG* may also be younger at 670 m.y. (Hayatsu and Palmer, 1975).

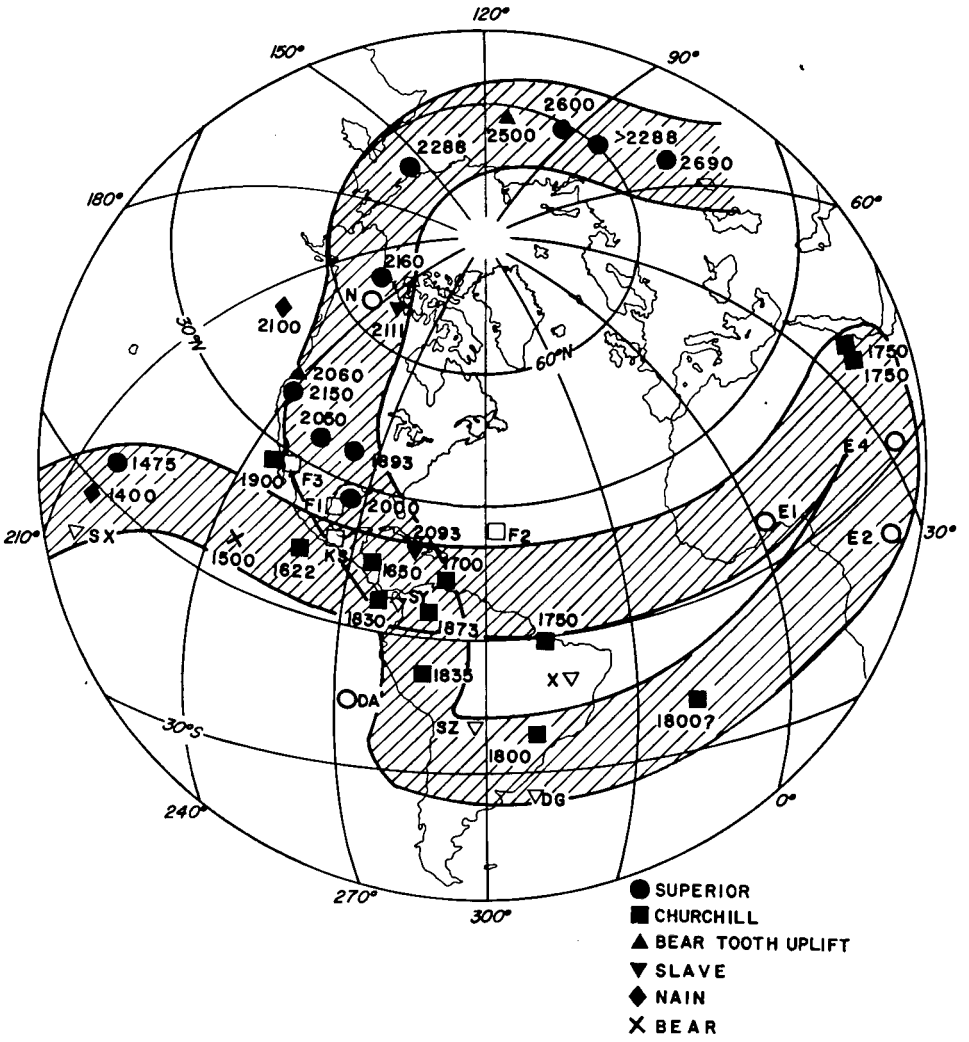

Fig. 8. Apparent polar wander path for North American cratons, 2700—1400 m.y. Symbols and sampling localities are as indicated in Fig. 7. Swathe width 15° at equator.

these discordant poles (the only convincing example of systematically discordant data known in the Precambrian of North America) have led to tectonic models based upon continental collision as well as models based upon internal (ensialic) mechanisms. Details of these respective models will not be presented here, the reader is referred to Irving et al. (1972, 1974b) and Buchan and Dunlop (1976) for examples of collisional interpretations. Non-collisional interpretations of these data can be found in Roy and Fahrig (1973), Fahrig et al. (1974) and McWilliams and Dunlop (1975, 1977).

It is widely accepted that the Grenville Front itself is not the site of a

collisional suture (e.g. Irving et al., 1972; Wynne-Edwards, 1972) Any suture zone if it exists must lie within the Grenville Province itself. Palaeomagnetic results from the northern Grenville (McWilliams and Dunlop, 1974, 1975; Ueno et al., 1975) limit the position of a hypothetical suture to within an 85-km zone adjacent to the Front in the western Grenville Province. No geological evidence for a suture is found in this zone, although as Dewey (1976, and this volume) rightly points out, such evidence may be difficult if not impossible to find.

The manner in which the remanent magnetization in rocks is gradually lost during the heating accompanying burial and metamorphism, and how it is replaced by a new remanence during uplift and cooling has been investigated both theoretically and experimentally by Pullaiah et al. (1975). These studies suggest that very little, if any, remanence can survive upper greenschist facies metamorphism. The age of the remanence in high-grade metamorphic rocks will fall in the range between the Rb—Sr whole-rock isochron and K—Ar biotite ages. Harper (1967) first suggested that the distribution of K—Ar ages from the Grenville Province formed a series of equal-age "thermochrons" parallel to and progressively younger with distance away from the Grenville Front (see inset of Fig. 7). This distribution strongly suggests a history of post-orogenic uplift and cooling progressing eastwards away from the Front. It is most likely therefore that the magnetizations measured in Grenville rocks were acquired during this post-orogenic uplift following the Grenville orogeny. Both geologic (Wynne-Edwards, 1972; Stockwell et al., 1970) and radiometric (Grant, 1964; Wanless et al., 1970) evidence show that the Grenville orogeny affected the Superior Province to the north and thus occurred whilst the Grenville was in approximately its present position. All of these observations then strongly suggest that the palaeomagnetism of Grenville rocks cannot describe the pre-orogenic drift history of the Grenville Province.

The above arguments show that the discordant poles observed from the Grenville Province must be related to post-orogenic uplift and cooling and thus the thermochron distribution proposed by Harper (1967). The poles will refer to a time sequence between about 1100 m.y. and 800 m.y. which post-dates the Logan Loop of Robertson and Fahrig (1971). The palaeomagnetic poles have been averaged (Table I) in zones represented by the thermochrons as shown in the inset of Fig. 7. The results define a time sequence which extends the Logan Loop into a Grenville polar loop (McWilliams and Dunlop, 1975, 1977) as shown in Fig. 9. The poles *SR* and *SN* are derived from secondary magnetizations possibly acquired during late-stage thermal events in the order suggested by Buchan and Dunlop (1976). That the Logan Loop should be extended southwards towards Australia is confirmed by preliminary palaeomagnetic results from the Grand Canyon sequence (Elston and Grommé, 1974). Unfortunately, there exist no corroborative data for the interval 850—700 m.y. from elsewhere in North America to confirm the remainder of the loop.

TABLE I

Thermochron zone poles. A summary of component poles can be found in Irving et al. (1974b) and Buchan and Dunlop (1976). Poles A—F are grouped according to sampling locality, with Grenville thermochrons (Harper, 1967) as a guide. Polarity: N = normal, R = reversed; M_N = mixed predominantly normal, M_R = mixed predominantly reversed; N = number of poles in zone; R = vector resultant length. Latitudes and longitudes are reckoned positive north and east, respectively.

Zone	Thermochron age range (m.y.)	Component poles	Polarity	Zone mean pole				Zone polarity
				N	R	long.E	lat.N	
A	1050—1000	Michael Gabbro	R	2	1.97	159	1	R
		Chibougamau *CH* component	R					
B	1000— 950	Grenville Front Anorthosites	R	5	4.86	164	2	M_R
		Mealy Mt. *NW* component	N					
		Seal Igneous Rocks	R					
		Croteau Igneous Rocks	R					
		Shabogamo Gabbro	R					
C	950— 925	Grenville Dykes	M_R	3	2.91	146	—15	M_N
		Whitestone *W* component	N					
		Magnetawan Metamorphic RX	N					

D	925— 900	Haliburton *A* component	N	3	2.95	149	—26	M_N
		Wilberforce Pyroxenite	N					
		Thanet Intrusives	R					
E	900— 850	Allard Lake Anorthosite	M_N	3	2.98	145	—38	M_N
		Morin Anorthosite Primary	N					
		Ottawa Intrusives	M_N					
F	850— 750	Indian Head Anorthosites	N	2	1.99	159	—11	M
		Frontenac Axis Dykes	R					
SR *	750 $\overset{?}{-}$ 650	Haliburton *C* component	R	3	2.99	166	— 3	R
		Whitestone *Y* component	R					
		Morin Secondary	R					
SN *	<SR	Haliburton *B* component	N	3	2.89	167	19	N
		Whitestone *Z* component	N					
		Mealy Mt. *E* component	N					
G	<SN	Tudor Gabbro	N	2	1.99	138	20	M
		Steel Mt. Anorthosite	R					

* SR and SN component poles are secondary magnetizations selected on basis of polarity, not relationship of sampling site to thermochron lines.

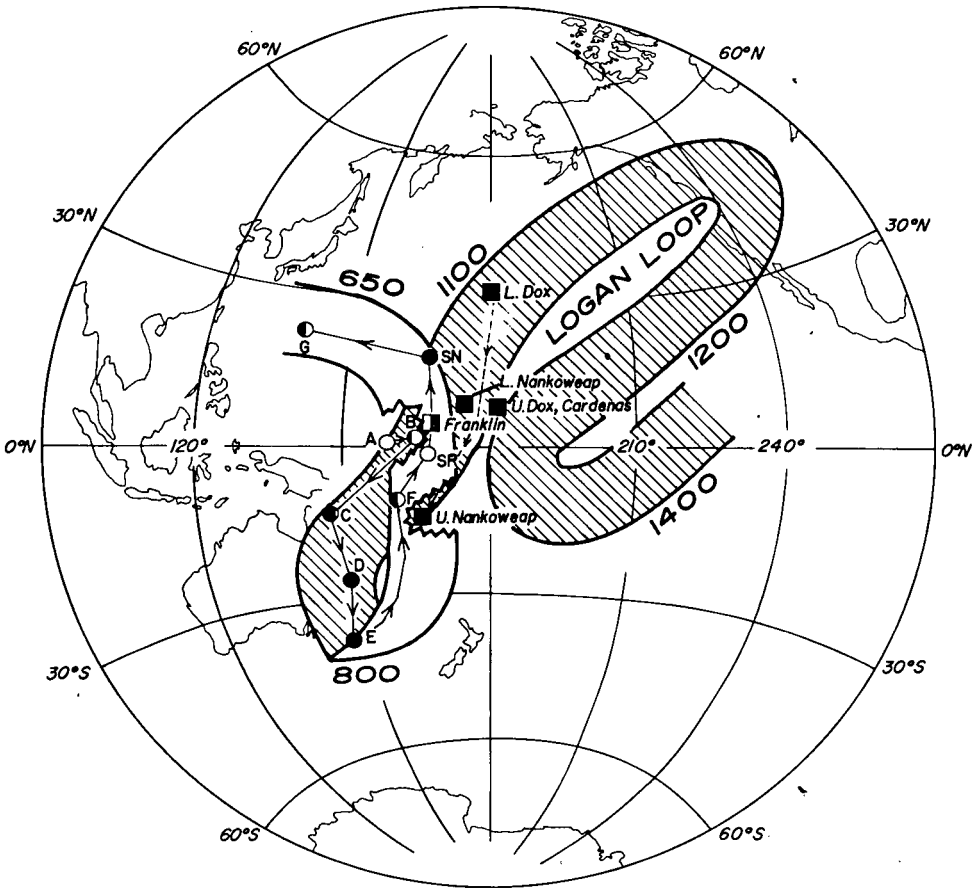

Fig. 9. Grenville apparent polar wander path, 1000—700 m.y. Thermochron zone poles *A—G*, *SR* and *SN* listed in Table I; solid symbols represent normal polarity, open symbols reversed. Mixed polarity indicated by partially filled symbols. Squares are poles from outside Grenville Province: Franklin diabase (Fahrig et al., 1971) and Grand Canyon rocks (Elston and Grommé, 1974), in stratigraphic order (see text). Underside of path is shaded, topside cut away to show A, B and upper Nankoweap. Swathe width 15° at equator, approximate path ages in m.y. A clockwise loop at approximately 700 m.y. (Irving and McGlynn, 1976) is also possible, in addition to the 800 m.y. loop.

The interpretation of the palaeomagnetic data in terms of Harper's (1967) thermochrons effectively invalidates both the collision (Irving et al., 1972, 1974b; Buchan and Dunlop, 1976) and non-collision models (Roy and Fahrig, 1973; Fahrig et al., 1974) proposed to fit the data On the model presented here, the exposed Grenville has maintained its present relative position to the remaining Precambrian shield before, during and after the Grenville orogeny. However, a plate-tectonic mechanism for the orogeny itself is not precluded, such as Burke and Dewey (1973) have suggested. In their inter-

pretation, the Grenville Province is a reactivated (Superior Province) terrain resulting from subduction and plate collision along a zone to the southeast (now covered or lost in the Appalachian orogen). Since the Grenville palaeomagnetic poles date from post-orogenic times, they have no bearing on such an interpretation.

DISCUSSION

It is well known (e.g. McElhinny, 1973) that the palaeomagnetic consequences of large-scale horizontal displacements as predicted by plate-tectonic theory are highly variable. This variability arises from the possible geometrical relationships between Euler rotation poles and successive palaeomagnetic poles in any given crustal block. In the simplest case maximum apparent polar motion occurs when the rotation pole and palaeomagnetic pole are orthogonal; conversely, no apparent polar motion will be observed when the two poles are coincident. Large apparent polar motion need not to be the result of large actual displacement. If the rotation pole is situated in or near the block under consideration, small rotations can give rise to large apparent polar motion if the position of the palaeomagnetic poles is favourable. We should then expect that during Precambrian time, if a plate-tectonic regime were operative, an entire spectrum of such geometrical arrangements would occur, manifesting themselves in a wide variety of palaeomagnetic signatures in distinct crustal units. Specifically, if the orogenic belts presently separating the cratons owe their origin to continent—continent collision on plate-tectonic theory, then it must be assumed that many of the cratons presently adjacent to one another were originally widely separated. Allowing for reversals of the earth's magnetic field this would mean that the poles for pre-collision times could be situated virtually anywhere over an entire hemisphere, the precise positions being determined only by the geometry of the plate-tectonic situation involved.

In the previous sections we have presented results from three continents that illustrate the continuity of apparent polar wander paths through six orogenies. The probabilities that in all six cases the pre-orogenic poles from adjacent cratons would all be in agreement (to 10° or 20°) and that a plate-tectonic regime involving continent—continent collision was operating are exceedingly small. The expected wide spectrum of possible polar distributions is not seen. We have previously noted that the inherent errors in the pole paths, as represented by the swathe of width 15°, does not preclude the creation and destruction of small oceans. However, it must be stressed again that these are very special oceans that open and close again so as to return the adjacent cratons to their same relative positions. Whereas this is certainly a form of plate motion that is possible on plate-tectonic theory it is not one that is predicted except in very special circumstances. It must be assumed that the motions of continents/cratons are constrained only by

the presence of other continents/cratons and their relation to plate boundaries.

Attempts have been made (Burke et al., 1976) to show that the apparent polar wander paths from different cratons are indeed widely different in the Precambrian. With the amount of palaeomagnetic data currently available from Precambrian rocks it is a relatively simple exercise to demonstrate the apparent divergences between the data from separate cratons when viewed separately. This arises because the data are incomplete and the comparison of two or more incomplete data sets will inevitably lead to apparent differences whatever hypothesis is valid. The observation of the existence of differences merely confirms the inadequacy of the data and says nothing about the validity or otherwise of the hypothesis being tested. The problem is basically to compare two data sets each having associated statistical errors and uncertainties and one needs to answer the question: are they the same or are they different? When using formal statistical comparisons the approach is always to use the null hypothesis. That is one does not test that two quantities are different but what the probabilities are that they are the same. If the probability is low that they are the same, the hypothesis of sameness can be rejected and one asserts that the quantities are different. This is essentially the technique that we have followed in analyzing Precambrian apparent polar wander paths in this paper. We find that these paths may be constructed irrespective of the presence of intervening orogenic belts between cratons. Although this conclusion is difficult to sustain in formal statistical terms, nevertheless it suggests that large-scale motions to explain these belts are unlikely. The approach used by Burke et al. (1976) is invalid because it fails to take into account the nature of the data being analyzed.

Although we find that the relative motion between Precambrian cratons over the time span 2500—700 m.y. has been small for presently adjoining cratons, it is clear that relative motion between these cratons and the pole was similar to that observed during the Phanerozoic. This suggests that there were continental units moving over the surface of the earth in Precambrian times. Orogenic belts did not arise from the formation and destruction of large oceans and resulting continent—continent collision but arose from internal deformation. It seems possible that plate tectonics has matured through the earth's history. Possibly there were initially only two or three continental blocks so that the probabilities of collision were small. At the same time rifting may have occurred within continents resulting in the formation of aulacogens which then closed again to produce many of the orogenic belts seen today. In any case, palaeomagnetic data strongly suggest that Precambrian tectonic mechanisms were not the same as present-day plate-tectonic mechanisms.

REFERENCES

As, J.A. and Zijderveld, J.D.A., 1958. Magnetic cleaning of rocks in palaeomagnetic research. Geophys. J. R. Astron. Soc., 1: 308—319.

Beck, M.E., 1970. Paleomagnetism of Keweenawan intrusive rocks, Minnesota. J. Geophys. Res., 75: 4985—4996.

Briden, J.C., 1976. Application of palaeomagnetism to Proterozoic tectonics. Philos. Trans. R. Soc. London, A280: 405—416.

Buchan, K.L. and Dunlop, D.J., 1976. Paleomagnetism of the Haliburton intrusions: superimposed magnetizations, metamorphism, and tectonics in the late Precambrian. J. Geophys. Res., 81: 2951—2967.

Burke, K. and Dewey, J.F., 1972. Orogeny in Africa. In: T.F.J. Dessauvagie and A.J. Whiteman (editors), African Geology Ibadan 1970. Ibadan Univ. Press, p. 583—608.

Burke, K., Dewey, J.F. and Kidd, W.S.F., 1976. Precambrian paleomagnetic results compatible with contemporary operation of the Wilson Cycle. Tectonophysics, 33: 287—299.

Clifford, T.N., 1968. Radiometric dating and the pre-Silurian geology of Africa. In: E.F. Hamilton and R.M. Farquhar (editors), Radiometric Dating for Geologists. Interscience, London, p. 299—416.

Dewey, J.F., 1969. Evolution of the Appalachian/Caledonian orogen. Nature, 221: 124—129.

Dewey, J.F., 1976. Ophiolite obduction. Tectonophysics, 31: 93—120.

Dewey, J.F., 1977. Suture zone complexities: a review. This volume.

Dewey, J.F. and Bird, J.M., 1970a. Mountain belts and the new global tectonics. J. Geophys. Res., 75: 2625—2647.

Dewey, J.F. and Bird, J.M., 1970b. Plate tectonics and geosynclines. Tectonophysics, 10: 625—638.

Dewey, J.F. and Burke, K., 1973. Tibetan, Variscan and Precambrian basement reactivation: products of continental collision. J. Geol., 81: 683—692.

Du Bois, P.M., 1962. Paleomagnetism and correlation of Keweenawan rocks. Geol. Surv. Can. Bull., 71: 75 pp.

Elston, D.P. and Grommé, S.C., 1974. Precambrian polar wandering from Unkar Group and Nankoweap formation, eastern Grand Canyon, Arizona. Paper presented at Geol. Soc. Am. Rocky Mtn. Soc. Meeting.

Fahrig, W.F., Irving, E. and Jackson, G.D., 1971. Paleomagnetism of the Franklin diabases. Can. J. Earth Sci., 8: 455—467.

Fahrig, W.F., Christie, K.W. and Schwarz, E.J., 1974. Paleomagnetism of the Mealy Mountain Anorthosite and of the Shabogamo Gabbro, Labrador, Canada. Can. J. Earth Sci., 11: 18—29.

Fujiwara, Y. and Schwarz, E.J., 1975. Paleomagnetism of the Circum-Ungava Proterozoic fold belt (I): Cape Smith Komatiitic basalts. Can J. Earth Sci., 12: 1785—1793.

Gough, D.I., Opdyke, N.D. and McElhinny, M.W., 1964. The significance of paleomagnetic results from Africa. J. Geophys. Res., 69: 2509—2519.

Grant, J.A., 1964. Rubidium—strontium isochron study of the Grenville Front near Lake Timigami, Ontario. Science, 146: 1049—1053.

Hamilton, W., 1970. The Uralides and the motion of the Russian and Siberian platforms. Geol. Soc. Am. Bull., 81: 2553—2576.

Harper, C.T., 1967. On the interpretation of potassium—argon ages from Precambrian shields and Phanerozoic orogens. Earth Planet. Sci. Lett., 3: 128—132.

Hayatsu, A. and Palmer, H.C., 1975. K—Ar isochron study of the Tudor Gabbro, Grenville Province, Ontaria. Earth Planet. Sci. Lett., 25: 208—212.

Irving, E., 1956. Palaeomagnetic and palaeoclimatological aspects of polar wandering. Geofis. Pura Appl., 33: 23—41.

Irving, E. and McGlynn, J.C., 1976. Proterozoic magnetostratigraphy and tectonic evolution of Laurentia. Philos. Trans. R. Soc. London, A280: 433—468.

Irving, E., Robertson, W.A., Stott, P.M., Tarling, D.H. and Ward, M.A., 1961. Treatment of partially stable sedimentary rocks showing planar distribution of directions of magnetization. J. Geophys. Res., 66: 1927—1933.

Irving, E., Park, J.K. and Roy, J.L., 1972. Palaeomagnetism and the origin of the Grenville Front. Nature, 236: 344—346.
Irving, E., Park, J.K. and Emslie, R.F., 1974a. Paleomagnetism of the Morin Complex. J. Geophys. Res., 79: 5482—5490.
Irving, E., Emslie, R.F. and Ueno, H., 1974b. Upper Proterozoic paleomagnetic poles from Laurentia and the history of the Grenville Structural Province. J. Geophys. Res., 79: 5491—5502.
Kröner, A. (editor), 1975. Twelfth Annual Report 1974, Precambrian Research Unit, University of Cape Town, 60 pp.
Leech, G.B., Lowdon, J.A., Stockwell, C.H. and Wanless, R.K., 1963. Age determinations and geological studies. Geol. Surv. Can. Pap., 61—71.
Le Pichon, X., 1968. Sea-floor spreading and continental drift. J. Geophys. Res., 73: 3661—3697.
McElhinny, M.W., 1973. Palaeomagnetism and Plate Tectonics. Cambridge University Press, London, 358 pp.
McElhinny, M.W. and Embleton, B.J.J., 1976. Precambrian and early Palaeozoic palaeomagnetism in Australia. Philos. Trans. R. Soc. London, A280: 417—431.
McElhinny, M.W., Briden, J.C., Jones, D.L. and Brock, A., 1968. Geological and geophysical implications of palaeomagnetic results from Africa, Rev. Geophys., 6: 201—238.
McKenzie, D.P. and Parker, R.L., 1967. The North Pacific: an example of tectonics on a sphere. Nature, 216: 1276—1280.
McWilliams, M.O. and Dunlop, D.J., 1974. Paleomagnetism of a folded Precambrian iron formation of Grenville age. EOS, Trans. Am. Geophys. Union, 55: 226 (abstract).
McWilliams, M.O. and Dunlop, D.J., 1975. Precambrian paleomagnetism: magnetizations reset by the Grenville orogeny. Science, 190: 269—272.
McWilliams, M.O. and Dunlop, D.J., 1977. Paleomagnetism of the Magnetawan metasediments (Grenville Supergroup) and tectonics of the Grenville Province. Can. J. Earth Sci. (in press).
Piper, J.D.A., 1976. Palaeomagnetic evidence for a Proterozoic super-continent. Philos. Trans. R. Soc. London, A280: 469—490.
Piper, J.D.A., Briden, J.C. and Lomax, K., 1973. Precambrian Africa and South America as a single continent. Nature, 245: 244—248.
Pullaiah, G., Irving, E., Buchan, K.L. and Dunlop, D.J., 1975. Magnetization changes caused by burial and uplift. Earth Planet. Sci. Lett., 28: 133—143.
Robertson, W.A. and Fahrig, W.F., 1971. The Great Logan Paleomagnetic Loop — The polar wandering path from Canadian shield rocks during the Neohelikian Era. Can. J. Earth. Sci., 8: 1355—1372.
Roy, J.L. and Fahrig, W.F., 1973. The paleomagnetism of Seal and Croteau rocks from the Grenville Front, Labrador: Polar wandering and tectonic implications. Can. J. Earth Sci., 10: 1279—1301.
Roy, J.L. and Lapointe, P.L., 1976. The paleomagnetism of Huronian redbeds and Nipissing diabase; post-Huronian igneous events and apparent polar path for the interval —2300 to —1500 Ma for Laurentia. Can. J. Earth Sci., 13: 749—773.
Roy, J.L. and Park, J.K., 1974. The magnetization process of certain redbeds. Vector analysis of chemical and thermal results. Can. J. Earth Sci., 11: 437—471.
Runcorn, S.K., 1956. Paleomagnetic comparisons between Europe and North America. Proc. Geol. Assoc. Can., 8: 77—85.
Rutland, R.W.R., 1976. Orogenic evolution in Australia. Earth Sci. Rev., 12: 161—196.
Spall, H., 1971. Precambrian apparent polar wandering evidence for North America. Earth Planet. Sci. Lett., 10: 273—280.
Stockwell, C.H., McGlynn, J.C., Emslie, R.F., Sanford, B.V., Norris, A.W., Donaldson, J.A., Fahrig, W.F. and Currie, K.L., 1970. Geology of the Canadian shield. In: R.J.W. Douglas (editor), Geology and Economic Minerals of Canada. Geol. Surv. Can., Econ. Geol. Rept., 1: 44—150.

Stumpfl, E.F., Clifford, T.N., Burger, A.J. and Van Zijl, D., 1976. The copper deposits of the O'Okiep district, South Africa: new data and concepts. Mineral. Deposita (Berl.), 11: 46—70.

Sutton, J. and Watson, J.V., 1974. Tectonic evolution of continents in early Proterozoic times. Nature, 247: 433—435.

Ueno, H., Irving, E. and McNutt, R.H., 1975. Paleomagnetism of the Whitestone anorthosite and diorite, the Grenville polar track, and relative motions of the Laurentian and Baltic shields. Can. J. Earth Sci., 12: 209—226.

Wanless, R.K., Stevens, R.D. and Loveridge, W.D., 1970. Anomalous parent—daughter isotopic relationships in rocks adjacent to the Grenville Front near Chibougamau, Quebec. Eclogae Geol. Hebr., 63: 345—364.

Wynne-Edwards, H.R., 1972. The Grenville Province. In: R.A. Price and R.J.W. Douglas (editors), Variations in Tectonic Style in Canada. Geol. Assoc. Can. Spec. Publ., 11: 263—334.